

Improving Practicality and Scope of Nickel-Catalyzed Coupling Reactions

By

Wei Li

**A dissertation submitted in partial fulfillment
of the requirements for the degree of
Doctor of Philosophy
(Chemistry)
in The University of Michigan
2012**

Doctoral Committee:

**Professor John Montgomery, Chair
Professor John R. Traynor
Professor Masato Koreeda
Associate Professor John P. Wolfe**

DEDICATION

This dissertation is dedicated to my family-the Li clan. Thanks to all your support, I am finally getting close to have a permanent head damage :).

ACKNOWLEDGEMENTS

I would like to first thank my advisor, Professor John Montgomery. Without your guidance and support, I would not be able to accomplish what I have done in graduate school. I mostly appreciated your inquisitive questions regarding chemistry in general and funny jokes, in addition to your brutal honesty in the wake of my mistakes. Going through graduate school with you as an advisor have been a fun and interesting process.

I would like to thank all my group members in the Montgomery lab, past and present. You guys have made my graduate school life so much more enjoyable. Besides the great insights you guys have contributed to my chemistry, the unlimited amount of uncensored humors will also be missed. I would like thank Anada Herath in particular for his mentorship as an older graduate student. I would also like to thank all the group members that have edited my thesis, you know who you are!

I would also like to thank all my committee members for all your help. In particular, my rotation advisor, Professor John Wolfe for his insights and suggestions on my project and improving as a chemist in general; Professor Masato Koreeda for being a great help throughout my GSI appointments and super fast in returning emails; Professor John Traynor for being my cognate committee member and active engagement in my candidacy and data meeting presentations. In addition, I want to thank you guys for being patient and understanding in scheduling my defense.

I would also like to give a shout out to some of my fellow classmates Zachary Buchan, Joshua Neukom and Peter Mai for all their help, encouragement and fun memories throughout their time here. I hope I have done the same for you!

I would also like to thank my undergraduate advisor, Professor Jeffrey Johnson, and graduate student mentors, Xin Linghu and Matthew Campbell for their mentorship and guidance throughout my undergraduate studies.

Lastly and most importantly, I want to thank my family for their unconditional love and support. I want to thank my dad and my mom for always being supportive. I want to thank my brother, Michael, for always being a fantastic brother. I want to thank my girlfriend, Lisa, for being my best friend and rationale voice! You have been everything to me!

To simply summarize what I have learned from graduate school, love your family, love your friends and love life! Thank you, God!

Table of Contents

DEDICATION.....	ii
ACKNOWLEDGEMENTS.....	iii
LIST OF SCHEMES	x
LIST OF TABLES.....	xiii
LIST OF ABBREVIATIONS	xiv
ABSTRACT	xvi
Chapter 1: Introduction.....	1
1.1 Significance of Catalytic Reductive Coupling Processes	1
1.2 Nickel-Catalyzed Aldehyde-Alkyne Couplings	3
1.3 Nickel-Catalyzed Enone-Alkyne Couplings	8
1.3.1 Cuprate Reagents	8
1.3.2 Hydrometallation in Conjugate Addition	9
1.3.3 Nickel-Catalyzed Reductive Couplings of Enones and Alkynes	10
1.4 Alcohols as Reducing Agents in Transition-Metal Catalyzed Reactions	20
1.5 Regioselective Coupling Processes.....	23

1.5.1	Challenges and Solutions in Regiocontrol of Alkyne and Allene Additions Reactions	23
1.5.2	Substrate-Control in Reductive Coupling Reactions with Alkynes	24
1.5.3	Ligand-Control of Regiochemistry of Alkynes	24
1.5.4	Reducing Agent Influence on Regiochemistry of Allene Additions.....	26
1.5.5	Process Control of Regiochemistry	27
Chapter 2: Nickel-Catalyzed Alcohol-Mediated Enones-Alkynes and Aldehydes-Alkynes Reductive Coupling Reactions.....		30
2.1	Nickel-Catalyzed Alcohol-Mediated Enone-Alkyne Reductive Coupling.....	30
2.1.1	Proposed Strategy for Utilizing Alcohol as Reducing Agent.....	30
2.1.2	Initial Studies and Optimization of the Nickel-Catalyzed Alcohol-Mediated Reductive Couplings of Enones / Alkynes	32
2.1.3	Mechanistic Studies and Comparison of Methanol-Mediated to Et ₃ B-Mediated Reductive Coupling Reactions.....	36

2.2	Nickel-Catalyzed Alcohol-Mediated Reductive Couplings of Aldehydes and Alkynes	39
2.2.1	Proposed Strategy and Challenges for utilizing Alcohol as Reducing Agent in Aldehyde / Alkyne Reductive Couplings	39
2.2.2	Reaction Optimization for the Alcohol-Mediated Aldehyde-Alkyne Reductive Coupling Reactions	42
2.3	Summary of Nickel-Catalyzed Alcohol Mediated Enone-Alkyne and Aldehyde-Alkyne Reductive Couplings	46
Chapter 3: Pathway to the Discovery of a Nickel-Catalyzed Internal Redox Reaction		48
3.1	Ligand Screening of the Nickel-Catalyzed Enal-Alkyne Coupling Reactions	48
3.2	Triarylphosphine-Promoted Nickel-Catalyzed [3+2] Reductive Cycloadditions and Alkylative Couplings of Enals and Alkynes	50
3.3	Discovery of Internal Redox Reactions of Enals, Alkynes and Methanol	54
Chapter 4: Regioselective Addition of Functional Groups to Allenes...59		

4.1	Hypothesis and Challenges of Allenes in Reductive Couplings	59
4.2	Optimization and Scope of Nickel-Catalyzed Enone / Allene Coupling with Et ₃ B as Reducing Agent	60
4.3	Hypothesis of using Et ₃ SiH in Nickel-Catalyzed Enone / Allene Couplings	66
4.4	Regioselective Nickel-Catalyzed Enone-Allene Coupling Reactions	67
4.5	Nickel-Catalyzed Regioselective Allene Hydrosilylation	73
Chapter 5: Experimental Section.....		78
5.1	Experimental Procedures and Spectra Data: Chapter 2.....	78
5.1.1	General Procedure A for the Ni(COD) ₂ /PBU ₃ Promoted Reductive Coupling of Enones and Alkynes using Et ₃ B as the Reducing Agent.....	79
5.1.2	General Procedure B for the Ni(COD) ₂ / PCy ₃ Catalyzed Reductive Coupling of Enones and Alkynes using MeOH as the Reducing Agent.....	79
5.2	Experimental Procedures and Spectra Data: Chapter 3.....	90
5.2.2	General Procedure for the Ni(COD) ₂ / IPr Promoted Coupling of Enals, Alkynes, and Alcohols	97

5.3	Experimental Procedures and Spectra Data: Chapter 4.....	101
5.3.1	General Procedure for the Ni(COD) ₂ /PBU ₃ Promoted Reductive Coupling of Enones and Alkynes.....	102
	References.....	153

List of Schemes

Scheme 1. Addition of Alkenyl Nucleophiles to Electrophiles	2
Scheme 2. Divergent Pathways of Nickel-Catalyzed Alkynal Couplings	4
Scheme 3. Et ₃ B as Reducing Agent in Intermolecular Aldehyde-Alkyne Couplings	5
Scheme 4. Et ₃ SiH as Reducing Agent in Alkynal Reductive Couplings	5
Scheme 5. Total Synthesis of Pumiliotoxin 339A	6
Scheme 6. Intermolecular Crossover Experiment Utilizing R ₃ SiH	7
Scheme 7. Proposed Mechanism for Nickel-Catalyzed Couplings of Aldehydes, Alkynes, and R ₃ SiH	7
Scheme 8. Organocuprate Formation	9
Scheme 9. Hydrometallation Strategy to Generate Vinyl Metal Species	10
Scheme 10. Alkynyl Transfer in Enone-Alkyne Alkylative Couplings	10
Scheme 11. Proposed Mechanism for Alkylative Coupling of Enones, Alkynes and Organostannanes	11
Scheme 12. Nickel-Catalyzed Tandem Coupling of Enones, Alkynes, Me ₂ Zn and TMSCl	11
Scheme 13. Alkylative and Reductive Coupling of Alkynyl Enones	12
Scheme 14. Metallacycle Isolation Attempt	13
Scheme 15. Diverse Reactivity of Nickellacycle	14
Scheme 16. Intermolecular Enone-Alkyne Reductive Couplings	15
Scheme 17. Formal [3+2] Reductive Cycloaddition Pathway	16

Scheme 18. Et ₃ SiH-Mediated Enal-Alkyne Reductive Couplings	17
Scheme 19. Proposed Et ₃ SiH-Mediated Enal-Alkyne Reductive Coupling Mechanism	17
Scheme 20. Cobalt-Catalyzed Zinc-Mediated Reductive Couplings	19
Scheme 21. Aldehyde Prenylation Process.....	21
Scheme 22. Reductive Cross Coupling Reactions.....	22
Scheme 23. Regioselectivity Problems in Alkyne and Allene Addition Reactions.....	23
Scheme 24. Alkyne Substrates with Exceptional Regio- Control	24
Scheme 25. Ligand Control of Regiochemistry in Reductive Coupling Reactions.....	25
Scheme 26. Ligand-Controlled Regioselectivity Reversal	26
Scheme 27. Regiochemical Influence from Reducing Agent.....	27
Scheme 28. Process Control of Regiochemistry in Formaldehyde-Aromatic Alkyne Couplings	28
Scheme 29. Key Regiodetermining Steps in Both Processes	28
Scheme 30. Nickel-Catalyzed Et ₃ B-Mediated Reductive Coupling of Enones and Alkynes	31
Scheme 31. Proposed Mechanism of the Et ₃ B-Mediated Enone Alkyne Couplings.....	31
Scheme 32. Hypothesis of Alcohols as Reducing Agent.....	32
Scheme 33. Alcohol-Mediated Reductive Coupling of Enones and Alkynes	33
Scheme 34. Deuterium-Labeling Studies	37
Scheme 35. Proposed Mechanism for the Alcohol-Mediated Enone-Alkyne Couplings...	38
Scheme 36. Proposed Strategy for Alcohol-Mediated Aldehyde/Alkyne Couplings.....	40
Scheme 37. Parallel Mechanistic Comparison of Alcohol-Mediated Enone-Alkyne with Aldehyde-Alkyne Couplings	40

Scheme 38. Deuterium Labeling Studies.....	44
Scheme 39. Reductive Coupling of <i>p</i> -Tolualdehyde and Alkyne.....	45
Scheme 40. Proposed Mechanism for Benzylalcohol as Reducing Agent	46
Scheme 41. Mechanistic Rationale for Ligand Control in Enal-Alkyne Couplings.....	51
Scheme 42. Discovery of an Internal Redox Process of Enals, Alkynes and Methanol..	54
Scheme 43. Observation of Ester Product in the Absence of Et ₃ B.....	55
Scheme 44. Proposed Mechanism of Enal, Alkyne, Methanol Couplings	57
Scheme 45. 1,3 Diketone Product Formation	58
Scheme 46. Regioselective Enone-Alkyne and Enone-Alkene Couplings.....	59
Scheme 47. Et ₃ B-Mediated Enone-Allene Reductive Coupling Reaction	60
Scheme 48. Possible Metallacycles in Enone-Allene Couplings.....	63
Scheme 49. Mechanistic Analysis of Et ₃ B-Mediated Enone-Allene Couplings	64
Scheme 50. Allene Scope of Et ₃ B-Mediated Enone Allene Couplings.....	65
Scheme 51. Allene Scope of Et ₃ B-Mediated Enone Allene Couplings.....	66
Scheme 52. Hypothesis of Interception of Nickellacycles	67
Scheme 53. Proposed Mechanism for Enone-Allene Reductive Couplings.....	72
Scheme 54. Proposed Regioselective Addition of A-B Functional Groups	73
Scheme 55. Ligand-Control Regioselective Allene Hydrosilylation.....	74
Scheme 56. Large Ligand Influence on Regioselectivity	75

List of Tables

Table 1. Scope of Methanol-Mediated Reductive Couplings	35
Table 2. Optimization of Alcohol-Mediated Aldehyde-Alkyne Reductive Couplings ...	43
Table 3. Ligand Effects in Reductive Couplings in Enal-Alkyne Couplings	49
Table 4. P(o-tol) ₃ -Promoted Alkylative Couplings of Enals and Alkynes	52
Table 5. P(2,4,6-trimethoxyphenyl) ₃ -Promoted Reductive Cycloadditions	53
Table 6. Three Component Enal, Alkyne and Alcohol Couplings	56
Table 7. Ligand Effects on Et ₃ B-Mediated Enone Allene Coupling Reaction	61
Table 8. Solvent and Temperature Effects on the Enone Allene Coupling Reaction	62
Table 9. Optimization of the Et ₃ SiH-Mediate Enone Allene Couplings	68
Table 10. Et ₃ SiH-Mediated Enone-Allene Couplings Substrate Scope	70

List of Abbreviations

<i>n</i> -Bu	butyl
<i>t</i> -Bu	<i>tert</i> -butyl
COD	1,5-cyclooctadiene
°C	temperature in degrees centigrade
Et	ethyl
equiv	equivalent
h	hour
Hex	hexyl
IMes	1,3-bis-(1,3,5-trimethylphenyl)imidazole-2-ylidene
IPr	1,3-bis-(2,6-diisopropylphenyl)imidazole-2-ylidene
Me	methyl
Min	minute(s)
NHC	N-heterocyclic carbene
Pent	pentyl
Ph	phenyl

<i>i</i> -Pr	isopropyl
rt	room temperature
TBAF	tetrabutylammonium fluoride
THF	tetrahydrofuran
TLC	thin layer chromatography

ABSTRACT

Improving Practicality and Scope of Nickel-Catalyzed Coupling Reactions

by

Wei Li

Chair: John Montgomery

Efficient organic synthesis in medicinal chemistry and in complex molecule preparation often requires expedient and inexpensive processes. Nickel-catalyzed reductive coupling reactions from our group fulfill these requirements by a swift union of two simple unsaturated π -fragments via C-C bond formations. The focus of this thesis is to qualitatively elucidating the role and influence of reducing agents in these nickel-catalyzed reductive coupling reactions and to apply the mechanistic insights learned to related reaction classes.

Common reducing agents in nickel-catalyzed reductive coupling reactions are metallic, flammable, expensive or highly mass intensive. Low molecular weight alcohols are mild and inexpensive reagents. The introduction of alcohols as reducing agents in reductive coupling reactions has been achieved in our work. Through ligand effects

studies, incorporation of the alcohol reducing reagent as part of the final product has been accomplished in an internal redox reaction. This internal redox reaction make the nickel-catalyzed coupling processes even more practical and atom economical. Two regioselectivity control strategies have been applied to the addition of functional groups to allenes. The application of these strategies resulted in highly regioselective allene addition processes that broaden the scope of products that can be obtained using existing methods. Through these studies, mechanistic insights in nickel-catalyzed coupling reactions have been gained and applied to other reaction classes.

Chapter 1: Introduction

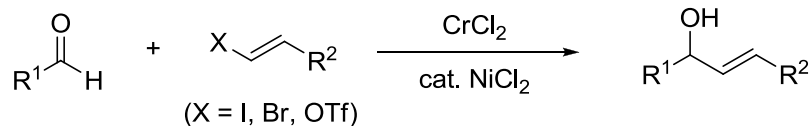
1.1 Significance of Catalytic Reductive Coupling Processes

In the context of organic synthesis, catalytic reductive coupling processes are powerful alternatives to traditional synthetic methods involving nucleophilic additions of functionalized vinyl metal reagents to electrophiles.¹ Although significant advances have been made in alkyne functionalization through carbometallation and hydrometallation, generation of stoichiometric metal reagents cannot be avoided by these routes. Catalytic reductive coupling processes have a major advantage over traditional processes by avoiding stoichiometric assembly of the vinyl organometallic reagents. This advantage can be translated in the shortening of synthetic sequences, in addition to being atom economical and environmentally friendly.

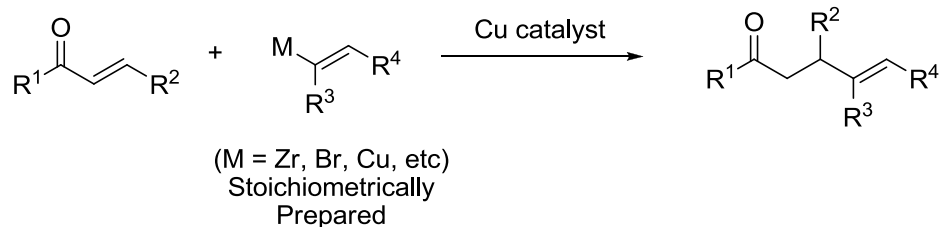
Processes involving addition of vinyl metal reagents to aldehydes or α,β -unsaturated carbonyls are particularly noteworthy because of the useful structures generated. While benchmark procedures for both processes have been developed in the forms of Nozaki-Hiyama-Kishi (NHK) couplings² and conjugate addition reactions,³ reductive coupling counterparts have also been developed into practical and versatile synthetic methods (Scheme 1).⁴

Scheme 1. Addition of Alkenyl Nucleophiles to Electrophiles

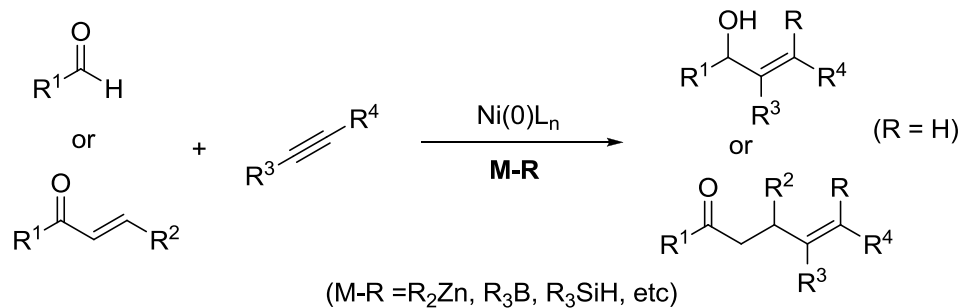
Nozaki Hiyama Kishi Coupling



Conjugate Addition



Catalytic Reductive Couplings



In the benchmark NHK coupling, nickel-catalyzed addition of vinyl halides to aldehydes can generate versatile allylic alcohol substructures.⁵ However, the synthesis of the stereochemically defined vinyl halides can be a complex process in itself. In addition, toxic stoichiometric chromium reagents are typically used in the reaction. On the other hand, catalytic reductive coupling approaches involve the direct union of aldehydes and alkynes *via* a C-C bond formation, thus avoiding pre-installation of any functional groups.⁽⁴⁾ In a similar fashion, installation of alkene functionality to α,β -unsaturated carbonyls through conjugate addition requires stoichiometric generation of vinyl organometallic species.⁶ Catalytic reductive coupling approaches can instead directly

couple α,β -unsaturated carbonyls with alkynes to generate analogous γ,δ -unsaturated carbonyl products without prior vinyl organometallic reagent synthesis.⁷

Nickel-catalyzed reductive coupling processes in general involve the direct union of two π -components *via* a C-C bond formation. For such processes to be catalytic in terms of the nickel reagent, a terminal reducing agent (M-R) is required.⁸ The identity of the reducing agent can significantly impact the practicality and efficiency of these coupling processes. This thesis introduces mild and practical reducing agents in nickel-catalyzed coupling reactions, and also studies the role and influence of reducing agents and ligands in these reactions.

An extensive body of work has been carried out on nickel-catalyzed reductive coupling processes from our lab and several other research groups. This body of work builds on the key advances and concepts detailed below.

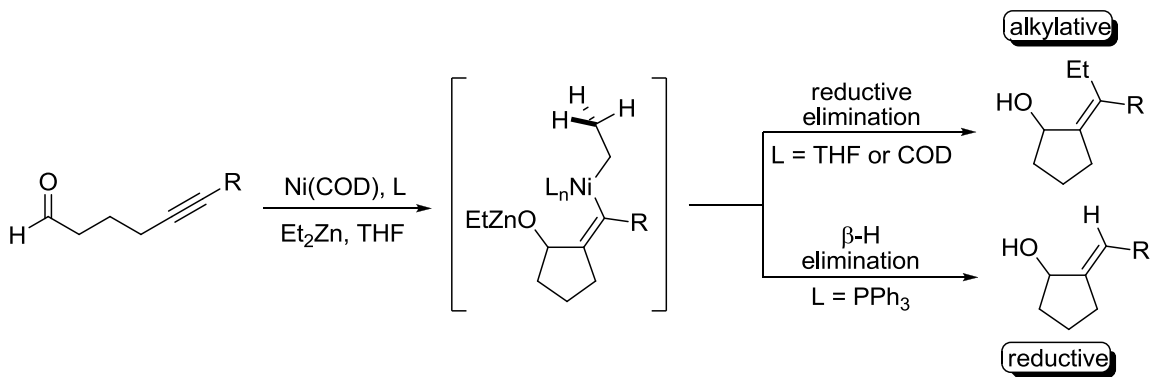
1.2 Nickel-Catalyzed Aldehyde-Alkyne Couplings

Allylic alcohols are a common structural motif in bioactive natural products and versatile precursors for a variety of synthetic transformations.^{9,10} While NHK couplings or addition of alkenyl metallated species to aldehydes have been widely used for the synthesis of these substructures, our group along with several other groups have recently developed nickel-catalyzed couplings of aldehydes and alkynes to afford allylic alcohols and their analogues in the presence of a variety of reducing agents.

The Montgomery group first identified Ni(COD)₂ as a competent catalyst for the alkylative coupling (transferring a carbon substituent) of aldehydes and alkynes in an intramolecular ynal cyclization.¹¹ These initial transformations generated tetrasubstituted

allylic alcohol products using organozinc reducing agents. Introduction of PBU_3 as a ligand in combination with using an organozinc reagent bearing β -hydrogens interestingly led to the formation of reductive coupling (transferring a hydrogen substituent) products in this nickel-catalyzed ynal cyclization (Scheme 2).

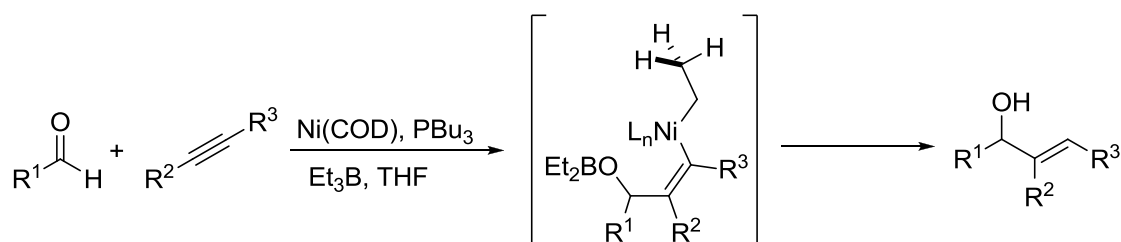
Scheme 2. Divergent Pathways of Nickel-Catalyzed Alkynal Couplings



Strong σ -donation from the phosphine ligand to the nickel catalyst could suppress the reductive elimination process by increasing electron density around the metal center. In the absence of a strong σ -donating ligand, π -acidic ligands such as the substrates can coordinate to the active catalyst to remove electron density from the metal center, and facilitate the reductive elimination process to generate the alkylation product.

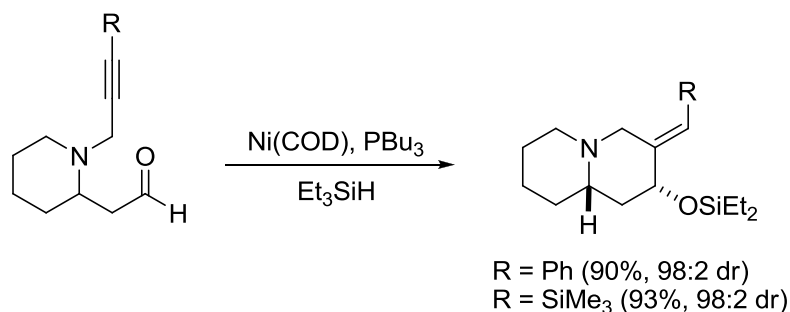
Analogous intermolecular aldehyde-alkyne reductive couplings have been reported by Jamison and coworkers utilizing Et_3B as a reducing agent.¹² This approach affords the allylic alcohol products directly and tolerates a variety of aldehydes and alkynes. The reaction presumably proceeds through similar intermediates proposed for the Et_2Zn -mediated reductive coupling pathway (Scheme 3).

Scheme 3. Et₃B as Reducing Agent in Intermolecular Aldehyde-Alkyne Couplings



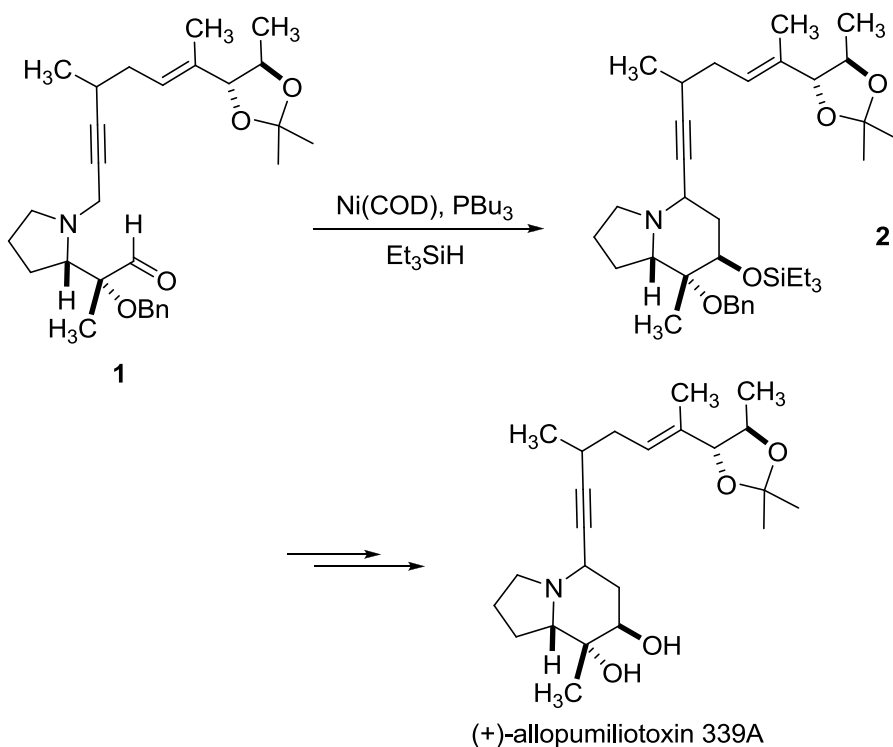
The reductive coupling variant of alkynes was further developed by the Montgomery group with the utilization of R₃SiH as reducing agent.¹³ The distinct advantage of this new methodology can be summarized as: 1) the removal of complications from alkylative transfer versus hydrogen transfer in the R₂Zn and R₃B cases; 2) the utilization of trialkylsilanes as more stable, less nucleophilic alternatives to pyrophoric R₂Zn and R₃B reagents; 3) the formation of a stereochemically defined silyl-protected allylic alcohol (Scheme 4).

Scheme 4. Et₃SiH as Reducing Agent in Alkynyl Reductive Couplings



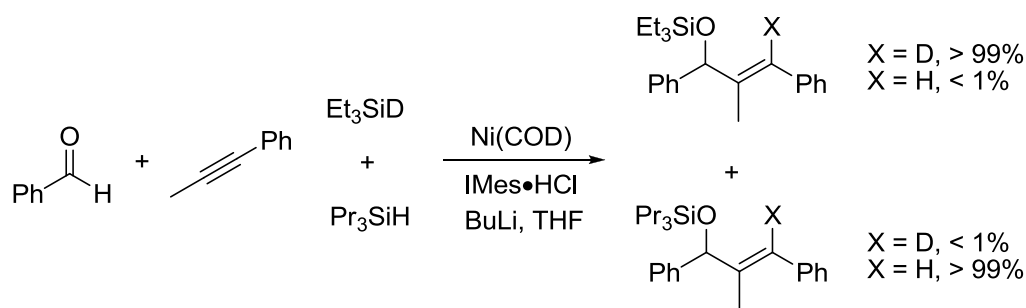
The synthetic utility of the Et₃SiH-mediated method was demonstrated in the total synthesis of allopumiliotoxin 339A.¹⁴ In the key step of the synthesis, the nickel-catalyzed reductive coupling of **1** using Et₃SiH as a reducing agent afforded the core structure **2** as a single diastereomer (Scheme 5).

Scheme 5. Total Synthesis of Pumiliotoxin 339A



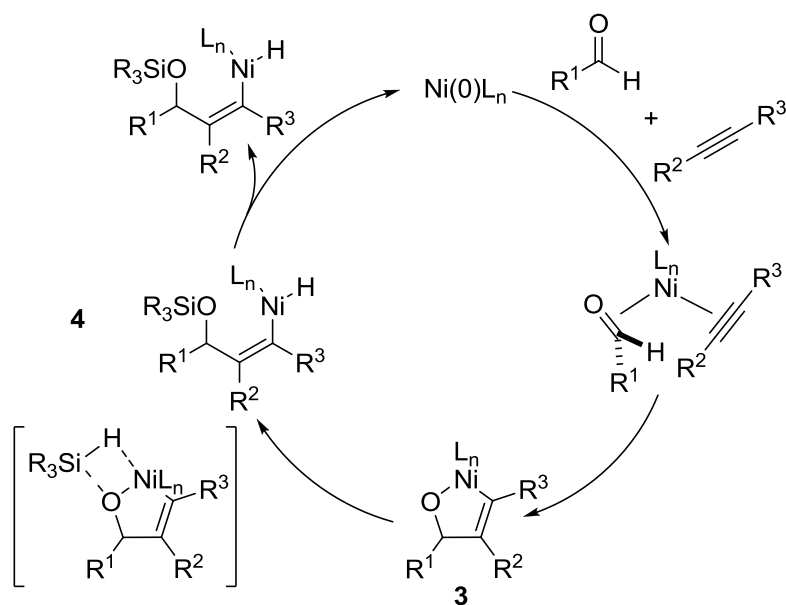
Although the $\text{Et}_3\text{SiH}/\text{PBU}_3$ protocol was not efficient for intermolecular aldehyde-alkyne reductive coupling reactions, the Montgomery group has developed an important NHC/ Et_3SiH combination for intermolecular variants.¹⁵ To elucidate the role of Et_3SiH in this intermolecular reductive coupling reaction, a crossover study utilizing Et_3SiD and Pr_3SiH were carried out. The two observed products suggested that there is essentially no crossover in the products with respect to the silanes and H/D. The generation of a Ni-H active catalyst would result in crossover of the silanes and the respective D/H in the product. Since no such crossover was observed in the product, this experiment suggested that reductive nickel hydrides were most likely not generated during the reaction (Scheme 6).

Scheme 6. Intermolecular Crossover Experiment Utilizing R₃SiH



Additional mechanistic studies suggested that aldehydes and alkynes can complex to the nickel catalyst first, followed by a rate determining oxidative cyclization step to generate metallacycle **3**.¹⁶ A rapid σ -bond metathesis of the Ni-O and Si-H bonds resulted in the formation of **4** and accounted for the absence of crossover products mentioned previously. Reductive elimination of **4** could then lead to the product and regenerate the catalyst. A simplified version of the mechanism was proposed below (Scheme 7).

Scheme 7. Proposed Mechanism for Nickel-Catalyzed Couplings of Aldehydes, Alkynes, and R₃SiH



Although different procedures have been elucidated for various reducing agents, further improvements are still needed. For example, metallic (Et_2Zn), pyrophoric (Et_3B), or high mass intensive (R_3SiH) reducing agents are used in these reactions. These limitations present a number of questions: Can we gain more insights in how these reducing agents function in these reactions? Can milder and less expensive alcohols be utilized as reducing agent in these reductive coupling reactions? Can alcohols be used as coupling partners in these reactions since primary alcohols can serve as precursors for aldehydes? Can regioselective addition to the aldehydes be achieved across different classes of alkynes or other nonpolar π components such as allenes? Can air stable Ni(II) catalysts be used in these reactions? While some of these issues are addressed in the introduction and the following Chapters, the underlying potential for this reductive coupling method is still to be fully explored.

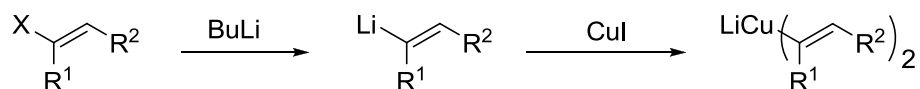
1.3 Nickel-Catalyzed Enone-Alkyne Couplings

1.3.1 Cuprate Reagents

Similar to the aldehyde-alkyne couplings being a useful synthetic method for the construction of allylic alcohols, nickel-catalyzed α,β -unsaturated carbonyl-alkyne couplings are efficient alternatives for the synthesis of γ,δ -unsaturated carbonyl compounds in comparison with traditional processes. Traditional processes often involved the conjugate additions of stoichiometric vinyl metal species to α,β -unsaturated carbonyls. One such variant is the conjugate addition of vinyl cuprates to α,β -unsaturated carbonyls. While useful, these cuprate reagents often require prior synthesis of vinyl

halides, followed by lithium halogen exchange, and then cuprate formation through transmetallation (Scheme 8).¹⁷

Scheme 8. Organocuprate Formation

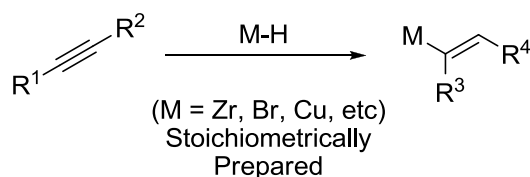


The application of vinyl cuprates is mitigated by several facts. First, vinyl cuprates must be generated from vinyl halides, which can be challenging to prepare. Second, prior to the lithium halogen exchange, any electrophilic functional groups need to be either protected or excluded, thus limiting tolerated functional groups. Third, a stoichiometric quantity of copper is often required, which is neither economical nor environmentally friendly. Alternative procedures have been developed to address some of the mentioned shortcomings of vinyl cuprates.

1.3.2 Hydrometallation in Conjugate Addition

One alternative procedure is the generation of vinyl metal reagents through alkyne hydrometalation strategies. A variety of vinyl metal reagents have been reported. Vinyl zirconocenes, derived from hydrometallation of alkynes using the Schwartz reagent are among the most prominent and useful examples.¹⁸ Many different transition metal reagents including copper,¹⁹ nickel,²⁰ and rhodium²¹ can then be used to catalyze the addition of the vinyl metal reagents to enones. Direct reduction of alkynes to vinyl metal reagents improved functional group tolerance compared to methods utilizing vinyl cuprates, however, the stoichiometric generation of vinyl metal reagents is still a major drawback for this method (Scheme 9).

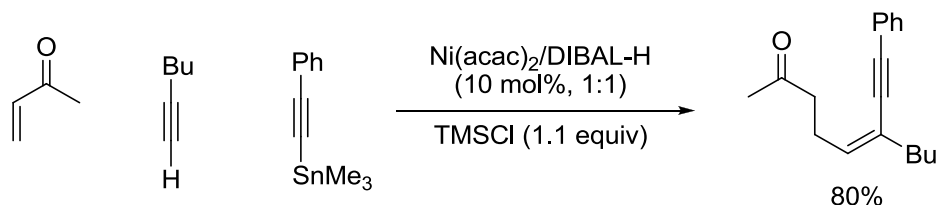
Scheme 9. Hydrometallation Strategy to Generate Vinyl Metal Species



1.3.3 Nickel-Catalyzed Reductive Couplings of Enones and Alkynes

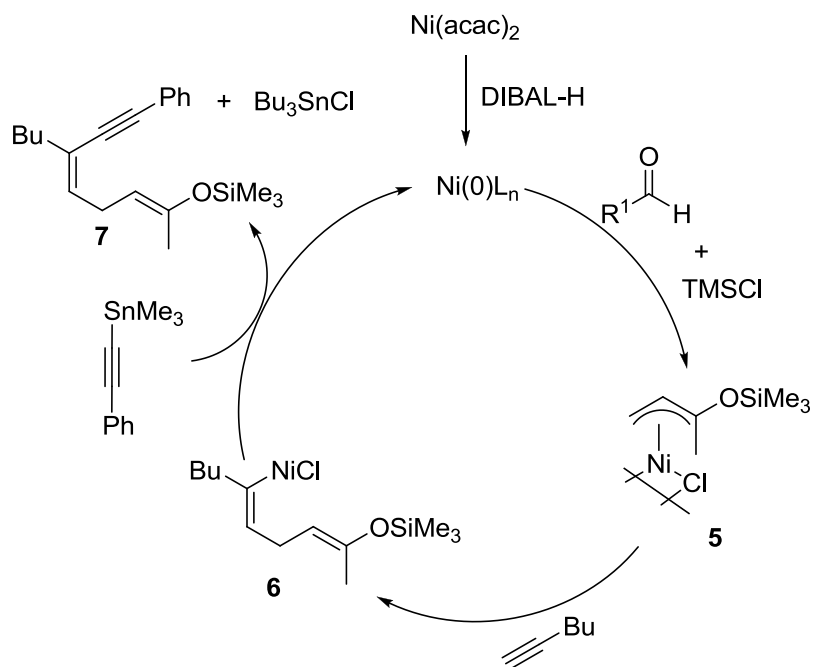
A more contemporary approach to the synthesis of γ,δ -unsaturated carbonyl compounds has been developed by the Montgomery group through the direct coupling of enones and alkynes. Early efforts toward the reductive coupling of enones and alkynes drew inspiration from seminal works by Ikeda and Sato, who demonstrated that nickel catalyzed the transfer of alkynyl groups from alkynylstannane reagents in an enone-alkyne alkylative coupling to produce conjugated enyne products (Scheme 10).²²

Scheme 10. Alkynyl Transfer in Enone-Alkyne Alkylative Couplings



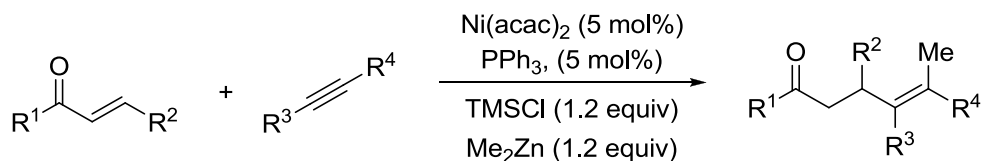
Ikeda and Sato proposed that the mechanism proceeded through the formation of a chlorine bridged nickel π -allyl dimer complex **5**. Migratory insertion of the terminal alkyne into intermediate **5** would result in the formation of species **6**. Transmetalation of **6** with organostannane reagents, followed by reductive elimination would generate **7**. Reaction workup would eventually desilylate the enol ether to afford the observed ketone product (Scheme 11).

Scheme 11. Proposed Mechanism for Alkylative Coupling of Enones, Alkynes and Organostannanes



Ikeda and Sato have also expanded the scope of transmetallation reagent from the toxic alkynyltin reagents to organozinc reagents. This reaction was proposed to go through similar intermediates as in the alkynyltin cases to eventually transfer a Me group to the alkenyl position in the product (Scheme 12).²³

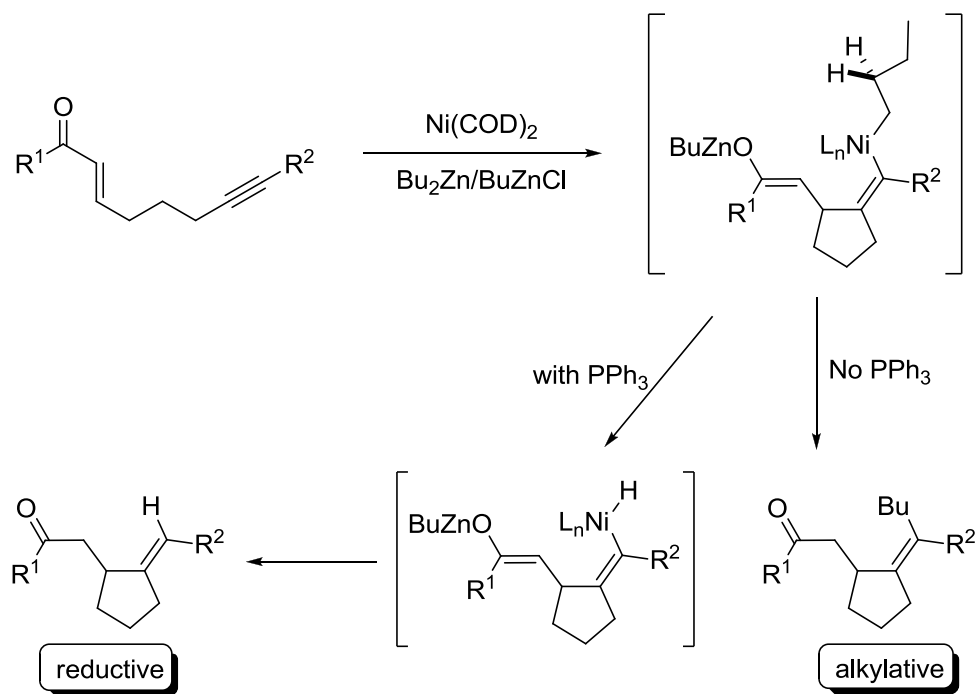
Scheme 12. Nickel-Catalyzed Tandem Coupling of Enones, Alkynes, Me_2Zn and TMSCl



Similar to the application of $\text{Ni}(\text{COD})_2$ as a competent catalyst in the aldehyde-alkyne coupling reactions, the Montgomery group sought to apply $\text{Ni}(\text{COD})_2$ in this enone, alkyne and organozinc coupling reaction, albeit in the absence of a TMSCl promoter.²⁴ Early studies from the group revealed that when Bu_2Zn was used with a σ -donating phosphine ligand, reductive transfer (hydrogen atom) was observed instead of

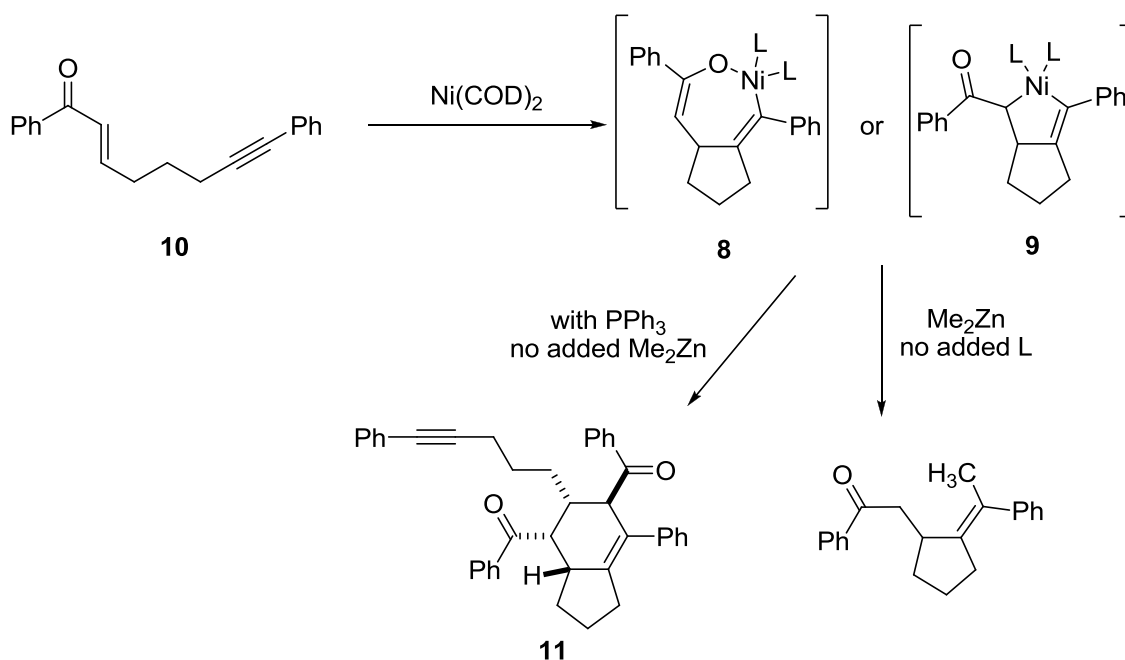
the alkylative transfer (carbon atom transfer) that was normally observed using Ikeda and Sato's method (Scheme 13). This has prompted the group to develop a series of intramolecular enone and alkyne couplings alongside the alkylative coupling processes.¹

Scheme 13. Alkylative and Reductive Coupling of Alkynyl Enones



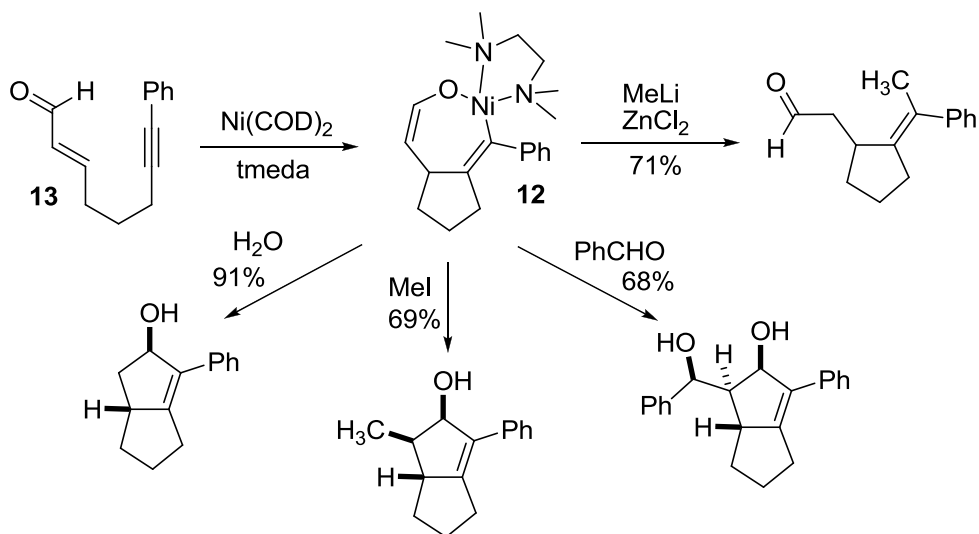
To shed light on whether a η^1 O-bound seven membered metallacycle **8** or a η^1 C-bound five membered metallacycle **9** was a more likely intermediate in this enone-alkyne reductive coupling reaction, the Montgomery group attempted to synthesize such metallacycles. Although attempts to synthesize such metallacycles from **10** with stoichiometric Ni(COD)₂ and various conditions did not lead to metallacycle isolation, product **11** was obtained from coupling with a second substrate (Scheme 14).²⁵

Scheme 14. Metallacycle Isolation Attempt



The formation of compound **11** suggested that a bidentate ligand could suppress the dimerization pathway and lead to the metallacycle formation. Metallacycle complex **12** could indeed be obtained using stoichiometric $\text{Ni}(\text{COD})_2$ and *tmeda* as the bidentate ligand from substrate **13**. NMR and crystallography studies strongly suggested the formation of a η^1 *O*-bound seven membered metallacycle **12**.²⁶ This metallacycle demonstrated interesting nucleophilic reactivity with a variety of electrophiles at the α -carbon of the enone.²⁷ In addition, the alkylative coupling product was also observed by reacting **12** with MeLi and ZnCl_2 (Scheme 15).

Scheme 15. Diverse Reactivity of Nickellacycle

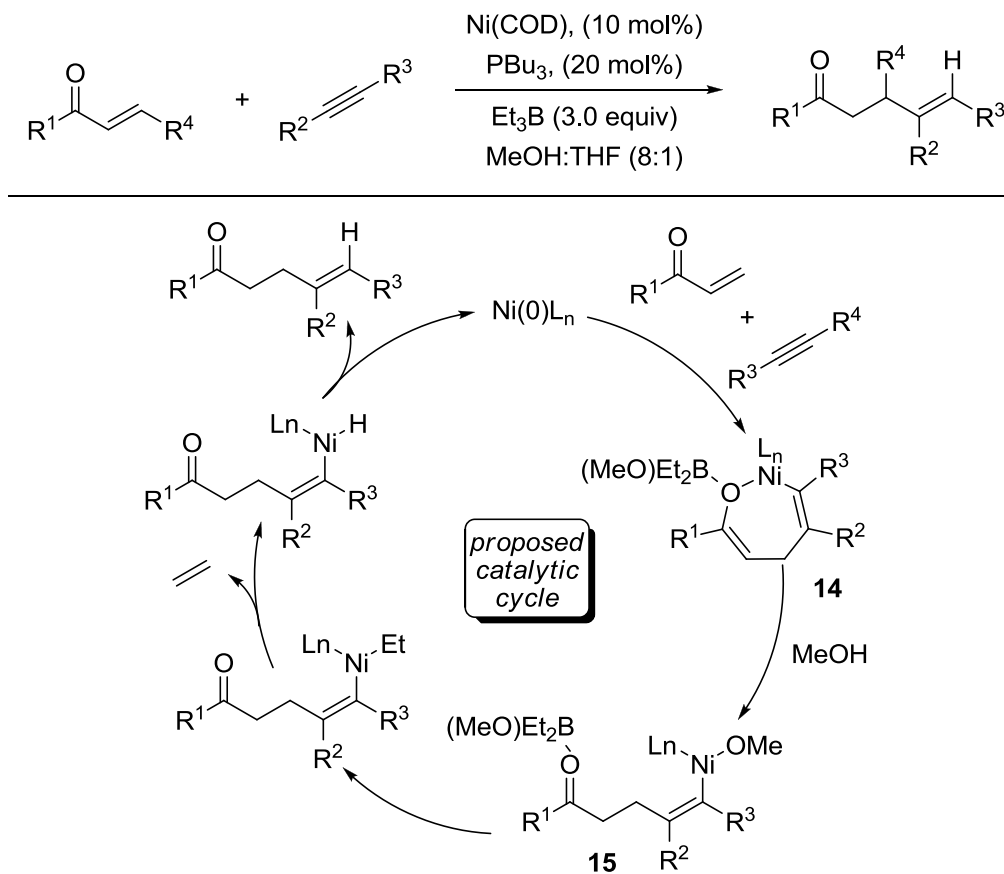


The isolation of metallacycle **12** was a major advancement in the nickel-catalyzed ynone cyclization reactions. Such metallacycle isolation not only shed light on potential intermediates in catalytic reactions, but also led to the development of new reaction pathways in catalytic variations. While these stoichiometric nickel-mediated ynone and ynol cyclizations generated interesting and useful structures, catalytic versions of these reactions were desirable for both intra- and intermolecular reactions.

Although Et_2Zn was an efficient reducing agent in the intramolecular reductive couplings of enones and alkynes, it was less effective in the intermolecular variants due to various competing side reactions. For example, addition of organozincs in conjugate additions to enones in the presence of a nickel catalyst was well preceded.²⁸ Two critical changes allowed efficient intermolecular reductive couplings.²⁹ The first change was the introduction of a methanol / THF mixed solvent system. The inclusion of methanol as a solvent was presumed to protonate the metallacycles generated from the oxidative cyclizations of nickel catalyst, enones and alkynes. Secondly, Et_3B was used as the reducing agent to alleviate nucleophilic side addition reactions as in the cases using

Et_2Zn . In addition, strong Lewis acidity from Et_3B could activate the enones toward metallacycle formation. With these changes, the new protocol allowed a variety of enones and alkynes to couple effectively. The proposed mechanism for the Et_3B -mediated reaction is shown below (Scheme 16).

Scheme 16. Intermolecular Enone-Alkyne Reductive Couplings

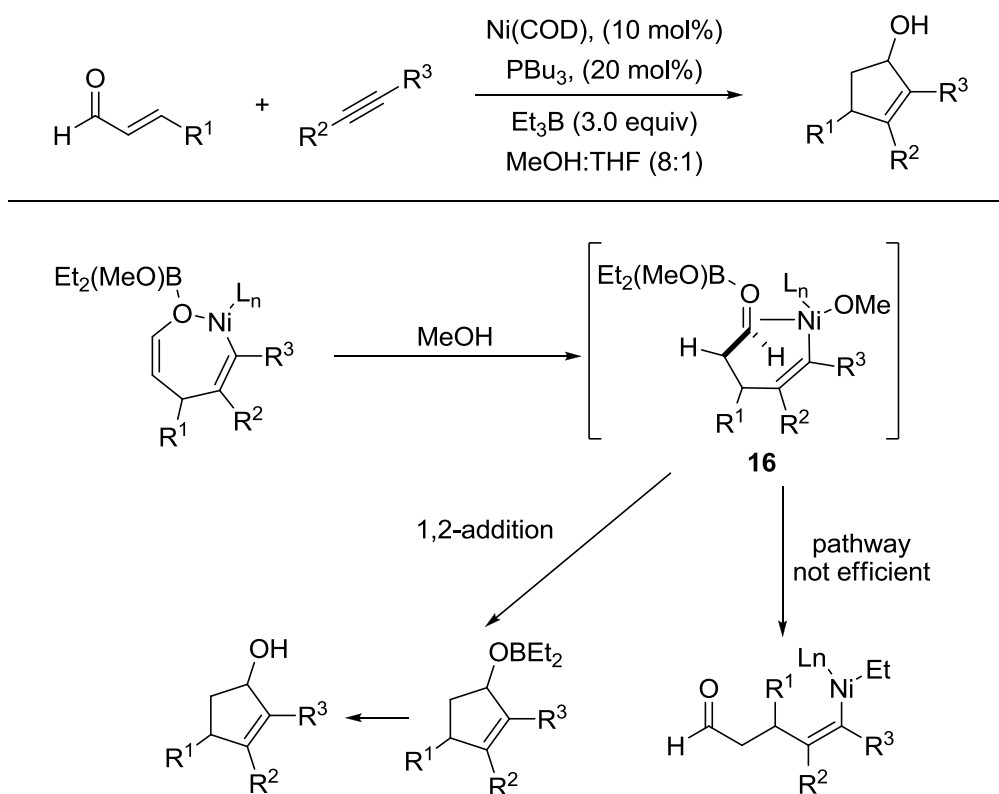


The enone and alkyne could undergo an oxidative cyclization with Ni(COD)_2 to generate 7-membered metallacycle **14**. Methanol protonation of the nickel enolate would generate species **15**. Subsequent reductions could then regenerate the catalyst and form the corresponding γ,δ -unsaturated ketone.

Products generated by the coupling of α,β -unsaturated carbonyls and alkynes in this reaction were highly dependent on the substrates used. In the case of enones as the

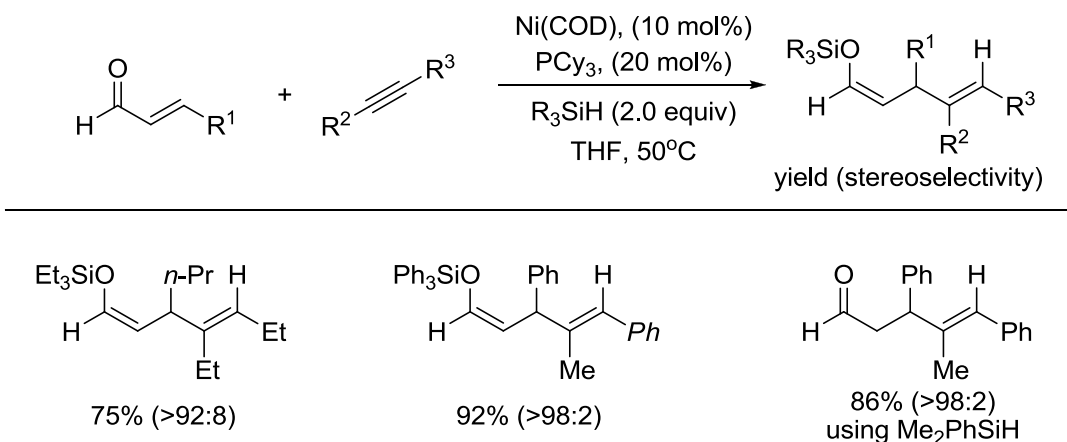
reagent, the reductive coupling product was observed. However, when an enal was introduced in the reaction, a cyclopentenol product was obtained instead.³⁰ The lower electrophilicity of the ketone versus aldehyde could likely lead to the product divergence. The reductive cycloaddition reaction was proposed to go through intermediate **16**. Instead of a transmetalation process, 1,2-addition of a vinyl nickel fragment into the aldehyde could occur to eventually generate cyclopentenol product (Scheme 17).

Scheme 17. Formal [3+2] Reductive Cycloaddition Pathway



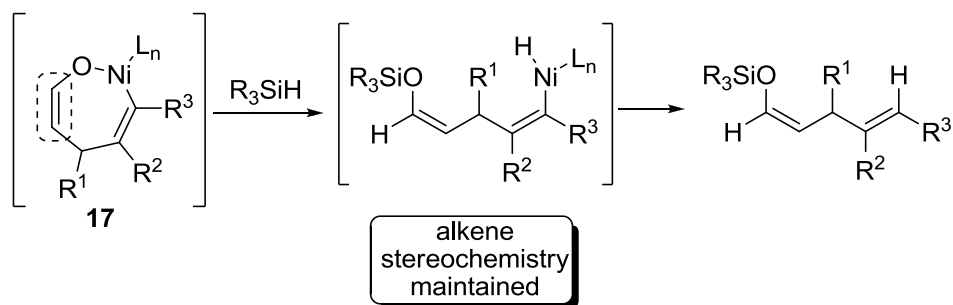
While the reductive cycloaddition of enals and alkynes could be achieved using Et_3B as a reducing agent, the reductive coupling of enals and alkynes could not be accomplished as the major reaction pathway. An alternative procedure introduced mild and non-pyrophoric R_3SiH as reducing agent in a nickel-catalyzed reductive coupling of enals and alkynes in an aprotic solvent, THF (Scheme 18).³¹

Scheme 18. Et₃SiH-Mediated Enal-Alkyne Reductive Couplings



Using this procedure, *Z*-enol silanes could be obtained in high stereoselectivity and regioselectivity. The high stereoselectivity of the *Z*-enol silane formation could be readily rationalized based on the proposed mechanism. Metallacycle **17** could be produced by oxidative cyclization of enals and alkynes in the absence of a Lewis acidic promoter. A direct interception of metallacycle **17** could then occur by a σ -bond metathesis process between the Ni-O and Si-H bonds. Such σ -bond metathesis steps were well preceded in Et₃SiH-mediated aldehyde and alkyne reductive couplings as mentioned in section 1.2 (Scheme 19).

Scheme 19. Proposed Et₃SiH-Mediated Enal-Alkyne Reductive Coupling Mechanism

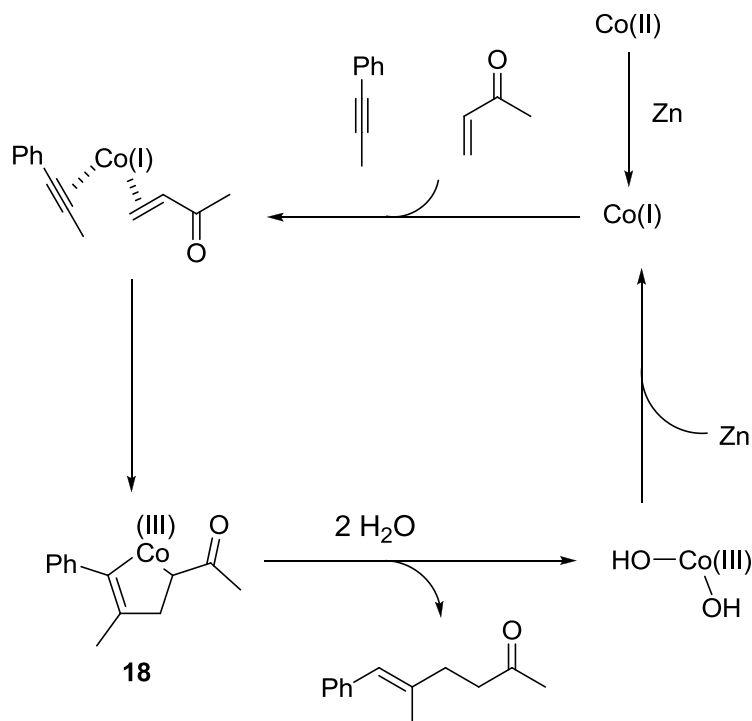
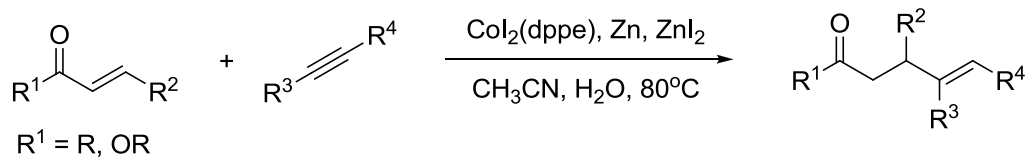


The consistently observed *Z*-enol silane stereochemistry suggested that the necessary *Z*-enolate stereochemistry formed in metallacycle **17** was maintained through subsequent mechanistic steps. In addition, the exclusion of a protic solvent from the

reaction conditions ensured that the opening of the metallacycle **17** would not proceed through a protonation process. This observation also provided evidence for the formation of a η^1 -*O*-bonded nickelacycle in a catalytic reaction.

Concurrently, zinc powder has also been used as a reducing agent by Cheng et al. in a cobalt-catalyzed reductive coupling process of enoates and enones with alkynes. (Scheme 20).³² This cobalt-catalyzed variant took advantage of the reduction potential of a metallic zinc reagent to reduce the Co(II) catalyst to the active Co(I) catalyst. The active catalyst could then undergo oxidative cyclization with the enone and alkyne substrates to generate metallacycle **18**. Double protonation of metallacycle **18**, would then afford the reductive coupling product and a Co(III) species, which could be reduced by Zn metal to regenerate the active catalyst. The ZnI₂ additive was suggested to help activate the catalyst and to act as a Lewis acid towards enone activation. Although this zinc-mediated protocol was a useful procedure across a variety of α,β -unsaturated carbonyls, use of multiple equivalents of zinc metal and the requirement of elevated temperature could be undesirable.

Scheme 20. Cobalt-Catalyzed Zinc-Mediated Reductive Couplings



This cobalt-catalyzed variant took advantage of the reduction potential of a metallic zinc reagent to reduce the Co(II) catalyst to the active Co(I) catalyst. The active catalyst could then undergo oxidatively cyclization with the enone and alkyne substrates to generate metallacycle **18**. Double protonation of metallacycle **18**, would then afford the reductive coupling product and a Co(III) species, which could be reduced by Zn metal to regenerate the active catalyst. The ZnI₂ additive was suggested to help activate the catalyst and to act as a Lewis acid towards enone activation. Although this zinc-mediated protocol was a useful procedure across a variety of α,β -unsaturated carbonyls, use of

multiple equivalents of zinc metal and the requirement of elevated temperature could be undesirable.

While near parallel success has been achieved in nickel-catalyzed enone-alkyne reductive coupling reactions and aldehyde-alkyne reductive coupling reactions, similar improvement questions for the enone-alkyne reductive coupling can also be asked. For example, metallic (Et_2Zn or Zn), pyrophoric (Et_3B), or high mass intensive (R_3SiH) reducing agents are used in these reactions. Can milder and less expensive alcohols be utilized as reducing agent? Can regioselective addition to enones be achieved across different classes of alkynes or allenes? While most of the questions will be addressed in the following chapters, the underlying potential for this reductive coupling reaction is still to be fully explored.

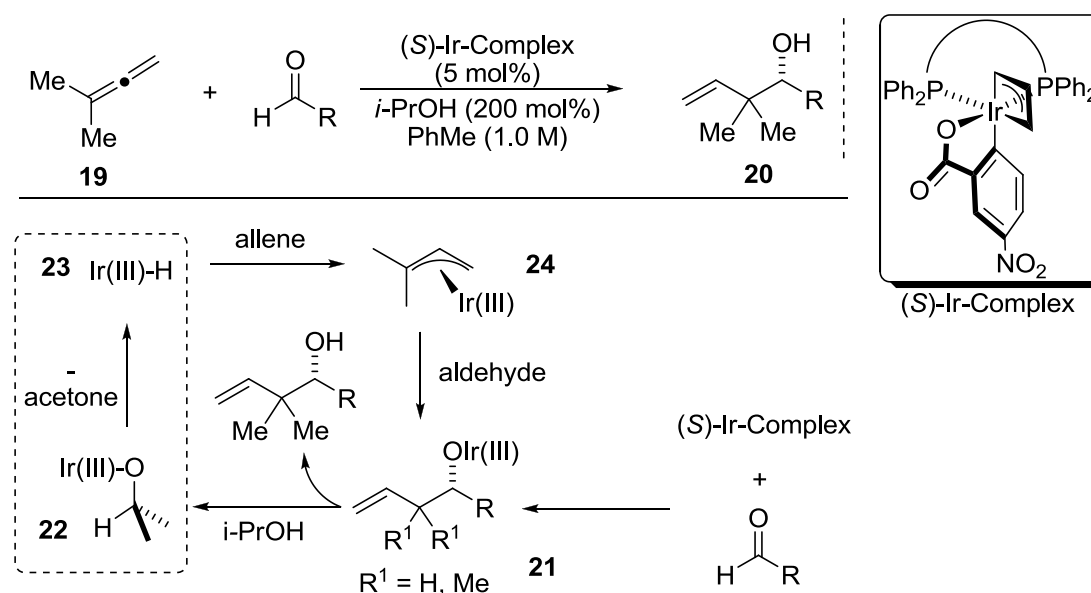
1.4 Alcohols as Reducing Agents in Transition-Metal Catalyzed Reactions

Alcohols are commonly oxidized to carbonyls, and an enormous body of literature is devoted to this transformation. The oxidation of an alcohol to a ketone formally generates an equivalent of hydride, and as such alcohols can be used as reducing agents. Compared to the previously mentioned reducing agents such as R_2Zn , Et_3B and R_3SiH , simple alcohols are a mild, inexpensive and practical alternative. The development of alcohols as reducing agents would indeed further advance the nickel-catalyzed reductive coupling processes mentioned in the previous sections.

The Krische group and Sigman group recently reported C-C bond forming reactions in different reductive coupling processes utilizing alcohols as the reducing

agent. The Krische group reported a reductive coupling of aldehydes and allene **19** using a chiral iridium catalyst with 2-propanol as the terminal reductant, which generated product **20** in high yield and ee. The proposed reaction mechanism is described in Scheme 21. Addition of the chiral iridium complex to the aldehyde resulted in species **21**, which could then be protonated to generate **22**. Intermediate **22** can then undergo β -hydrogen elimination to generate an Ir(III)-H intermediate **23**. Insertion of **23** into the allene **19** can then generate the π -allyl intermediate **24**, which can then add to the aldehyde to reinitiate the catalytic cycle (Scheme 21).^{33, 34, 35}

Scheme 21. Aldehyde Prenylation Process



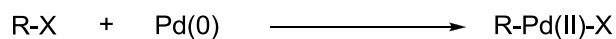
The authors were also able to utilize carbonyls generated *in situ* from alcohols in these coupling reactions. Thus, alcohols may serve as both a hydrogen donor and as a carbonyl precursor. In the highlighted mechanistic step, Ir(III)-H was formed with a concomitant oxidation of 2-propanol to acetone. When a primary alcohol RCH_2OH was used as the hydride source, the resulting aldehyde in the same process could then be consumed *via* reductive coupling with an unsaturated π -component. These advances not

only highlighted the utility of alcohols as reducing agent, but also introduced primary alcohols as synthetic precursors to aldehydes.

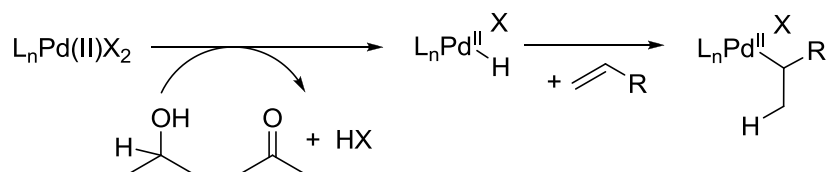
Sigman also reported reductive cross-coupling reactions that use alcohols as reducing agent. In a traditional cross coupling reaction, oxidative addition of Pd(0) to a C-heteroatom bond (R-X) can generate a R-Pd(II)-X species. Although cross couplings are powerful and ubiquitous reactions, the methodology is limited by the scope of C-heteroatom bonds that can successfully generate the R-Pd(II)-X species (Scheme 22).³⁶

Scheme 22. Reductive Cross Coupling Reactions

Oxidative Addition Process from Traditional Cross Coupling



Reductive Cross Coupling Initiation Step



In the reductive cross coupling process, Sigman reported the use of alcohol as a reducing agent to generate a X-Pd(II)-H species from a Pd(II)X₂ precatalyst, which can then insert into an alkene to generate the R-Pd(II)-X species similar to that generated in a traditional cross coupling reaction. The R-Pd(II)-X species can then go on to cross couple with a variety of transmetallating reagents. This reduction-insertion sequence significantly increases the scope of coupling partners by including unsaturated π -components (Scheme 22).

Considering the tremendous success of utilizing alcohols as reducing agent achieved in these two separate reaction classes, we hypothesized that alcohols could also

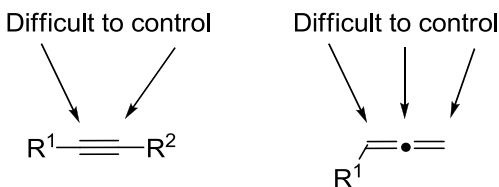
be utilized in nickel-catalyzed reductive coupling reactions of enones or aldehydes with alkynes. Studies pertaining to this hypothesis will be covered in Chapter 2.

1.5 Regioselective Coupling Processes

1.5.1 Challenges and Solutions in Regiocontrol of Alkyne and Allene Additions Reactions

The development of reductive coupling processes has met with great success in many areas. One area that has caught significant attention recently is the control of regiochemistry in these reactions (Scheme 23). Often, poor regiocontrol of additions of alkynes and allenes diminishes the applicability of these types of transformations. To overcome difficulties in this area, different regiochemical control strategies have been realized to influence the final regiochemical outcome of these reactions. Four particular categories include: 1) substrate-control; 2) ligand-control; 3) reducing agent influence; 4) process control. Process control is defined here as two or more distinct processes that can provide products with a complementary regiochemical outcome. These strategies have all been shown to have significant impact on regiochemistry in these alkyne and allene addition reactions.

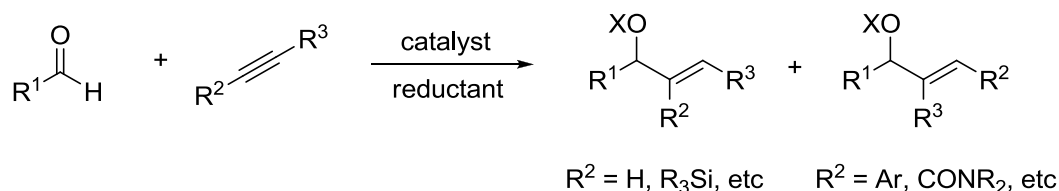
Scheme 23. Regioselectivity Problems in Alkyne and Allene Addition Reactions



1.5.2 Substrate-Control in Reductive Coupling Reactions with Alkynes

Although the regiocontrol of additions to alkynes can be difficult, alkynes with substituents that possess strong electronic or steric bias can result in excellent regiochemical outcome for reductive coupling reactions. For example, substrate classes such as aromatic alkynes,¹ terminal alkynes,¹ silyl alkynes,¹ ynamides,³⁷ conjugated diynes,³⁸ enynes,³⁹ in addition to alkynes with remote directing alkenes⁴⁰ and alcohols⁴¹ have all demonstrated exceptional regioselectivity in metal-catalyzed reductive coupling reactions (Scheme 24).

Scheme 24. Alkyne Substrates with Exceptional Regio- Control



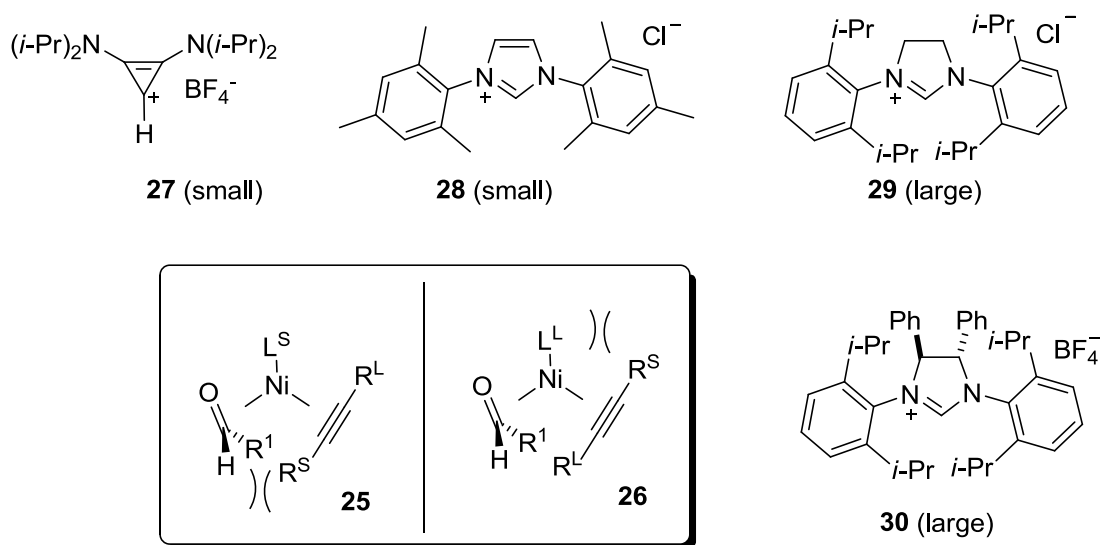
While reductive coupling products derived from these biased substrates can be very useful, specific products will require specific substrates to be used. Also, in cases when a product with the unfavored regiochemistry is needed for the biased substrates, alternative synthetic routes are generally required. Most importantly, when alkyne substrates lack such strong electronic or steric bias, they often participate in the reductive coupling reactions with poor regioselectivity.

1.5.3 Ligand-Control of Regiochemistry of Alkynes

To overcome the difficulties in regiocontrol for unbiased alkynes and in reversal of regiocontrol for biased alkynes, the Montgomery group has recently developed a ligand-control strategy to influence the regiochemical outcome of the aldehyde-alkyne

reductive coupling reactions.⁴² The key underlying feature for this strategy is to take advantage of the minimization of steric interactions between the ligands and the substrates prior to an oxidative cyclization step that sets the regioselectivity. Because the ligand size effect was thought to be substantial, using ligand that are characterized as either small ligands or large ligands can potentially override substrate-derived regiochemical influences (Scheme 25).

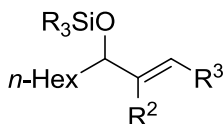
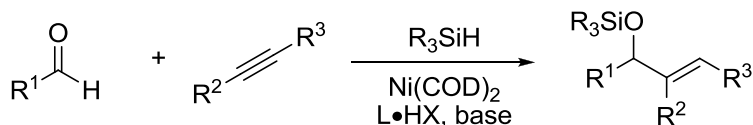
Scheme 25. Ligand Control of Regiochemistry in Reductive Coupling Reactions



Using this simple model, the ligand control of regiochemistry can be readily rationalized. In π -complex **26** with a large ligand present on the metal center, steric interaction between ligand and substrate substituents could force the large group to be positioned distal to the ligand, thus resulting in a C-C bond formation between the carbonyl carbon and the alkynyl carbon substituted by the large substituent. In π -complex **25** with a small ligand on the metal catalyst, the steric interaction between the carbonyl substituent and the alkyne substituent now becomes the dominant deciding factor. This steric interaction would then force the large substituent proximal to the ligand, resulting in a C-C bond formation between the carbonyl carbon and the alkynyl

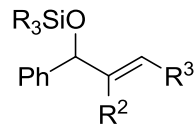
carbon close to the small substituent. Using this concept, reductive coupling of aldehydes with unbiased aliphatic alkynes, or with biased alkynes such as aromatic alkynes and terminal alkynes could result in either allylic alcohol product showing high regioselectivity (Scheme 26)

Scheme 26. Ligand-Controlled Regioselectivity Reversal



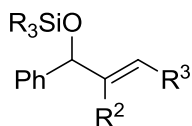
29 (large), R² = *n*-Pr, R³ = Me, 85% (93:7)

27 (small), R² = *n*-Pr, R³ = Me, 78% (12:88)



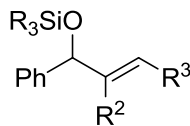
29 (large), R² = *n*-Pr, R³ = Me, 86% (>98:2)

27 (small), R² = *n*-Pr, R³ = Me, 72% (16:84)



29 (large), R² = Me, R³ = Ph, 99% (81:19)

28 (small), R² = Me, R³ = Ph, 84% (<2:98)



30 (large), R² = *n*-Hex, R³ = H, 71% (88:12)

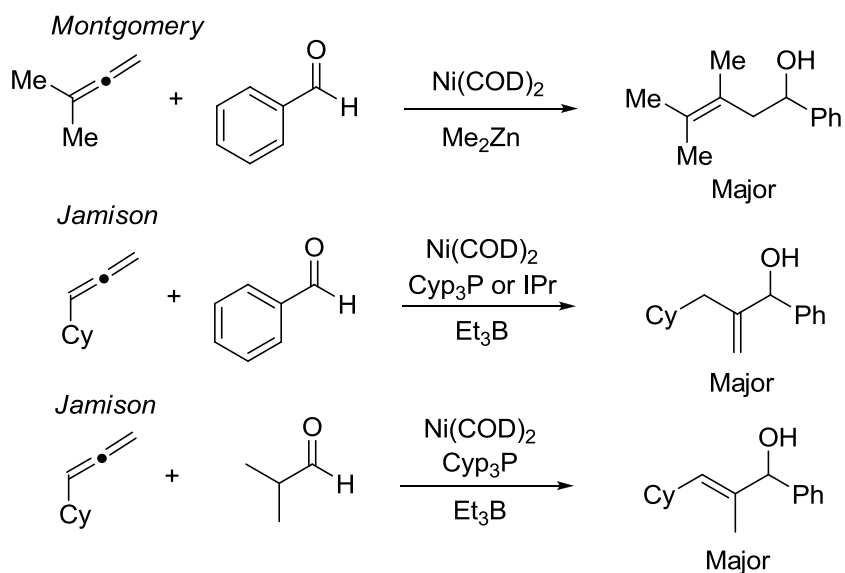
28 (small), R² = *n*-Hex, R³ = H, 82% (3:97)

1.5.4 Reducing Agent Influence on Regiochemistry of Allene Additions

In the aldehyde-allene reductive coupling reaction, the Montgomery and Jamison groups have observed a strong regioselectivity dependence based on the nature and Lewis acidity of the reducing agent used. In allene-aldehyde reductive couplings using R₃SiH, addition of the aldehyde to the allene at the allene central carbon was observed to generate a 1,1-disubstituted allylic alcohol product.⁴³ When Et₃B was employed as the reducing agent, addition to the allene central carbon was once again observed, however,

to generate a 1,2-trisubstituted allylic alcohol product.⁴³ When Me_2Zn was used as the reductant, aldehyde addition to the least hindered allene terminal carbon was observed to afford the alkylative homoallylic alcohol product.⁴⁴ The regiochemical outcome of these three reactions have demonstrated strong dependence on the identity of the reducing agent (Scheme 27).

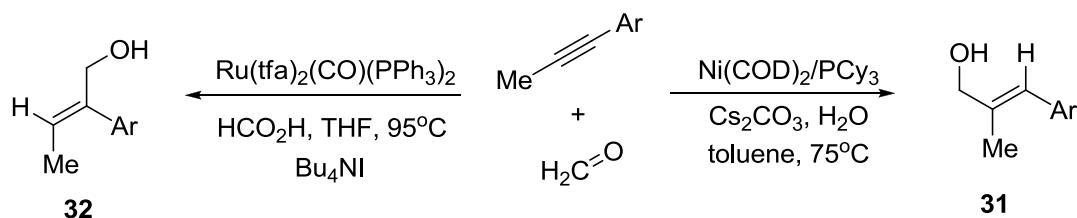
Scheme 27. Regiochemical Influence from Reducing Agent



1.5.5 Process Control of Regiochemistry

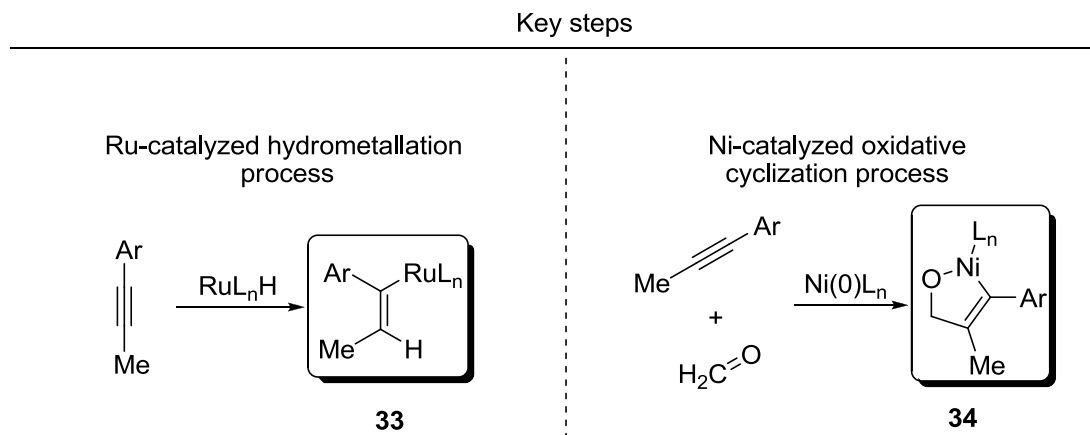
To distinguish from the above-mentioned regiocontrol categories, process control of regiochemistry refers to two distinct coupling processes that provide products with a complementary regiochemical outcome. A unique example that illustrates this factor is the recent coupling reactions of paraformaldehyde and aromatic alkynes using either a nickel-catalyzed process or a ruthenium-catalyzed process (Scheme 28).⁴⁵

Scheme 28. Process Control of Regiochemistry in Formaldehyde-Aromatic Alkyne Couplings



The complementary regioselectivity in these two reactions were attributed to the distinct process pertaining to each individual reaction. In the nickel-catalyzed couplings, oxidative cyclization of the alkyne and formaldehyde resulted in the formation of **31** presumably by proceeding through metallacycle intermediate **34** to stabilize developing charge on the catalyst center through the electronic bias inherent in the aromatic alkynes. In the ruthenium-catalyzed couplings, hydrometallative pathways resulted in the formation of **32** by going through a vinyl metallated species, **33** allowing the electronic bias of the aromatic alkyne to stabilize the developing charge on the Ru metal center. While both coupling reactions take advantage of the electronic bias of the alkyne substrate, the distinct hydrometallative and oxidative coupling processes would lead to divergent regiochemical outcomes (Scheme 29).

Scheme 29. Key Regiodetermining Steps in Both Processes



While nickel-catalyzed reductive couplings of allenes have achieved considerable success, the application of these substrates in a variety of reductive coupling reactions have yet to be fully explored, in particular regarding the regioselectivity issues resulting from these reactions. To address the challenges in regioselective allene additions, reducing agent control and ligand control strategies can be applied and will be discussed in detail in chapter 4.

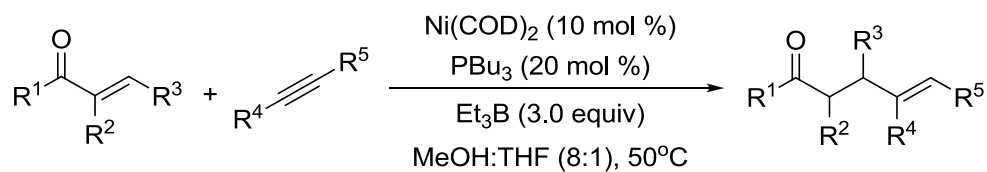
Chapter 2: Nickel-Catalyzed Alcohol-Mediated Enones-Alkynes and Aldehydes-Alkynes Reductive Coupling Reactions

2.1 Nickel-Catalyzed Alcohol-Mediated Enone-Alkyne Reductive Coupling

2.1.1 Proposed Strategy for Utilizing Alcohol as Reducing Agent

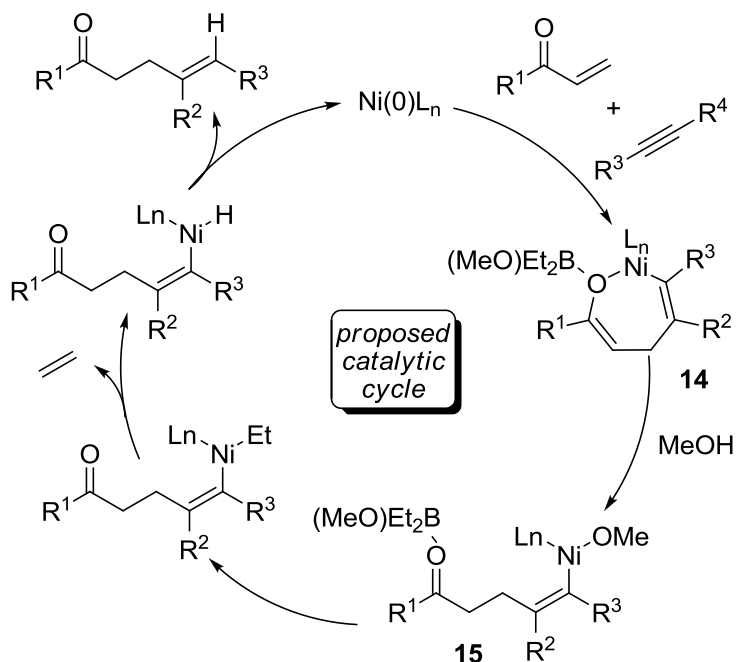
The choice of reducing agents is highly important to the practicality of nickel-catalyzed enone-alkyne reductive coupling reactions. As discussed in section 1.3.3, our group has developed a nickel-catalyzed Et₃B-mediated reductive coupling reaction of enones and alkynes with MeOH:THF as a cosolvent system (Scheme 30). While this intermolecular reaction tolerates a variety of enones and alkynes, the high flammability of the reducing agent Et₃B is a limiting factor to the reaction's practicality. To further improve the practical end of this coupling reaction, a mild and inexpensive reducing agent is highly desired. The utilization of alcohols as reducing agent has been discussed in section 1.4. The mild and economical nature of alcohols makes them an attractive alternative to Et₃B. Thus, we hoped to introduce alcohols for the first time as a reducing agent in nickel-catalyzed enone-alkyne reductive coupling reactions.

Scheme 30. Nickel-Catalyzed Et₃B-Mediated Reductive Coupling of Enones and Alkynes



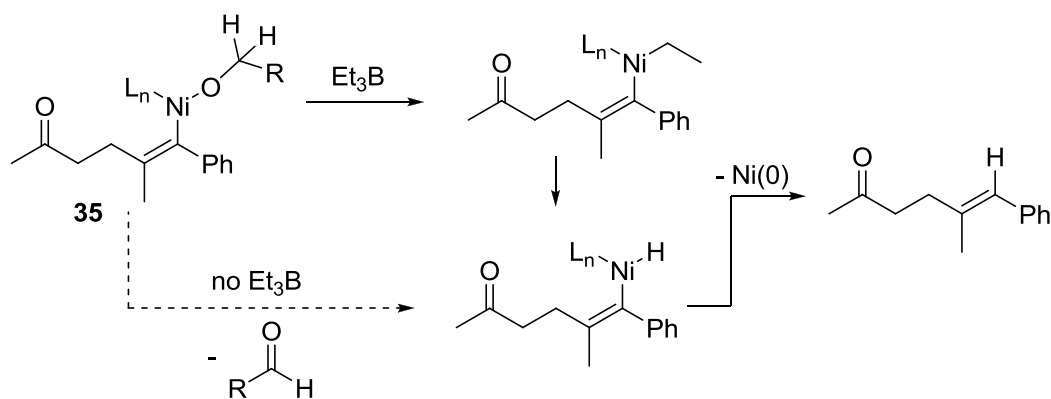
To achieve that goal, we have closely analyzed the proposed mechanism of the Et₃B-mediated reductive coupling variant (Scheme 31). Based on the mechanistic understanding at the time, a nickel catalyst could oxidatively cyclize the enone and alkyne to generate a seven-membered metallacycle **14**. Protonation of metallacycle **14** can then generate intermediate **15**. Transmetalation of Et₂B(OMe) with **15**, followed by subsequent reduction steps would eventually form product and regenerate the active catalyst.

Scheme 31. Proposed Mechanism of the Et₃B-Mediated Enone Alkyne Couplings



The proposed formation of intermediate **15**, in particular, intrigued us because as discussed in section 1.4, similar X-M-OCH₂R species can undergo β-H elimination in other transition metal catalyzed reactions that utilize alcohols as the reducing agent. This recognition prompted us to investigate whether intermediate **15** could undergo direct β-H elimination to generate the R-M-H instead of the transmetalation process with Et₃B. Therefore, the success of this proposed strategy is pending upon smooth β-H elimination from intermediate **35**; in addition, the metallacycle needs to be formed in the absence of a Lewis acidic borane reagent (Scheme 32).

Scheme 32. Hypothesis of Alcohols as Reducing Agent



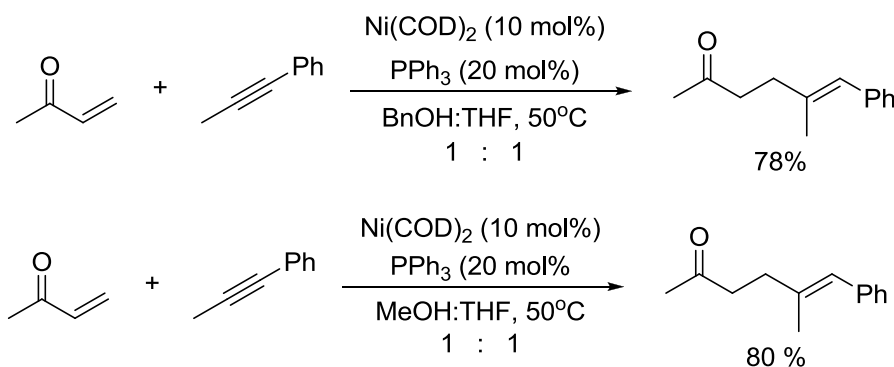
2.1.2 Initial Studies and Optimization of the Nickel-Catalyzed Alcohol-Mediated Reductive Couplings of Enones / Alkynes

Our first set of reaction conditions to test the hypothesis was carried out based on the Et₃B-mediated reaction protocol with a few modifications. The first modification is the use of benzyl alcohol as a reducing agent and part of the solvent system. We hoped that the β-hydrogen of the R-Ni-OCH₂Ph would be activated toward β-H elimination using benzyl alcohol. Another modification is the use of PPh₃ as ligand. As discussed in

section 1.3.3, the Montgomery group has demonstrated that PPh_3 facilitates β -H elimination from an R-Ni-R species. This effect was attributed to the strong σ -donating ability of PPh_3 to the nickel catalyst that could suppress the competing reductive elimination pathway. That same σ -donation from PPh_3 should apply in the β -H elimination of a $\text{R-Ni-OCH}_2\text{Ph}$ species. Finally, a minor modification of using 1:1 $\text{BnOH}:\text{THF}$ solvent ratio is used for workup purposes due to the high boiling point of BnOH .

To our delight, the reductive coupling of methylvinylketone (MVK) and 1-phenyl-1-propyne proceeded to yield the desired product in 78% yield in the first trial reaction. A few interesting observations need to be pointed out here. Both crude NMR and GCMS suggested that benzaldehyde was generated as a side product. Although the reductive coupling of benzaldehyde and 1-phenyl-1-propyne was well documented by several groups using Et_3B or Et_3SiH as reducing agent, such a reaction was not observed here. The formation of the aldehyde side product also did not appear to slow or shut down the reaction by binding to the nickel catalyst. The rationale behind this observation derived from considering that an enone is a better ligand for the nickel catalyst than an aldehyde (Scheme 33).

Scheme 33. Alcohol-Mediated Reductive Coupling of Enones and Alkynes



Switching BnOH to MeOH in a 1:1 MeOH:THF cosolvent system improved the yield to 80% (Scheme 30). Although no direct evidence suggested the formation of formaldehyde, the precipitation of white powder during the reaction suggested that the monomeric formaldehyde maybe formed and instantaneously polymerized to its insoluble paraformaldehyde form under the reaction condition. In addition, the paraformaldehyde peak was often observed in the crude NMR.

The yield was further improved to 83% when an 8:1 MeOH:THF cosolvent system was used. Using this standard protocol, ligands were also tested. While PPh₃ and PCy₃ are both very effective ligands in this methanol-mediated reductive coupling reaction, PBu₃ led to inefficient couplings. NHC carbene ligands only led to modest yields of the coupling products with internal alkyne substrates. The optimized reaction condition and scope for the methanol-mediated reductive couplings of enones and alkynes are summarized in Table 1.⁴⁶

Table 1. Scope of Methanol-Mediated Reductive Couplings

Entry	Ligand	Product (yield, regioselectivity)	Entry	Ligand	Product (yield, regioselectivity)
1	PCy ₃	 86% (>95:5)	8	PCy ₃	 66%
2	PCy ₃	 63% (94:6)	9	PCy ₃	 52% (>95:5)
3	PCy ₃	 90%	10	PPh ₃	 83% (93:7)
4	PCy ₃	 93% (>95:5)	11	PPh ₃	 81% (>95:5)
5	PPh ₃	 70% (>95:5)	12	PCy ₃	 94% (>95:5) ^a
6	PPh ₃	 76% (>95:5)	13	IMes	 47% (75:25) ^a
7	PCy ₃	 58% (>95:5)	14	PCy ₃	 47% (>95:5) ^b

^a Alkyne was added by syringe drive.

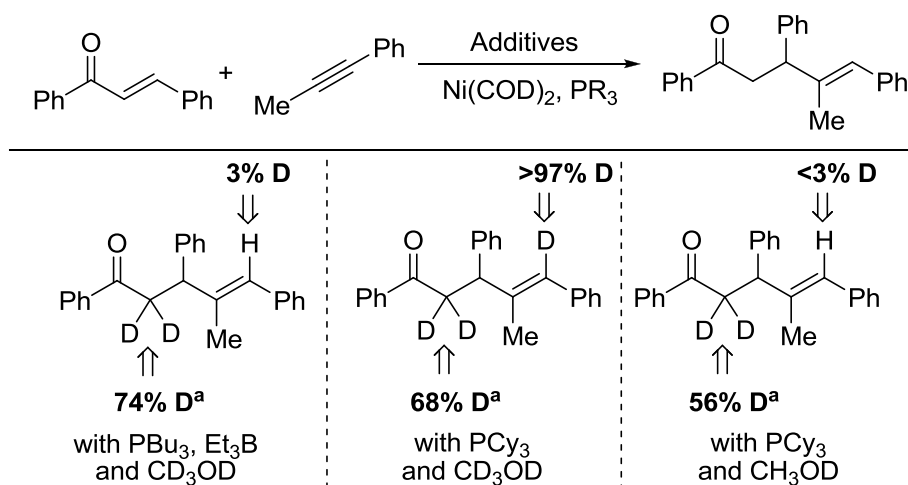
^b Additionally, 13% yield of the alcohol derived from deprotection of the product acetate was obtained, giving an overall 60% yield for desired coupling.

While the scope of this procedure closely resembles the Et₃B-based procedure, a few notable distinctions can be pointed out here. While PCy₃ and PPh₃ are interchangeable ligands, PCy₃ was generally preferred with α - or β - substituted enones, whereas PPh₃ suited better for enones that lack substitution at both the α - and β - positions. Secondly, terminal alkynes required slow additions. Fast, problematic oligomerization processes of terminal alkynes are the main reason for slow addition requirement. NHC ligands were inefficient in the oligomerization of alkynes compared with the desired reductive coupling pathway in the aldehyde-alkyne reductive couplings. The application of NHC ligands here also improved the yield of the benzylidene acetone and cyclohexyl acetylene reductive coupling product from 24% to 47%.

2.1.3 Mechanistic Studies and Comparison of Methanol-Mediated to Et₃B-Mediated Reductive Coupling Reactions

While we were pleased with the development of a novel methanol-mediated reductive couplings of enones and alkynes, several mechanistic questions remain unanswered for this reaction and the Et₃B-mediated variant. For example, the presence of both Et₃B and methanol in the Et₃B-based reaction raises the question of which reagent assumes the role of reducing agent. In the methanol-mediated variant, we can safely assume that methanol is the reducing agent because of the absence of Et₃B and any other reducing agent. Another question relates to how methanol acts as a reducing agent in the methanol-mediated reaction. To elucidate the exact nature of the reducing agents in both reactions, a series of deuterium labeling studies were carried out (Scheme 34).

Scheme 34. Deuterium-Labeling Studies



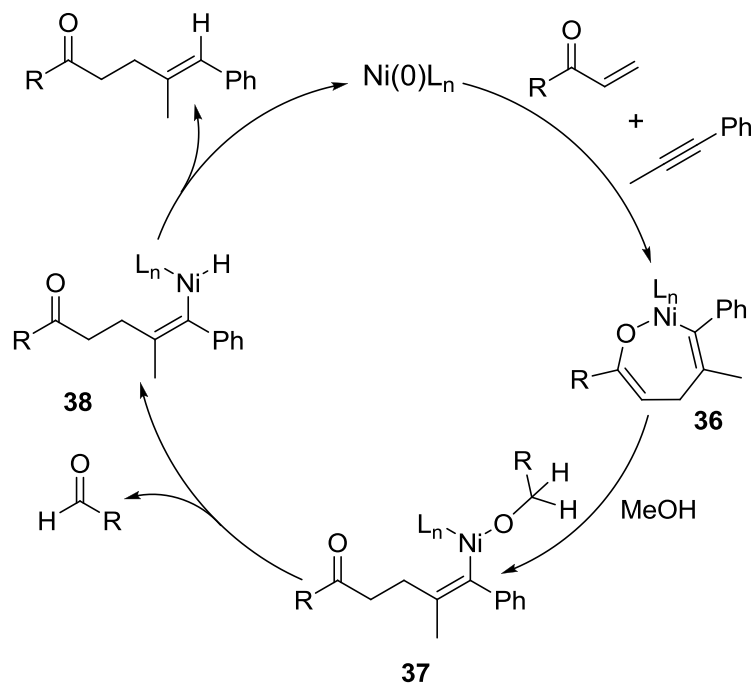
^a Percent D incorporation of the CH_2 moiety α to the ketone is given relative to 2 hydrogen atom units.

To address the question of the ambiguity of Et_3B and methanol as reducing agent in the Et_3B -mediated case, a deuterium labeling reaction employs the standard Et_3B -based coupling reaction condition using Ni(COD)_2 , PBu_3 , and Et_3B in a $\text{CD}_3\text{OD/THF}$ solvent system. The coupling product shows less than 3% deuterium incorporation at the alkenyl position and 74% deuterium incorporation per hydrogen atom at the α -C of the phenyl ketone. This experiment suggested that Et_3B was indeed the reducing agent since Et_3B is the only possible source besides methanol to deliver a hydrogen at the alkenyl position. The 74% deuterium incorporation per hydrogen atom at the α -C of the phenyl ketone can be explained by the combination of enolate kinetic protonation in addition to H/D exchange at this acidic position.

To address the question of how methanol functions as a reducing agent, two separate deuterium labeling reactions were carried out. The first experiment was performed with Ni(COD)_2 and PCy_3 in $\text{CD}_3\text{OD/THF}$ solvent system. From this reaction, the coupling product obtained resulted in greater than 97% deuteration at the alkenyl

position. This experiment confirmed the role of methanol as a reducing agent since CD_3OD is the only deuterium source. In the second experiment with $\text{CH}_3\text{OD}/\text{THF}$ solvent system, the coupling product had less than 3% deuteration at the alkenyl position. This $\text{CH}_3\text{OD}/\text{THF}$ experiment in conjunction with the observation of benzaldehyde or paraformaldehyde formation in the optimization studies strongly suggested that methanol transferred a hydrogen atom from the CH_3 group rather than from the OH group. Thus based on the deuterium labeling studies, empirical observations during optimization and previously documented seven-membered metallacycle formation, the mechanism for the alcohol-mediated enone-alkyne coupling reaction is proposed below (Scheme 35).

Scheme 35. Proposed Mechanism for the Alcohol-Mediated Enone-Alkyne Couplings



The nickel-catalyst could oxidatively cyclize the enone and alkyne to generate the seven-membered nickelacycle **36**. Methanol protonation of **36** could then generate intermediate **37**. Subsequent β -hydride elimination would afford **38**. Reductive elimination from **38** would result in the coupling product and regenerate the nickel

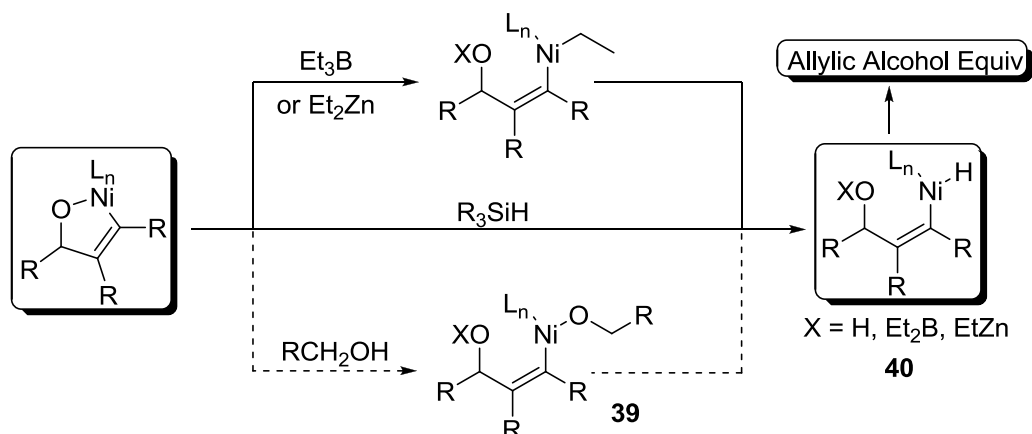
catalyst. The paraformaldehyde or benzaldehyde formation could be explained by the β -hydride elimination step from **37** to **38**, in which concomitant oxidation of the alcohol could occur. To summarize, we have developed a novel nickel-catalyzed alcohol-mediated reductive coupling of enones and alkynes, and elucidated the nature of methanol functioning as a reducing agent in this reaction. To expand on the mechanistic understanding we have gained from this reaction, we decided to apply them to similar classes of reactions.

2.2 Nickel-Catalyzed Alcohol-Mediated Reductive Couplings of Aldehydes and Alkynes

2.2.1 Proposed Strategy and Challenges for utilizing Alcohol as Reducing Agent in Aldehyde / Alkyne Reductive Couplings

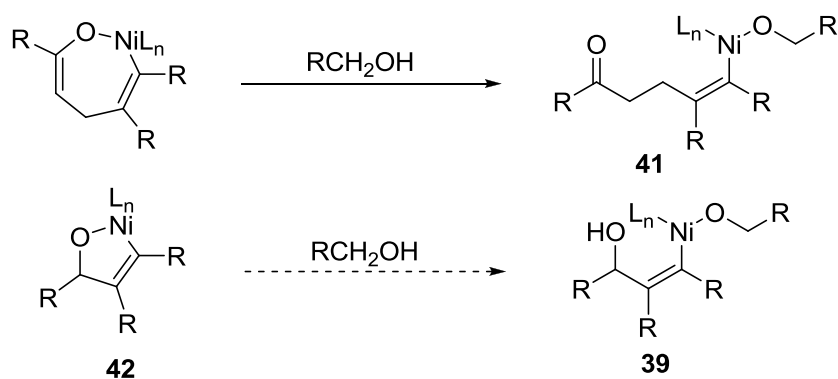
As discussed in section 1.2, allylic alcohols are important molecules, and significant efforts have been put forth for the development of synthetic methods for their preparation. Considerable success has been achieved in using mild and inexpensive alcohols as reducing agent in the reductive couplings of enones and alkynes. The lack of mild and inexpensive reducing agents in the aldehyde-alkyne reductive couplings motivates us to utilize alcohols as reducing agent in this reductive coupling reaction. Based on mechanistic understanding gained from the alcohol-mediated enone-alkyne reactions, the proposed strategy is outlined below (Scheme 36).

Scheme 36. Proposed Strategy for Alcohol-Mediated Aldehyde/Alkyne Couplings



Comparing the previously developed reductive couplings using Et_3B , Et_2Zn or Et_3SiH , the proposed strategy using alcohol could go through intermediate **39**. β -Hydride elimination would then afford intermediate **40**. Reductive elimination from **40** would finally afford the allylic alcohol product (Scheme 36). Although the proposed strategy seemed plausible, potential challenges needed to be addressed. Parallel mechanistic analogies could be drawn from the alcohol-mediated enone-alkyne reductive couplings for the development of this alcohol-mediated aldehyde-alkyne reductive coupling (Scheme 37).

Scheme 37. Parallel Mechanistic Comparison of Alcohol-Mediated Enone-Alkyne with Aldehyde-Alkyne Couplings



Based on qualitative rationale of these two mechanistic steps, we envisioned several challenges may arise in the alcohol-mediated aldehyde-alkyne couplings. The first challenge resides in the decreasing Bronsted-basicity difference of the Ni-O and Ni-C in the five membered metallacycle. In the seven membered metallacycle, the protonation step proceeds smoothly because an enolate has a greater kinetic basicity than a Ni-C bond. Without the enolate presence, the Ni-O bond in **42** is significantly less basic, and methanol can potentially protonate both the Ni-O and Ni-C bonds. If the Ni-C is protonated first, a RO-Ni-OR species would be generated and the fate of such a species is unclear.

The second challenge relates to whether **39** can undergo β -hydride elimination in the presence of a remote alcohol functional group. An alcohol is normally regarded as a σ -donating ligand. While **41** is observed to undergo smooth β -hydride elimination, a remote π -acidic ketone functional group is present. How will the change in the electronic nature of a remote functional group in the key intermediates affect β -hydride elimination?

The third challenge comes from the formation of the aldehyde side product. Reductive elimination from both **39** and **41** can result in the concomitant formation of aldehydes. In the enone-alkyne coupling case, the aldehyde byproduct is an innocent bystander because enones are generally thought of as better binding ligands than aldehydes for nickel-catalyst. However, in the proposed aldehyde-alkyne coupling reaction, the potential aldehyde byproducts are not innocent bystanders anymore. Rather, they can participate in the reaction as coupling partners. Thus, chemoselectivity issue may arise between the original aldehyde reagent and the aldehyde byproduct. While this challenge may seem like a challenge initially, one can imagine that a methodology

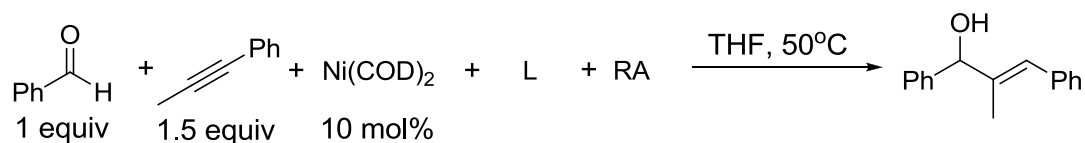
coupling of alcohols and alkynes can be developed. Since the alcohols can be precursors to aldehydes *in-situ*, they can be used as an aldehyde equivalent in the reaction. Finally, the allylic alcohol product can potentially act as a reducing agent source in the reaction. Therefore, chemoselectivity issues can also occur between the original alcohol reducing reagent and the allylic alcohol product.

While the alcohol-mediated reductive couplings of aldehydes and alkynes may seem like a daunting task, the development of such a protocol would substantially improve the practicality of aldehyde-alkyne coupling reactions by introducing a mild and inexpensive alternative reducing agent. In addition, the incorporation of alcohol as an aldehyde synthetic equivalent to generate allylic alcohols is highly desirable in the nickel-catalyzed reductive couplings.

2.2.2 Reaction Optimization for the Alcohol-Mediated Aldehyde-Alkyne Reductive Coupling Reactions

Our initial efforts focused on using methanol as the alcohol reducing agent. Based on the empirical observation that formaldehyde could polymerize quickly to the rather stable paraformaldehyde form in the enone-alkyne coupling reaction condition, we have hoped that such a process would remove the complication of chemoselectivity issues from the aldehyde side products. Our model reaction used benzaldehyde and 1-phenyl-1-propyne as the coupling partners in various reaction conditions (Table 2).

Table 2. Optimization of Alcohol-Mediated Aldehyde-Alkyne Reductive Couplings

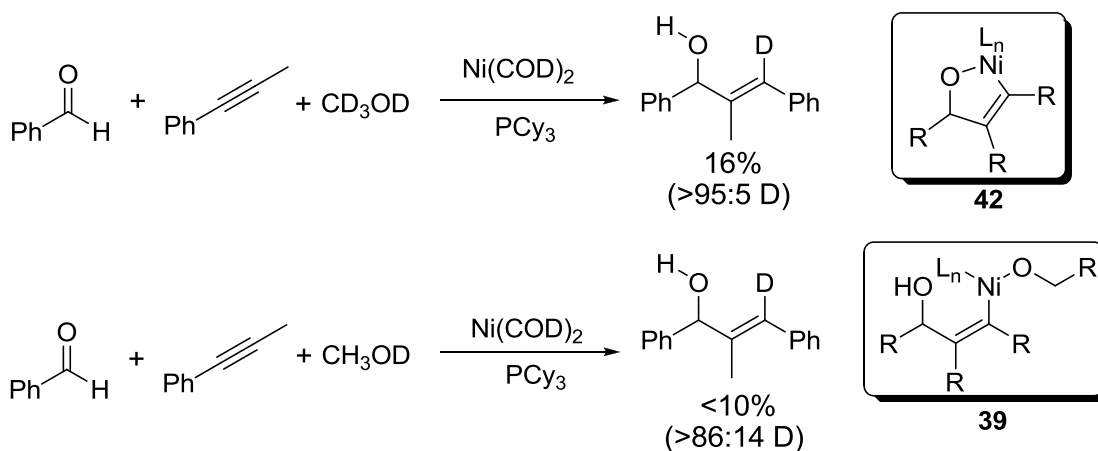


Entry	RA	Ligand	yield (regioselectivity)
1	MeOH (10 eq)	PCy ₃	<10%
2	MeOH (4.4 mL)	IMes	<10%
3	MeOH (4.4 mL)	IPr	12% (61:39)
4	EtOH (10 eq)	PCy ₃	<10%
5	iPrOH (10 eq)	PCy ₃	<10%
6	BnOH (3 eq)	PCy ₃	33%
7	BnOH (5 eq)	PCy ₃	37%
8	BnOH (10 eq)	PCy ₃	42%
9	BnOH (5 eq)	PCy ₃	33% ^a
10	BnOH (5 eq) ^b	PCy ₃	24%
11	BnOH (5 eq)	PPh ₃	<10%
12	BnOH (5 eq)	IMes:	30%

a. Syringe addition of alkyne
 b. Toluene is used as solvent

While conditions involving methanol resulted in noncatalytic yields regardless of ligands, methanol equivalence and Lewis acidic additives, ethanol and isopropanol were also ineffective as reducing agents under these reaction conditions. Disappointed with the initial screening, we carried out two deuterium labeling studies to draw insights from the potential reaction mechanism. Such insights could potentially help to generate new reaction conditions for the development of the reaction (Scheme 38).

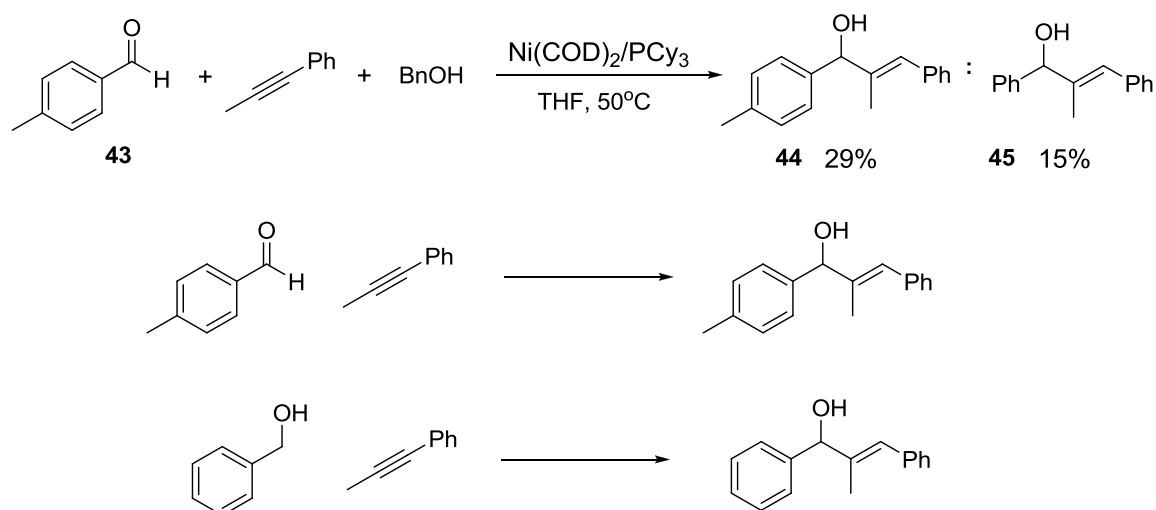
Scheme 38. Deuterium Labeling Studies



The deuterium labeling studies revealed that protons from CH₃ of methanol were not predominantly incorporated into the alkene product. These studies suggested that direct protonation of either **42** or **39** could occur to result in deuterium incorporation at the alkenyl position of the product. In addition, Ni-D generated from the nickel catalyst and deuterated methanol also could not be excluded to account for the observed products.

Somewhat disappointed with the initial results, further screening of alcohols revealed that catalytic activity could be observed using benzyl alcohol (Table 2, entry 10). Current optimal conditions involving coupling of the substrates in 10 equiv. of benzyl alcohol afforded 42% yield of the reductive coupling product. While excited with the observed catalytic activity using alcohols, complications can result from chemoselectivity of the original benzaldehyde reagent and the possible benzaldehyde side product generated. To clarify this complication, *p*-tolualdehyde was used as the aldehyde reagent, and benzyl alcohol was used as the reducing agent (Scheme 39). Interestingly, coupling products from both *p*-tolualdehyde and benzyl alcohol were observed in 29% and 15% yield, respectively. This led us to believe that not only catalytic reductive coupling of aldehydes and alkynes is possible, but also couplings of alcohols and alkynes are possible.

Scheme 39. Reductive Coupling of *p*-Tolualdehyde and Alkyne

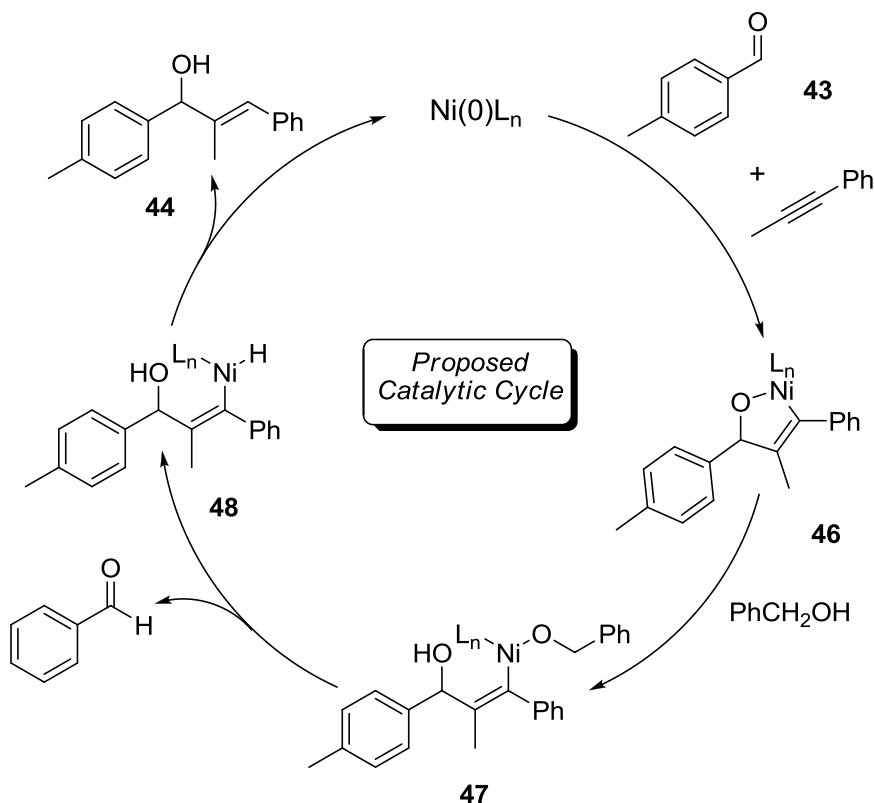


Although the reaction efficiency for both processes needs to be further optimized, the interesting reactivity from both processes has suggested many possibilities. For example, the potential to incorporate alcohol as the reducing agent in aldehyde-alkyne reductive coupling processes is partially achieved here. The ability to utilize alcohols as coupling partners in reductive coupling processes is highly desirable and partially realized here. In addition, varying amounts of enone products derived from oxidation of the allylic alcohol products were often observed in these reactions. Such enone formation processes could also be optimized to generate useful entries to substituted enones.

Finally, to rationalize the formation of both allylic alcohol products in the *p*-tolualdehyde case, a preliminary reaction mechanism is proposed here for further refinement (Scheme 40). As previous aldehyde-alkyne reductive coupling reactions suggested, oxidative cyclization of aldehyde **43** and alkyne by the nickel catalyst can generate metallacycle **46**. Protonation of the metallacycle then affords intermediate **47**. β -Hydrogen elimination of **47** can result in the formation of **48** with concomitant extrusion of benzaldehyde. Reductive elimination from **48** affords product **44** and regenerates the

active catalyst. The benzaldehyde side product can also participate in this catalytic cycle to generate the allylic alcohol product **45**.

Scheme 40. Proposed Mechanism for Benzylalcohol as Reducing Agent



2.3 Summary of Nickel-Catalyzed Alcohol Mediated Enone-Alkyne and Aldehyde-Alkyne Reductive Couplings

In this chapter, we have developed a nickel-catalyzed alcohol-mediated enone-alkyne reductive coupling reaction. Mechanistic insights for this reaction were probed to validate the role of methanol as a viable reducing agent. We have also initiated the development of an alcohol-mediated aldehyde-alkyne reductive coupling reaction. Although further work is needed to develop this reaction into an efficient process, we have confirmed the potential to utilize alcohols as reducing agents in such coupling

reactions. In addition, we have discovered pathways to potentially utilize primary alcohols as synthetic equivalents of aldehydes in aldehyde-alkyne reductive coupling reactions.

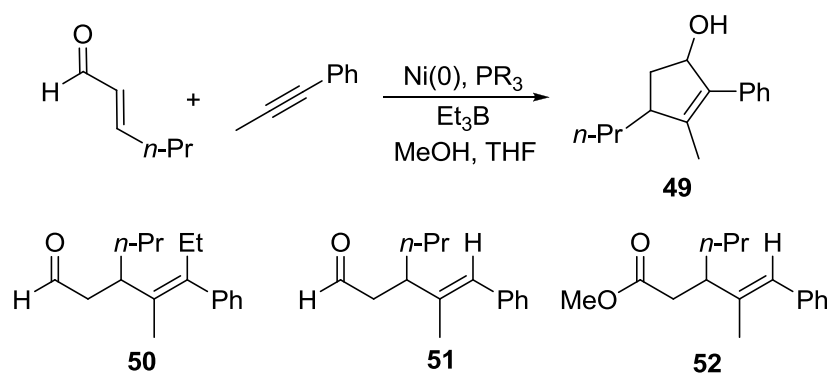
Chapter 3: Pathway to the Discovery of a Nickel-Catalyzed Internal Redox Reaction

3.1 Ligand Screening of the Nickel-Catalyzed Enal-Alkyne Coupling Reactions

As discussed in section 1.3.3, our group has disclosed the formation and isolation of seven membered metallacycles from alkynal substrates. From these versatile metallacycle structures or intermediates, various reaction pathways exist with simple modifications in substrates, ligands, reducing agents, additives, solvents, and metal stoichiometry. In particular, former co-worker Ananda Herath has observed ligand effects in the nickel-catalyzed coupling reaction of enals and alkynes using Et₃B as the reducing agent in an 8:1 MeOH:THF solvent system. To systematically illustrate ligand effects in selecting for reaction pathways, we have decided to screen a range of monodentate phosphine structures.

Our standard reaction conditions involve the coupling of trans-2-hexen-1-al and 1-phenyl-1-propyne employing 10 mol% Ni(COD)₂, 20 mol% of a monodentate phosphine ligand, and 3.0 equiv Et₃B in an 8:1 methanol:THF cosolvent system (Table 3).⁴⁷

Table 3. Ligand Effects in Reductive Couplings in Enal-Alkyne Couplings



entry	Ligand	% 49 (dr) ^a	% 50	% 51	% 52
1	PBu ₃	85 (87:13)			
2	PPh ₃	46 (87:13)	14	25	
3	P(<i>o</i> -tolyl) ₃	<10	76	19	
4	P(1-naphthyl) ₃		57	<10	
5	P[4-(MeO)C ₆ H ₄] ₃	72 (65:35)	<10	<10	
6	P[2,4,6-(MeO) ₃ C ₆ H ₂] ₃	79 (36:64)			
7	PCy ₃			12	45
8	P(<i>t</i> -Bu) ₃	<10	17	18	
9	P(C ₆ F ₅) ₃		NR		

^aDiastereomeric ratio of **A** is reported as cis:trans ratio.

As the ligand screen results show, a variety of different products were observed. As discussed in section 1.3.3, [3+2] reductive cycloaddition product **49** using PBu₃ has been reported by the Montgomery group. However, the alkylative coupling product **50** had not been disclosed in previous couplings of enals and alkynes. While the reductive coupling product **51** was usually obtained as the minor product, our group reported a Et₃SiH-mediated reductive coupling of enals and alkynes to generate an alternative enol silane reductive coupling product as discussed in section 1.3.3. In addition, an ester product **52** was also observed using PCy₃. The formation and preliminary optimization

of the [3+2] adducts and alkylative coupling products will be discussed in the following section 3.2. The formation of the ester product **52** will be discussed in section 3.3.

3.2 Triarylphosphine-Promoted Nickel-Catalyzed [3+2] Reductive Cycloadditions and Alkylative Couplings of Enals and Alkynes

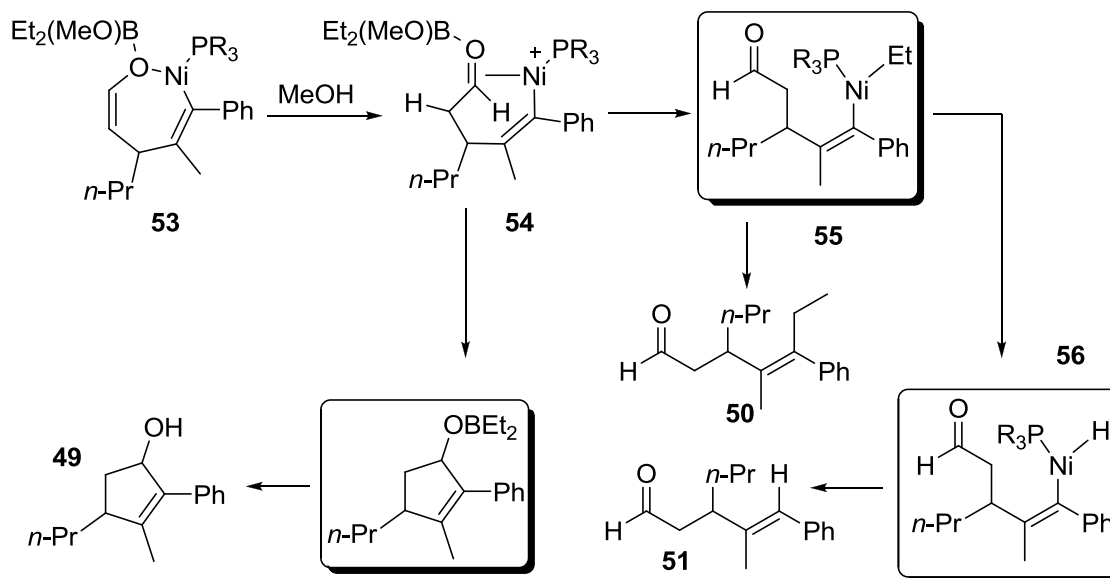
As shown in the previous section, PBu_3 predominantly leads to [3+2] reductive cycloaddition products, while the use of triaryl phosphine ligands in enal-alkyne coupling reactions mainly leads to three different products: [3+2] cycloaddition product **49**, reductive coupling product **51**, and alkylative product **50**. In the case of PPh_3 as the ligand, although the dr of the [3+2] cycloaddition product can match that of PBu_3 , the yield of the [3+2] products are much lower because of the formation of two other competing products.

To rationalize the divergent reactivity behavior from PBu_3 to PPh_3 , a common intermediate **54** was proposed to form following the protonation of a metallacycle intermediate **53** (Scheme 41). While the strong σ -donating capability of PBu_3 would promote the addition of the vinyl nickel fragment to the coordinated aldehyde, that same capability would also disfavor an ethyl transfer to generate intermediate **55**. The addition of the vinyl nickel fragment to the aldehyde would eventually lead to the cyclopentenol product, thus explaining the exclusive formation of [3+2] reductive cycloaddition product using PBu_3 .

On the other hand, the less σ -donating triaryl phosphines would facilitate the ethyl transfer process to form **55**. Two separate pathways could then occur from **55**. The first pathway involves a direct reductive elimination to generate the alkylative product **50**.

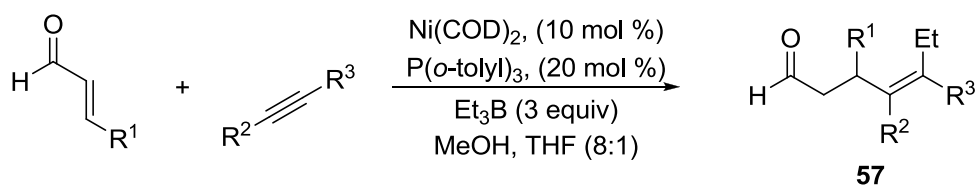
The second pathway resulted in β -hydride elimination from **55**, followed by reductive elimination of **56** to generate the reductive coupling product **51**. Since PPh_3 only partially facilitated the ethyl transfer process, distribution of all three coupling products would then be observed (Scheme 41).

Scheme 41. Mechanistic Rationale for Ligand Control in Enal-Alkyne Couplings



The mechanistic analysis here is further validated using triaryl phosphine ligands that have either increased sterics or increased σ -donating capability compared to PPh_3 . Phosphine ligands such as $\text{P}(o\text{-tol})_3$ and $\text{P}(1\text{-naphthyl})_3$ both have an alkyl substitution at the ortho-position of the aromatic ring. The increased sterics from these two ligands not only strongly disfavours the addition of the alkenyl nickel fragments to the aldehyde, but significantly facilitates the reductive elimination process to generate the alkylative coupling product as the major product. A preliminary scope of the alkylative coupling process using $\text{P}(o\text{-tol})_3$ is shown below (Table 4).

Table 4. P(*o*-tol)₃-Promoted Alkylative Couplings of Enals and Alkynes



entry	R ¹	R ²	R ³	% 57 ^a
1	<i>n</i> -Pr	Me	Ph	76
2	<i>n</i> -Pr	Ph	Ph	52
3	H	Ph	Ph	53
4	<i>n</i> -Pr	Et	Et	57

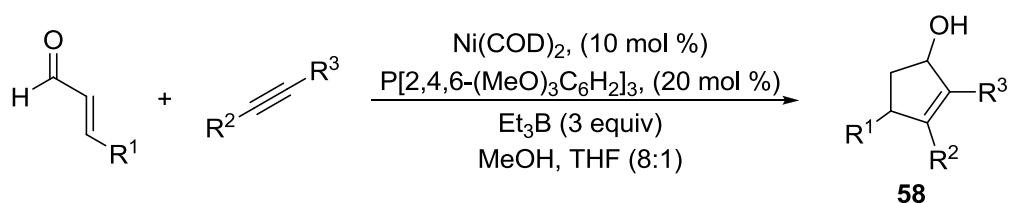
^aIsolated yields are shown. Only a single regio- and stereoisomer was observed.

The choice of P(*o*-tol)₃ instead of P(1-naphthyl)₃ for the alkylative coupling process is due to several factors. Although P(1-naphthyl)₃ generally gives better selectivity for the alkylative coupling product than P(*o*-tol)₃, it consistently gives lower isolated yield. In addition, the workup process can be more complex with P(1-naphthyl)₃ due to solubility issues. Using P(*o*-tol)₃, alkylative couplings with phenylpropyne or diphenylacetylene with *trans*-hexenal were effective. Alkylative coupling of acrolein and diphenylacetylene proceeded with moderate yield. Additionally, a nonaromatic alkyne is also a viable substrate for this alkylative coupling process.

Although the Ni(0)/PBU₃ combination is very effective in forming the [3+2] cycloaddition adducts, PBU₃ is very sensitive and prone to air oxidation. PBU₃ needs to be distilled from commercially available sources and stored in a Schlenk flask. In the ligand screening study in the section 3.1, we observed the formation of [3+2] product using the much more stable PPh₃ as the ligand. Although the isolated yield of [3+2] product is low for PPh₃ because of other competing product formation, switching to P(*p*-

methoxyphenyl)₃ and P(2,4,6-trimethoxyphenyl)₃ that are considerably more σ -donating than PPh₃ resulted in higher yields, albeit with lower dr. These two electron-rich ligands can closely match the electronic biases of PBu₃ to produce cyclopentenol **58** while displaying the crystallinity and stability of other triaryl phosphines. The preliminary scope of the nickel-catalyzed P(2,4,6-trimethoxyphenyl)₃-promoted [3+2] reductive cycloaddition process is shown below (Table 5).

Table 5. P(2,4,6-trimethoxyphenyl)₃-Promoted Reductive Cycloadditions



entry	R ¹	R ²	R ³	% 58 (dr) ^a
1	<i>n</i> -Pr	Et	Et	51 (48:52)
2	<i>n</i> -Pr	Ph	Ph	70 (53:47)
3	<i>n</i> -Pr	Me	Ph	79 (36:64)
4	<i>n</i> -Pr	H	Ph	71 (64:36)
5	<i>n</i> -Pr	(CH ₂) ₃ OH	Ph	65 (62:38)
6	H	Me	Ph	31

^aDiastereomeric ratio of **58** is reported as *cis:trans* ratio

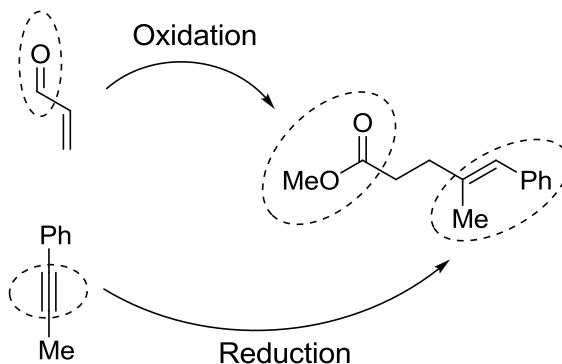
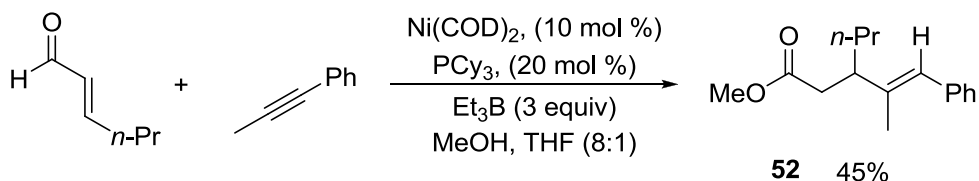
Although the diastereocontrol for the [3+2] adducts is low, couplings of β -substituted enals with symmetrical, unsymmetrical and terminal alkynes proceeded efficiently. Alkynes possessing an unprotected hydroxyl could also be effectively coupled. Reductive cycloaddition of acrolein with 1-phenyl-1-propyne proceeded only in low yield.

In summary, stable electron-rich aryl phosphines can be used as a convenient substitute for more sensitive PBU_3 in reductive cycloaddition process. Sterically bulky phosphines can lead to an alkylative coupling process that has not been previously disclosed in enal-alkyne couplings to generate useful tetrasubstituted alkene products.

3.3 Discovery of Internal Redox Reactions of Enals, Alkynes and Methanol

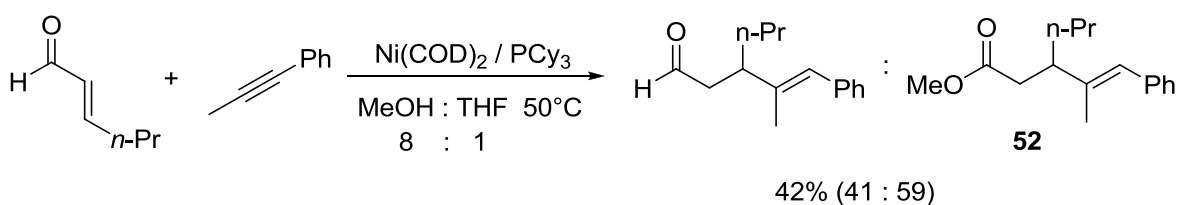
During the ligand screen for the enal-alkyne coupling reactions, we came across the formation of an ester product **52** in 45% yield using PCy_3 as the ligand. Initially, we simply thought that **52** was just an esterification product from the reductive coupling product **51**. However, analyzing the formation of this product in detail, we were puzzled by the formation of this product in the absence of an oxidant. Comparison of the product to the starting materials quickly led us to a surprising conclusion (Scheme 42).

Scheme 42. Discovery of an Internal Redox Process of Enals, Alkynes and Methanol



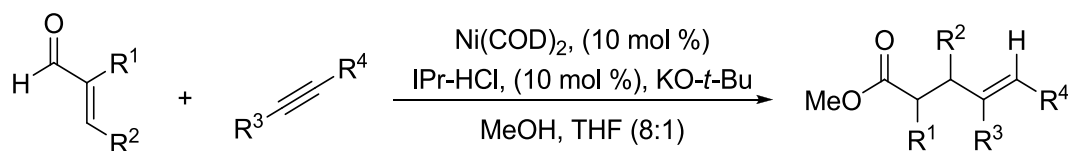
While formal reductive cycloaddition or coupling are common processes in our laboratory, the generation of **52** could instead involve an internal redox process, in which the aldehyde is oxidized to an ester and the alkyne is reduced to an alkene in the product. This mechanistic analysis suggested to us that the ester product **52** should still form in the absence of an external reducing agent. Carrying out the same reaction in the absence of Et₃B, product **52** was indeed formed (Scheme 43).

Scheme 43. Observation of Ester Product in the Absence of Et₃B



Optimization of the reaction with PCy₃ as ligand consistently gives moderate yields because of the competing reductive coupling formation. The use of IPr as a ligand suppresses the reductive coupling pathway and leads to significant yield improvement for the ester product. An optimized condition involving treatment of an enal and alkyne with Ni(COD)₂ and IPr in a MeOH/THF solvent system resulted in formation of **52** as a regioisomeric mixture. Using the optimized reaction condition, the scope of enals and alkynes was examined in this reaction (Table 6).⁴⁸

Table 6. Three Component Enal, Alkyne and Alcohol Couplings



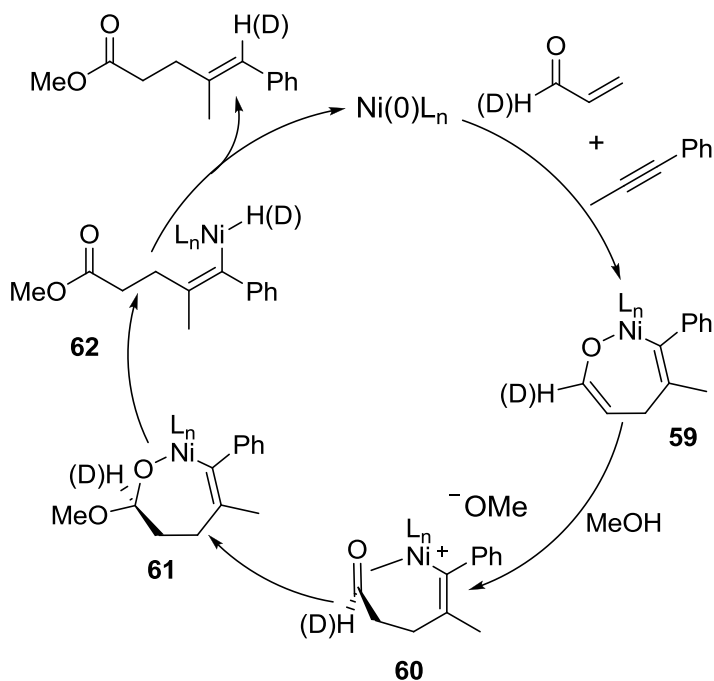
entry	R ¹	R ²	R ³	R ⁴	% A (regioselectivity)
1	H	<i>n</i> -Pr	Ph	Me	75 (53:47)
2	H	<i>n</i> -Pr	Et	Et	52
3	H	<i>n</i> -Pr	<i>n</i> -Pent	Me	76 (73:27)
4	Me	H	Ph	Me	85 (75:25)
5	H	(CH ₂) ₂ Ph	Et	Et	45
6	H	<i>n</i> -Pr	Me	CH ₂ OH	70 (90:10)

The process tolerated substitution at either the α - or β -position of the enal. Both internal aliphatic and aromatic alkynes underwent efficient coupling. A remaining problem for this reaction is regioselectivity. Although the IPr ligand gives the highest yield, the ester product was formed in a regioisomeric mixture when unsymmetric alkynes were used. However, when an alkyne has a primary hydroxyl group at the propargyl- or homopropargyl- position, the C-C formation occurred exclusively close to the hydroxyl group (Table 6).

In light of the previously proposed mechanism for formation of the reductive coupling and [3+2] products, we suggested that the formation of product involves seven membered metallacycle **59** (Scheme 44). Protonation of the enolate unit of **59** would generate **60**. Either MeO⁻ addition to the aldehyde or aldehyde insertion into the Ni-OMe bond would form **61**. β -Hydride elimination from intermediate **61** would then afford the

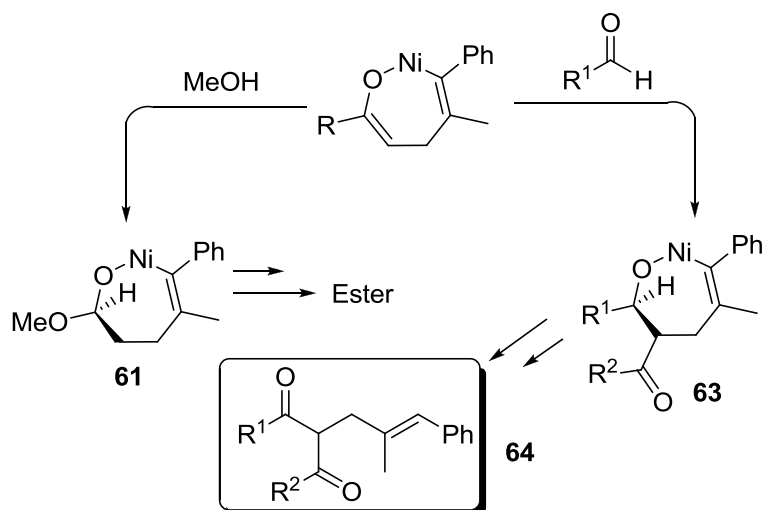
Ni-H intermediate **62**, and reductive elimination from **62** would eventually afford the ester product and regenerate the nickel catalyst.

Scheme 44. Proposed Mechanism of Enal, Alkyne, Methanol Couplings



This mechanistic proposal was further validated with a deuterium labeling study. As illustrated in the proposed mechanism, the aldehydic proton would eventually become the alkenyl proton. This suggested to us that deuterium incorporation at the aldehydic position would lead to deuteration at the alkene C-H in the final product. Carrying out the internal redox reaction with a deuterated enal at the aldehydic position led to >95% deuterium incorporation at the expected alkene position in the product (Table 6, entry 5). This result cannot rule out the addition of uncomplexed NHC carbenes to the aldehyde of **60** that could be responsible for hydride transfer to nickel, followed by acyl transfer to methanol. This deuterium labeling study unambiguously rules out the possibility that methanol serves as a hydride source concomitant with formaldehyde generation.

Scheme 45. 1,3 Diketone Product Formation



While it is not a focus of this thesis, my coworker Ananda Herath has extended this concept to generate 1,3-diketone products (Scheme 45). In the ester formation reaction, the enolate in the metallacycle is protonated. Instead of a proton source as an electrophile, this 1,3-diketone product formation utilizes an aldehyde as the electrophile to generate metallacycle **63** instead by an aldol addition. β-Hydrogen elimination and reductive elimination from **63** would eventually afford the 1,3 diketone product **64**.

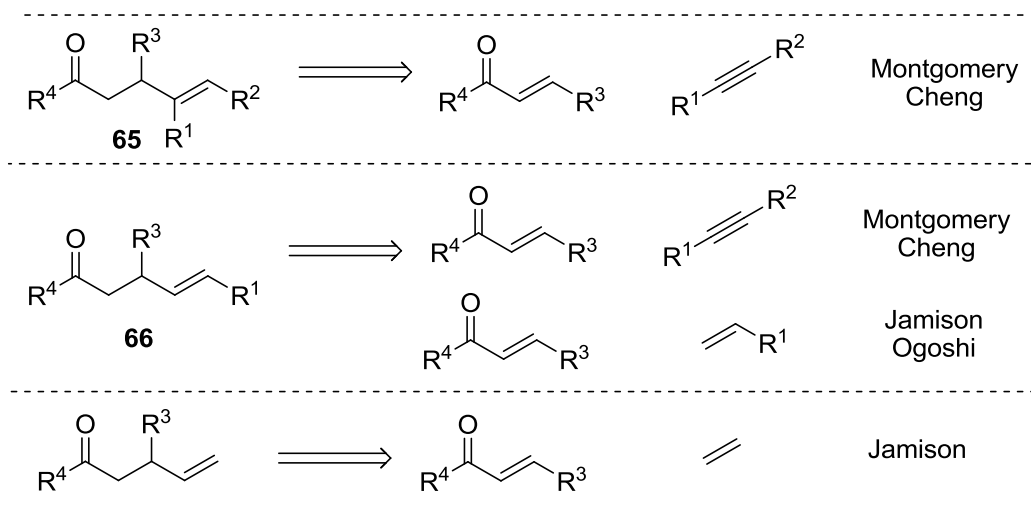
To summarize, alkylative couplings and reductive cycloadditions of enals and alkynes have been developed using stable and crystalline triaryl phosphine ligands. An internal redox reaction pathway of enals, alkynes and methanol was discovered from the surprising formation of an ester product. Observation of such interesting new pathways has led to development of new reaction variants.

Chapter 4: Regioselective Addition of Functional Groups to Allenes

4.1 Hypothesis and Challenges of Allenes in Reductive Couplings

As discussed in section 1.3, γ,δ -unsaturated carbonyl compounds are useful synthetic structures, which can be prepared by the application of reductive couplings of enones and alkynes. One significant advantage to these methods when compared with organocuprate and hydrometallative processes is avoiding the stoichiometric preparation of an alkenyl metal species as discussed in section 1.1 and 1.3. While 1,2-disubstituted and 1,2-trisubstituted alkenes **65** and **66** are easily accessible *via* enone-alkyne reductive coupling methods, entries to 1,1-disubstituted alkenes remain considerably more difficult by these methods (Scheme 46).^{49, 50, 51, 52}

Scheme 46. Regioselective Enone-Alkyne and Enone-Alkene Couplings

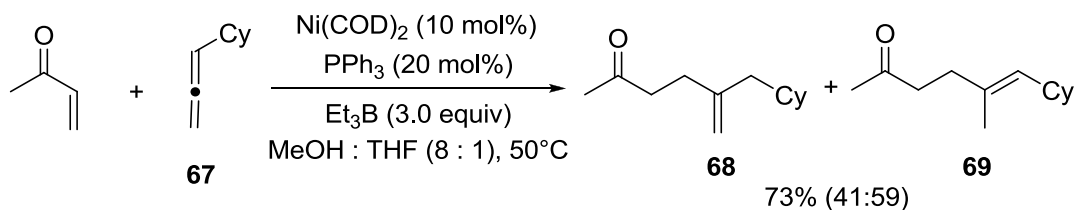


While allenes have unique reactivity because of their orthogonal π bonds, difficulties in controlling regioselectivity and chemoselectivity often plague synthetic reactions utilizing allenes as substrates. Enone-allene couplings have provided efficient entries into 1,3-dienes,⁵³ cyclopentenols,⁵⁴ and δ,ϵ -unsaturated carbonyl compounds⁵⁵; however, direct reductive coupling of enones and allenes has not been previously reported. We envisioned that enone-allene couplings would proceed through seven-membered metallacycles similar to the enone-alkyne or enal-alkyne reductive couplings described in the previous chapters. The success of such enone-allene reductive couplings could provide efficient entries into various alkene stereoisomers. Thus, we have decided to pursue the enone-allene reductive coupling process using typical reductive coupling conditions developed by the Montgomery group.

4.2 Optimization and Scope of Nickel-Catalyzed Enone / Allene Coupling with Et₃B as Reducing Agent

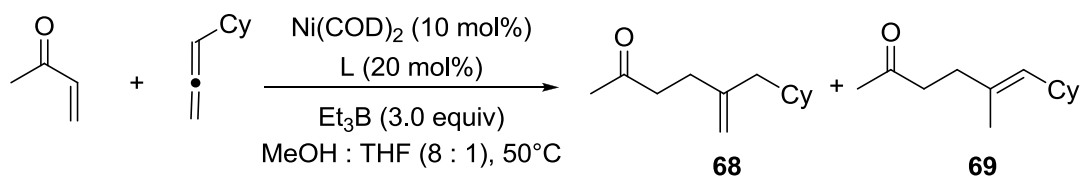
Our efforts to develop the regioselective reductive coupling of enones and allenes started with using Et₃B as the reducing agent. Thus, coupling of methyl vinyl ketone and allene **67**, using Ni(COD)₂ / PPh₃ as the catalyst and Et₃B in 8:1 MeOH:THF afforded a mixture of regioisomers **68** and **69** (Scheme 47).

Scheme 47. Et₃B-Mediated Enone-Allene Reductive Coupling Reaction



Although disappointed with the regioselectivity of the reaction, we were excited that the targeted 1,1-disubstituted regioisomer **68** was formed, albeit as the minor regioisomer. In addition, both regioisomeric products derive from the addition of the central carbon of the allene to the β -carbon of the enone. A quick ligand screen revealed that the ligand has minimal impact on the regioselectivity. While the yield of the reaction fluctuated around 60%, regioselectivity changed marginally based on ligand structure (Table 7).

Table 7. Ligand Effects on Et₃B-Mediated Enone Allene Coupling Reaction



Ligand	Yield	Regioselectivity (1 : 2)
PPh ₃	73%	41 : 59
P(o-tol) ₃	63%	31 : 69
PCy ₃	71%	31 : 69
P(2-furyl) ₃	70%	39 : 61
Xantphos	41%	36 : 64
BINAP	-	30 : 70
Dpe-phos	-	40 : 60

Table 8. Solvent and Temperature Effects on the Enone Allene Coupling Reaction

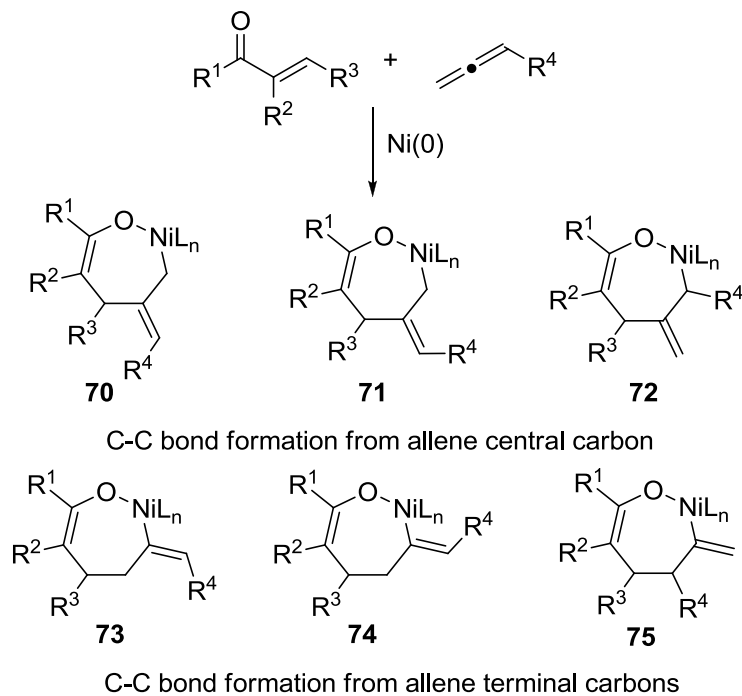
Solvent	Temperature	Yield	Regioselectivity (1 : 2)
MeOH : THF (8 : 1)	50°C	80%	40:60
MeOH : THF (1 : 8)	50°C	87%	47:53
MeOH : Toluene (8 : 1)	50°C	-	32:68
THF	50°C	39%	43:57
MeOH : THF (8 : 1)	R.T.	39%	29:79

Changing solvent composition and temperature only slightly impacted the regioselectivity of the reaction (Table 8). Despite our inability to affect the regiochemical outcome of the reaction by optimization, we did gain several mechanistic insights. First, ligand structures have minimal impact on the regioselectivity determining step. Secondly, the reaction proceeded in moderate yield with no methanol. This observation suggested that while methanol improved the reaction efficiency, Et₃B alone can directly intercept the metallacycle structure formed from the nickel catalyst, enone and allene. This result suggested that the regioselectivity derived from metallacycle formation could potentially be intercepted with the assumption that later mechanistic steps would not interfere with the regiochemical outcome.

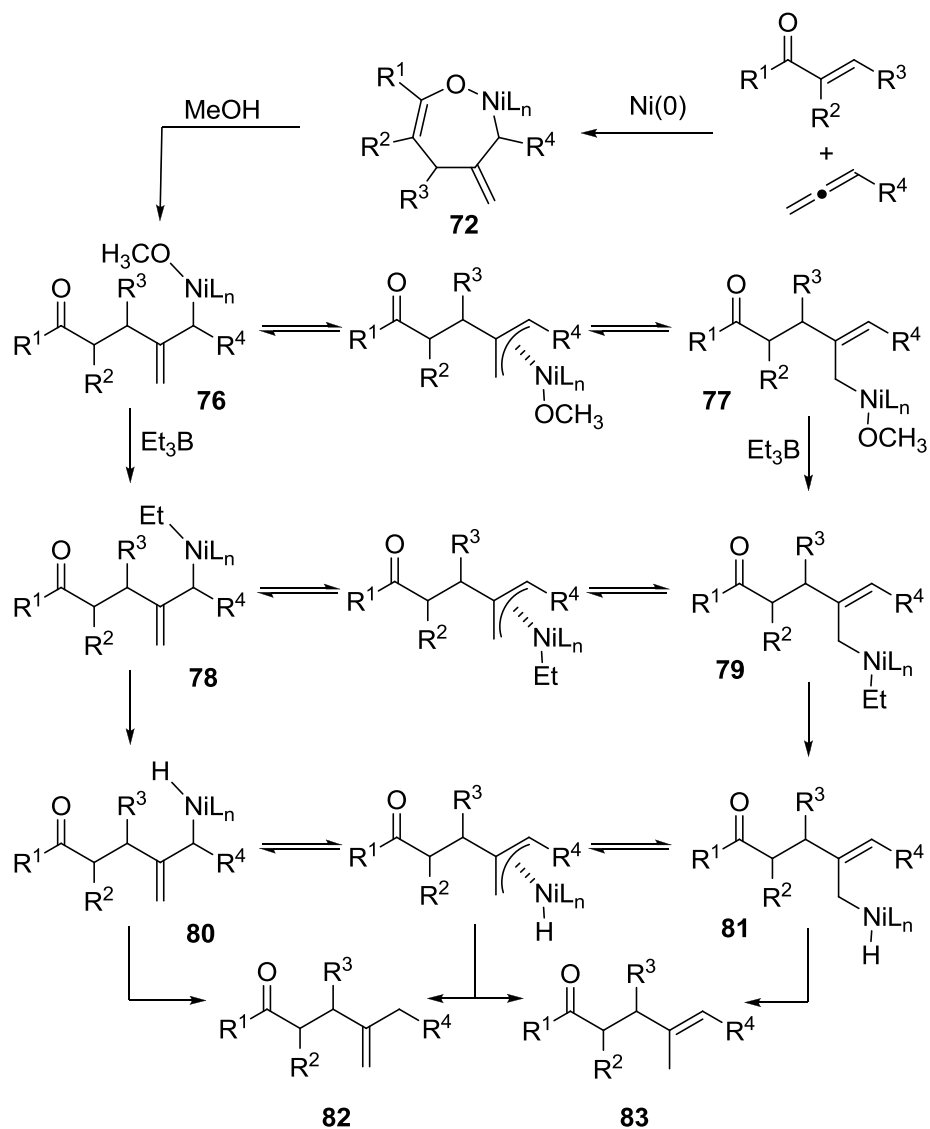
In light of previously proposed mechanisms of enone-allene coupling reactions, six possible stereoisomeric metallacycles could be formed (Scheme 48). The observation of product **68** and **69** excluded the involvement of metallacycles **73**, **74**, and

75 since the C-C bond formation step is from the central carbon of the allene. While metallacycle **70**, **71**, and **72** could all lead to the formation of the observed products, The observed regioselectivity is most readily rationalized by the involvement of metallacycle **72**. When conducted in a methanol/THF co-solvent system, protonation of metallacycle **72** could occur to generate intermediate **76**, which could readily isomerize through its π -allyl intermediate to another η^1 intermediate **77**. Et transfer from Et_3B with **76** could lead to the formation of **78**, that could further isomerize via another π -allyl intermediate **79**. β -Hydride elimination from **78** would eventually generate the Ni-H species **80**, followed by reductive elimination to afford the product in a regioisomeric mixture (Scheme 49).

Scheme 48. Possible Metallacycles in Enone-Allene Couplings



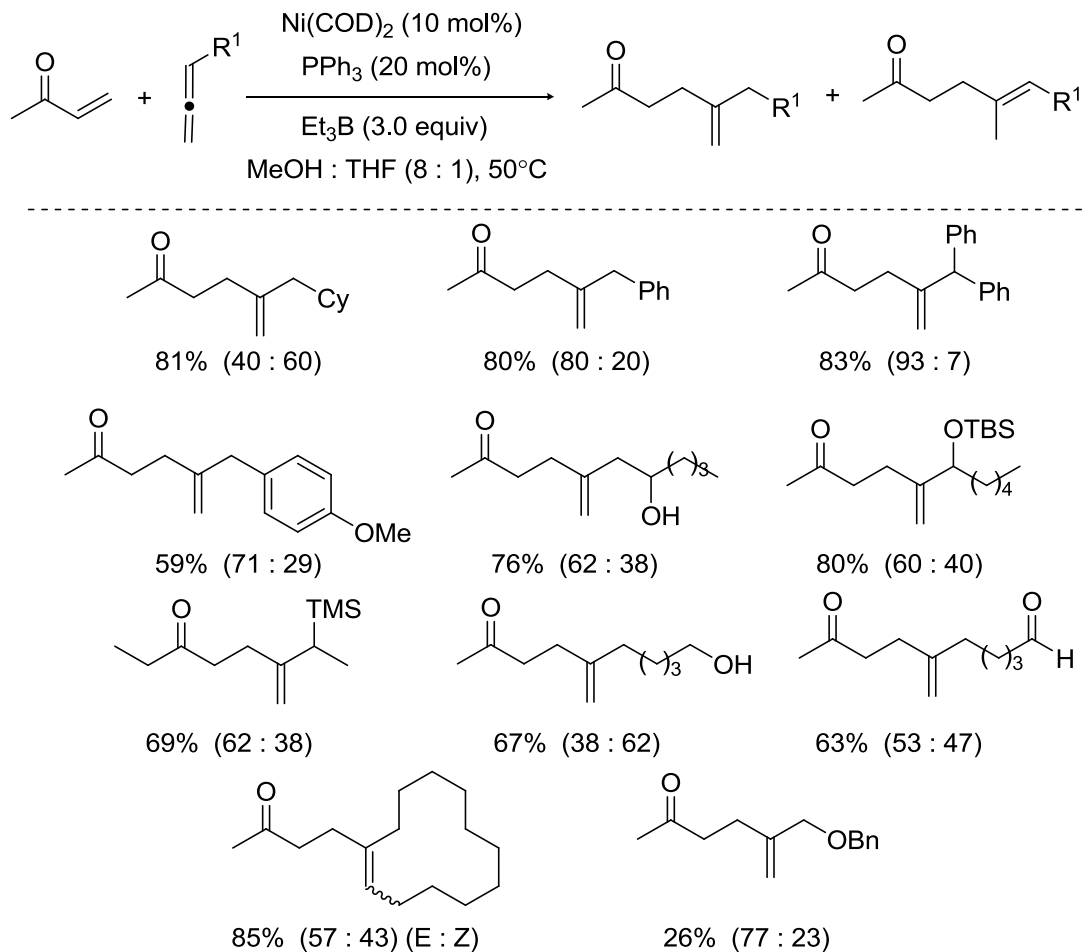
Scheme 49. Mechanistic Analysis of Et₃B-Mediated Enone-Allene Couplings



Based on this proposed mechanism, the observed regioselectivity can be derived from four different mechanistic stages of the reaction. The first step is the metallacycle formation stage. Assuming later steps do not influence regioselectivity, nonselective formation of metallacycles **71** and **72** can lead to the observed regioselectivity in products **82** and **83**. The second stage is the isomerization from **76** to **77** that can also lead to the observed regioselectivity. The third stage and the fourth stage are the isomerization of **78** to **79**, and **80** to **81**, respectively. Such isomerizations could be

translated in the eventual non-regioselective process. With the proposed mechanism in hand, we decided to determine if substrate structure would have any influence on the product regioselectivity (Scheme 50 and 51).

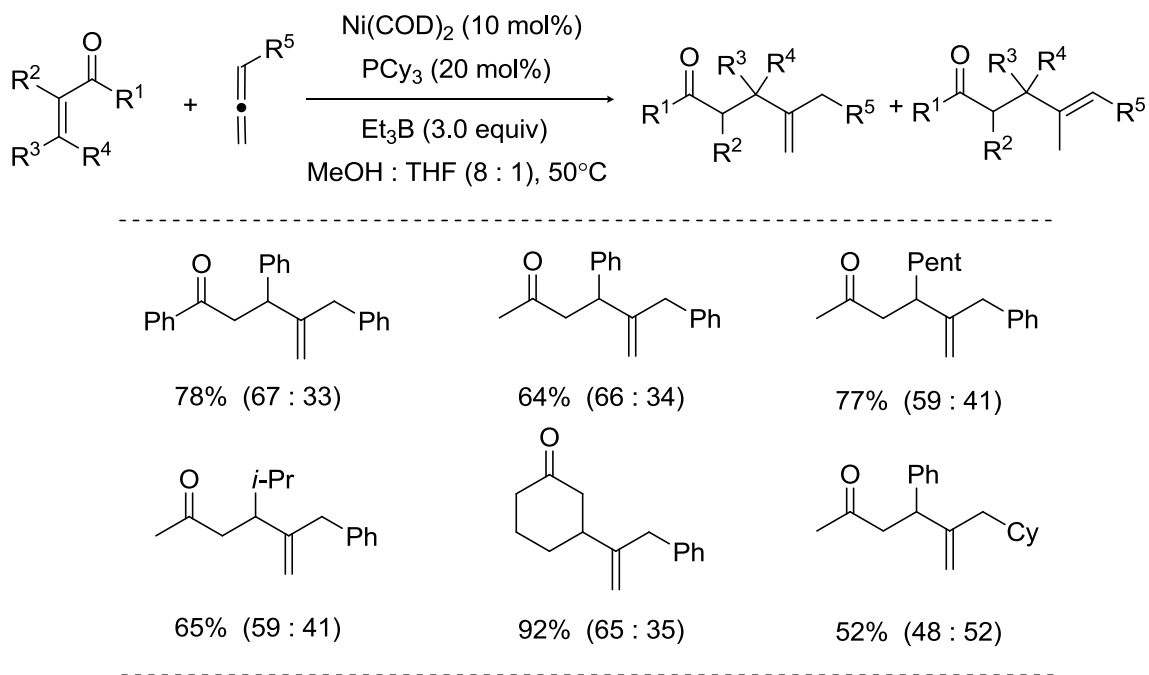
Scheme 50. Allene Scope of Et₃B-Mediated Enone Allene Couplings



Better regioselectivity was observed for the 1,1-disubstituted alkene products when charge stabilizing substituents were attached to the allene. However, allene substrates without such electronic bias resulted in non-regioselective formation of both regioisomers. Even remote directing groups such as alcohols, silyl groups, or aldehydes did not seem to affect regioselectivity for this reaction (Scheme 50). In addition, enone

substrates also have minimal impact on the regioselectivity of this Et₃B-mediated reaction as similar regioselectivity was observed across different enones (Scheme 51).

Scheme 51. Allene Scope of Et₃B-Mediated Enone Allene Couplings

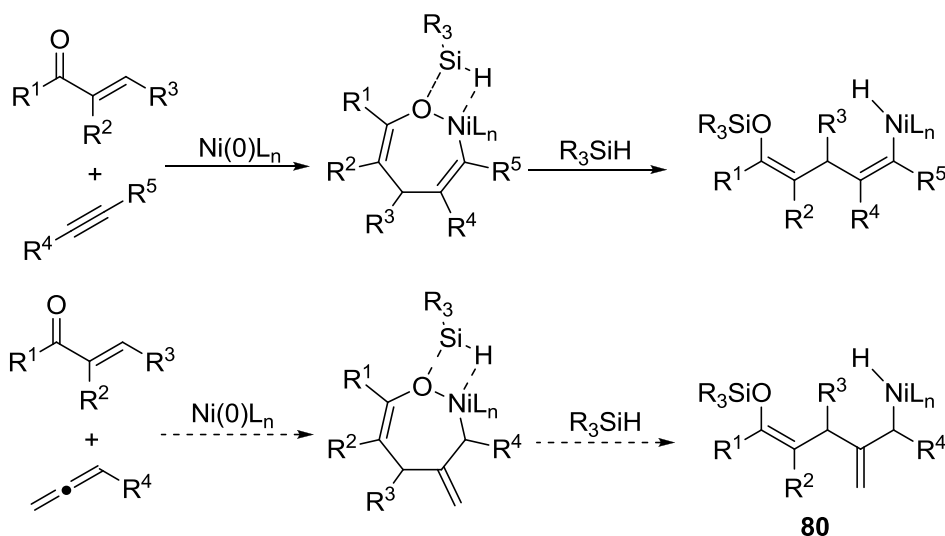


4.3 Hypothesis of using Et₃SiH in Nickel-Catalyzed Enone / Allene Couplings

Although the utilization of Et₃B as a reducing agent did not lead to highly regioselective enone-allene reductive couplings, valuable mechanistic insight was gained, in particular, the possible origin of regiochemical erosion. In addition, we have learned that direct interception of metallacycles derived from enones, allenes and a nickel catalyst by the reducing agent is possible. To improve on the regioselectivity of this enone-allene coupling reaction, we decided to move to the use Et₃SiH as the reducing agent. As discussed in section 1.3.3, our group has disclosed the direct interception of metallacycles generated from enones and alkynes to afford enol silane structures. We envisioned that

enone-allene metallacycles could also proceed efficiently in similar processes (Scheme 52).

Scheme 52. Hypothesis of Interception of Nickellacycles



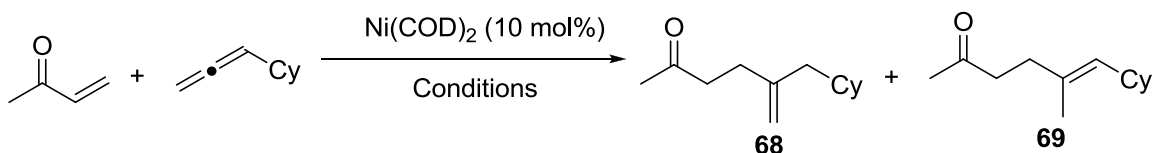
Using this σ -bond metathesis concept, the potential regioisomeric erosion steps are now minimized from four steps in the Et_3B -mediated case to two steps here. Depending on how readily intermediate **80** isomerizes, the control of regioselectivity could be significantly simplified. Since reductive eliminations of a R-Ni-H species are generally considered as fast processes, isomerization from this intermediate is less likely to occur. Therefore, the regioselectivity of this reaction can be simplified to a single mechanistic step, the formation of the metallacycle. The removal of potential isomerization complications motivated us to utilize Et_3SiH as a reducing agent in the enone-allene reductive coupling reactions.

4.4 Regioselective Nickel-Catalyzed Enone-Allene Coupling Reactions

To test this hypothesis, optimization of enone-allene couplings using Et_3SiH was carried out. A few entries of prior Et_3B -mediated reactions were included from Table 7

and **8** to illustrate the difference between the two reducing agents in addition to the role of methanol in the enone-allene reductive coupling reactions (Table 9).⁵⁶ As discussed in the previous sections, presence of Et₃B and/or methanol in the enone-allene coupling reaction produces a mixture of regioisomers (Table 9, entry 1-4, 7). The introduction of Et₃SiH as a reducing agent, however, afforded the desired product **1** in high yield and selectivity upon TBAF work up (Table 9, entry 5). Further optimization revealed toluene as the optimal solvent to afford **68** in 84% yield and 93:7 regioselectivity. While Et₃SiH alone afforded product **68** in high selectivity, the combination of MeOH and Et₃SiH resulted in a mixture of **68** and **69** as predicted. Coupling of an enone and allene using other ligands such PCy₃ or IMes provided lower yields and selectivity.

Table 9. Optimization of the Et₃SiH-Mediate Enone Allene Couplings



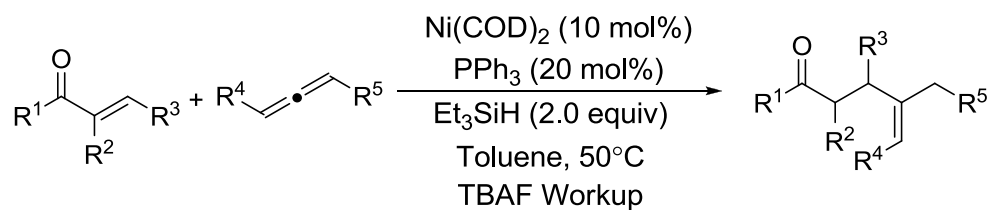
entry	ligand	solvent	reductant	% yield (68:69)
1	PPh ₃	THF	Et ₃ B	39 % (43:57)
2	PPh ₃	THF:MeOH (1:8)	Et ₃ B	73 % (41:59)
3	PCy ₃	THF:MeOH (1:8)	Et ₃ B	71 % (31:69)
4	P(<i>o</i> -tol) ₃	THF:MeOH (1:8)	Et ₃ B	63 % (31:69)
5	PPh ₃	THF	Et ₃ SiH	77 % (93:7)
6	PPh ₃	Toluene	Et ₃ SiH	84 % (93:7)
7	PPh ₃	THF:MeOH (1:8)	Et ₃ SiH	58 % (62:38)
8	PCy ₃	Toluene	Et ₃ SiH	27 % (81:19)
9	IMes	THF	Et ₃ SiH	<10%

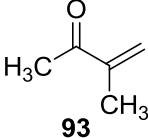
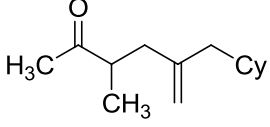
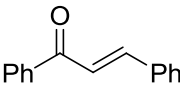
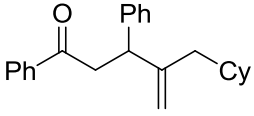
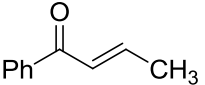
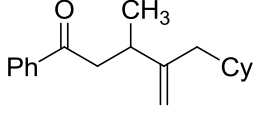
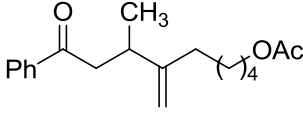
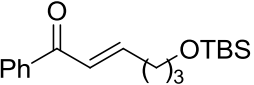
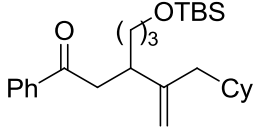

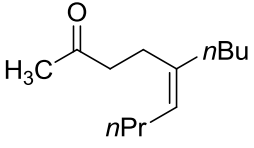
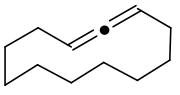
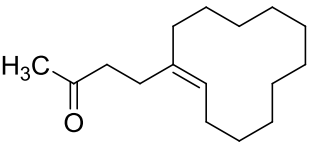
With an optimized procedure developed (Table 9, entry 6), the substrate scope of the enones and allenes was explored. Under the optimized reaction conditions, reductive couplings of methyl vinyl ketone with a variety of allenes were carried out. Allenes with functional groups including aliphatic, aromatic, hydroxy, silyloxy, acetoxy, and ethereal functionalities at remote positions were all efficient coupling partners. While all the allenes are selective towards the desired 1,1-disubstituted alkene products, an allene with a hydroxyl group afforded a mixture of stereoisomeric products. The same rationale of how methanol erodes regioselectivity can also explain the non-regioselective product formation from hydroxy-containing allenes (Table 10).

A variety of enone substrates also underwent efficient coupling with allene **67** in high selectivity. α - and β -Substituted aliphatic and aromatic enones all afforded the desired products in moderate to good yield. While monosubstituted allenes were the primary focus for accessing the 1,1-disubstituted alkene products, we also examined the viability of internal allenes in this reaction. Internal cyclic and acyclic allenes **97** and **98** were indeed efficient coupling partners with MVK. These coupling reactions afforded a mixture of trisubstituted alkenyl diastereomers with the *Z*-alkene stereochemistry being favored (Table 10).

Table 10. Et₃SiH-Mediated Enone-Allene Couplings Substrate Scope

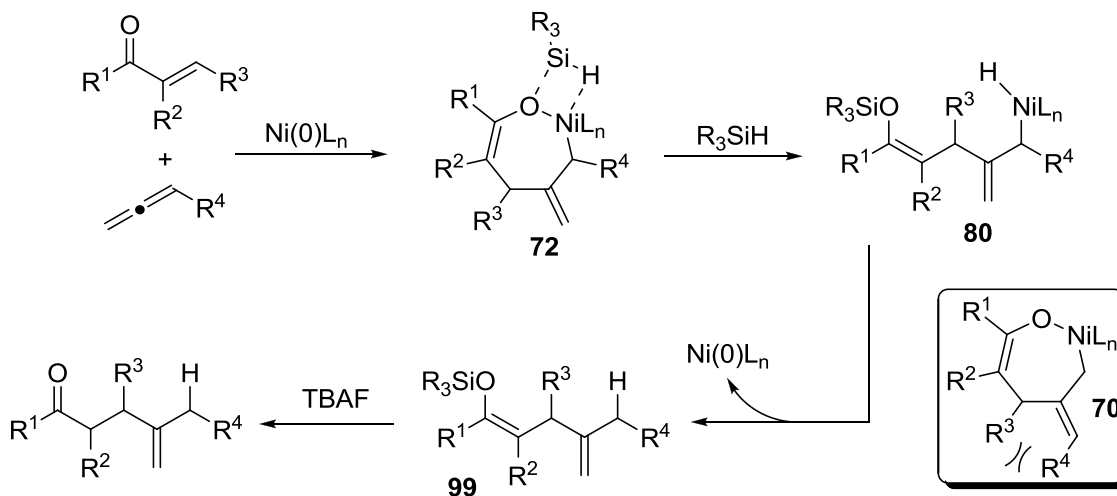
Entry	Enone	Allene	Product yield [%] (isomer ratio)
1			 73 (78:15:7)
2	84		 50 (90:10)
3	84		 85 (>95:5)
4	84		 68 (79:21)
5	84		 85 (78:13:9)
6	84		 63 (79:21)
7			 71 (>95:5)



Entry	Enone	Allene	Product yield [%] (isomer ratio)
8	 93	67	 51 (>95:5)
9	 94	67	 90 (>95:5)
10	 95	67	 72 (93:5:2)
11	95	88	 70 (90:5:5)
12	 96	67	 78 (>95:5)
13	84	 97	 59 (78:22)
14	84	 98	 78 (87:13)

The observed regioselectivity from the substrate studies can be readily rationalized by the formation of the metallacycles derived from C-C bond formation of the allene central carbon. Enones with β -substitution did not favor the formation of metallacycle **70** because of the allylic strain derived from the steric interaction of R^3 and R^4 groups. Based on the product formation, metallacycle **72** is the most likely major metallacycle isomer formed. Selective formation of **72** and subsequent σ -bond metathesis of the Ni-O and Si-H bonds would afford the Ni-H intermediate **80**. Direct reductive elimination from **80** would then afford the enol silane compound **99**, presumably without isomerization from **80**. The 1,1-disubstituted alkene product could then be obtained upon hydrolysis of the enol silane (Scheme 53).

Scheme 53. Proposed Mechanism for Enone-Allene Reductive Couplings



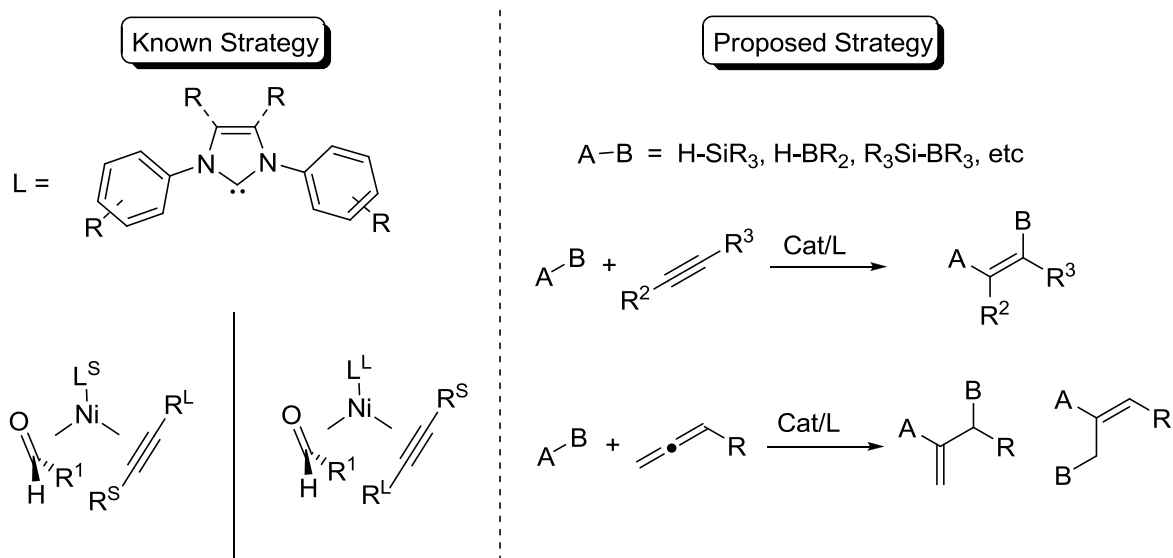
Although isomerization from the Ni-H intermediate **80** is possible, the high regioselectivity observed in most cases strongly suggested that the opportunity for isomerization is minimal. In addition, using hydroxy-containing allenes resulted in formation of a mixture of isomers, which could be readily explained by a fast protonation step of metallacycle **72** with the hydroxyl functionality. This protonation process would

then generate a nickel alkoxy intermediate, which is likely to lead to an isomerization pathway similar to the Et₃B-mediated reactions with methanol as part of the solvent.

4.5 Nickel-Catalyzed Regioselective Allene Hydrosilylation

With the success of regioselective addition of enone functional groups to allenes, we wondered if the regioselective addition of other functional groups to allenes could be achieved. As discussed in section 1.5.3, the Montgomery group has recently demonstrated highly regioselective aldehyde-alkyne reductive couplings through a ligand-controlled strategy. The ligand-controlled strategy involves steric interactions between the ligand and substituents of a five membered metallacycle derived from the nickel catalyst, aldehyde and alkyne. The underlying synthetic significance of this strategy resides in the reversal of regiocontrol of alkyne additions to aldehydes. Through this strategy, we envisioned that regioselective additions of A-B functional groups could be achieved across a variety of unsaturated π -systems (Scheme 54).

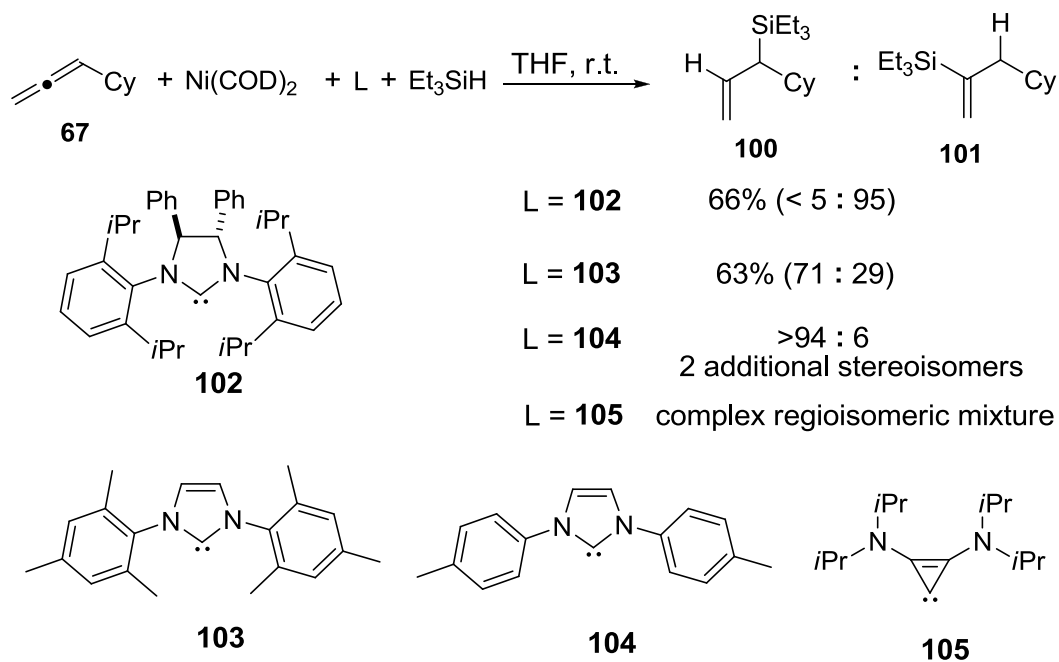
Scheme 54. Proposed Regioselective Addition of A-B Functional Groups



While this proposed strategy lacks the well-organized five-membered cyclic intermediate presented in the aldehyde-alkyne coupling reaction, we thought the potential minimization of steric interactions between the ligand, A-B group and the unsaturated π -component would still determine the regiochemical outcome of the reaction. Although multiple regioisomers could be generated in the case of A-B addition to allenes, selective formation of each regioisomer based on ligand controlled strategy would be particularly impressive and useful entries to variable alkene structures. With this goal in mind, we decided to study the hydrosilylation of allenes as an entry point.

A 2 hour syringe drive addition of a solution of allene **67** in THF to a mixture of $\text{Ni}(\text{COD})_2$, IMes and Et_3SiH afforded a regioisomeric mixture of **100** and **101** in 63% yield. Both products were derived from the addition of Et_3SiH to the internal double bond of the allene (Scheme 55).

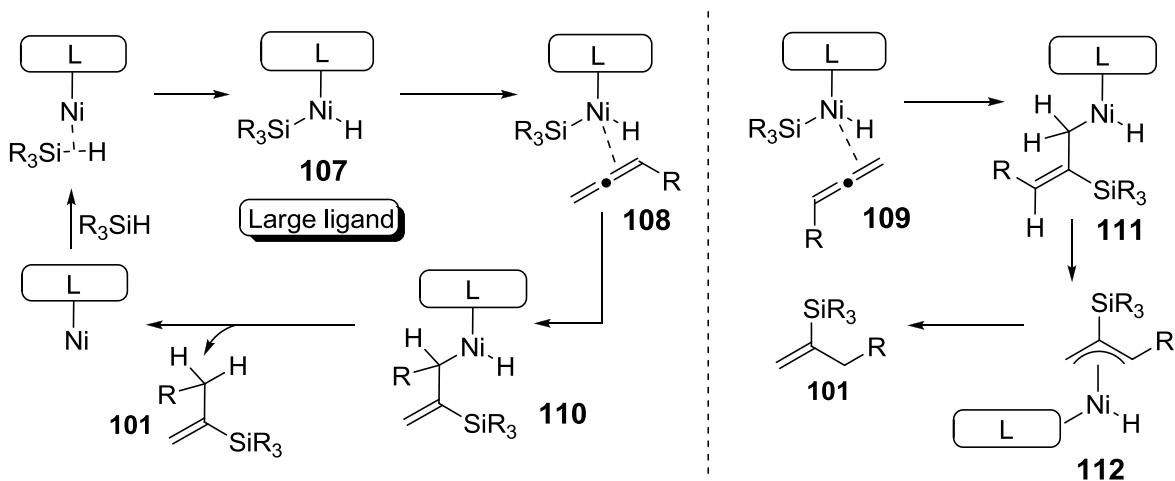
Scheme 55. Ligand-Control Regioselective Allene Hydrosilylation



Although disappointed to obtain a mixture of two products, we were excited that out of six possible isomers, only two regioisomers were formed. Based on this result, we carried out this allene hydrosilylation with a large ligand NHC ligand **102**. Surprisingly, only product **100** was formed in 66% yield and >95:5 regioselectivity. Utilizing a small ligand **104** resulted in the reversal of regioselectivity regarding the formation of products **100** and **101**. However, two additional isomers were formed in addition to **100** and **101**. An even smaller ligand **106** afforded a complex mixture of diastereomers and was completely nonselective in product formation. This allene hydrosilylation project is currently being studied by Zachary Miller from our group to selectively form both product **100** and **101** in high regioselectivity.

Based on the preliminary data observed, two possible mechanisms were proposed to account for the regioselectivities. The first possible mechanism to rationalize the regioselectivity is based on a regioselective insertion step from **108** to **110**. The second potential mechanism is based on a regioselective reductive elimination process from π -allyl intermediate **112**. (Scheme 36)

Scheme 56. Large Ligand Influence on Regioselectivity



The initial step of this reaction is likely the insertion of the nickel catalyst into the Si-H bond to generate intermediate **107**. This intermediate can bind to the allene through either the internal or the terminal double bond. If binding to the internal double bond occurs, for large ligands, **108** is the most likely intermediate to minimize steric interactions between the R₃Si group and the allene substituent R. Insertion of the silyl group to the electrophilic allene central carbon, followed by a fast reductive elimination from **110** can form the product **101**. The presence of a large ligand on the nickel catalyst can exacerbate potential steric interactions between R₃Si and R, thus resulting in good regioselectivity. If binding to the terminal double bond occurs, insertion of the silyl group to the allene central carbon can occur to generate **111**. Isomerization of **111** can result in a π -allyl intermediate **112**. The regioselectivity most likely arises from the minimization of steric interactions between the ligand and the allene substituent R. The presence of small ligands in either mechanism can result in poor regioselectivity because of poor minimization of steric interactions during the key steps. These two possible mechanisms generate a preliminary discussion point for rationalizing the regioselectivities observed.

To summarize, a highly regioselective nickel-catalyzed enone-allene reductive coupling process was developed to generate very useful 1,1-disubstituted alkene products that complement existing reductive coupling methods. Highly regioselective allene hydrosilylation protocols have been initiated and are currently being developed by Zachary Miller to generate useful vinyl silane and allyl silane structures. While the regiochemical outcome in the enone-allene reductive coupling process has shown high

dependence on the reducing agent choice, ligand control could instead influence the regiochemical outcome in the allene hydrosilylation reactions.

To summarize the overall work in this thesis, we have introduced mild and inexpensive alcohol reducing agents in nickel-catalyzed reductive coupling reactions in chapter 2. These alcohol reducing agents are practical alternatives to the currently used reducing agents. In addition, we have discovered the potential to utilize primary alcohols as synthetic precursors for aldehydes in nickel-catalyzed reductive couplings. In chapter 3, we have observed divergent enal-alkyne coupling pathways based on triaryl phosphine ligand structure. We have disclosed a novel enal-alkyne alkylative coupling reaction, and utilized stable triaryl phosphines as practical alternatives to the air sensitive PBU_3 for [3+2] enal-alkyne reductive cycloaddition reactions. We have also uncovered an internal redox reaction of enals, alkynes and methanol. This internal redox reaction demonstrated an interesting mechanistic departure from reductive coupling reactions. In chapter 4, we have developed a highly regioselective nickel-catalyzed enone-allene reductive coupling process to generate very useful 1,1-disubstituted alkene products that complement existing reductive coupling methods. In addition, a highly regioselective allene hydrosilylation reaction was discovered based on a ligand control strategy. In broader terms, we have elucidated the role and influence of reducing agents across several coupling reactions. We hope such clarification can lead to new reaction design and discovery.

Chapter 5: Experimental Section

5.1 Experimental Procedures and Spectra Data: Chapter 2

All reagents were used as received unless otherwise noted. Solvents were purified under nitrogen using a solvent purification system (Innovative Technology, inc., Model # SPS-400-3 and PS-400-3). Enals were distilled prior to use. Tributylphosphine (PBU₃) was freshly distilled and stored in an inert atmosphere schlenk tube. Ni(COD)₂ (Strem Chemicals, Inc., used as received), triphenylphosphine (PPh₃) and tricyclohexylphosphine (PCy₃) were stored and weighed in an inert atmosphere glovebox. All reactions were conducted in flame-dried glassware under a nitrogen atmosphere. ¹H and ¹³C spectra were obtained in CDCl₃ at rt, unless otherwise noted, on a Varian Mercury 400 or Varian Unity 500 MHz instrument. Chemical shifts of ¹H NMR spectra were recorded in parts per million (ppm) on the δ scale from an internal standard of residual chloroform (7.27 ppm). Chemical shifts of ¹³C NMR spectra were recorded in ppm from the central peak of CDCl₃ (77.0 ppm) on the δ scale. High resolution mass spectra (HRMS) were obtained on a VG-70-250-s spectrometer manufactured by Micromass Corp. (Manchester UK) at the University of Michigan Mass Spectrometry Laboratory.

Regioisomeric ratios were determined on crude reaction mixtures using NMR or GC methods. GC with FID detection were carried on an Agilent 6890N Network GC System with a HP-5MS column (30m x 0.252mm x 0.25 μ m). GCMS analyses were carried out on an HP6890 Series GC System with a HP-5MS column (30m x 0.252 mm x 0.25 μ m). The trisubstituted alkene stereochemistry was determined by NOE in the following cases: Table 1, entries 4 and 7.

5.1.1 General Procedure A for the Ni(COD)₂/PBU₃ Promoted Reductive Coupling of Enones and Alkynes using Et₃B as the Reducing Agent.

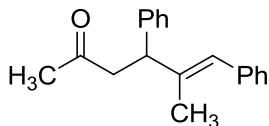
To a solution of Ni(COD)₂ (0.1 equiv) in THF (0.6 mL) was added dropwise tributylphosphine (PBU₃) (0.2 equiv) at rt. After stirring for 5-10 min at rt, the reaction mixture became bright yellow. A solution of enone (1.0 equiv) and alkyne (1.5 equiv) at rt in MeOH (4.4 mL) was added, and then Et₃B (3.0 equiv) was added. The reaction mixture was stirred at 50 °C until TLC analysis indicated disappearance of the enone. The reaction mixture was quenched with a saturated aqueous solution of NH₄Cl and extracted three times with diethyl ether. The combined organic layers were washed with brine, dried over magnesium sulfate, filtered, and concentrated, and the residue was purified by column chromatography on silica gel.

5.1.2 General Procedure B for the Ni(COD)₂ / PCy₃ Catalyzed Reductive Coupling of Enones and Alkynes using MeOH as the Reducing Agent

THF (0.5 mL) was added to a solid mixture of Ni(COD)₂ (0.1 equiv) and ligand (0.2 equiv) at rt. The resulting solution was stirred for 5 min. Then a solution of enone

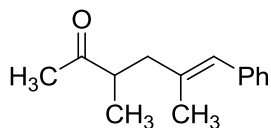
(1 equiv) and alkyne (1.5 equiv) in methanol (4 mL) was added. With terminal alkynes, a solution of enone (1 equiv) in methanol (2 mL) was added, followed by syringe addition of the alkyne (1.5 equiv) as a solution in methanol (2 mL) at 50 °C. The reaction mixture was stirred at 50 °C until TLC analysis indicated the disappearance of the enone. The reaction was quenched with saturated solution of NH₄Cl, extracted with ethyl acetate, washed with brine, dried over MgSO₄ and concentrated. The residue was purified via flash chromatography (SiO₂) to afford the desired product.

(E)-5-Methyl-4,6-diphenylhex-5-en-2-one (Table 1, entry 1)



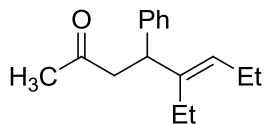
Following the general procedure **B**, benzylideneacetone (44 mg, 0.3 mmol), 1-phenyl-1-propyne (52 mg, 0.45 mmol), Ni(COD)₂ (8 mg, 0.03 mmol) and PCy₃ (17 mg, 0.06 mmol) were stirred for 3 h at 50 °C. The product (68 mg, 86%, >95:5) was afforded as a clear liquid after SiO₂ chromatography (5% EtOAc in hexanes). ¹H NMR (400 MHz, CDCl₃) δ 7.22 (m, 10H), 6.42 (s, 1H), 3.98 (t, *J* = 7.6 Hz, 1H), 3.02 (dd, *J* = 7.6, 16.0 Hz, 1H), 2.93 (dd, *J* = 7.6, 16.0 Hz, 1H), 2.09 (s, 3H), 1.69 (d, *J* = 1.2 Hz, 3H); ¹³C NMR (100 MHz, CDCl₃) δ 207.2, 142.2, 139.9, 137.9, 128.9, 128.4, 128.0, 127.7, 126.6, 126.2, 125.2, 49.5, 47.5, 30.5, 16.8; IR (film, cm⁻¹) 3024, 2915, 1714, 1492; HRMS (ESI) *m/z* calcd for C₁₉H₂₀O [M⁺] 264.1514, found 264.1514.

(E)-3,5-Dimethyl-6-phenylhex-5-en-2-one (Table 1, entry 2)



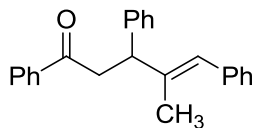
Following the general procedure **B**, 3-methyl-3-buten-2-one (25 mg, 0.3 mmol), 1-phenyl-1-propyne (52 mg, 0.45 mmol), Ni(COD)₂ (8 mg, 0.03 mmol) and PCy₃ (17 mg, 0.06 mmol) were stirred for 3 h at 50 °C. The product (38 mg, 63%, 94:6) was afforded as a light yellow oil after SiO₂ chromatography (10% EtOAc in hexanes). Spectral data for this compound was previously reported and matched with current data.⁵⁷

(E)-5-Ethyl-4-phenyloct-5-en-2-one (Table 1, entry 3)



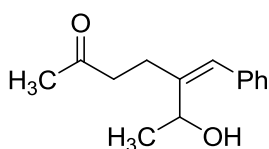
Following the general procedure **B**, benzylideneacetone (44 mg, 0.3 mmol), 3-hexyne (37 mg, 0.45 mmol), Ni(COD)₂ (8 mg, 0.03 mmol) and PCy₃ (17 mg, 0.06 mmol) were stirred for 3 h at 50 °C. The product (62 mg, 90%) was afforded as a clear liquid after SiO₂ chromatography (5% EtOAc in hexanes). Spectral data for this compound was previously reported and matched with the current data.⁵⁸

(E)-4-Methyl-1,3,5-triphenylpent-4-en-1-one (Table 1, entry 4)



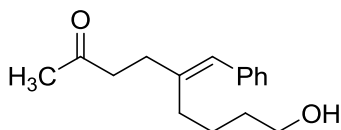
Following the general procedure **B**, *trans*-Chalcone (62 mg, 0.3 mmol) with THF (0.5 mL), 1-phenyl-1-propyne (52 mg, 0.45 mmol), Ni(COD)₂ (8 mg, 0.03 mmol) and PCy₃ (17 mg, 0.06 mmol) were stirred overnight at 50 °C. The product (90 mg, 93%, >95:5) was afforded as a clear liquid after SiO₂ chromatography (5% EtOAc in hexanes). Spectral data for this compound was previously reported and matched with current data.⁵⁷

(Z)-5-Benzylidene-6-hydroxyheptan-2-one (Table 1, entry 5)



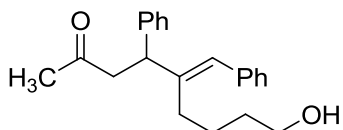
Following the general procedure **B**, 3-buten-2-one (21 mg, 0.3 mmol), 4-phenylbut-3-yn-2-ol (66 mg, 0.45 mmol), Ni(COD)₂ (8 mg, 0.03 mmol) and PPh₃ (16 mg, 0.06 mmol) were stirred for 3 h at 50 °C. The product (46 mg, 70%, >95:5) was afforded as a light yellow oil after SiO₂ chromatography (25% EtOAc in hexanes). ¹H NMR (400 MHz, CDCl₃) δ 7.27 (t, *J* = 7.6 Hz, 2H), 7.18 (t, *J* = 7.2 Hz, 1H), 7.11 (d, *J* = 7.6 Hz, 2H), 6.26 (s, 1H), 4.85 (q, *J* = 6.4 Hz, 1H), 2.77 (m, 2H), 2.60 (m, 1H), 2.37 (m, 1H), 2.23 (bs, 1H), 2.15 (s, 3H), 1.28 (d, *J* = 6.4 Hz, 3H); ¹³C NMR (100 MHz, CDCl₃) δ 209.0, 143.8, 136.9, 128.6, 128.1, 126.6, 126.5, 65.8, 43.3, 30.0, 23.6, 21.7; IR (film, cm⁻¹) 3408, 2971, 1710; HRMS (ESI) *m/z* calcd for C₁₄H₁₈O₂Na [M+Na]⁺ 241.1204, found 241.1214.

(E)-5-Benzylidene-9-hydroxynonan-2-one (Table 1, entry 6)



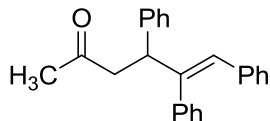
Following the general procedure **B**, 3-buten-2-one (21 mg, 0.3 mmol), 6-phenylhex-5-yn-1-ol (78 mg, 0.45 mmol), Ni(COD)₂ (8 mg, 0.03 mmol) and PPh₃ (16 mg, 0.06 mmol) were stirred for 4 h at 50 °C. The product (56 mg, 76%, >95:5) was afforded as a clear liquid after SiO₂ chromatography (30% EtOAc in hexanes). ¹H NMR (400 MHz, CDCl₃) δ 7.19 (m, 5H), 6.22 (s, 1H), 3.54 (m, 2H), 2.62 (m, 2H), 2.40 (m, 2H), 2.19 (m, 2H), 2.14 (s, 3H), 1.55 (bs, 1H), 1.49 (m, 4H); ¹³C NMR (100 MHz, CDCl₃) δ 208.4, 141.5, 138.0, 128.5, 128.0, 126.1, 125.5, 62.4, 42.3, 32.4, 30.6, 30.3, 29.9, 24.2; IR (film, cm⁻¹) 3414, 2933, 1713, 1443; HRMS (ESI) *m/z* calcd for C₁₆H₂₂O₂Na [M+Na]⁺ 269.1517, found 269.1528.

(E)-5-Benzylidene-9-hydroxyl-4-phenylnonan-2-one (Table 1, entry 7)



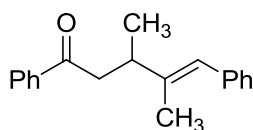
Following the general procedure **B**, benzylideneacetone (44 mg, 0.6 mmol), 6-phenylhex-5-yn-1-ol (78 mg, 0.3 mmol), Ni(COD)₂ (8 mg, 0.03 mmol) and PCy₃ (17 mg, 0.06 mmol) were stirred for 4 h at 50 °C. The product (56 mg, 58%, >95:5) was afforded as a light yellow oil after SiO₂ chromatography (5% EtOAc in hexanes). ¹H NMR (500 MHz, CDCl₃) δ 7.27 (m, 10H), 6.42 (s, 1H), 4.08 (t, *J* = 7.5 Hz, 1H), 3.51 (m, 2H), 3.09 (dd, *J* = 7.5, 16.5 Hz, 1H), 2.90 (dd, *J* = 7.5, 16.5 Hz, 1H), 2.32 (m, 1H), 2.10 (s, 3H), 1.87 (m, 1H), 1.40 (m, 5H); ¹³C NMR (100 MHz, CDCl₃) δ 207.2, 144.3, 142.7, 137.9, 128.6, 128.5, 128.1, 127.9, 126.6, 126.3, 124.9, 62.3, 48.6, 46.0, 32.4, 30.7, 30.4, 24.3; IR (film, cm⁻¹) 3405, 2930, 2862, 1714, 1451; HRMS (ESI) *m/z* calcd for C₂₂H₂₆O₂Na [M+Na]⁺ 345.1830, found 345.1823.

(Z)-4,5,6-Triphenylhex-5-en-2-one (Table 1, entry 8)



Following the general procedure **B**, benzylideneacetone (44 mg, 0.3 mmol), diphenylacetylene (80 mg, 0.45 mmol) with THF (0.5 mL), Ni(COD)₂ (8 mg, 0.03 mmol) and PCy₃ (17 mg, 0.06 mmol) were stirred for 3 h at 50 °C. The product (65 mg, 66%) was afforded as a light yellow oil after SiO₂ chromatography (5% EtOAc in hexanes). ¹H NMR (500 MHz, CDCl₃) δ 7.09 (m, 15H), 6.53 (s, 1H), 4.40 (t, *J* = 7.5 Hz, 1H), 3.09 (dd, *J* = 7.5, 17.0 Hz, 1H), 2.98 (dd, *J* = 8.0, 17.0 Hz, 1H), 2.12 (s, 3H); ¹³C NMR (125 MHz, CDCl₃) δ 206.7, 144.5, 141.5, 140.2, 136.8, 129.1, 129.0, 128.4, 128.3, 128.1, 127.7, 127.1, 127.0, 126.6, 126.4, 49.6, 47.5, 30.5; IR (film, cm⁻¹) 3025, 1667, 1449; HRMS (ESI) *m/z* calcd for C₂₄H₂₂ONa [M+Na]⁺ 349.1568, found 349.1571.

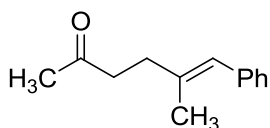
(Z)-3,4-Dimethyl-1,5-diphenylpent-4-en-1-one (Table 1, entry 9)



Following the general procedure **B**, phenyl 1-propenyl ketone (43 mg, 0.3 mmol), 1-phenyl-1-propyne (52 mg, 0.45 mmol), Ni(COD)₂ (8 mg, 0.03 mmol) and PCy₃ (17 mg, 0.06 mmol) were stirred for 3 h at 50 °C. The product (97 mg, 93%, >95:5) was afforded as a light yellow oil after SiO₂ chromatography (5% EtOAc in hexanes). ¹H NMR (400 MHz, CDCl₃) δ 7.93 (d, *J* = 8.4 Hz, 2H), 7.52 (tt, *J* = 1.2, 8.4 Hz, 1H), 7.43 (t, *J* = 8.0

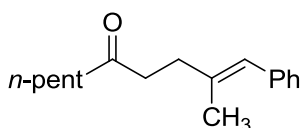
Hz, 2H), 7.26 (t, $J = 8.0$ Hz, 2H), 7.15 (d, $J = 8.0$ Hz, 3H), 6.28 (s, 1H), 3.15 (m, 1H), 2.99 (m, 2H), 1.83 (d, $J = 1.2$ Hz, 3H), 1.16 (d, $J = 6.4$ Hz, 3H); ^{13}C NMR (100 MHz, CDCl_3) δ 199.6, 141.9, 138.2, 137.3, 132.9, 128.8, 128.5, 128.0, 127.9, 125.9, 124.5, 44.3, 39.5, 19.4, 15.1; IR (film, cm^{-1}) 3055, 2961, 1683, 1447; HRMS (ESI) m/z calcd for $\text{C}_{19}\text{H}_{20}\text{ONa}$ $[\text{M}+\text{Na}]^+$ 287.1412, found 287.1410.

(E)-5-Methyl-6-phenylhex-5-en-2-one (Table 1, entry 10)



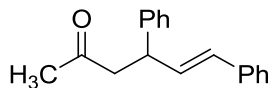
Following the general procedure **B**, 3-buten-2-one (21 mg, 0.3 mmol), 1-phenyl-1-propyne (52 mg, 0.45 mmol), $\text{Ni}(\text{COD})_2$ (8 mg, 0.03 mmol) and PPh_3 (16 mg, 0.06 mmol) were stirred for 3 h at 50 °C. The product (47 mg, 83%, 93:7) was afforded as a light yellow oil after SiO_2 chromatography (5% EtOAc in hexanes). Spectral data for this compound was previously reported and matched with the current data.⁵⁷

(E)-2-Methyl-1-phenyldec-1-en-5-one (Table 1, entry 11)



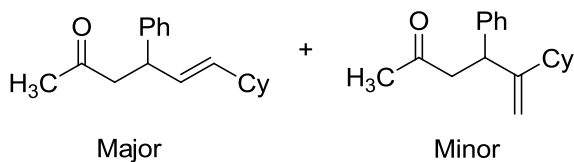
Following the general procedure **B**, 1-octen-3-one (38 mg, 0.3 mmol), 1-phenyl-1-propyne (52 mg, 0.45 mmol), $\text{Ni}(\text{COD})_2$ (8 mg, 0.03 mmol) and PPh_3 (16 mg, 0.06 mmol) were stirred for 3 h at 50 °C. The product (59 mg, 81%, 92:8) was afforded as a light yellow oil after SiO_2 chromatography (10% EtOAc in hexanes). Spectral data for this compound was previously reported and matched with the current data.⁵⁷

(E)-4,6-Diphenylhex-5-en-2-one (Table 1, entry 12)



Following the general procedure **B**, benzylideneacetone (44 mg, 0.3 mmol), phenylacetylene (46 mg, 0.45 mmol), Ni(COD)₂ (8 mg, 0.03 mmol) and PCy₃ (17 mg, 0.06 mmol) were stirred for 4 h at 50 °C. The product (70 mg, 93%, 95:5) was afforded as a light yellow oil after SiO₂ chromatography (5% EtOAc in hexanes). Spectral data for this compound was previously reported and matched with the current data.⁵⁸ Characteristic ¹H NMR signals for minor regioisomer: δ 5.40 (s, 1H), 5.10 (s, 1H), 4.51 (t, *J* = 7.5 Hz, 1H).

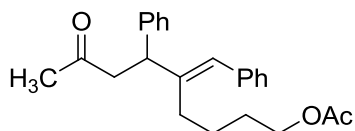
(E)-6-Cyclohexyl-4-phenylhex-5-en-2-one (Table 1, entry 13)



General procedure **B** was followed with the following modification: THF (0.5 mL) was added to a solid mixture of Ni(COD)₂ (8 mg, 0.03 mmol), IMes·HCl (11 mg, 0.03 mmol) and potassium *t*-butoxide (4 mg, 0.03 mmol) at rt. The resulting dark solution was stirred for 5 min. Then a solution of benzylideneacetone (44 mg, 0.3 mmol) in methanol (2 mL) was added, followed by syringe addition of cyclohexylacetylene (52 mg, 0.45 mmol) in methanol (2 mL) at 50 °C. The reaction mixture was stirred for 4 h at 50 °C. The product (36 mg, 47%, 75:25) was afforded as a light yellow oil after SiO₂ chromatography (5% EtOAc in hexanes). ¹H NMR (400 MHz, CDCl₃) δ 7.20 (m, 5H_{maj}+5H_{min}), 5.47 (ddd, *J* =

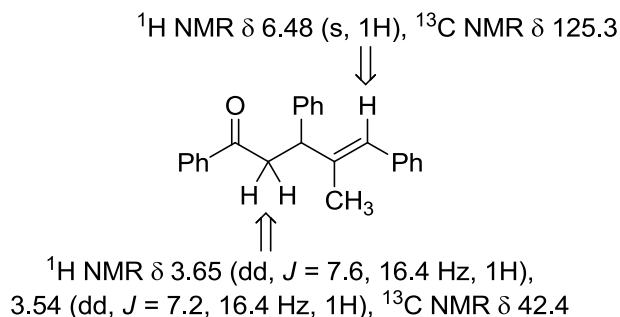
0.8, 7.2, 16.4 Hz, 1H_{maj}), 5.36 (dd, $J = 6.4, 15.6$ Hz, 1H_{maj}), 4.91 (s, 1H_{min}), 4.84 (s, 1H_{min}), 3.88 (t, $J = 7.6$ Hz, 1H_{min}), 3.78 (q, $J = 7.2$ Hz, 1H_{maj}), 2.90 (dd, $J = 7.6, 16.4$ Hz, 1H_{min}), 2.75 (m, 2H_{maj}), 2.75 (m, 1H_{min}), 2.03(s, 3H_{maj}), 2.00 (s, 3H_{min}), 1.86 (m, 1H_{maj} + 1H_{min}), 1.55 (m, 4H_{maj} + 4H_{min}), 0.93-1.26 (m, 6H_{maj} + 6H_{min}); ¹³C NMR (100 MHz, CDCl₃) δ 207.4, 207.3, 156.7, 143.8, 142.9, 136.8, 129.5, 128.4, 128.3, 127.9, 127.4, 126.4, 126.3, 107.3, 49.9, 49.3, 45.8, 43.9, 43.7, 40.5, 33.6, 33.0, 32.9, 32.5, 30.6, 30.5, 26.8, 26.6, 26.2, 26.1, 25.9; IR (film, cm⁻¹) 2924, 2851, 1718, 1449; HRMS (ESI) m/z calcd for C₁₈H₂₄ONa [M+Na]⁺ 279.1725, found 279.1715.

(E)-5-Benzylidene-8-oxyl-6-phenylonyl-acetate (Table 1, entry 14)

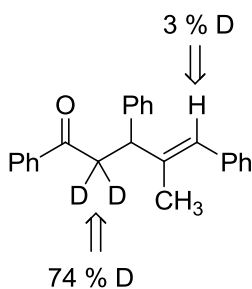


Following the general procedure **B**, benzylideneacetone (44 mg, 0.6 mmol), 6-phenylhex-5-ynyl acetate (98 mg, 0.45 mmol), Ni(COD)₂ (8 mg, 0.03 mmol) and PCy₃ (17 mg, 0.06 mmol) were stirred for 4 h at 50 °C. The product (51 mg, 47%, >95:5; and 13mg, 13%, >95:5 was obtained as the deacylated product) was afforded as a clear liquid after SiO₂ chromatography (20% EtOAc in hexanes). ¹H NMR (400 MHz, CDCl₃) δ 7.22 (m, 10H), 6.39 (s, 1H), 4.01 (t, $J = 7.6$ Hz, 1H), 3.89 (t, $J = 6.0$ Hz, 2H), 3.03 (dd, $J = 7.6, 16.4$ Hz, 1H), 2.87 (dd, $J = 7.6, 16.4$ Hz, 1H), 2.27 (m, 1H), 2.05 (s, 3H), 1.96 (s, 3H), 1.85 (m, 1H), 1.43 (m, 4H); ¹³C NMR (100 MHz, CDCl₃) δ 206.9, 171.0, 144.2, 142.6, 137.8, 128.6, 128.5, 128.1, 127.9, 126.7, 126.4, 125.1, 64.0, 48.6, 46.2, 30.7, 30.4, 28.4, 24.6, 20.9; IR (film, cm⁻¹) 2922, 1737, 1598; HRMS (ESI) m/z calcd for C₂₄H₂₈O₃Na [M+Na]⁺ 387.1936, found 387.1940.

Undeuterated Standard for Deuterium Labelling Study (from Table 1, entry 4 and Scheme 34)

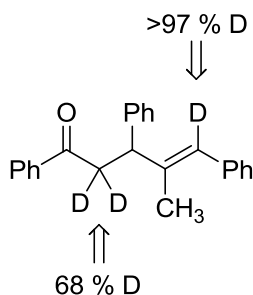


Deuterium Labelling Study with PBu_3 , Et_3B and CD_3OD



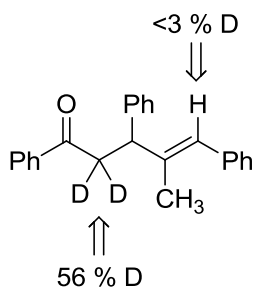
Following the general procedure **A**, *trans*-chalcone (62 mg, 0.30 mmol), 1-phenyl-1-propyne (52 mg, 0.45 mmol), $\text{Ni}(\text{COD})_2$ (8 mg, 0.03 mmol), PBu_3 (16 μL , 0.06 mmol), and Et_3B (130 μL , 0.90 mmol) were stirred for 12 h at 50 $^\circ\text{C}$. The product (44 mg, 45 %) was obtained as a colorless oil after SiO_2 chromatography (5% EtOAc in hexanes). $^1\text{H NMR}$ (400 MHz, CDCl_3) δ 7.91 (m, 2H), 7.52 (m, 1H), 7.42 (m, 2H), 7.21 (m, 10H), 6.41 (s, 1H), 4.19 (d, $J = 7.2$ Hz, 1H), 3.54 (d, $J = 7.2$ Hz, 0.52H), 1.73 (d, $J = 1.2$ Hz, 3H); $^{13}\text{C NMR}$ (125 MHz, CDCl_3) δ 198.6, 142.5, 139.9, 137.9, 137.2, 132.9, 128.9, 128.5, 128.4, 128.0, 127.9, 127.8, 126.5, 126.1, 125.3, 49.5, 16.9; IR (film, cm^{-1}) 3058, 2916, 1682, 1448; HRMS (ESI) m/z calcd for $\text{C}_{24}\text{H}_{21}\text{DONa}$ $[\text{M}+\text{Na}]^+$ 350.1631, found 350.1624.

Deuterium Labelling Study with PCy₃ and CD₃OD



Following the general procedure **B**, *trans*-Chalcone (62 mg, 0.3 mmol), 1-phenyl-1-propyne (52 mg, 0.45 mmol), Ni(COD)₂ (8 mg, 0.03 mmol) and PCy₃ (17 mg, 0.06 mmol) were stirred overnight at 50 °C. The product (53 mg, 54%) was afforded as a clear liquid after SiO₂ chromatography (5% EtOAc in hexanes). ¹H NMR (400 MHz, CDCl₃) δ 7.92 (m, 2H), 7.52 (m, 1H), 7.42 (m, 2H), 7.22 (m, 10H), 4.19 (d, *J* = 7.2 Hz, 1H), 3.54 (d, *J* = 7.2 Hz, 0.63H), 1.74 (d, *J* = 1.2 Hz, 3H); ¹³C NMR (100 MHz, CDCl₃) δ 198.6, 142.5, 139.9, 139.8, 137.9, 137.2, 132.9, 128.9, 128.5, 128.4, 128.0, 127.9, 127.8, 126.5, 126.1, 49.6, 42.1, 16.9; IR (film, cm⁻¹) 3057, 2914, 1683, 1447; HRMS (ESI) *m/z* calcd for C₂₄H₂₀D₂ONa [M+Na]⁺ 351.1691, found 351.1693.

Deuterium Labelling Study with PCy₃ and CH₃OD



Following the general procedure **B**, *trans*-Chalcone (62 mg, 0.3 mmol), 1-phenyl-1-propyne (52 mg, 0.45 mmol), Ni(COD)₂ (8 mg, 0.03 mmol) and PCy₃ (17 mg, 0.06 mmol)

were stirred overnight at 50 °C. The product (79 mg, 81%) was afforded as a clear liquid after SiO₂ chromatography (5% EtOAc in hexanes). ¹H NMR (400 MHz, CDCl₃) δ 7.91 (m, 2H), 7.52 (m, 1H), 7.42 (m, 2H), 7.22 (m, 10H), 6.42 (s, 1H), 4.19 (d, *J* = 7.6 Hz, 1H), 3.54 (d, *J* = 7.6 Hz, 0.88 H), 1.73 (d, *J* = 1.2 Hz, 3H); ¹³C NMR (100 MHz, CDCl₃) δ 198.6, 142.5, 140.0, 137.9, 137.2, 132.9, 128.9, 128.5, 128.4, 128.0, 127.9, 127.8, 126.5, 126.1, 125.3, 49.6, 42.1, 17.0; IR (film, cm⁻¹) 3058, 2928, 1684, 1447; HRMS (ESI) *m/z* calcd for C₂₄H₂₁DO₂Na [M+Na]⁺ 350.1631, found 350.1633.

5.2 Experimental Procedures and Spectra Data: Chapter 3

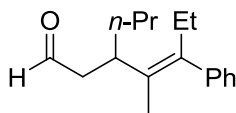
All reagents were used as received unless otherwise noted. All enals were distilled using a Büchi GKR-51 Kugelrohr instrument, stored in a vial under nitrogen environment and used immediately after distillation. Solvents were purified under nitrogen using a solvent purification system (Innovative Technology, inc., Model # SPS-400-3 and PS-400-3). Ni(COD)₂ (Strem Chemicals, Inc., used as received), 1,3-Bis(2,6-di-*iso*-propylphenyl) imidazolium chloride (IPr·HCl), all phosphine ligands and potassium *tert*-butoxide were stored and weighed in an inert atmosphere glovebox. All reactions were conducted in flame-dried glassware under a nitrogen atmosphere. ¹H and ¹³C spectra were obtained in CDCl₃ at rt, unless otherwise noted, on a Varian Mercury 400 or Varian Unity 500 MHz instrument. Chemical shifts of ¹H NMR spectra were recorded in parts per million (ppm) on the δ scale from an internal standard of residual chloroform (7.27 ppm). Chemical shifts of ¹³C NMR spectra were recorded in ppm from the central peak of CDCl₃ (77.0 ppm) on the δ scale. High resolution mass spectra (HRMS) were obtained on a VG-70-250-s spectrometer manufactured by Micromass Corp. (Manchester UK) at the University of Michigan Mass Spectrometry Laboratory.

Diastereomeric ratios and Regioisomeric ratios were determined on crude reaction mixtures using NMR and/or GCMS. GCMS analyses were carried out on an HP6890 Series GC System with a HP-5MS column (30m x 0.252 mm x 0.25 μ m). Stereochemistry was determined by NOE in the following case: Table 5, entries 4. The alkene stereochemistry was determined by NOE in the following cases: Table 6, entry 4.

5.2.1 General Procedure for the Ni(COD)₂/Phosphine Promoted Reductive Cycloadditions and Alkylative Couplings of Enals and Alkynes

To a solid mixture of Ni(COD)₂ (0.03 mmol) and monodentate phosphine ligand (0.06 mmol) was added THF (0.6 mL) at rt. After stirring for 5-10 min at rt, enal (0.3 mmol), alkyne (0.45 mmol), MeOH (4.4 mL) and Et₃B (0.9 mmol) were sequentially added at rt. The reaction mixture was then stirred at 50 °C until TLC analysis indicated disappearance of the enal. The reaction mixture was concentrated *in vacuo*. The residue was purified by column chromatography on silica gel to afford the desired product.

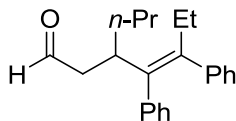
(*E*)-4-methyl-5-phenyl-3-propylhept-4-enal (Table 4, entry 1)



Following the general procedure, *trans*-2-hexen-1-al (35 μ L, 0.30 mmol), 1-phenyl-1-propyne (56 μ L, 0.45 mmol), Ni(COD)₂ (8 mg, 0.03 mmol), P(*o*-tol)₃ (18 mg, 0.06 mmol), and Et₃B (130 μ L, 0.90 mmol) were stirred for 5 h at 50 °C. The product (56 mg, 76 %) was obtained as a colorless oil after SiO₂ chromatography (3 % ethyl acetate in hexanes). ¹H NMR (500 MHz, CDCl₃) δ 9.77 (t, *J* = 2.0 Hz, 1H), 7.33-7.02 (m, 5H), 3.34 (quint, *J* = 2.0 Hz, 1H), 2.48 (m, 2H), 2.41 (m, 2H), 1.47-1.26 (m, 4H), 1.35 (s, 3H),

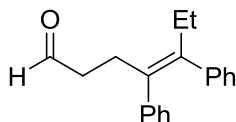
0.96 (t, $J = 7.5$ Hz, 3H), 0.87 (t, $J = 7.5$ Hz, 3H); ^{13}C NMR (125 MHz, CDCl_3) δ 202.6, 143.7, 140.0, 130.3, 128.8, 127.9, 125.9, 47.8, 35.6, 35.3, 26.9, 20.6, 14.3, 14.0, 13.1; GCMS (EI) m/z calcd for $\text{C}_{17}\text{H}_{24}\text{O}$ $[\text{M}]^+$ 244, found 244.

(Z)-4,5-diphenyl-3-propylhept-4-enal (Table 4, entry 2)



Following the general procedure, *trans*-2-hexen-1-al (35 μL , 0.30 mmol), diphenylacetylene (80 mg, 0.45 mmol), $\text{Ni}(\text{COD})_2$ (8 mg, 0.03 mmol), $\text{P}(o\text{-tol})_3$ (18 mg, 0.06 mmol), and Et_3B (130 μL , 0.90 mmol) were stirred for 5 h at 50 $^\circ\text{C}$. The product (48 mg, 52 %) was obtained as a colorless oil after SiO_2 chromatography (3 % ethyl acetate in hexanes). ^1H NMR (500 MHz, CDCl_3) δ 9.84 (t, $J = 2.0$ Hz, 1H), 7.08-6.82 (m, 10H), 3.59 (m, 1H), 2.70-2.56 (m, 2H), 2.46 (ddd, $J = 2.5, 8.0, 16.5$ Hz, 1H), 2.35 (ddd, $J = 2.0, 6.5, 17.0$ Hz, 1H), 1.63-1.33 (m, 4H), 1.00 (m, 6H); ^{13}C NMR (125 MHz, CDCl_3) δ 202.6, 143.0, 139.4, 138.1, 130.6, 129.2, 127.2, 127.1, 125.7, 125.4, 48.0, 36.0, 35.6, 27.0, 21.0, 14.2, 13.0; GCMS (EI) m/z calcd for $\text{C}_{22}\text{H}_{26}\text{O}$ $[\text{M}]^+$ 306, found 306.

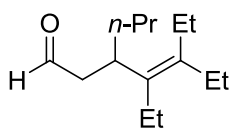
(Z)-4,5-diphenylhept-4-enal (Table 4, entry 3)



Following the general procedure, acrolein (21 μL , 0.30 mmol), diphenylacetylene (80 mg, 0.45 mmol), $\text{Ni}(\text{COD})_2$ (8 mg, 0.03 mmol), $\text{P}(o\text{-tol})_3$ (18 mg, 0.06 mmol), and Et_3B (130 μL , 0.90 mmol) were stirred for 5 h at 50 $^\circ\text{C}$. The product (42 mg, 53 %) was obtained as

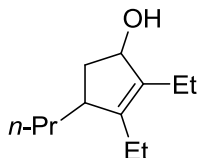
a colorless oil after SiO₂ chromatography (3 % ethyl acetate in hexanes). ¹H NMR (500 MHz, CDCl₃) δ 9.73 (s, 1H), 7.10-6.93 (m, 10H), 2.91 (t, *J* = 8.0 Hz, 2H), 2.59 (q, *J* = 7.5 Hz, 2H), 2.47 (dt, *J* = 1.5, 8.0 Hz, 2H), 1.00 (t, *J* = 7.5 Hz, 3H); ¹³C NMR (125 MHz, CDCl₃) δ 202.0, 142.5, 141.9, 141.1, 135.1, 129.7, 129.6, 127.6, 127.4, 125.9, 125.7, 42.6, 27.6, 26.4, 13.1; GCMS (EI) *m/z* calcd for C₁₉H₂₀O [M]⁺ 264, found 264.

(*E*)-4,5-diethyl-3-propylhept-4-enal (Table 4, entry 4)



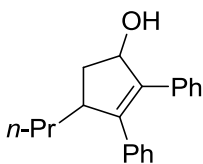
Following the general procedure, *trans*-2-hexen-1-al (35 μL, 0.30 mmol), 3-hexyne (51 μL, 0.45 mmol), Ni(COD)₂ (8 mg, 0.03 mmol), P(*o*-tol)₃ (18 mg, 0.06 mmol), and Et₃B (130 μL, 0.90 mmol) were stirred for 5 h at 50 °C. The product (36 mg, 57 %) was obtained as a colorless oil after SiO₂ chromatography (3 % ethyl acetate in hexanes). ¹H NMR (500 MHz, CDCl₃) δ 9.65 (t, *J* = 2.5 Hz, 1H), 3.14 (quint, *J* = 7.5 Hz, 1H), 2.40 (m, 2H), 2.06 (m, 4H), 1.95 (m, 2H), 1.43-1.22 (m, 4H), 1.02-0.87 (m, 12H); ¹³C NMR (125 MHz, CDCl₃) δ 203.3, 139.4, 133.5, 48.4, 36.2, 35.9, 24.4, 23.4, 20.8, 15.5, 14.2, 13.7, 13.3; GCMS (EI) *m/z* calcd for C₁₄H₂₆O [M]⁺ 210, found 210.

(1*R,4*R**)-2,3-Diethyl-4-propylcyclopent-2-enol (Table 5, entry 1)**



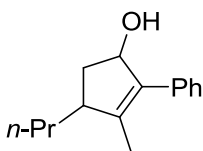
Following the general procedure, *trans*-2-hexen-1-al (35 μ L, 0.30 mmol), 3-hexyne (51 μ L, 0.45 mmol), Ni(COD)₂ (8 mg, 0.03 mmol), P[2,4,6-(MeO)₃C₆H₂]₃ (32 mg, 0.06 mmol), and Et₃B (130 μ L, 0.90 mmol) were stirred for 5 h at 50 °C. The product (28 mg, 51 %, dr 52:48) was obtained as a colorless oil after SiO₂ chromatography (10 % ethyl acetate in hexanes). Spectra data for this compound was previously reported and matched with the current data.⁵⁹

(1R*,4R*)-2,3-Diphenyl-4-propylcyclopent-2-enol (Table 5, entry 2)



Following the general procedure, *trans*-2-hexen-1-al (35 μ L, 0.30 mmol), diphenylacetylene (80 mg, 0.45 mmol), Ni(COD)₂ (8 mg, 0.03 mmol), P[2,4,6-(MeO)₃C₆H₂]₃ (32 mg, 0.06 mmol), and Et₃B (130 μ L, 0.90 mmol) were stirred overnight at 50°C. The product (58 mg, 70 %, dr 47:53) was obtained as a colorless oil after SiO₂ chromatography (10 % ethyl acetate in hexanes). Spectra data for this compound was previously reported and matched with the current data.⁵⁹

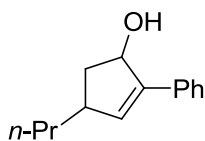
(1R*,4R*)-3-methyl-2-phenyl-4-propylcyclopent-2-enol (Table 5, entry 3)



Following the general procedure, *trans*-2-hexen-1-al (35 μ L, 0.30 mmol), 1-phenyl-1-propyne (56 μ L, 0.45 mmol), Ni(COD)₂ (8 mg, 0.03 mmol), P[2,4,6-(MeO)₃C₆H₂]₃ (32

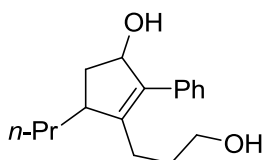
mg, 0.06 mmol), and Et₃B (130 μL, 0.90 mmol) were stirred for 5 h at 50 °C. The product (51 mg, 79 %, dr 64:36) was obtained as a colorless oil after SiO₂ chromatography (10 % ethyl acetate in hexanes). Spectra data for this compound was previously reported and matched with the current data.⁵⁹

(1R*,4R*)-2-phenyl-4-propylcyclopent-2-enol (Table 5, entry 4)



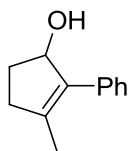
Following the general procedure, *trans*-2-hexen-1-al (35 μL, 0.30 mmol), phenylacetylene (50 μL, 0.45 mmol), Ni(COD)₂ (8 mg, 0.03 mmol), P[2,4,6-(MeO)₃C₆H₂]₃ (32 mg, 0.06 mmol), and Et₃B (130 μL, 0.90 mmol) were stirred for 5 h at 50 °C. The product (43 mg, 71 %, dr 36:64) was obtained as a yellow oil after SiO₂ chromatography (10 % ethyl acetate in hexanes). ¹H NMR (500 MHz, CDCl₃) δ 7.58(m, 2H_{maj}+2H_{min}), 7.36 (m, 2H_{maj}+2H_{min}), 7.26 (m, 1H_{maj}+1H_{min}), 6.31(d, *J* = 2.5 Hz, 1H_{maj}), 6.26 (d, *J* = 2.0 Hz, 1H_{min}), 5.23 (m, 1H_{maj}+1H_{min}), 3.03 (m, 1H_{maj}), 2.67 (m, 2H_{min}), 2.16 (ddd, *J* = 2.0, 7.5, 16.0 Hz, 1H_{maj}), 1.91 (m, 1H_{maj}), 1.66 (bs, 1H_{maj}+1H_{min}), 1.44 (m, 4H_{maj}+5H_{min}), 0.97 (m, 3H_{maj}+3H_{min}); ¹³C NMR (125 MHz, CDCl₃) δ 143.7, 143.5, 134.7, 134.6, 134.1, 128.5, 128.4, 127.4, 127.3, 126.2, 126.0, 76.8, 76.6, 43.2, 43.0, 41.3, 40.6, 39.2, 38.0, 21.0, 20.9, 19.3, 14.2; GCMS (EI) *m/z* calcd for C₁₄H₁₈O [M] 202, found 202.

(1R*,4R*)-3-(3-hydroxypropyl)-2-phenyl-4-propylcyclopent-2-enol (Table 5, entry 5)



Following the general procedure, *trans*-2-hexen-1-al (35 μ L, 0.30 mmol), 5-phenylpent-4-yn-1-ol (72 mg, 0.45 mmol), Ni(COD)₂ (8 mg, 0.03 mmol), P[2,4,6-(MeO)₃C₆H₂]₃ (32 mg, 0.06 mmol), and Et₃B (130 μ L, 0.90 mmol) were stirred for 5 h at 50 °C. The product (51 mg, 65 %, 38:62) was obtained as a colorless oil after SiO₂ chromatography (30 % ethyl acetate in hexanes). ¹H NMR (500 MHz, CDCl₃) δ ; ¹³C NMR (125 MHz, CDCl₃) δ 7.39-7.27 (m, 5H), 5.05 (dd, *J* = 5.5, 6.5 Hz, 1H), 3.54-3.43 (m, 2H), 2.67 (m, 1H), 2.57 (dt, *J* = 9.0, 13.0 Hz, 1H), 2.40 (m, 1H), 2.19 (m, 1H), 1.78-1.66 (m, 2H), 1.55-1.20 (m, 6H), 1.26 (m, 1H), 0.97 (t, *J* = 6.0 Hz, 3H); diagnostic signal for minor diastereomer: (2.96 ppm); ¹³C NMR (125 MHz, CDCl₃) δ 144.9, 139.7, 136.2, 128.5, 128.4, 126.9, 78.5, 62.4, 44.4, 38.3, 36.6, 30.6, 23.1, 20.6, 14.3; GCMS ((EI) *m/z* calcd for C₁₇H₂₄O₂ [M]⁺ 260, found 260).

3-methyl-2-phenylcyclopent-2-enol (Table 5, entry 6)

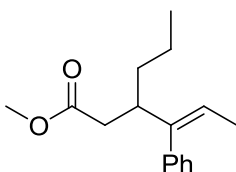


Following the general procedure, acrolein (21 μ L, 0.30 mmol), 1-phenyl-1-propyne (56 μ L, 0.45 mmol), Ni(COD)₂ (8 mg, 0.03 mmol), P[2,4,6-(MeO)₃C₆H₂]₃ (32 mg, 0.06 mmol), and Et₃B (130 μ L, 0.90 mmol) were stirred for 5 h at 50 °C. The product (16 mg, 31 %) was obtained as a colorless oil after SiO₂ chromatography (15 % ethyl acetate in hexanes). Spectra data for this compound was previously reported and match with the current data.⁶⁰

5.2.2 General Procedure for the Ni(COD)₂/ IPr Promoted Coupling of Enals, Alkynes, and Alcohols

THF (0.6 mL) was added to a solid mixture of IPr•HCl (0.03 mmol), potassium *t*-butoxide (0.03 mmol) and Ni(COD)₂ (0.03 mmol) at rt. The resulting solution was stirred for 20-30 min until the color turned to dark green. A small portion of methanol (0.5 mL) was added to the mixture, followed by the addition of enal (0.3 mmol), alkyne (0.45 mmol) and the remaining methanol (4.0 mL). The reaction mixture was stirred at 50 °C until TLC analysis indicated disappearance of the enal. The reaction mixture was concentrated *in vacuo*. The residue was purified via flash chromatography (SiO₂) to afford the desired product.

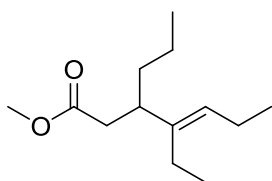
(*Z*)-Methyl 4-phenyl-3-propylhex-4-enoate (Table 6, entry 1)



Following the general procedure, *trans*-2-hexenal (34 μL, 0.3 mmol), 1-phenyl-1-propyne (56 μL, 0.45 mmol), Ni(COD)₂ (8 mg, 0.03 mmol), IPr•HCl (13 mg, 0.03 mmol), and *t*-BuOK (3 mg, 0.03 mmol) were stirred for 2 h at 50 °C. The product (55 mg, 75 %, 53:47) was obtained as a colorless oil after SiO₂ chromatography (5 % diethyl ether in hexanes). ¹H NMR (400 MHz, CDCl₃) δ 7.32-7.04 (m, 5H_{major} + 5H_{minor}), 6.30 (s, 1H_{minor}), 5.52 (q, *J* = 6.8 Hz, 1H_{major}), 3.62 (s, 3H_{major}), 3.61 (s, 3H_{minor}), 2.79 (m, 1H_{major}), 2.68 (m, 1H_{minor}), 2.41 (m, 1H_{major} + 2H_{minor}), 2.26 (dd, *J* = 7.2, 15.0 Hz, 1H_{major}), 1.74 (d, *J* = 1.6 Hz, 3H_{minor}), 1.50-1.16 (m, 4H_{major} + 4H_{minor}), 1.41 (d, *J* = 6.8 Hz

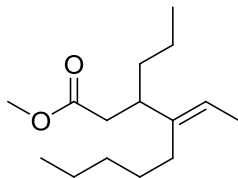
, 3H_{major}), 0.89 (t, $J = 7.0$ Hz, 3H_{major}), 0.85 (t, $J = 7.2$ Hz, 3H_{minor}); ¹³C NMR (100 MHz, CDCl₃) δ 173.4, 173.1, 143.1, 139.8, 139.2, 138.1, 129.2, 128.9, 128.0, 127.9, 126.8, 126.4, 126.0, 122.6, 51.4, 51.3, 46.0, 44.2, 39.3, 39.1, 35.5, 35.2, 20.5, 20.3, 14.5, 14.0, 13.6; IR (film, cm⁻¹) 3054, 2955, 1738, 1599, 1435; HRMS (ESI) m/z calcd for C₁₆H₂₂O₂Na [M+Na]⁺ 269.1517, found 269.1526.

(Z)-Methyl 4-ethyl-3-propylhept-4-enoate (Table 6, entry 2)



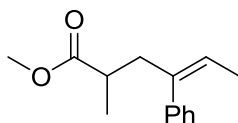
Following the general procedure, trans-2-hexenal (25 μ L, 0.3 mmol), 3-hexyne (51 μ L, 0.45 mmol), Ni(COD)₂ (8 mg, 0.03 mmol), IPr•HCl (13 mg, 0.03 mmol), and *t*-BuOK (3 mg, 0.03 mmol) were stirred for 2 h at 50 °C. The product (33mg, 52%) was obtained as a colorless oil after SiO₂ chromatography (5 % diethyl ether in hexanes). ¹H NMR (500 MHz, CDCl₃) δ 5.12 (t, $J = 7.0$ Hz, 1H), 3.64 (s, 3H), 2.48 (m, 1H), 2.37 (dd, $J = 7.5$, 14.5 Hz, 1H), 2.33 (dd, $J = 7.5$, 14.5 Hz, 1H), 1.98 (m, 4H), 1.44-1.18 (m, 4H); 0.97 (t, $J = 8.0$ Hz, 3H), 0.94 (t, $J = 7.5$ Hz, 3H), 0.88 (t, $J = 7.0$ Hz, 3H); ¹³C NMR (100 MHz, CDCl₃) δ 173.5, 141.3, 127.7, 51.3, 43.1, 39.8, 36.1, 21.8, 20.9, 20.4, 14.6, 14.10, 14.08; IR (film, cm⁻¹) 2960, 1742, 1456, 1435; HRMS (ESI) m/z calcd for C₁₃H₂₄O₂Na [M+Na]⁺ 235.1674, found 235.1664.

(Z)-Methyl 4-ethylidene-3-propylnonanoate (Table 6, entry 3)



Following the general procedure, *trans*-2-hexenal (34 μ L, 0.3 mmol), 2-octyne (65 μ L, 0.45 mmol), Ni(COD)₂ (8 mg, 0.03 mmol), IPr•HCl (13 mg, 0.03 mmol), and *t*-BuOK (3 mg, 0.03 mmol) were stirred for 2 h at 50 °C. The product (55 mg, 76 %, 73:27) was obtained as a colorless oil after SiO₂ chromatography (5 % diethyl ether in hexanes). ¹H NMR (400 MHz, CDCl₃) δ 5.22 (m, 1H_{major} + 1H_{minor}), 3.63 (s, 3H_{major}), 3.62 (s, 3H_{minor}), 2.48 (m, 1H_{major} + 1H_{minor}), 2.34 (m, 2H_{major} + 2H_{minor}), 1.94 (m, 2H_{major} + 2H_{minor}), 1.58 (d, J = 6.4 Hz, 3H_{major}), 1.50 (s, 3H_{minor}), 1.40-1.15 (m, 10H_{major} + 10H_{minor}), 0.88 (m, 6H_{major} + 6H_{minor}); ¹³C NMR (100 MHz, CDCl₃) δ 173.5, 173.4, 141.7, 135.0, 127.0, 119.6, 51.3, 51.2, 45.4, 43.1, 39.8, 39.4, 36.2, 35.1, 32.3, 31.4, 29.4, 29.1, 28.6, 27.6, 22.6, 22.5, 20.4, 14.09, 14.06, 14.0, 13.3, 11.7; IR (film, cm⁻¹) 2926, 1741, 1433; HRMS (ESI) m/z calcd for C₁₅H₂₈O₂Na [M+Na]⁺ 263.1987, found 263.1982.

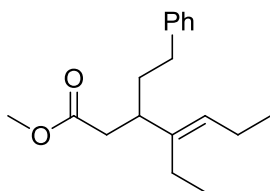
(Z)-Methyl 2-methyl-4-phenylhex-4-enoate (Table 6, entry 4)



Following the general procedure, methacrolein (25 μ L, 0.3 mmol), 1-phenyl-1-propyne (56 μ L, 0.45 mmol), Ni(COD)₂ (8 mg, 0.03 mmol), IPr•HCl (13 mg, 0.03 mmol), and *t*-BuOK (3 mg, 0.03 mmol) were stirred for 2 h at 50 °C. The product (55 mg, 84 %, 75:25) was obtained as a colorless oil after SiO₂ chromatography (5 % diethyl ether in hexanes). ¹H NMR (400 MHz, CDCl₃) δ 7.21 (m, 5H_{major} + 5H_{minor}), 6.25 (s, 1H_{minor}),

5.54 (q, $J = 6.8$ Hz, 1H_{major}), 3.64 (s, 3H_{minor}), 3.54 (s, 3H_{major}), 2.73 (m, 1H_{major} + 1H_{minor}), 2.52 (ddd, $J = 0.8$ Hz, $J = 7.4$ Hz, $J = 13.3$ Hz, 1H_{minor}), 2.34 (m, 2H_{major}), 2.20 (ddd, $J = 0.8$ Hz, $J = 7.6$ Hz, $J = 13.2$ Hz, 1H_{minor}), 1.81 (d, $J = 1.2$ Hz, 3H_{minor}), 1.52 (d, $J = 6.8$ Hz, 3H_{major}), 1.15 (d, $J = 7.2$ Hz, 3H_{minor}), 1.05 (m, $J = 6.8$ Hz, 3H_{major}); ¹³C NMR (100 MHz, CDCl₃) δ 176.9, 176.8, 139.9, 138.8, 138.1, 135.8, 128.8, 128.6, 128.1, 128.0, 127.2, 126.6, 126.1, 123.8, 51.6, 51.4, 44.9, 43.3, 38.1, 37.9, 17.5, 16.7, 16.5, 14.7; IR (film, cm⁻¹) 2915, 1735, 1599, 1439; HRMS (ESI) m/z calcd for C₁₄H₁₈O₂Na [M+Na]⁺ 241.1204, found 241.1205.

(Z)-methyl 4-ethyl-3-phenethylhept-4-enoate (Table 6, entry 5)



Following the general procedure, 5-phenylpent-2-enal (38 mg, 0.24 mmol), 3-hexyne (40 μ L, 0.36 mmol), Ni(COD)₂ (6.6 mg, 0.024 mmol), IPr•HCl (10.2 mg, 0.024 mmol), and *t*-BuOK (3 mg, 0.024 mmol) were stirred for 4 h at 50 °C. The product (30 mg, 45 %) was obtained as a colorless oil after SiO₂ chromatography (5 % diethyl ether in hexanes). ¹H NMR (400 MHz, CDCl₃) δ 7.18 (m, 5H), 5.16 (t, $J = 7.2$ Hz, 1H), 3.59 (s, 3H), 2.60-2.30 (m, 5H), 2.00 (m, 4H), 1.67 (m, 2H), 0.97 (t, $J = 7.6$ Hz, 3H), 0.93 (t, $J = 7.6$ Hz, 3H); ¹³C NMR (100 MHz, CDCl₃) δ 173.2, 142.5, 140.8, 128.4, 128.3, 128.3, 125.7, 51.3, 43.2, 39.8, 35.5, 33.6, 21.8, 20.9, 14.6, 14.1; IR (film, cm⁻¹) 3025, 2962, 1740, 1603, 1453; HRMS (ESI) m/z calcd for C₁₈H₂₆O₂Na [M+Na]⁺ 297.1830, found missing 297.1834.

Deuterated enal was prepared by LiAlD_4 reduction of methyl-5-phenylpent-2-enoate, followed by PCC oxidation. Repeating the above three component coupling on the deuterated enal afforded the product with >95% deuterium incorporation of the alkenyl CH (δ 5.16).

5.3 Experimental Procedures and Spectra Data: Chapter 4

All reagents were used as received unless otherwise noted. Solvents were purified under nitrogen using a solvent purification system (Innovative Technology, inc., Model # SPS-400-3 and PS-400-3). $\text{Ni}(\text{COD})_2$ (Strem Chemicals, Inc., used as received) and triphenylphosphine (PPh_3) were stored and weighed in an inert atmosphere glovebox. All reactions were conducted in flame-dried glassware under a nitrogen atmosphere. ^1H and ^{13}C spectra were obtained in CDCl_3 at rt, unless otherwise noted, on a Varian Mercury 400 or Varian Unity 500 MHz instrument. Chemical shifts of ^1H NMR spectra were recorded in parts per million (ppm) on the δ scale from an internal standard of residual chloroform (7.27 ppm). Chemical shifts of ^{13}C NMR spectra were recorded in ppm from the central peak of CDCl_3 (77.0 ppm) on the δ scale. High resolution mass spectra (HRMS) were obtained on a VG-70-250-s spectrometer manufactured by Micromass Corp. (Manchester UK) at the University of Michigan Mass Spectrometry Laboratory.

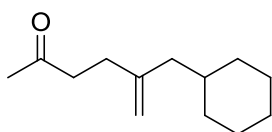
Compounds **67**⁶¹, **85**⁶¹, **86**⁶¹, **87**⁶², **88**⁶³, **89**⁶⁴, **90**⁶⁵, **96**⁶⁶ and **97**⁶⁷ were prepared according to literature procedure. Enone reagents were used as received.

Regioisomeric ratios were determined on crude reaction mixtures using NMR and/or GCMS. GCMS analyses were carried out on an HP6890 Series GC System with a HP-5MS column (30m x 0.252 mm x 0.25 μ m). The trisubstituted alkene stereochemistry was determined by NOE in the following cases: compound **69** and Table 2, entries 12 and 13.

5.3.1 General Procedure for the Ni(COD)₂/PBU₃ Promoted Reductive Coupling of Enones and Alkynes

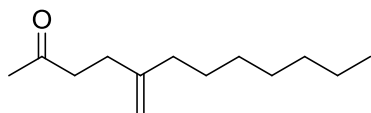
To a solid mixture of Ni(COD)₂ (0.03 mmol) and triphenylphosphine (PPh₃) (0.06 mmol) was added toluene (1 mL) at rt. After stirring for 5-10 min at rt, triethylsilane (0.6 mmol) and then enone (0.3 mmol) were added by syringe to the dark red mixture, followed by syringe drive addition of allene (0.45 mmol) in toluene (4 mL) at 1 mL/hr at 50 °C. The reaction mixture was stirred at 50 °C until TLC analysis indicated disappearance of the enone. The reaction mixture was concentrated, and then diluted with ethyl acetate. A solution of tetrabutylammonium fluoride (*n*-Bu₄NF) (0.6 mmol) in THF was added to the reaction mixture and stirred until TLC analysis indicated disappearance of the enol silane product. The reaction mixture was washed with brine, dried over magnesium sulfate, filtered, concentrated, and the residue was purified by column chromatography on silica gel.

5-(Cyclohexylmethyl)hex-5-en-2-one (Table 9, entry 6)



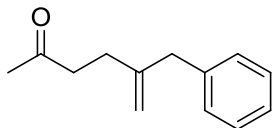
Following the general procedure, 3-buten-2-one (25 mg, 0.30 mmol), propa-1,2-dienylcyclohexane (55 mg, 0.45 mmol), Ni(COD)₂ (8 mg, 0.03 mmol), PPh₃ (16 mg, 0.06 mmol), and Et₃SiH (97 μL, 0.60 mmol) were stirred for 6 h at 50 °C. The product (49 mg, 84 %, 93:7) was obtained as a colorless oil after SiO₂ chromatography (2 % ethyl acetate in hexanes). ¹H NMR (500 MHz, CDCl₃) δ 4.70 (br s, 2H), 2.56 (m, 2H), 2.24 (m, 2H), 2.16 (s, 3H), 1.90 (d, *J* = 7.5 Hz, 2H), 1.66 (m, 5H), 1.39 (m, 1H), 1.17 (m, 3H), 0.83 (dq, *J* = 3.5, 12.0 Hz, 2H); ¹³C NMR (125 MHz, CDCl₃) δ 208.4, 146.6, 110.2, 44.7, 41.8, 35.4, 33.2, 29.8, 29.4, 26.5, 26.2; IR (film, cm⁻¹) 2922, 2851, 1719, 1448; HRMS (ESI) *m/z* calcd for C₁₃H₂₂ONa [M+Na]⁺ 217.1568, found 217.1560.

5-Methylenedodecan-2-one (Table 10, entry 1)



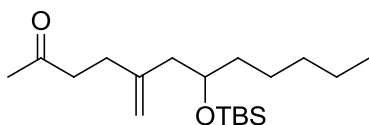
Following the general procedure, 3-buten-2-one (25 mg, 0.30 mmol), nona-1,2-diene (55 mg, 0.45 mmol), Ni(COD)₂ (8 mg, 0.03 mmol), PPh₃ (16 mg, 0.06 mmol), and Et₃SiH (97 μL, 0.60 mmol) were stirred for 6 h at 50 °C. The product (43 mg, 73 %, 78:15:7) was obtained as a colorless oil after SiO₂ chromatography (2 % ethyl acetate in hexanes). ¹H NMR (500 MHz, CDCl₃) δ 4.74 (s, 1H), 4.67 (s, 1H), 2.58 (app t, *J* = 7.0 Hz, 2H), 2.28 (app t, *J* = 7.5 Hz, 2H), 2.16 (s, 3H), 2.01 (app t, *J* = 7.5 Hz, 2H), 1.42 (m, 2H), 1.28 (m, 8H), 0.88 (t, *J* = 7.0 Hz, 3H); diagnostic signal for minor regioisomer: (5.16 ppm); ¹³C NMR (100 MHz, CDCl₃) δ 208.5, 148.6, 108.8, 41.9, 36.3, 31.8, 29.8, 29.7, 29.3, 29.1, 27.7, 22.6, 14.0; IR (film, cm⁻¹) 2927, 2856, 1720, 1442; HRMS (ESI) *m/z* calcd for C₁₃H₂₄O [M]⁺ 196.1827, found 196.1831.

5-Benzylhex-5-en-2-one (Table 10, entry 2)



Following the general procedure, 3-buten-2-one (25 mg, 0.30 mmol), propa-1,2-dienylbenzene (52 mg, 0.45 mmol), Ni(COD)₂ (8 mg, 0.03 mmol), PPh₃ (16 mg, 0.06 mmol), and Et₃SiH (97 μL, 0.60 mmol) were stirred for 6 h at 50 °C. The product (28 mg, 50 %, 91:9) was obtained as a colorless oil after SiO₂ chromatography (2 % ethyl acetate in hexanes). ¹H NMR (500 MHz, CDCl₃) δ 7.29 (m, 2H), 7.21 (m, 3H), 4.81 (s, 2H), 3.36 (s, 2H), 2.57 (t, *J* = 7.5 Hz, 2H), 2.27 (t, *J* = 8.0 Hz, 2H), 2.12 (s, 3H); ¹³C NMR (100 MHz, CDCl₃) δ 208.1, 147.4, 139.2, 128.9, 128.3, 126.1, 111.4, 43.3, 41.7, 29.7, 29.1; IR (film, cm⁻¹) 3026, 2922, 1716, 1440; HRMS (ESI) *m/z* calcd for C₁₃H₁₆O [M]⁺ 188.1201, found 188.1197.

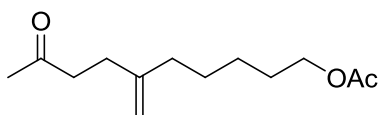
7-(*tert*-Butyldimethylsilyloxy)-5-methylenedodecan-2-one (Table 10, entry 3)



Following the general procedure, 3-buten-2-one (25 mg, 0.30 mmol), *tert*-butyldimethyl(nona-1,2-dien-4-yloxy)silane (114 mg, 0.45 mmol), Ni(COD)₂ (8 mg, 0.03 mmol), PPh₃ (16 mg, 0.06 mmol), and Et₃SiH (97 μL, 0.60 mmol) were stirred for 6 h at 50 °C. The product (83 mg, 85 %, >95:5) was obtained as a colorless oil after SiO₂ chromatography (2 % ethyl acetate in hexanes). ¹H NMR (400 MHz, CDCl₃) δ 4.75 (s, 1H), 4.73 (s, 1H), 3.77 (quint, *J* = 6.0 Hz, 1H), 2.57 (dd, *J* = 7.0, 9.5 Hz, 2H), 2.29 (t, *J* =

7.5 Hz, 2H), 2.18 (dd, $J = 6.0, 13.5$ Hz, 1H), 2.15 (s, 3H), 2.14 (dd, $J = 6.5, 14.0$ Hz, 1H), 1.20–1.47 (m, 8H), 0.88 (t, $J = 7.0$ Hz, 3H), 0.87 (s, 9H), 0.04 (s, 3H), 0.03 (s, 3H); ^{13}C NMR (100 MHz, CDCl_3) δ 208.2, 145.4, 111.8, 71.1, 44.4, 41.8, 36.8, 31.9, 30.0, 29.8, 25.8, 24.8, 22.6, 18.0, 14.0, -4.4, -4.5; IR (film, cm^{-1}) 2930, 1720, 1644, 1462; HRMS (ESI) m/z calcd for $\text{C}_{19}\text{H}_{38}\text{O}_2\text{SiNa}$ $[\text{M}+\text{Na}]^+$ 349.2539, found 349.2530.

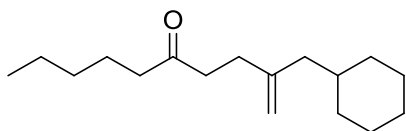
6-Methylene-9-oxodecyl acetate (Table 10, entry 4)



Following the general procedure, 3-buten-2-one (25 mg, 0.3 mmol), hepta-5,6-dienyl acetate (69 mg, 0.45 mmol), $\text{Ni}(\text{COD})_2$ (8 mg, 0.03 mmol), PPh_3 (16 mg, 0.06 mmol), and Et_3SiH (97 μL , 0.60 mmol) were stirred for 6 h at 50 $^\circ\text{C}$. The product (46 mg, 68 %, 79:21) was obtained as a colorless oil after SiO_2 chromatography (10 % ethyl acetate in hexanes). ^1H NMR (500 MHz, CDCl_3) δ 4.73 (s, 1H), 4.68 (s, 1H), 4.05 (t, $J = 6.5$ Hz, 2H), 2.57 (app t, $J = 7.5$ Hz, 2H), 2.27 (app t, $J = 7.5$ Hz, 2H), 2.15 (s, 3H), 2.04 (s, 3H), 2.02 (t, $J = 8.0$ Hz, 2H), 1.62 (m, 2H), 1.46 (m, 2H), 1.36 (m, 2H); diagnostic signal for minor regioisomer: (5.13 ppm); ^{13}C NMR (100 MHz, CDCl_3) (signals for both isomers included) δ 208.5, 208.3, 171.1, 148.0, 133.9, 125.7, 124.5, 109.1, 64.4, 42.3, 42.0, 41.8, 36.1, 33.5, 29.8, 29.5, 28.5, 28.4, 28.2, 28.1, 27.3, 27.2, 26.4, 26.1, 25.9, 25.5, 23.0, 20.9, 16.0; IR (film, cm^{-1}) 2936, 1738, 1644, 1440; HRMS (ESI) m/z calcd for $\text{C}_{13}\text{H}_{22}\text{O}_3$ $[\text{M}]^+$ 226.1569, found 226.1580.

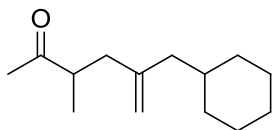
(10 % ethyl acetate in hexanes). Spectral data for this compound was previously reported and matched with the current data.⁶⁸

2-(Cyclohexylmethyl)dec-1-en-5-one (Table 10, entry 7)



Following the general procedure, 1-octen-3-one (38 mg, 0.30 mmol), propa-1,2-dienylcyclohexane (55 mg, 0.45 mmol), Ni(COD)₂ (8 mg, 0.03 mmol), PPh₃ (16 mg, 0.06 mmol), and Et₃SiH (97 μL, 0.60 mmol) were stirred for 6 h at 50 °C. The product (53 mg, 71 %, >95:5) was obtained as a colorless oil after SiO₂ chromatography (2 % ethyl acetate in hexanes). ¹H NMR (400 MHz, CDCl₃) δ 4.70 (s, 2H), 2.54 (dd, *J* = 7.6, 9.6 Hz, 2H), 2.42 (t, *J* = 7.2 Hz, 2H), 2.25 (app t, *J* = 8.0 Hz, 2H), 1.91 (d, *J* = 7.2 Hz, 2H), 1.55-1.74 (m, 7H), 1.10-1.47 (m, 8H), 0.89 (t, *J* = 7.2 Hz, 3H), 0.84 (dq, *J* = 3.2, 12.0 Hz, 2H); ¹³C NMR (100 MHz, CDCl₃) δ 210.9, 146.9, 110.2, 44.7, 42.8, 40.9, 35.4, 33.2, 31.4, 29.4, 26.5, 26.3, 23.5, 22.4, 13.9; IR (film, cm⁻¹) 2924, 1716, 1643, 1448; HRMS (ESI) *m/z* calcd for C₁₇H₃₀ONa [M+Na]⁺ 273.2194, found 273.2188.

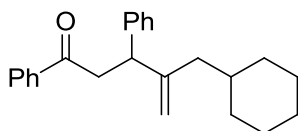
5-(Cyclohexylmethyl)-3-methylhex-5-en-2-one (Table 10, entry 8)



Following the general procedure, 3-methyl-3-buten-2-one (25 mg, 0.30 mmol), propa-1,2-dienylcyclohexane (55 mg, 0.45 mmol), Ni(COD)₂ (8 mg, 0.03 mmol), PPh₃ (16 mg, 0.06 mmol), and Et₃SiH (97 μL, 0.60 mmol) were stirred for 6 h at 50 °C. The product

(32 mg, 51 %, >95:5) was obtained as a colorless oil after SiO₂ chromatography (2 % ethyl acetate in hexanes). ¹H NMR (500 MHz, CDCl₃) δ 4.74 (s, 1H), 4.72 (s, 1H), 2.70 (sextet, *J* = 7.0 Hz, 1H), 2.36 (dd, *J* = 6.5, 14.5 Hz, 1H), 2.14 (s, 3H), 1.95 (dd, *J* = 8.0, 14.5 Hz, 1H), 1.89 (dd, *J* = 7.0, 14.0 Hz, 1H), 1.86 (dd, *J* = 7.0, 13.5 Hz, 1H), 1.67 (m, 5H), 1.39 (m, 1H), 1.10-1.27 (m, 3H), 1.07 (d, *J* = 7.0 Hz, 3H), 0.84 (dq, *J* = 4.0, 13.5 Hz, 2H); ¹³C NMR (100 MHz, CDCl₃) δ 212.3, 145.1, 112.2, 45.1, 44.0, 38.9, 35.4, 33.4, 33.1, 28.0, 26.5, 26.3, 26.2, 16.2; IR (film, cm⁻¹) 2924, 1713, 1642, 1449; HRMS (EI) *m/z* calcd for C₁₄H₂₄ONa [M+Na]⁺ 231.1725, found 231.1715.

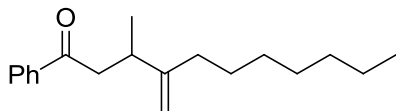
4-(Cyclohexylmethyl)-1,3-diphenylpent-4-en-1-one (Table 10, entry 9)



Following the general procedure, *trans*-chalcone (63 mg, 0.30 mmol), propa-1,2-dienylcyclohexane (55 mg, 0.45 mmol), Ni(COD)₂ (8 mg, 0.03 mmol), PPh₃ (16 mg, 0.06 mmol), and Et₃SiH (97 μL, 0.60 mmol) were stirred overnight at 50 °C. The product (90 mg, 90 %, >95:5) was obtained as a colorless oil after SiO₂ chromatography (2 % ethyl acetate in hexanes). ¹H NMR (500 MHz, CDCl₃) δ 7.93 (dd, *J* = 1.5, 7.0 Hz, 2H), 7.55 (tt, *J* = 1.0, 8.5 Hz, 1H), 7.45 (t, *J* = 8.0 Hz, 2H), 7.29 (d, *J* = 4.5 Hz, 4H), 7.21 (dd, *J* = 4.0, 8.5 Hz, 1H), 4.96 (s, 1H), 4.91 (s, 1H), 4.08 (t, *J* = 7.0 Hz, 1H), 3.57 (dd, *J* = 7.5, 16.5 Hz, 1H), 3.34 (dd, *J* = 7.0, 17.0 Hz, 1H), 1.86 (dd, *J* = 6.5, 14.5 Hz, 1H), 1.82 (dd, *J* = 8.0, 14.5 Hz, 1H), 1.67 (m, 5H), 1.48 (m, 1H), 1.18 (m, 3H), 0.83 (dq, *J* = 2.5, 11.5 Hz, 1H), 0.76 (dq, *J* = 3.0, 12.5 Hz, 1H); ¹³C NMR (100 MHz, CDCl₃) δ 198.4, 149.3, 142.9, 137.2, 132.8, 128.4, 128.3, 128.0, 127.9, 126.4, 110.1, 45.9, 44.0, 43.7, 35.5, 33.6, 32.7,

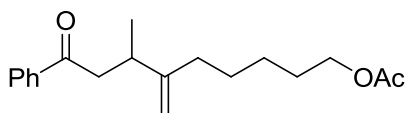
26.5, 26.3, 26.2; IR (film, cm^{-1}) 3061, 2920, 1689, 1642, 1448; HRMS (ESI) m/z calcd for $\text{C}_{24}\text{H}_{28}\text{ONa}$ $[\text{M}+\text{Na}]^+$ 355.2038, found 355.2036.

3-Methyl-4-methylene-1-phenylundecan-1-one (Table 10, entry 10)



Following the general procedure, 1-phenyl-but-2-en-1-one (44 mg, 0.30 mmol), nona-1,2-diene (55 mg, 0.45 mmol), $\text{Ni}(\text{COD})_2$ (8 mg, 0.03 mmol), PPh_3 (16 mg, 0.06 mmol), and Et_3SiH (97 μL , 0.60 mmol) were stirred for 6 h at 50 $^\circ\text{C}$. The product (59 mg, 72 %, 93:5:2) was obtained as a colorless oil after SiO_2 chromatography (2 % ethyl acetate in hexanes). ^1H NMR (500 MHz, CDCl_3) δ 7.96 (dd, $J = 1.0, 6.5$ Hz, 2H), 7.56 (tt, $J = 1.5, 8.0$ Hz, 1H), 7.46 (t, $J = 8.0$ Hz, 2H), 4.79 (s, 1H), 4.76 (s, 1H), 3.16 (dd, $J = 5.0, 16.0$ Hz, 1H), 2.91 (dd, $J = 8.5, 16.0$ Hz, 1H), 2.85 (m, 1H), 2.06 (m, 2H), 1.46 (quint, $J = 6.5$ Hz, 2H), 1.29 (m, 8H), 1.10 (d, $J = 6.5$ Hz, 3H), 0.89 (t, $J = 7.0$ Hz, 3H); diagnostic signal for minor regioisomer: (5.17 ppm); ^{13}C NMR (100 MHz, CDCl_3) δ 199.7, 154.2, 137.3, 132.8, 128.5, 128.0, 107.6, 44.8, 35.4, 34.7, 31.8, 29.4, 29.2, 28.0, 22.6, 20.0, 14.0; IR (film, cm^{-1}) 3067, 2927, 1688, 1642, 1448; HRMS (ESI) m/z calcd for $\text{C}_{19}\text{H}_{28}\text{ONa}$ $[\text{M}+\text{Na}]^+$ 295.2038, found 295.2036.

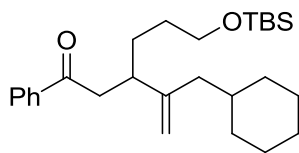
7-Methyl-6-methylene-9-oxo-9-phenylnonyl acetate (Table 10, entry 11)



Following the general procedure, 1-phenyl-but-2-en-1-one (44 mg, 0.30 mmol), hepta-5,6-dienyl acetate (69 mg, 0.45 mmol), Ni(COD)₂ (8 mg, 0.03 mmol), PPh₃ (16 mg, 0.06 mmol), and Et₃SiH (97 μL, 0.60 mmol) were stirred for 6 h at 50 °C. The product (63 mg, 70 %, 90:5:5) was obtained as a colorless oil after SiO₂ chromatography (5 % ethyl acetate in hexanes). ¹H NMR (500 MHz, CDCl₃) δ 7.95 (dd, *J* = 1.0, 8.0 Hz, 2H), 7.56 (tt, *J* = 1.0, 6.0 Hz, 1H), 7.46 (t, *J* = 8.0 Hz, 2H), 4.80 (s, 1H), 4.75 (d, *J* = 1.5 Hz, 1H), 4.06 (t, *J* = 6.5 Hz, 2H), 3.14 (dd, *J* = 5.5, 16.0 Hz, 1H), 2.92 (dd, *J* = 8.0, 15.5 Hz, 1H), 2.85 (sextet, *J* = 7.0 Hz, 1H), 2.08 (dt, *J* = 3.0, 7.5 Hz, 2H), 2.05 (s, 3H), 1.64 (m, 2H), 1.49 (quint, *J* = 7.5 Hz, 2H), 1.37 (m, 2H), 1.10 (d, *J* = 6.5 Hz, 3H); ¹³C NMR (100 MHz, CDCl₃) δ 199.5, 171.1, 153.7, 137.2, 132.9, 128.5, 128.0, 107.8, 64.5, 44.7, 35.2, 34.5, 28.4, 27.5, 25.7, 20.9, 20.1; IR (film, cm⁻¹) 3068, 2934, 1738, 1687, 1448; HRMS (ESI) *m/z* calcd for C₁₉H₂₆O₃Na [M+Na]⁺ 325.1780, found 325.1777.

6-(*tert*-Butyldimethylsilyloxy)-3-(3-cyclohexylprop-1-en-2-yl)-1-phenylhexan-1-one

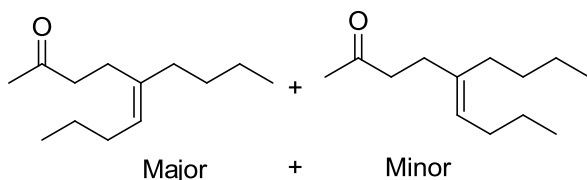
(Table 10, entry 12)



Following the general procedure, 6-(*tert*-butyldimethylsilyloxy)-1-phenylhex-2-en-1-one (91 mg, 0.30 mmol), propa-1,2-dienylcyclohexane (55 mg, 0.45 mmol), Ni(COD)₂ (8 mg, 0.03 mmol), PPh₃ (16 mg, 0.06 mmol), and Et₃SiH (97 μL, 0.60 mmol) were stirred for 6 h at 50 °C. The product (100 mg, 78 %, >95:5) was obtained as a colorless oil after SiO₂ chromatography (2 % ethyl acetate in hexanes). ¹H NMR (500 MHz, CDCl₃) δ 7.93 (dd, *J* = 5.5, 7.0 Hz, 2H), 7.55 (tt, *J* = 0.5, 7.0 Hz, 1H), 7.46 (t, *J* = 8.5 Hz, 2H), 4.82 (s, 1H),

4.77 (d, $J = 1.0$ Hz, 1H), 3.58 (m, 2H), 3.08 (dd, $J = 6.5, 16.0$ Hz, 1H), 2.96 (dd, $J = 7.5, 16.5$ Hz, 1H), 2.75 (quint, $J = 6.0$ Hz, 1H), 1.91 (dd, $J = 7.5, 15.0$ Hz, 1H), 1.87 (dd, $J = 7.0, 14.5$ Hz, 1H), 1.68 (m, 5H), 1.52 (m, 5H), 1.18 (m, 3H), 0.88 (s, 9H), 0.84 (m, 2H), 0.03 (s, 6H); ^{13}C NMR (100 MHz, CDCl_3) δ 199.6, 149.6, 137.3, 132.8, 128.5, 128.0, 110.3, 63.1, 43.4, 42.7, 40.9, 35.3, 33.5, 33.4, 30.3, 29.8, 26.6, 26.3, 25.9, 18.3, -5.3; IR (film, cm^{-1}) 3070, 2926, 1689, 1641, 1448; HRMS (ESI) m/z calcd for $\text{C}_{27}\text{H}_{44}\text{O}_2\text{SiNa}$ $[\text{M}+\text{Na}]^+$ 451.3008, found 451.3010.

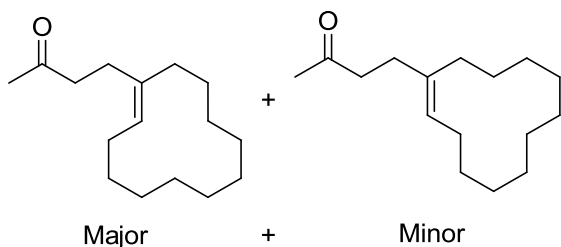
(Z, E)-5-Butylnon-5-en-2-one (Table 10, entry 13)



Following the general procedure, 3-buten-2-one (25 mg, 0.3 mmol), nona-4,5-diene (56 mg, 0.45 mmol), $\text{Ni}(\text{COD})_2$ (8 mg, 0.03 mmol), PPh_3 (16 mg, 0.06 mmol), and Et_3SiH (97 μL , 0.60 mmol) were stirred for 6 h at 50 $^\circ\text{C}$. The product (35 mg, 59 %, 78:22) was obtained as a colorless oil after SiO_2 chromatography (2 % ethyl acetate in hexanes). ^1H NMR (500 MHz, CDCl_3) δ 5.14 (t, $J = 7.5$ Hz, 1H_{maj}), 5.09 (t, $J = 7.0$ Hz, 1H_{min}), 2.52 (app t, $J = 8.0$ Hz, 2H_{min}), 2.46 (app t, $J = 7.0$ Hz, 2H_{maj}), 2.27 (app t, $J = 9.0$ Hz, $2\text{H}_{\text{maj}} + 2\text{H}_{\text{min}}$), 2.15 (s, 3H_{maj}), 2.14 (s, 3H_{min}), 1.98 (m, 4H_{min}), 1.95 (app t, $J = 7.0$ Hz, 4H_{maj}), 1.31 (m, $6\text{H}_{\text{maj}} + 6\text{H}_{\text{min}}$), 0.89 (m, $6\text{H}_{\text{maj}} + 6\text{H}_{\text{min}}$); All observable signals are reported as a mixture of the two stereoisomers. ^{13}C NMR (125 MHz, CDCl_3) (major and minor peak listings given) δ 208.8, 137.9, 137.7, 125.8, 125.1, 42.7, 42.6, 36.4, 30.7, 30.6, 30.3, 29.9,

29.8, 29.7, 24.1, 23.1, 22.7, 22.4, 18.4, 14.0, 13.9, 13.8; IR (film, cm^{-1}) 2958, 1719, 1641, 1461; HRMS (ESI) m/z calcd for $\text{C}_{13}\text{H}_{24}\text{ONa}$ $[\text{M}+\text{Na}]^+$ 219.1725, found 219.1721.

(Z, E)-4-Cyclododecenylbutan-2-one (Table 10, entry 14)



Following the general procedure, 3-buten-2-one (25 mg, 0.3 mmol), cyclododeca-1,2-diene (74 mg, 0.45 mmol), $\text{Ni}(\text{COD})_2$ (8 mg, 0.03 mmol), PPh_3 (16 mg, 0.06 mmol), and Et_3SiH (97 μL , 0.60 mmol) were stirred for 6 h at 50 $^\circ\text{C}$. The product (55 mg, 78 %, 87:13) was obtained as a colorless oil after SiO_2 chromatography (2 % ethyl acetate in hexanes). ^1H NMR (500 MHz, CDCl_3) δ 5.32 (t, $J = 7.5$ Hz, 1Hmaj), 5.10 (t, $J = 8.0$ Hz, 1Hmin), 2.52 (app t, $J = 7.5$ Hz, 2Hmin), 2.46 (app t, $J = 7.5$ Hz, 2Hmaj), 2.30 (app t, $J = 8.5$ Hz, 2Hmaj), 2.26 (app t, $J = 7.5$ Hz, 2Hmin), 2.14(s, 3Hmaj + 3Hmin), 2.03 (m, 4Hmaj + 4Hmin), 1.42 (m, 6Hmaj + 6Hmin), 1.24 (m, 10Hmaj + 10Hmin); ^{13}C NMR (100 MHz, CDCl_3) (major and minor peak listings given) δ 208.9, 137.5, 136.0, 129.1, 126.3, 42.5, 42.4, 35.2, 30.0, 29.9, 29.8, 27.3, 27.2, 26.8, 26.4, 25.9, 25.8, 25.3, 25.0, 24.9, 24.7, 24.6, 24.5, 24.3, 24.2, 23.9, 23.7, 22.8, 22.4, 22.2; IR (film, cm^{-1}) 2928, 1717, 1641, 1445; HRMS (ESI) m/z calcd for $\text{C}_{16}\text{H}_{28}\text{ONa}$ $[\text{M}-\text{H}]^+$ 235.2062, found 235.2068.

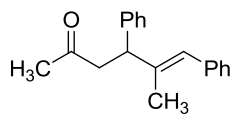
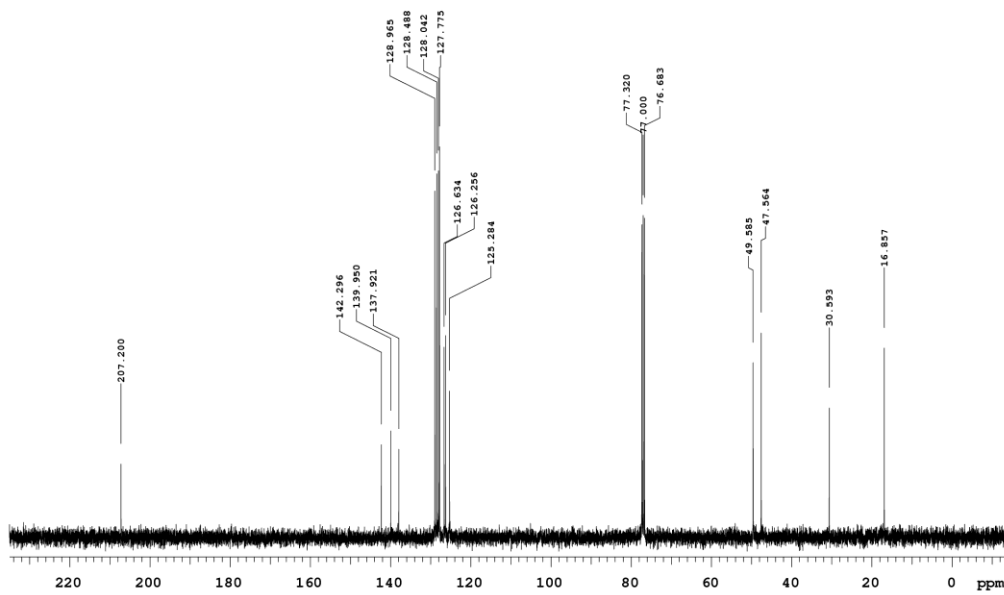
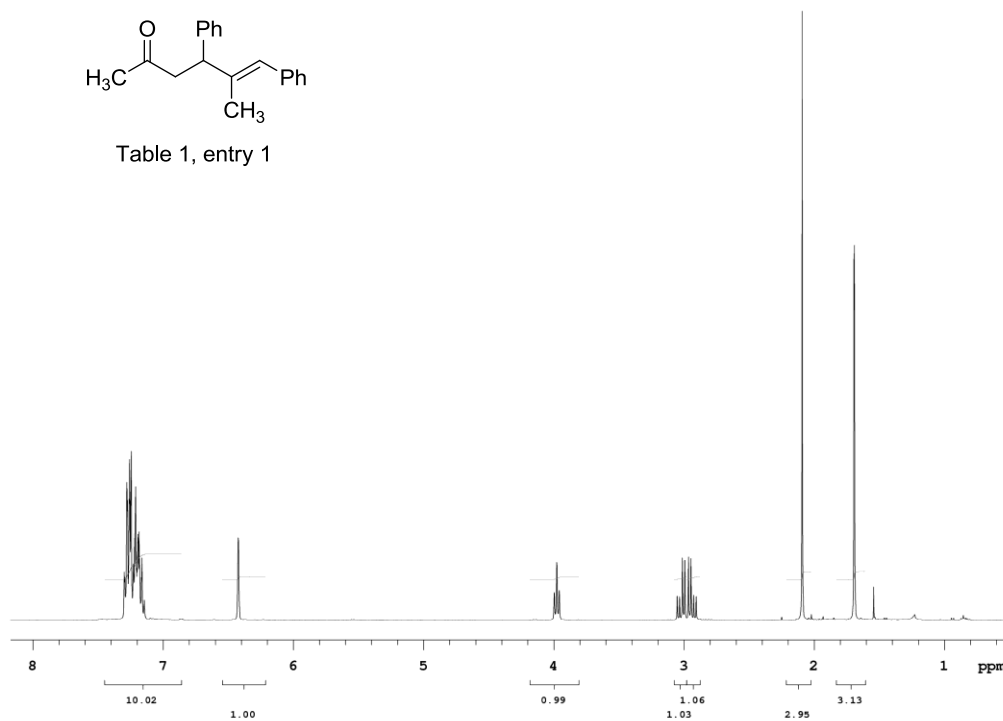
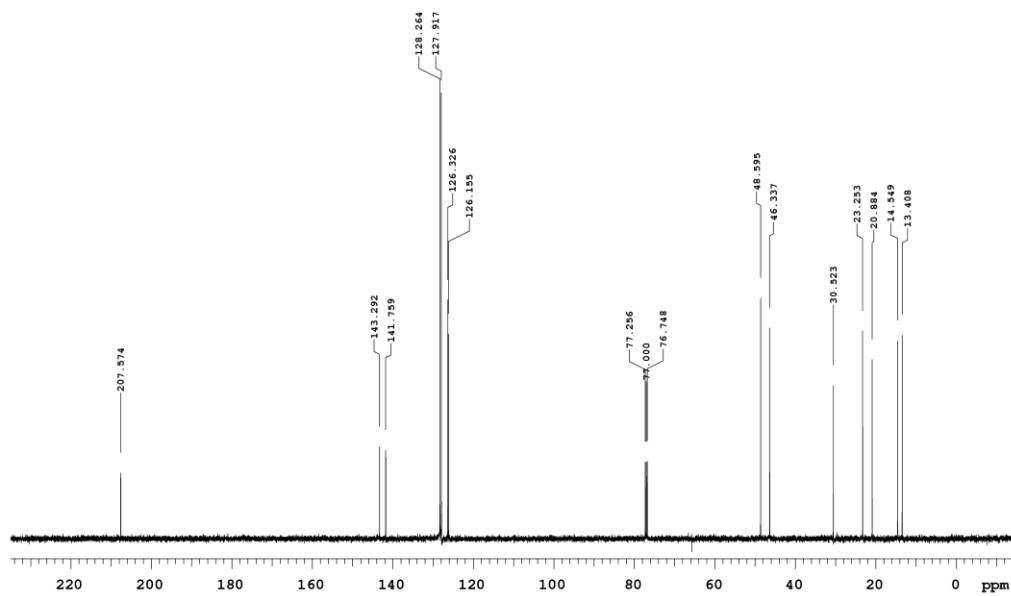
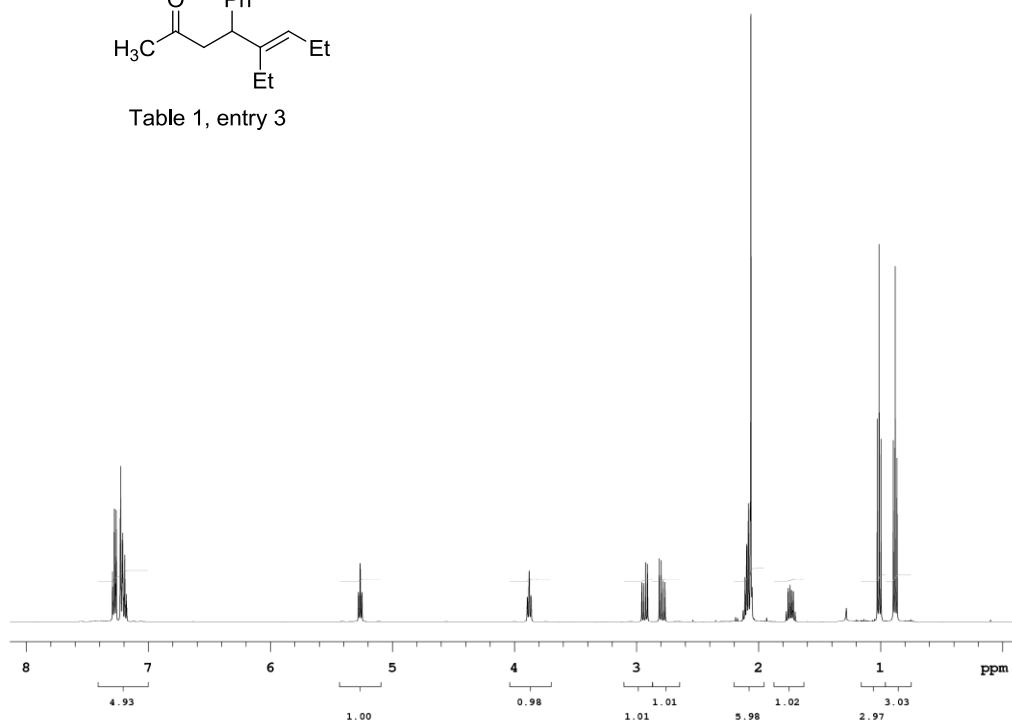
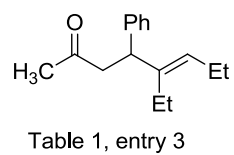


Table 1, entry 1





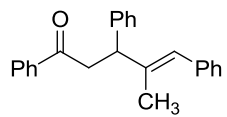
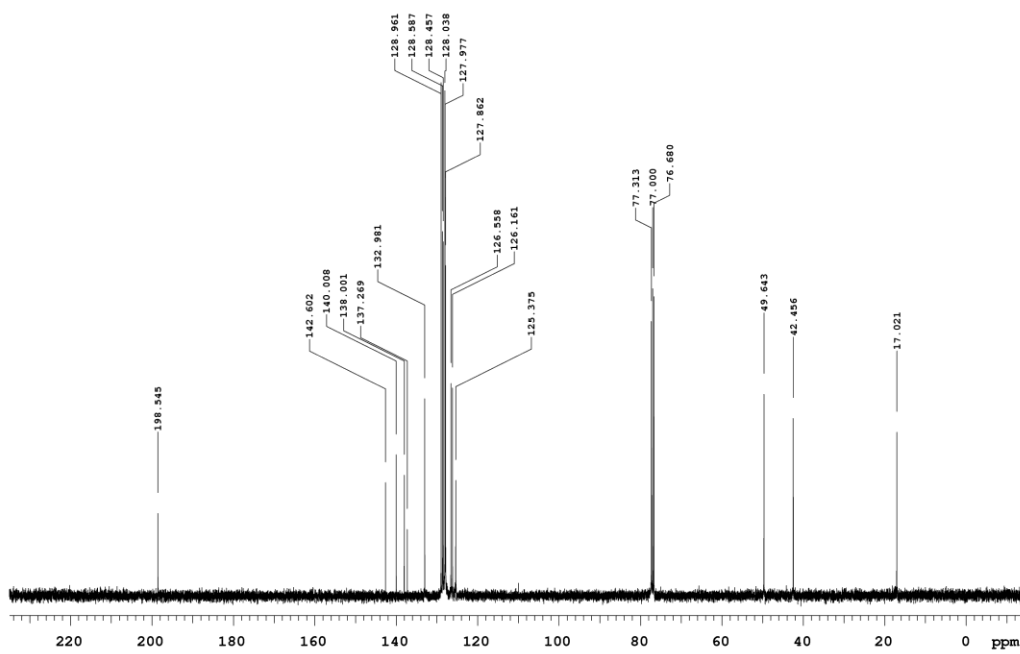
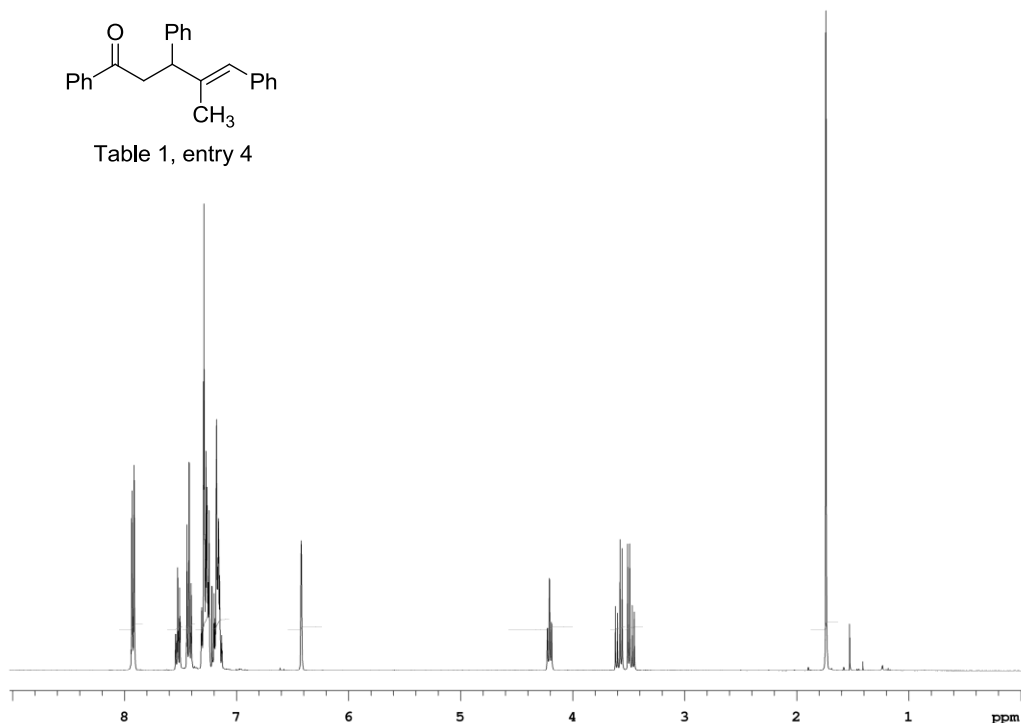


Table 1, entry 4



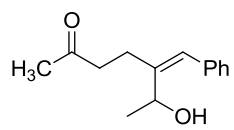
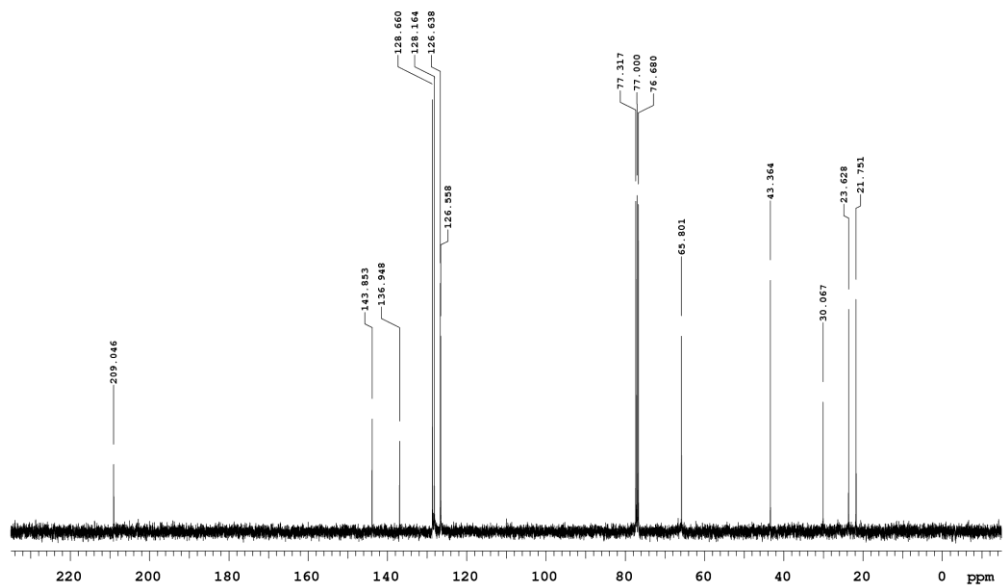
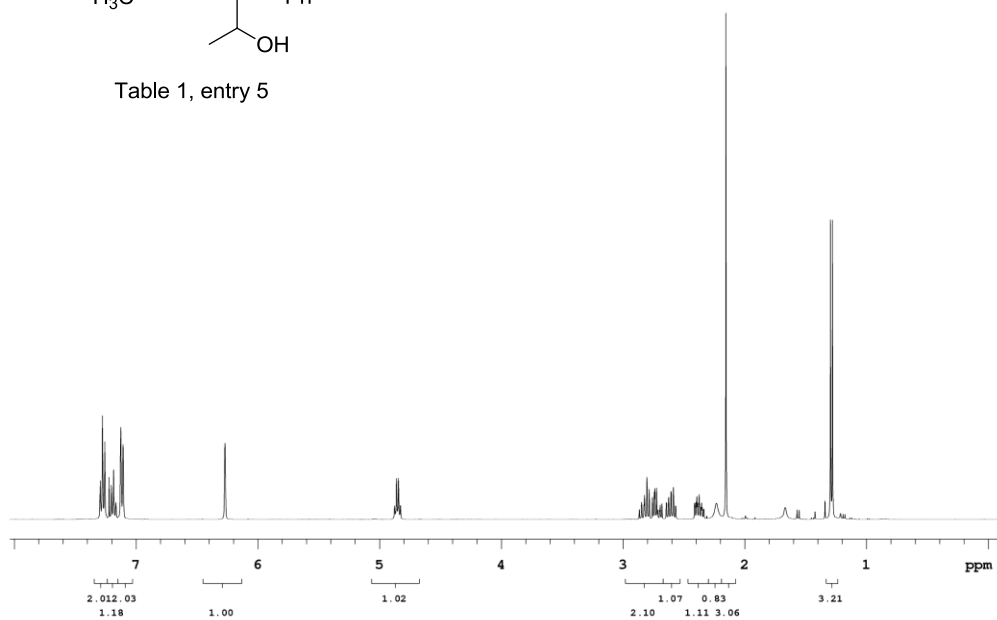


Table 1, entry 5



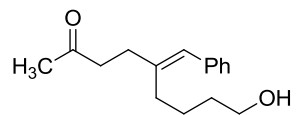
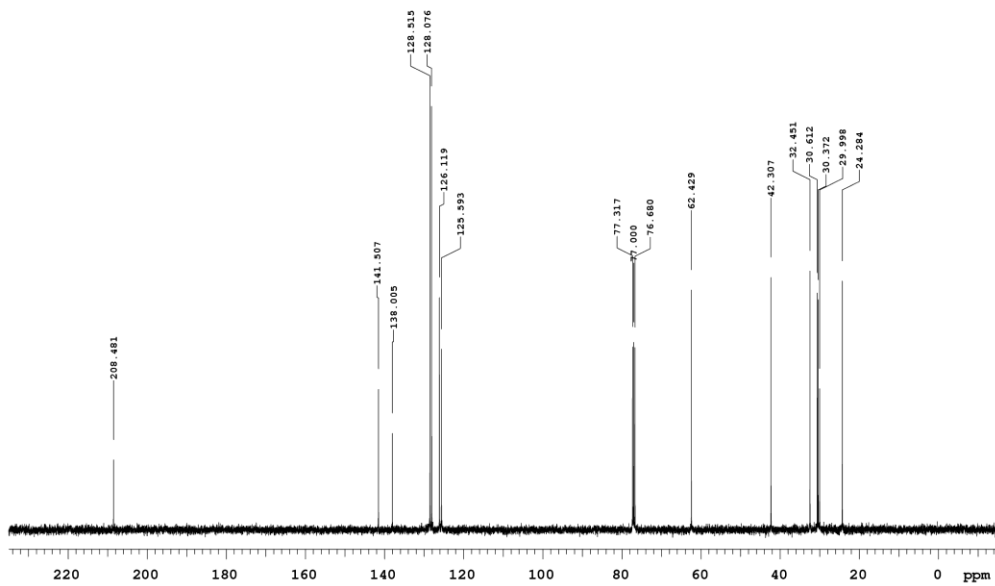
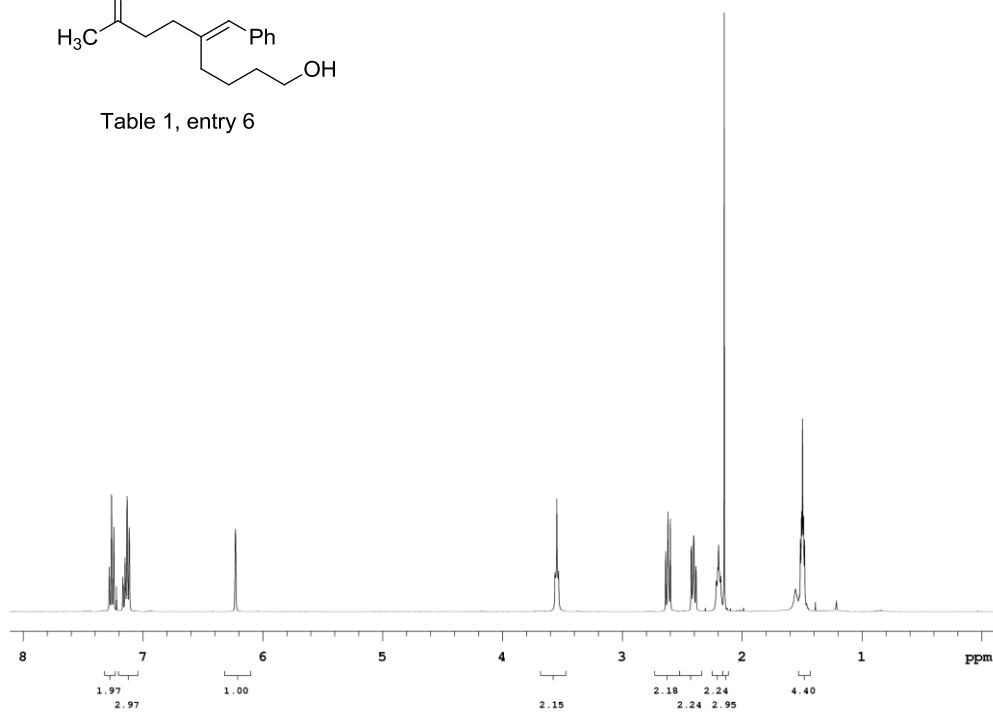


Table 1, entry 6



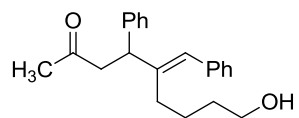
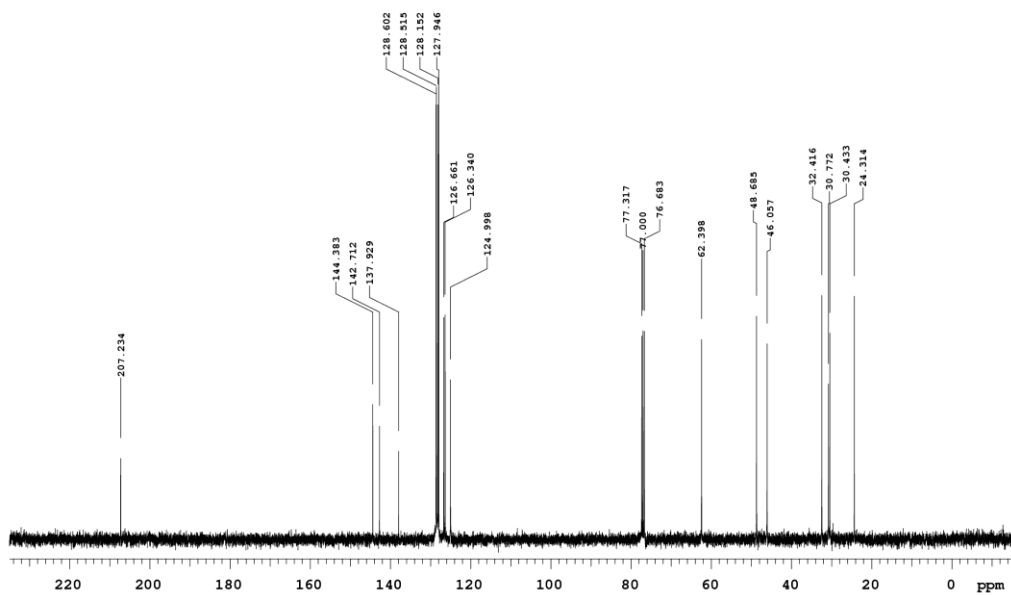
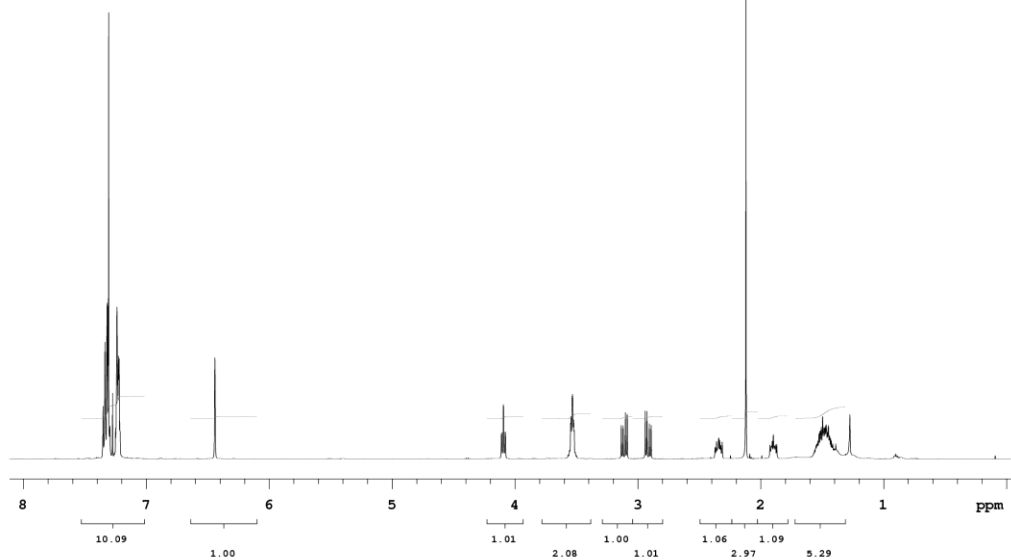


Table 1, entry 7



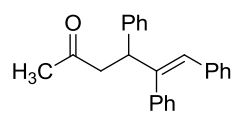
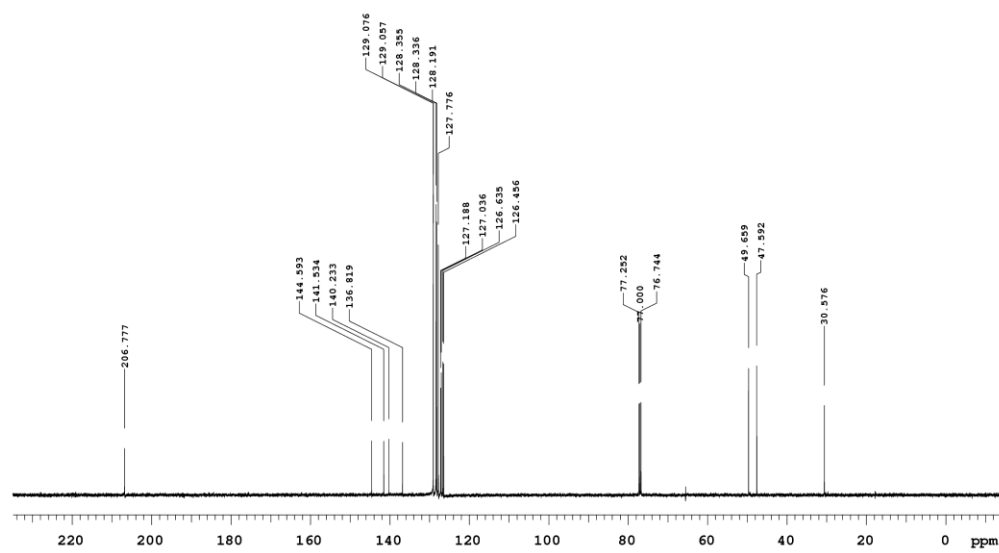
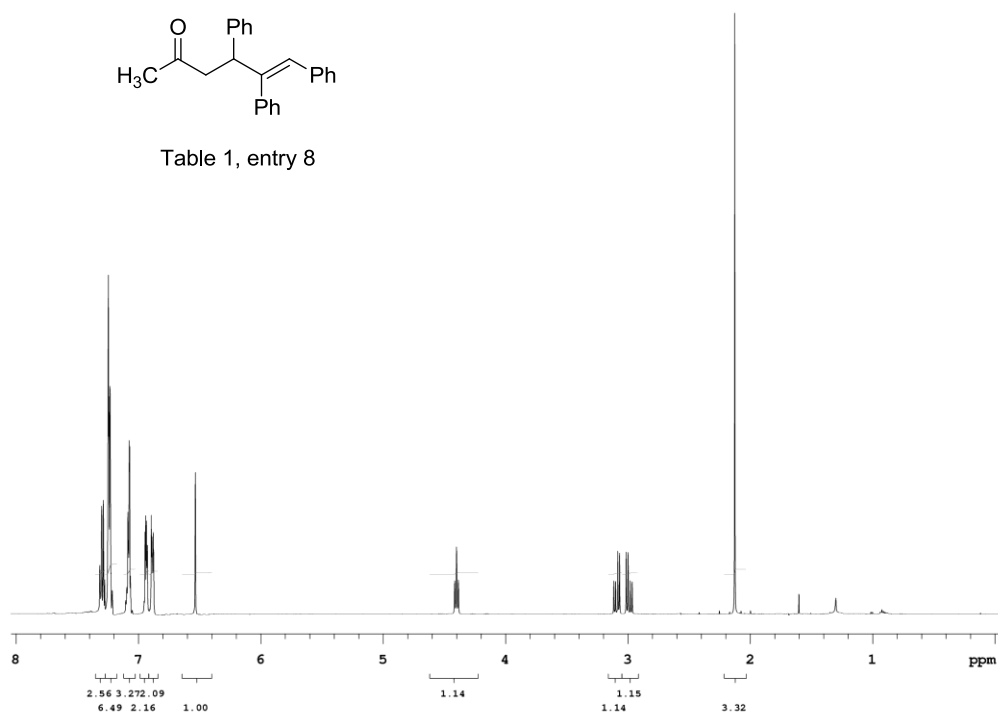


Table 1, entry 8



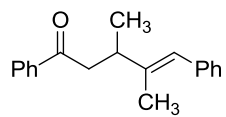
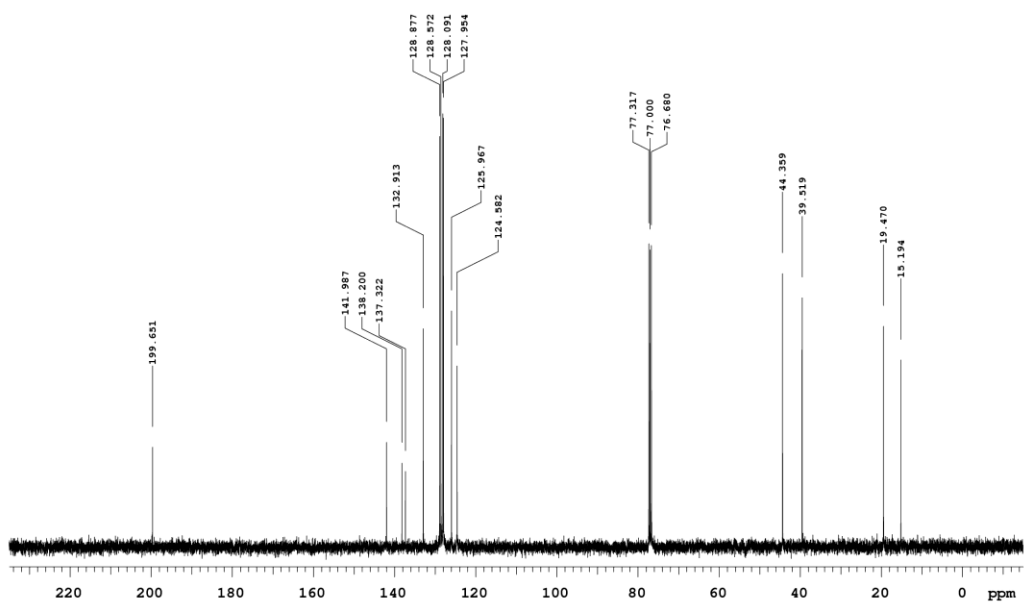
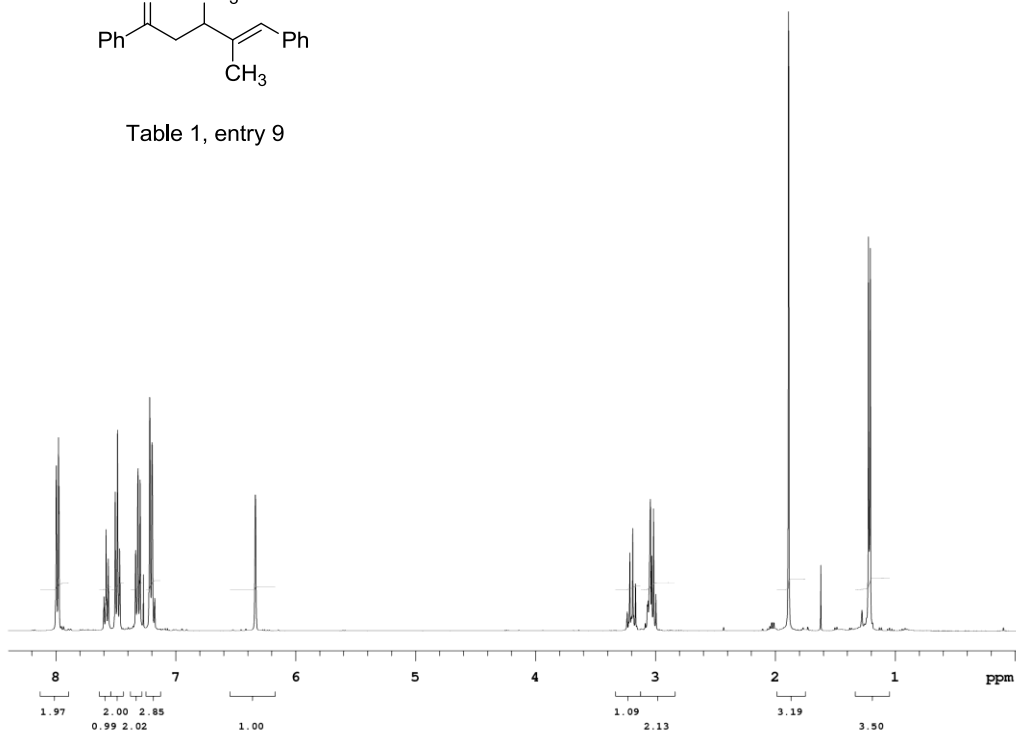


Table 1, entry 9



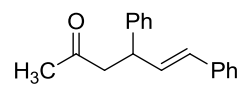
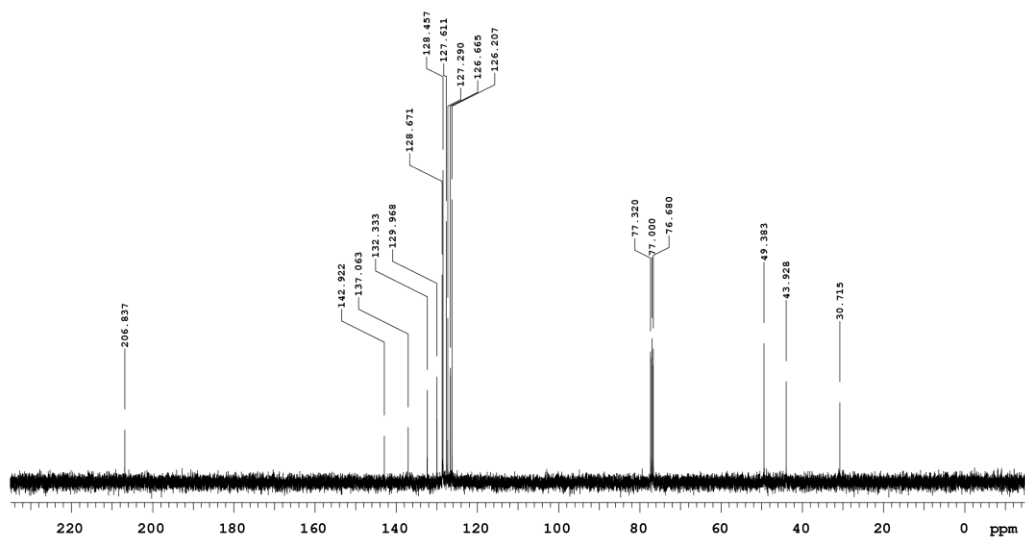
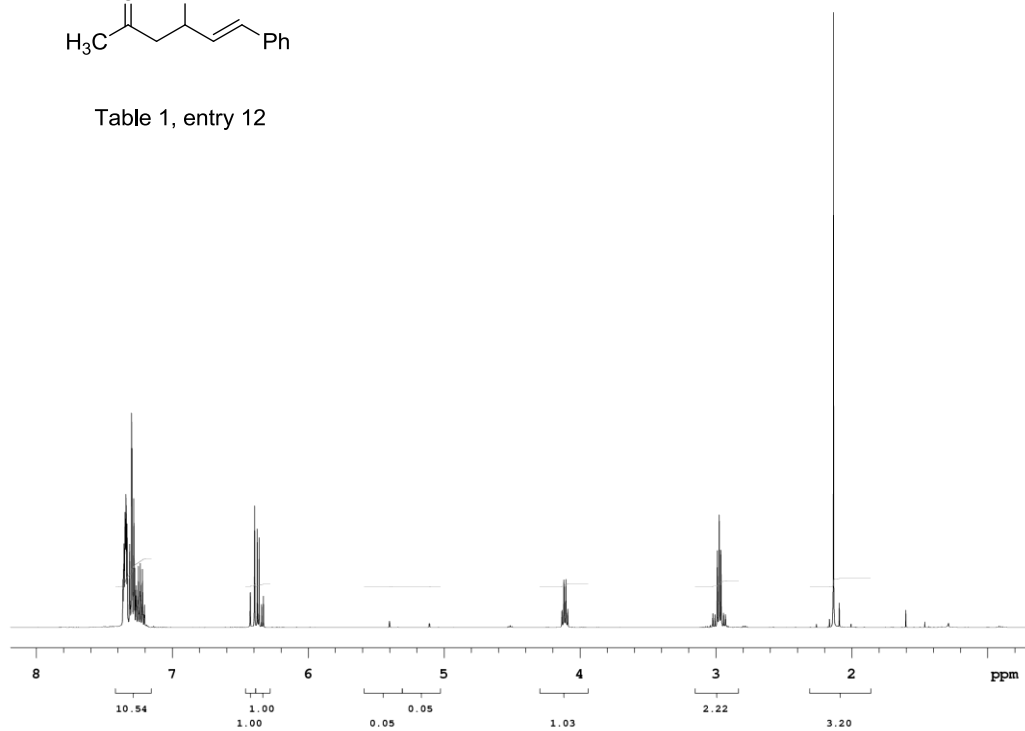


Table 1, entry 12



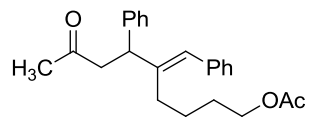
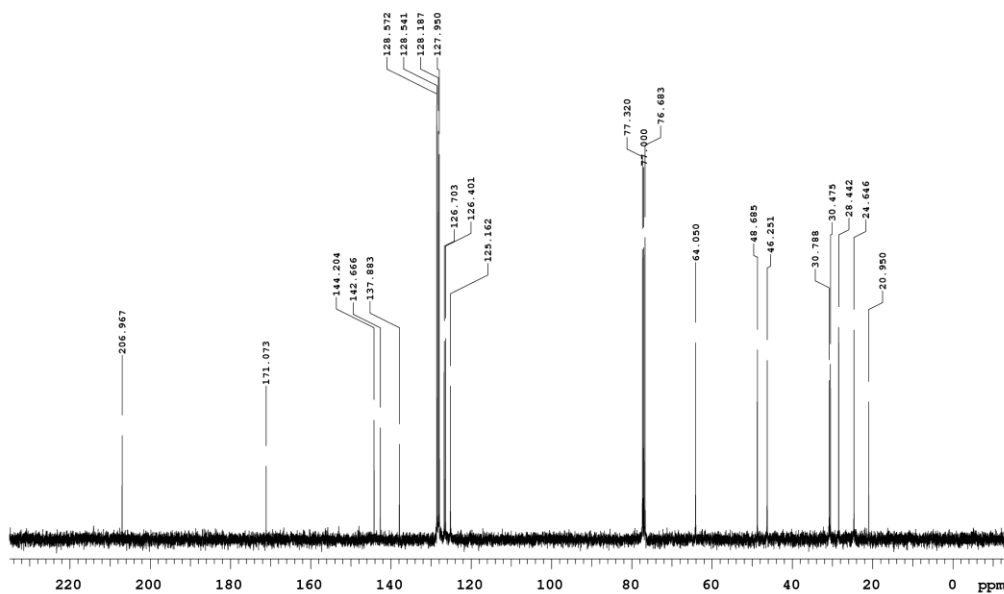
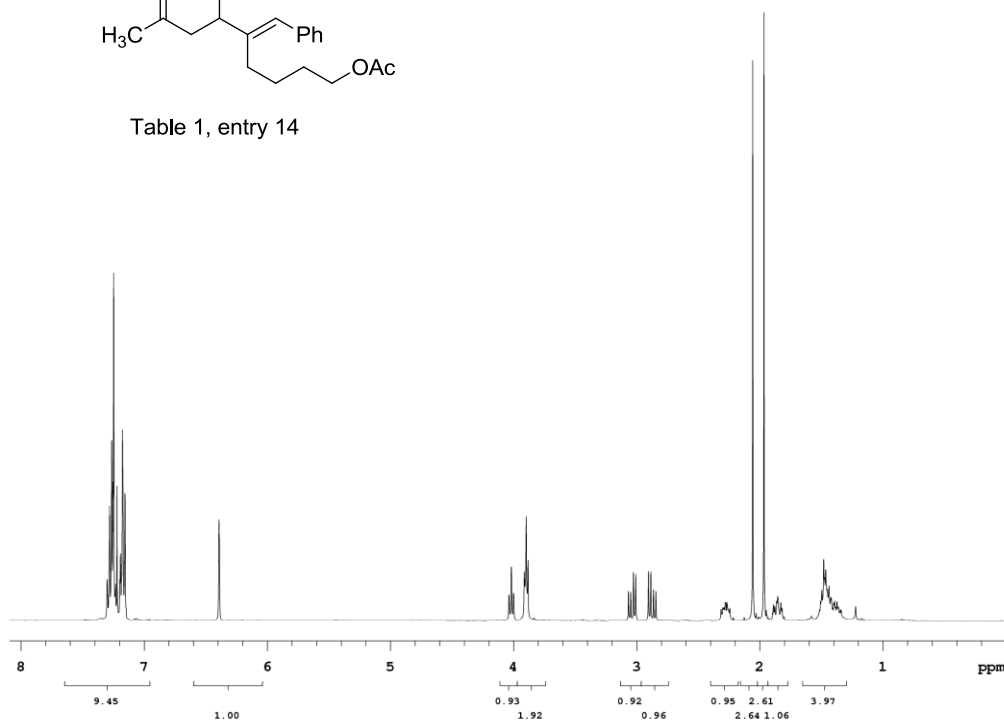
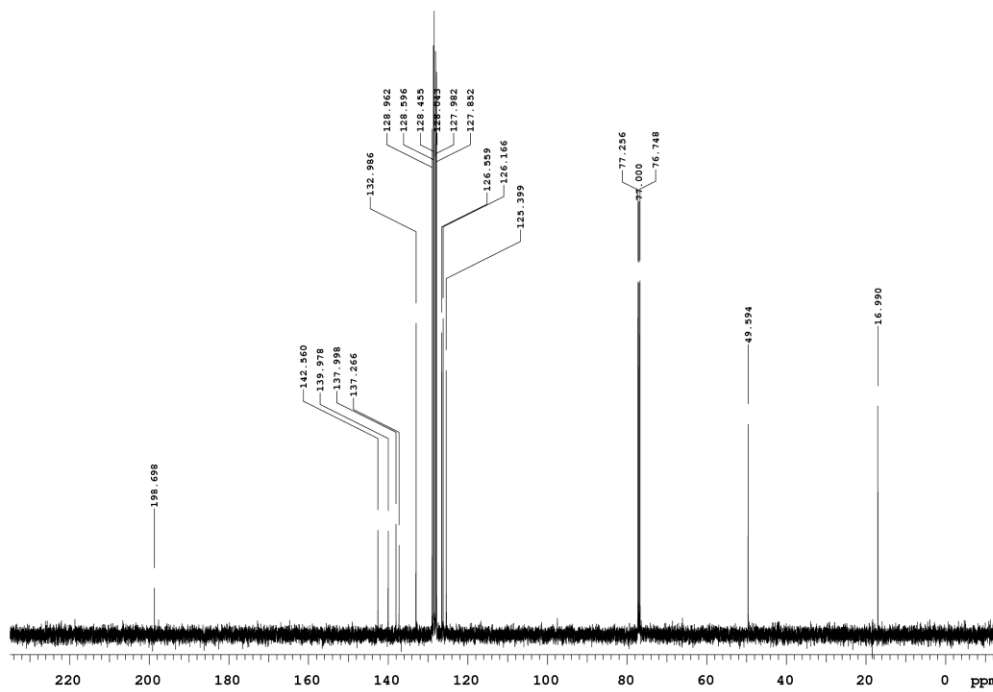
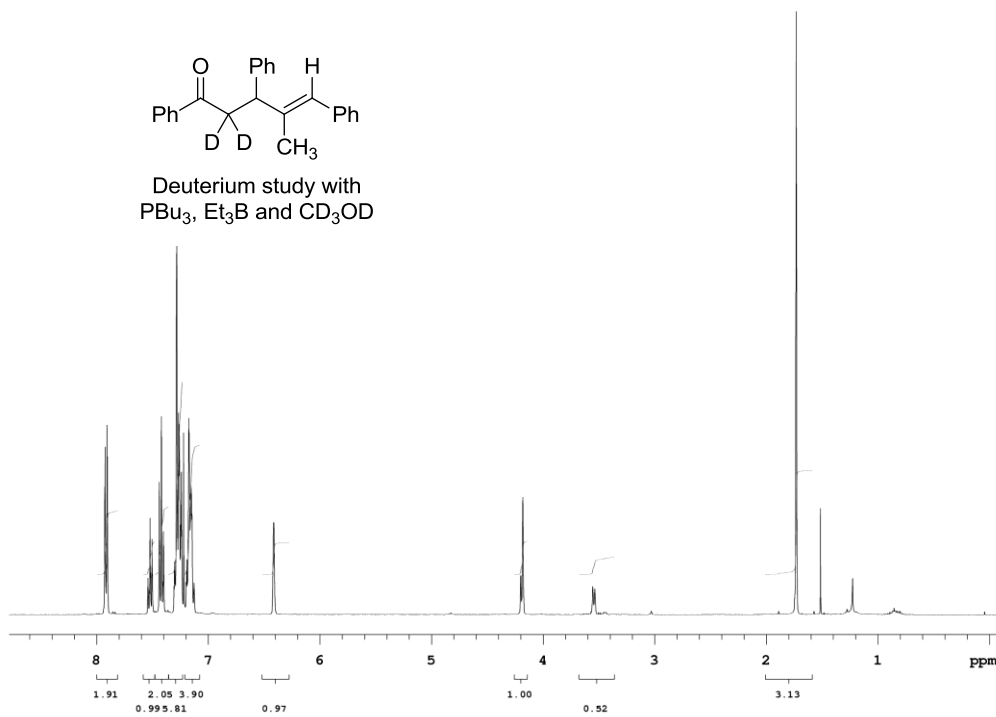
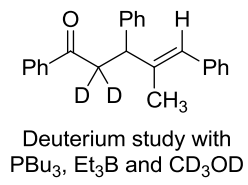
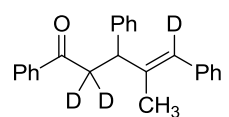


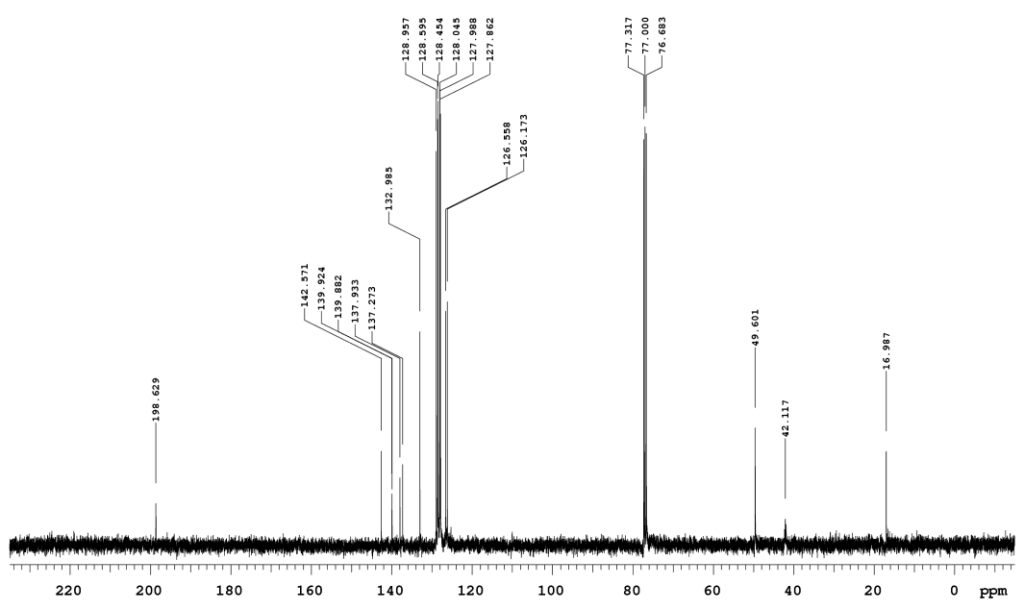
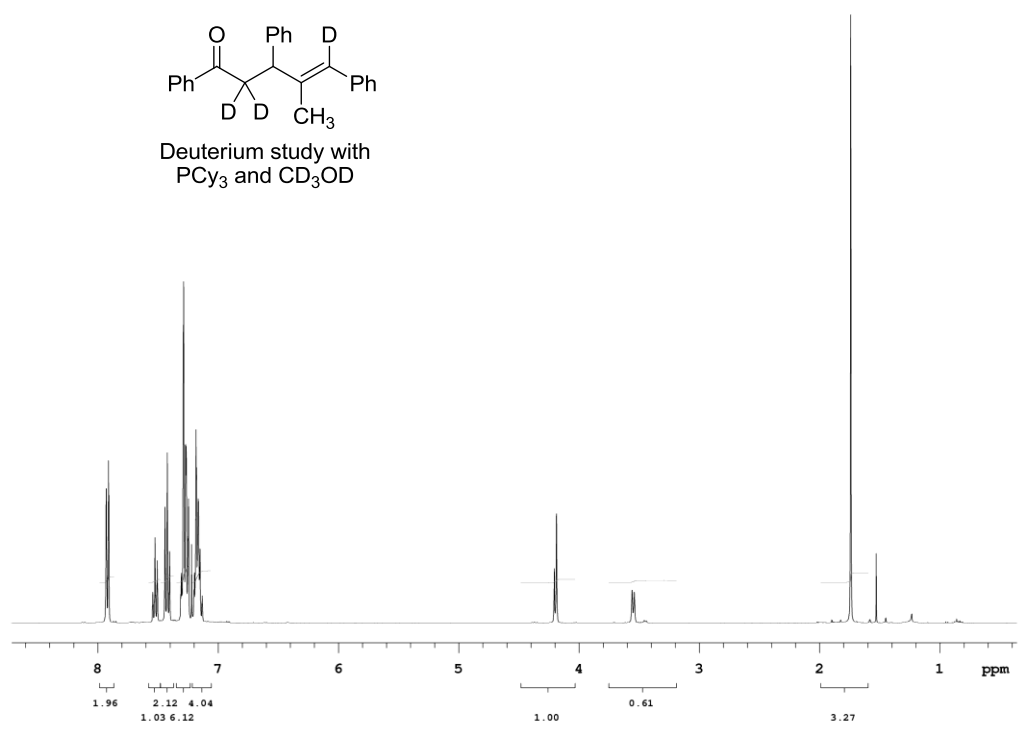
Table 1, entry 14

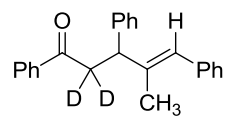




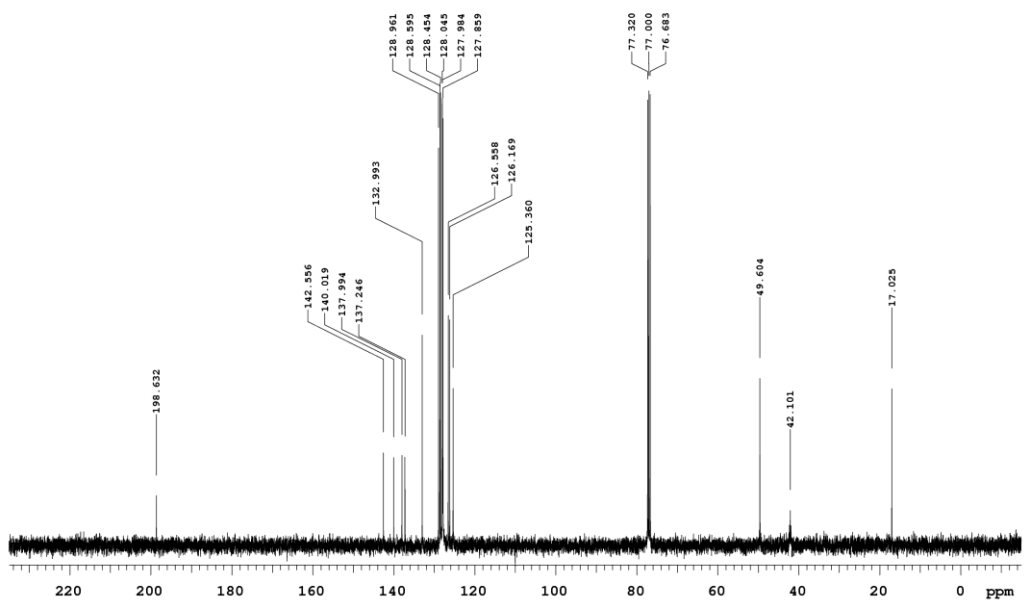
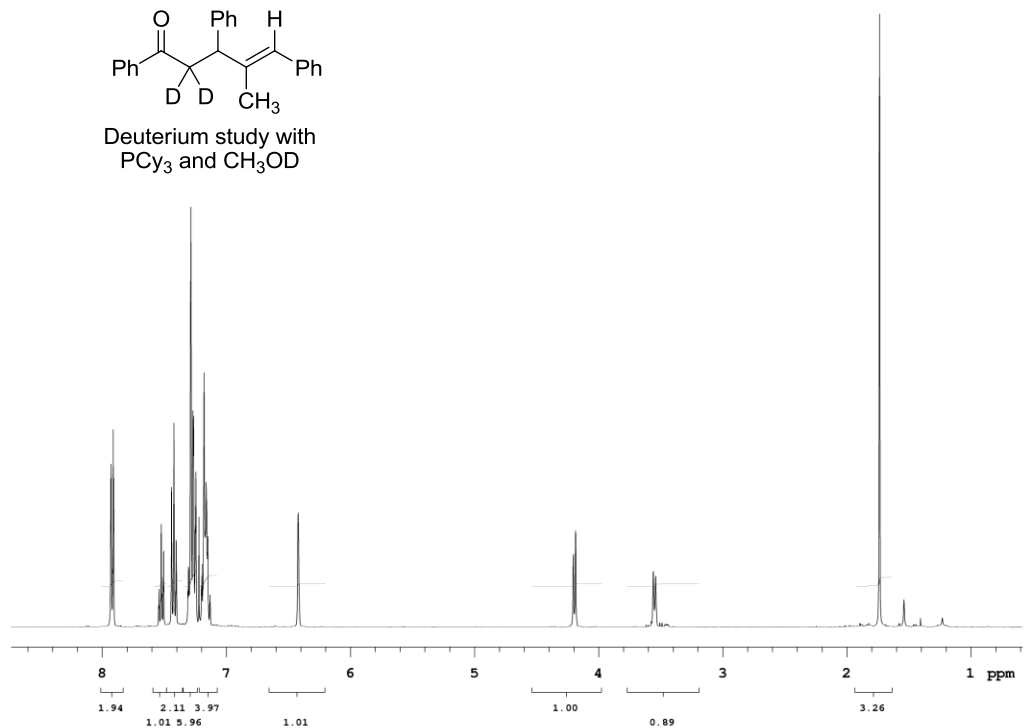


Deuterium study with PCy₃ and CD₃OD





Deuterium study with
PCy₃ and CH₃OD



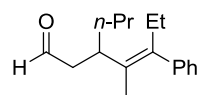
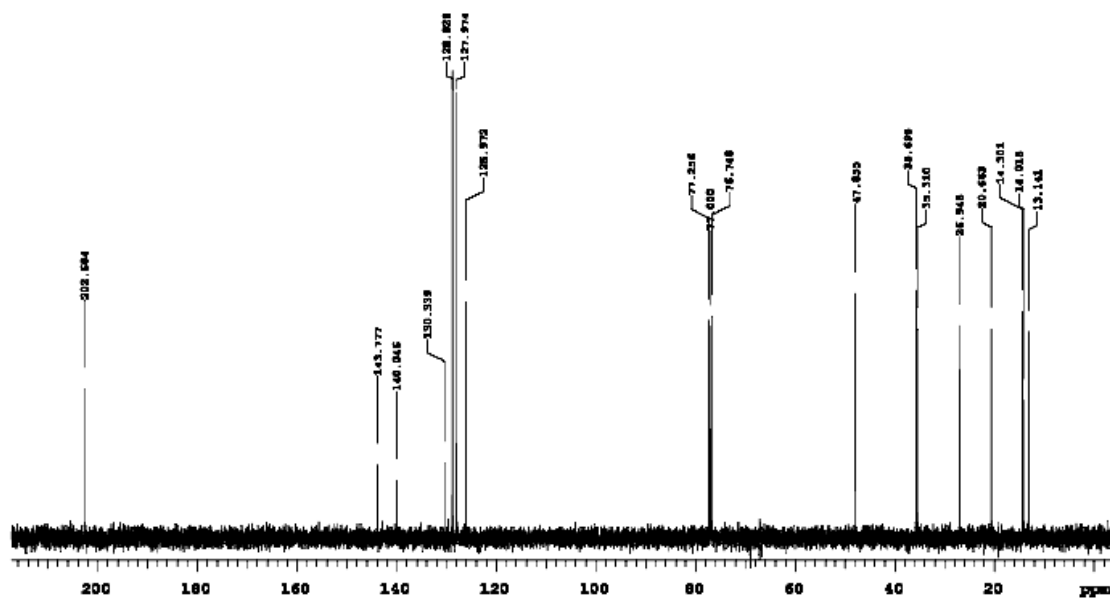
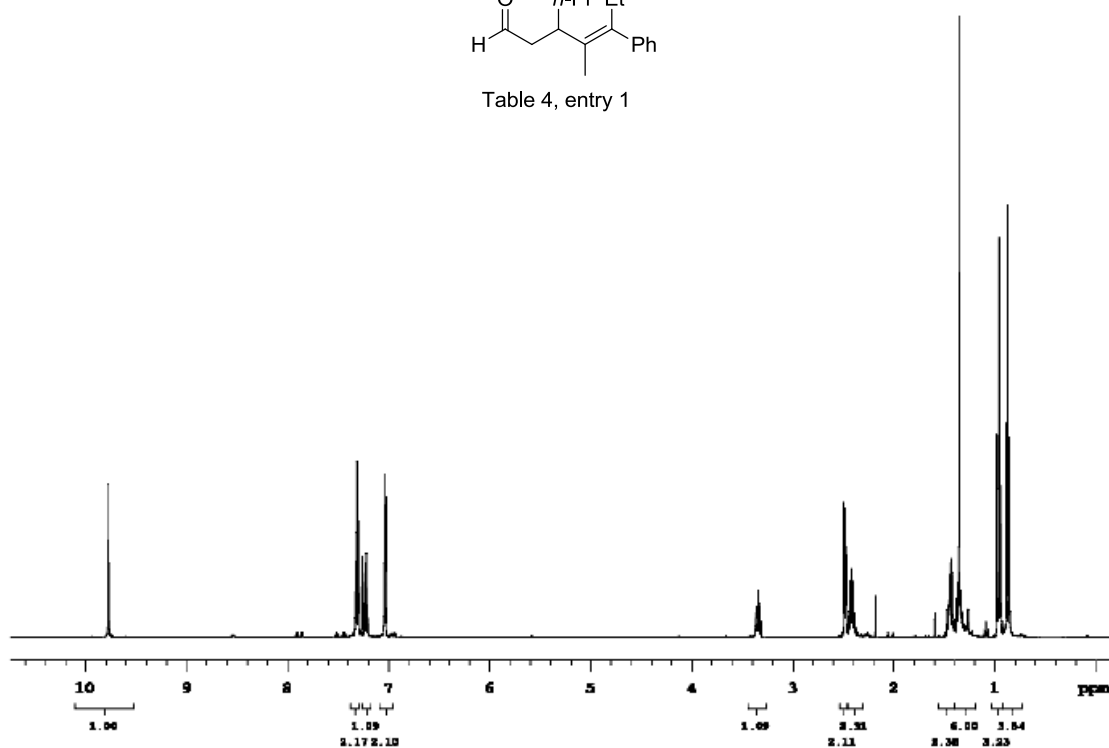


Table 4, entry 1



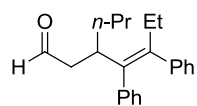
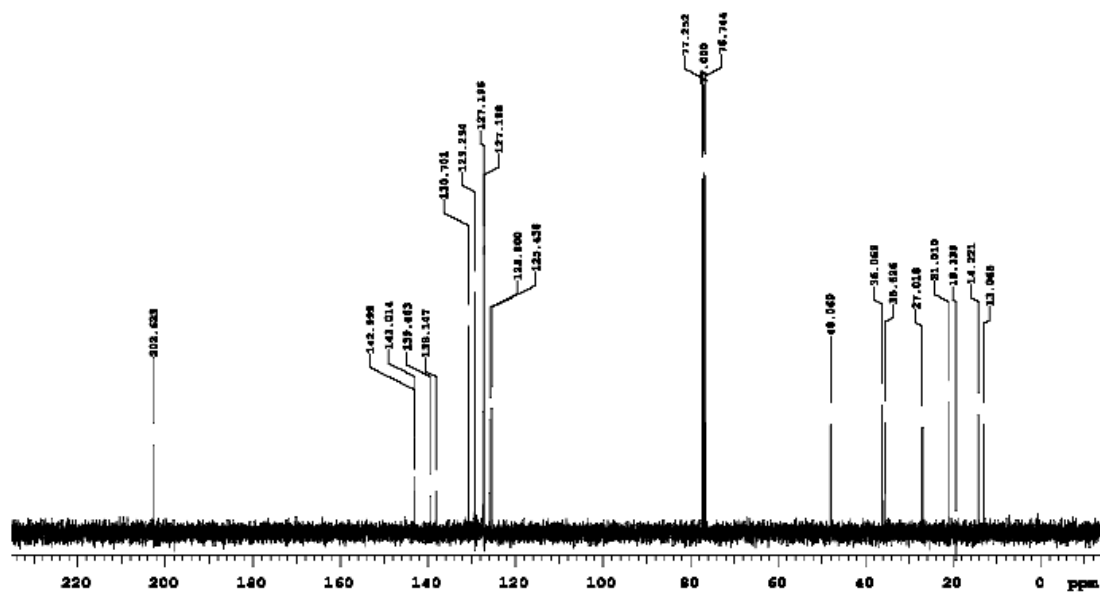
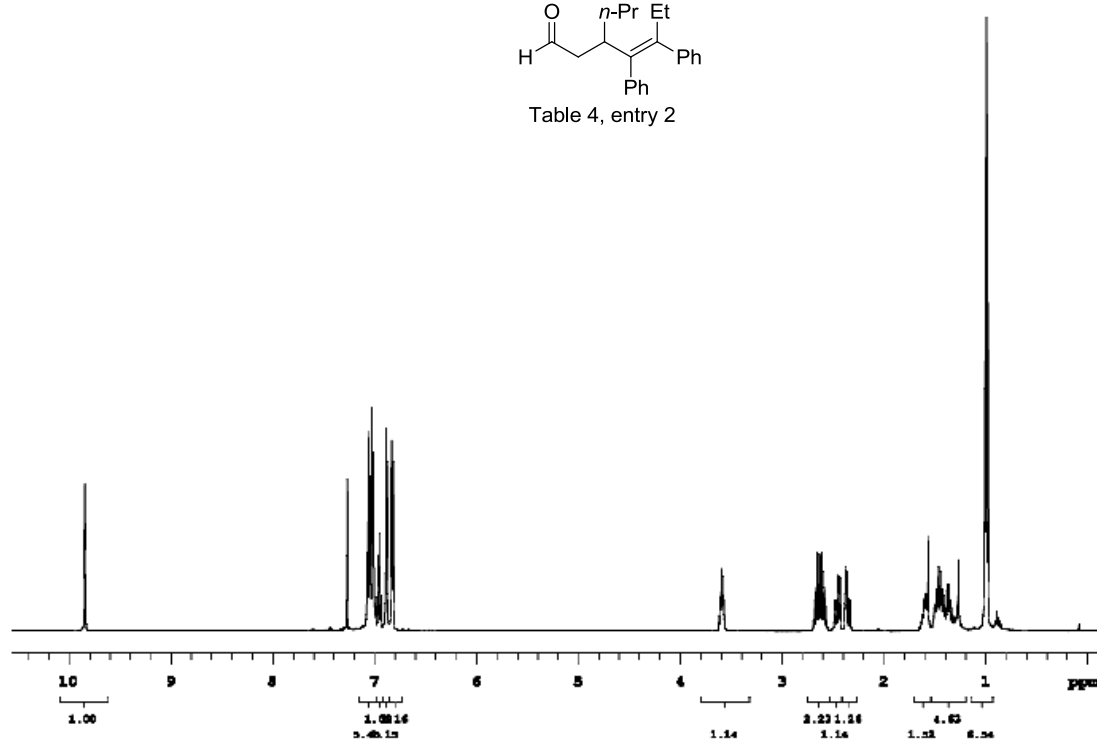


Table 4, entry 2



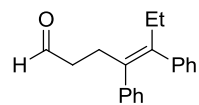
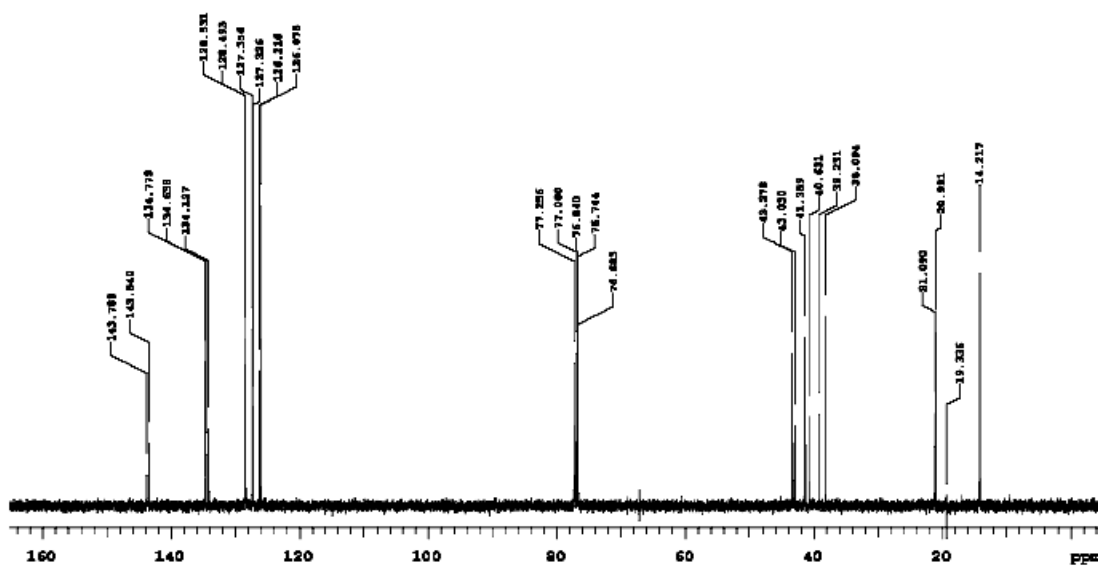
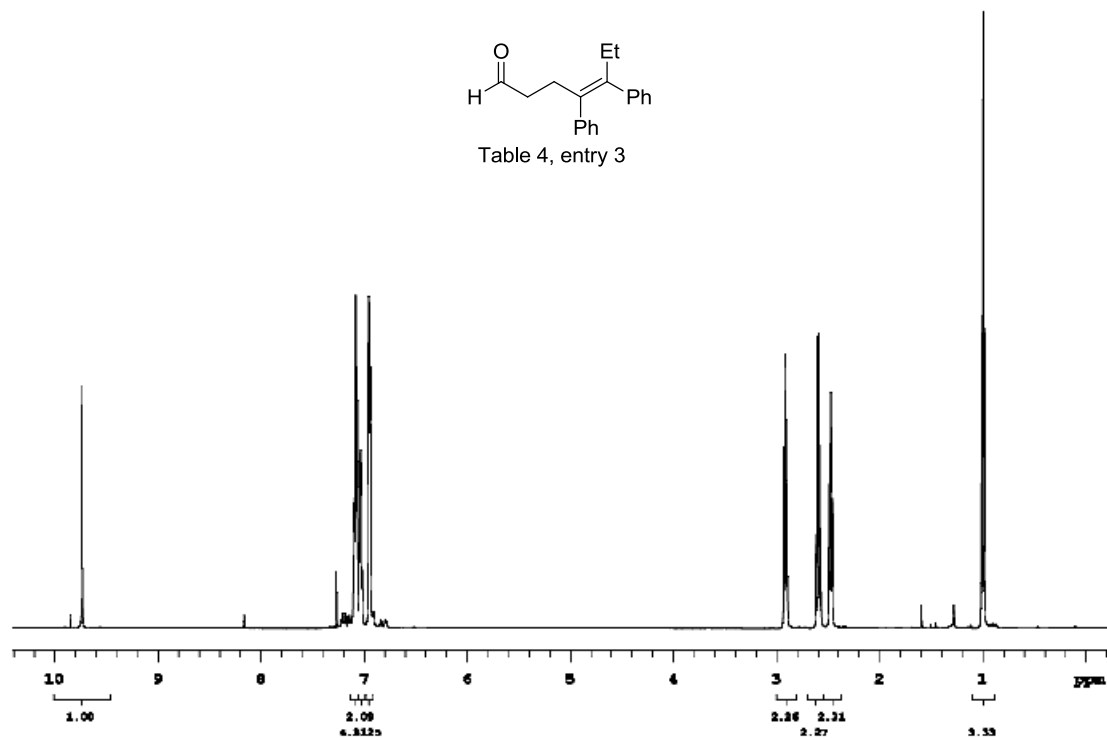


Table 4, entry 3



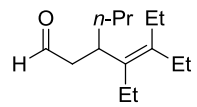
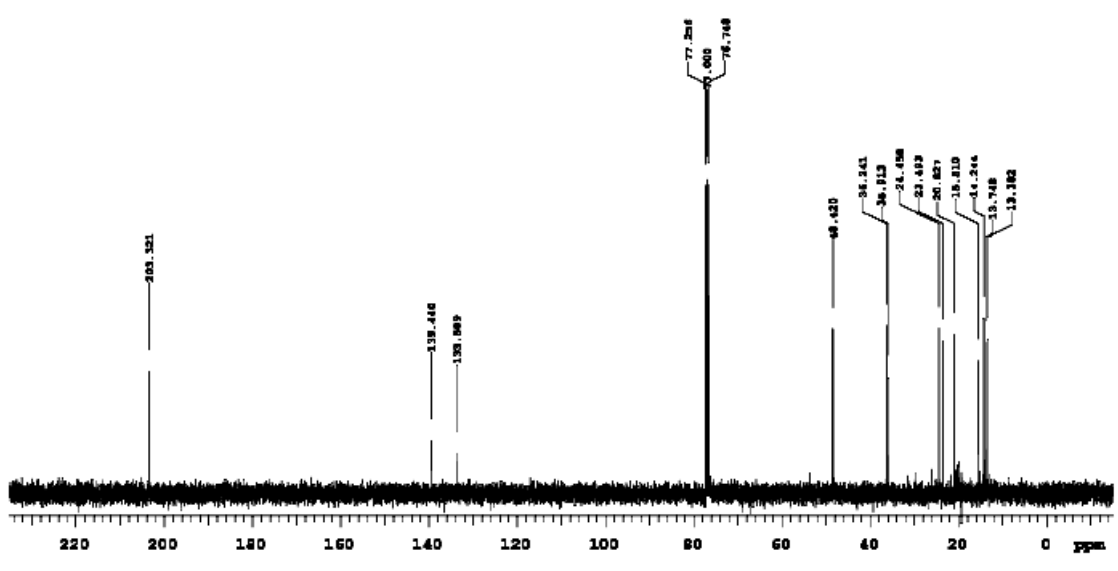
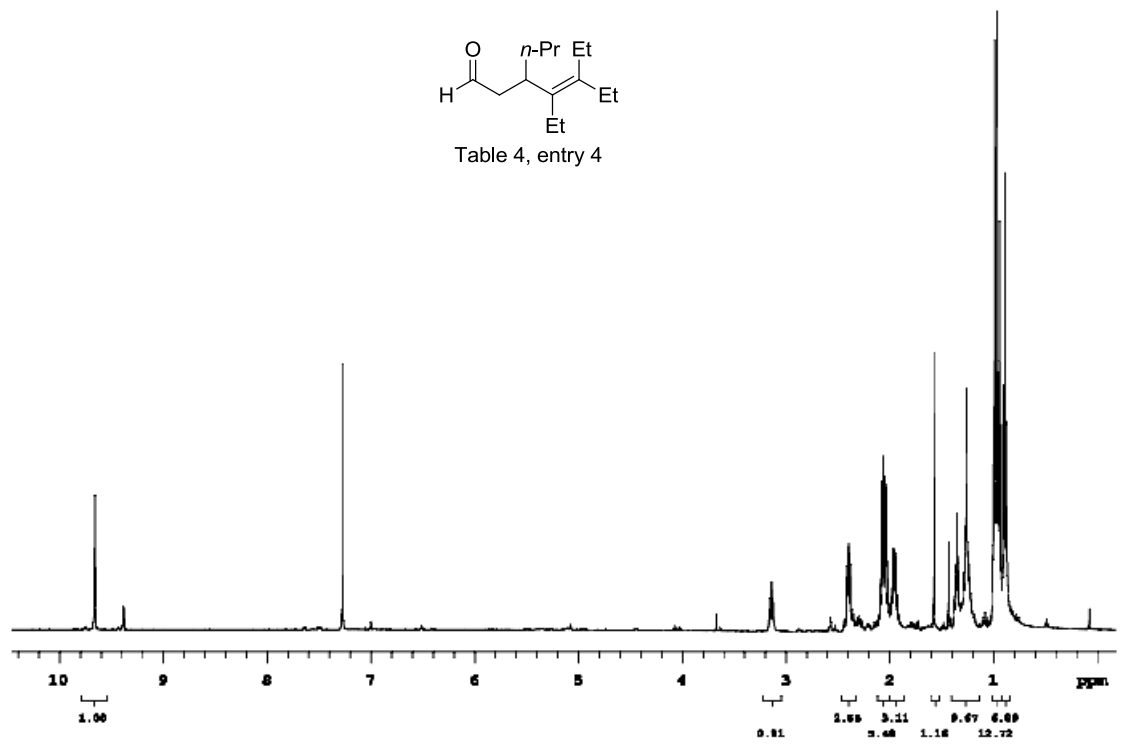


Table 4, entry 4



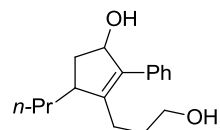
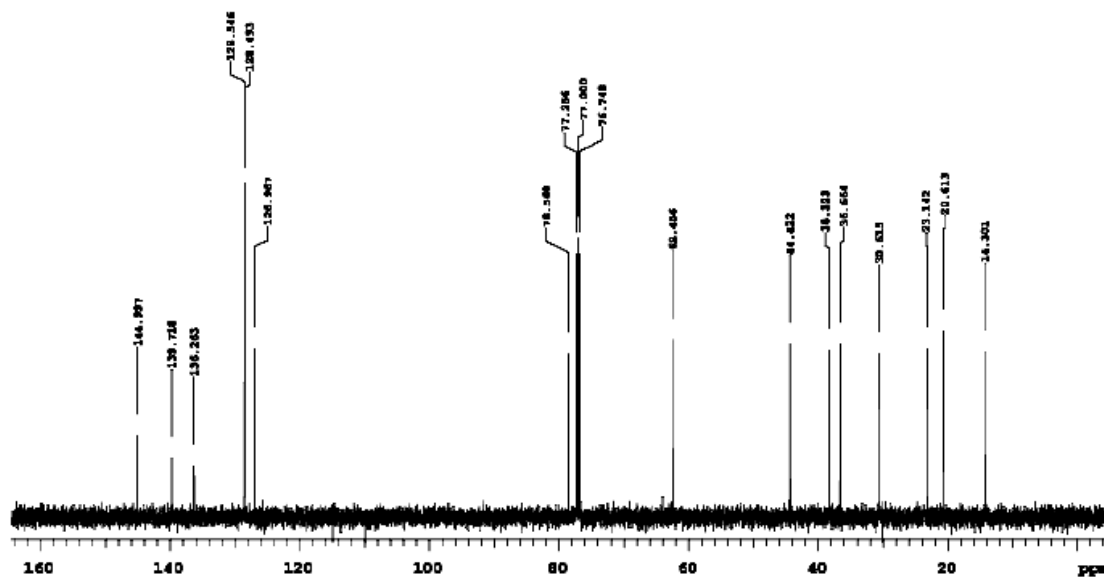
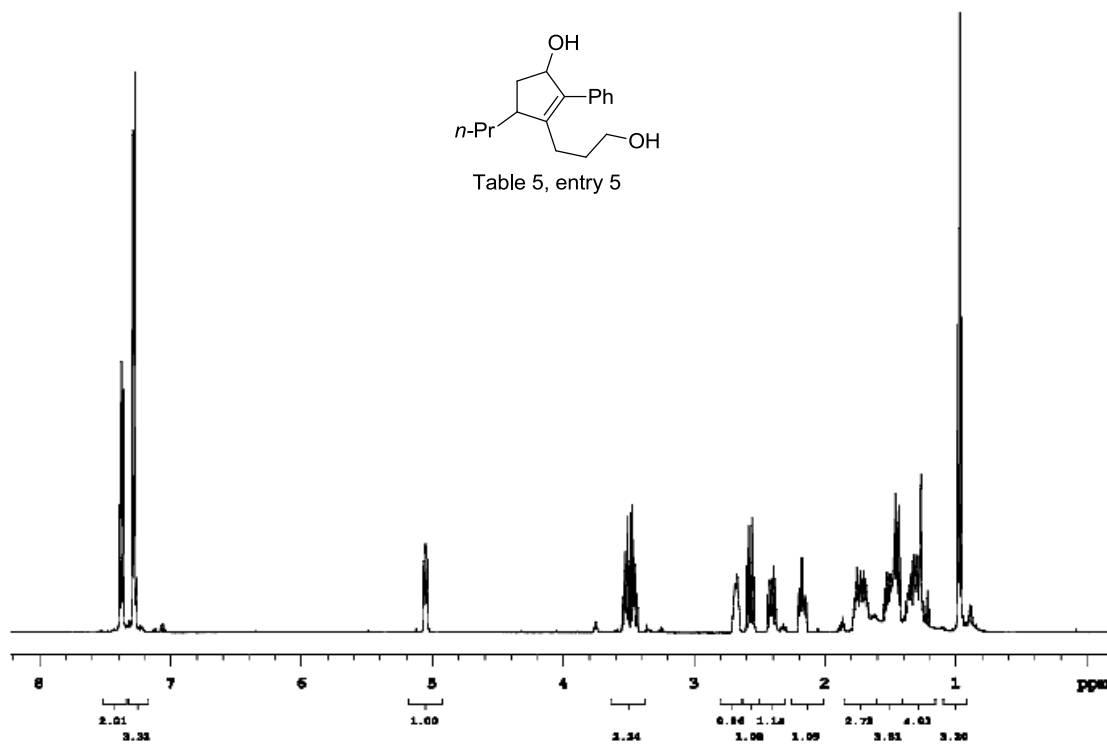


Table 5, entry 5



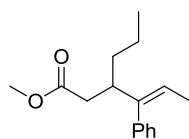
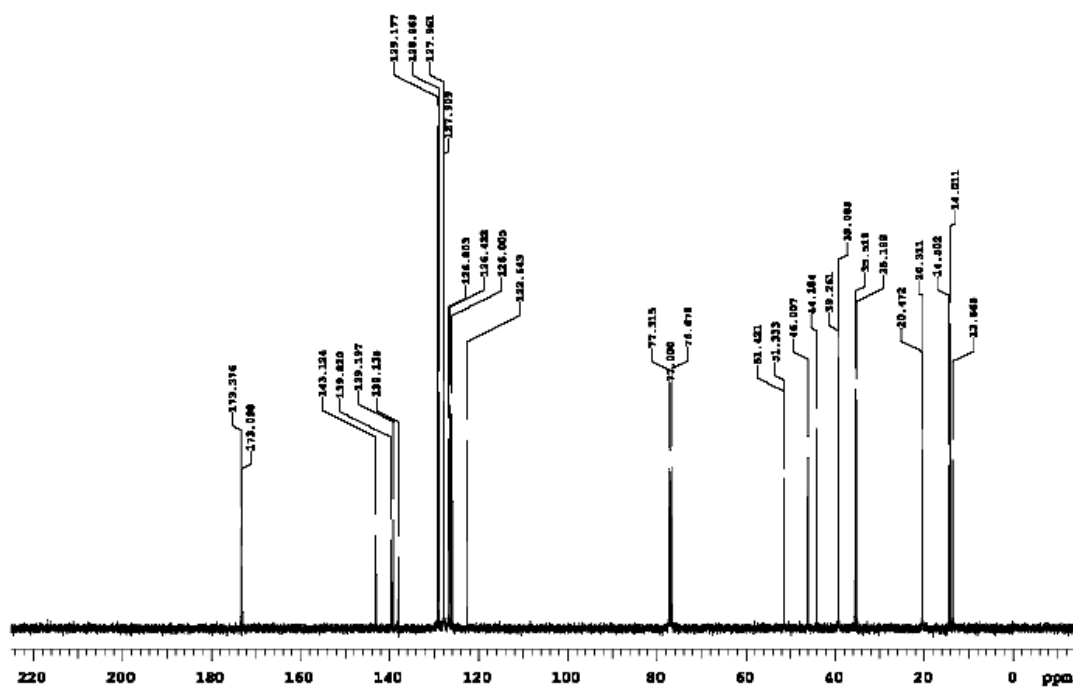
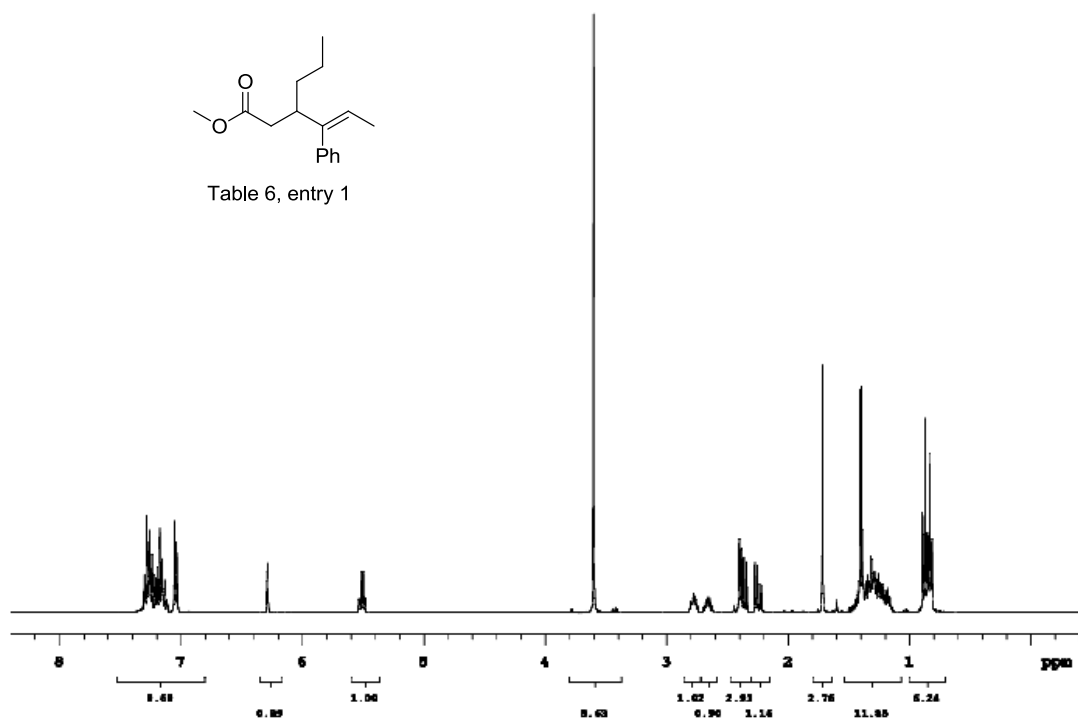


Table 6, entry 1



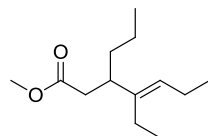
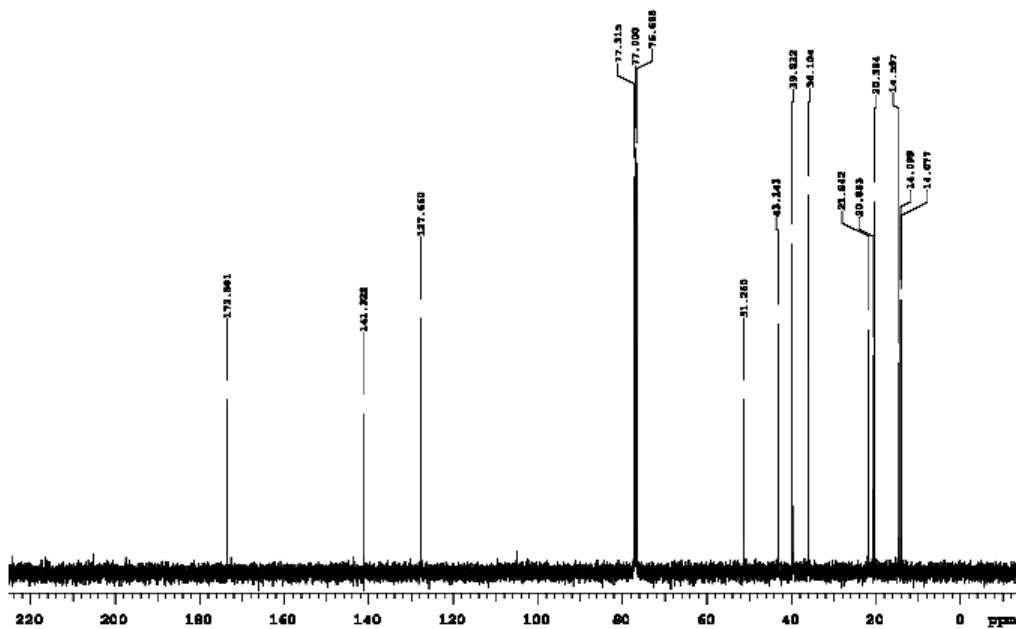
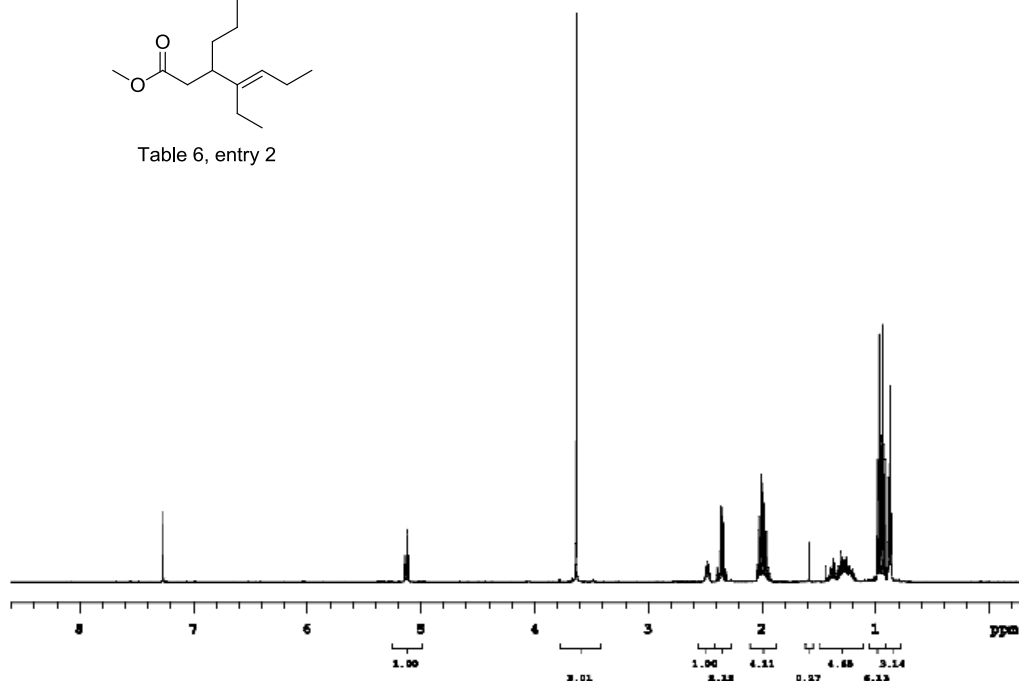


Table 6, entry 2



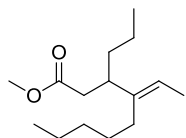
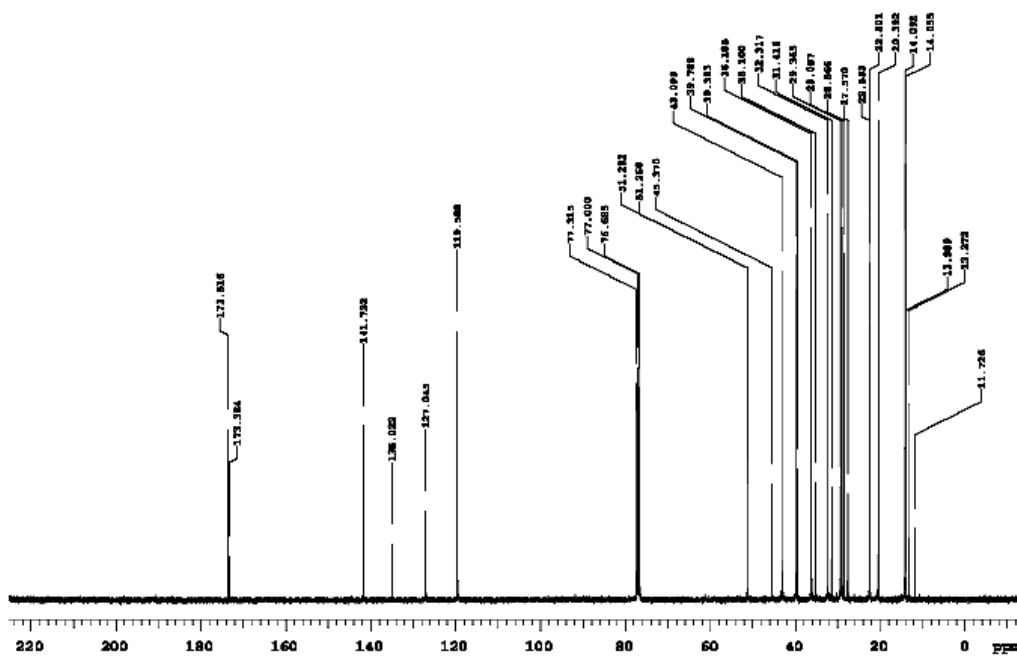
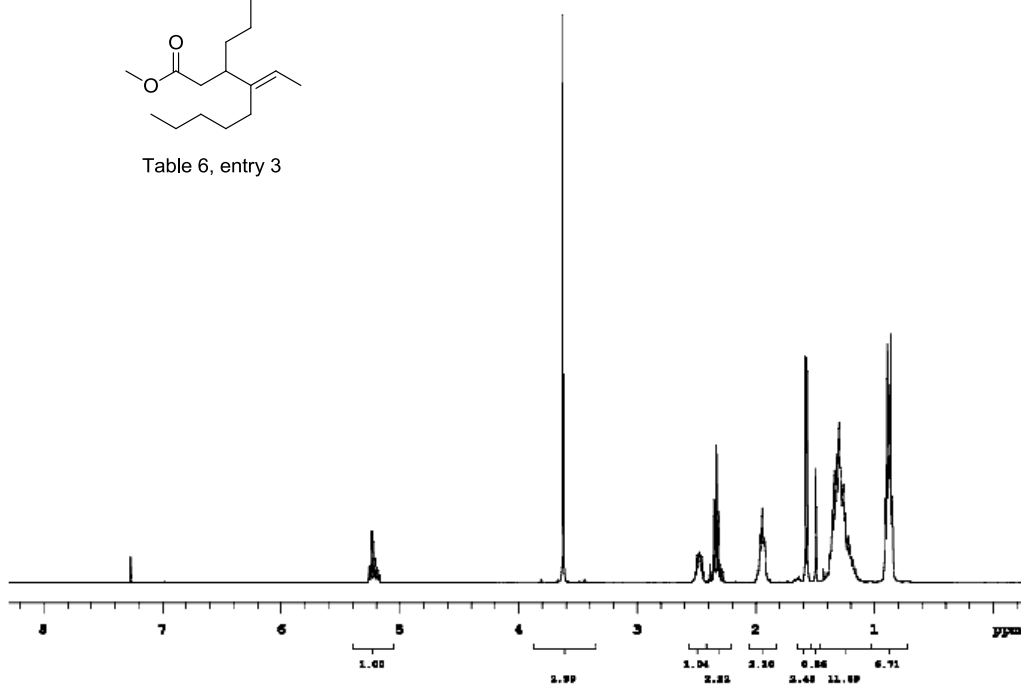


Table 6, entry 3



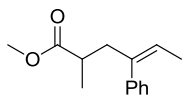
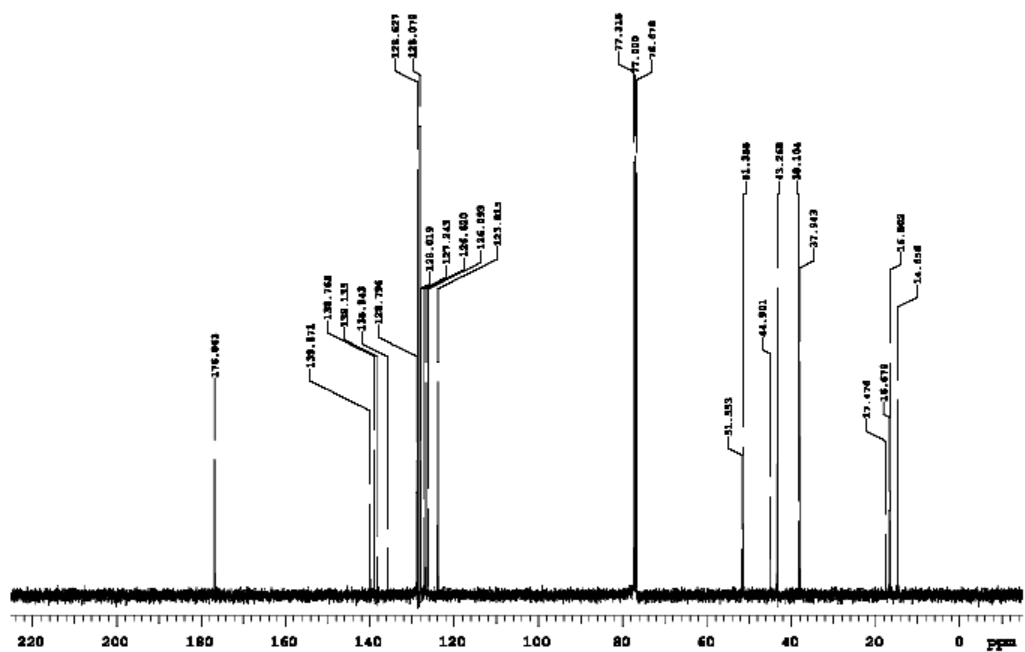
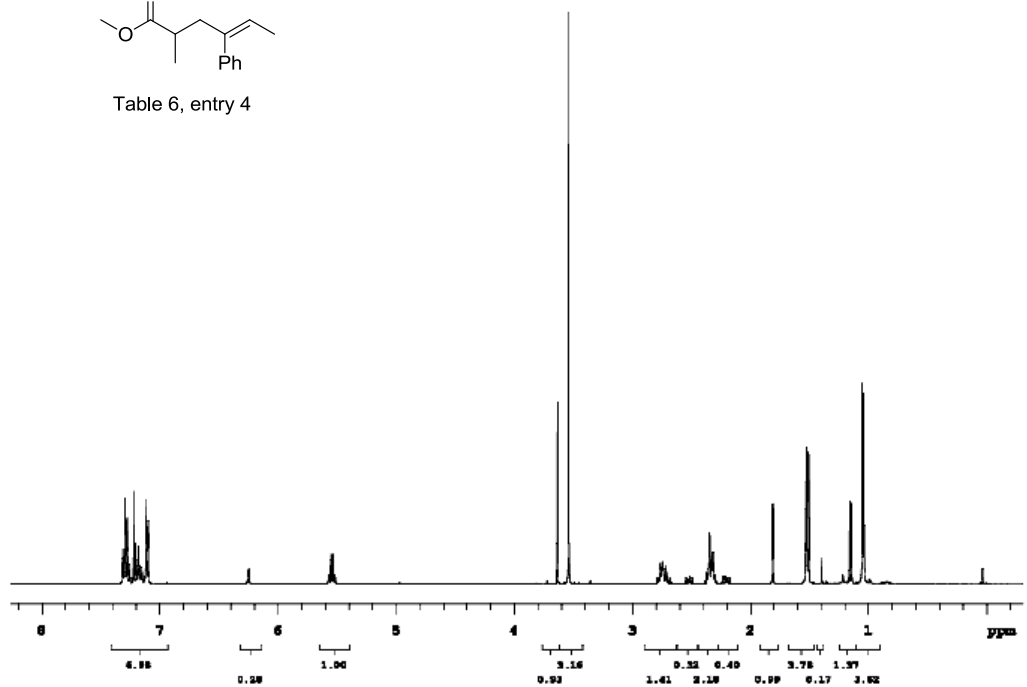


Table 6, entry 4



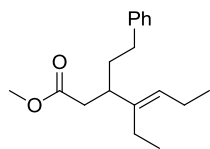
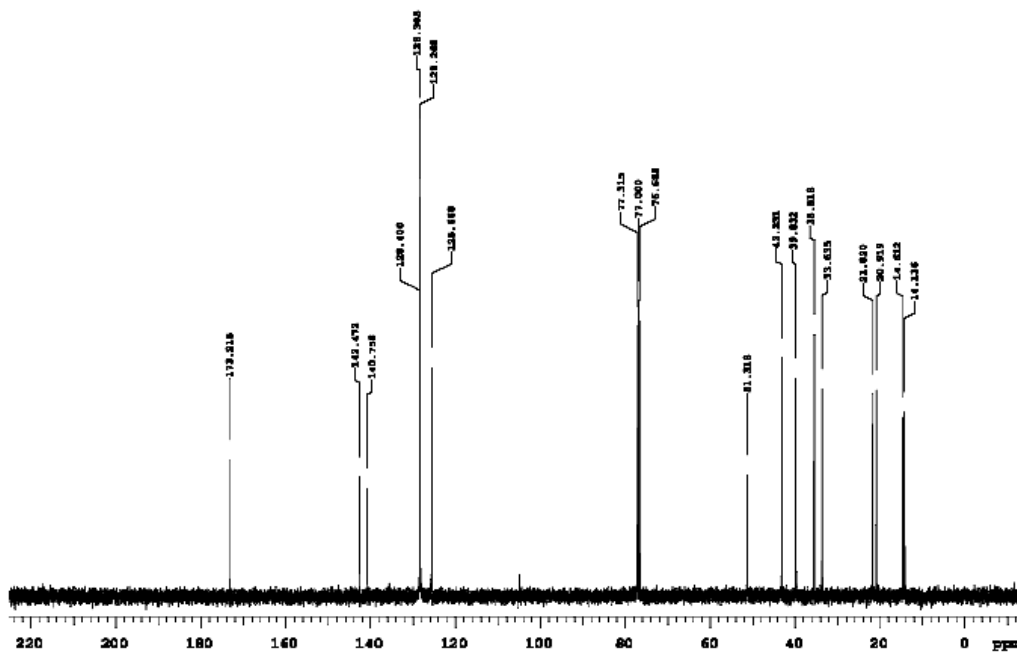
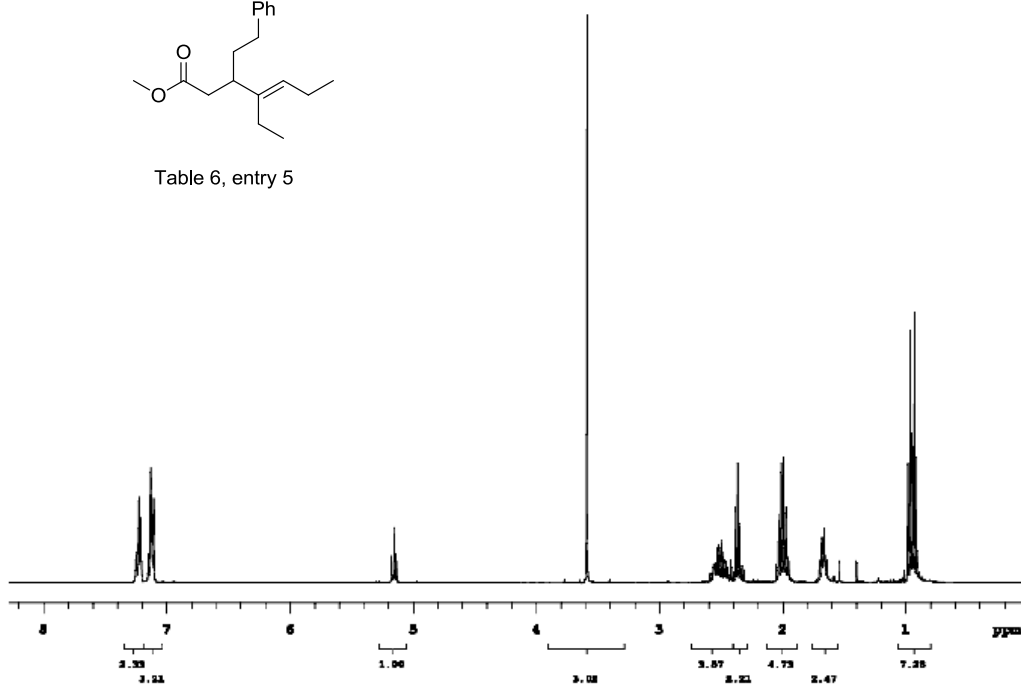


Table 6, entry 5



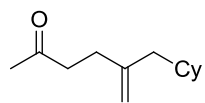
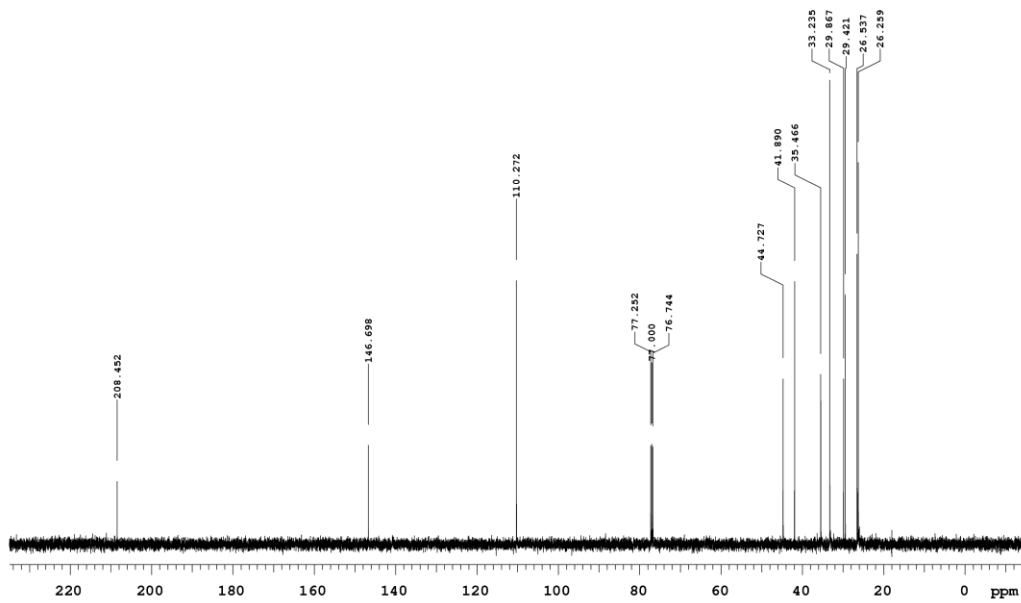
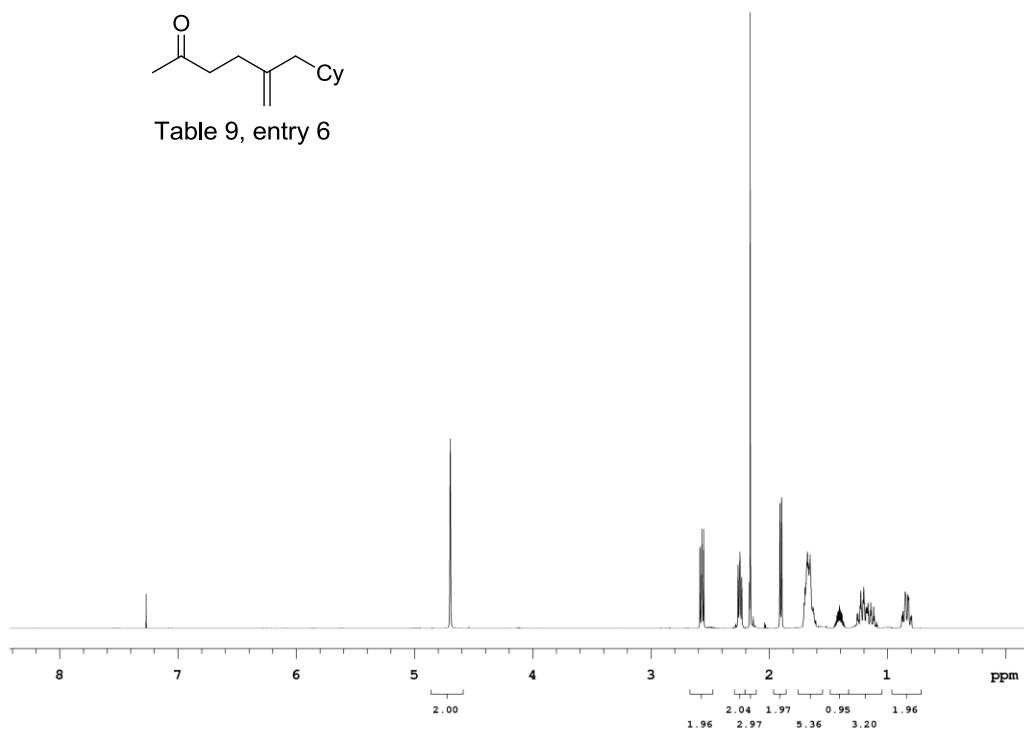


Table 9, entry 6



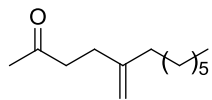
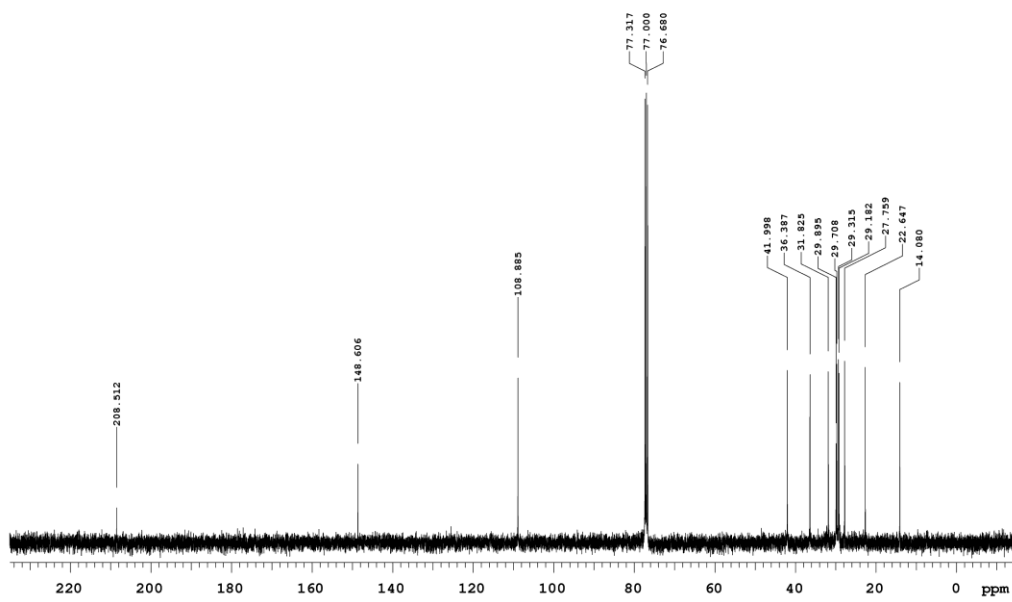
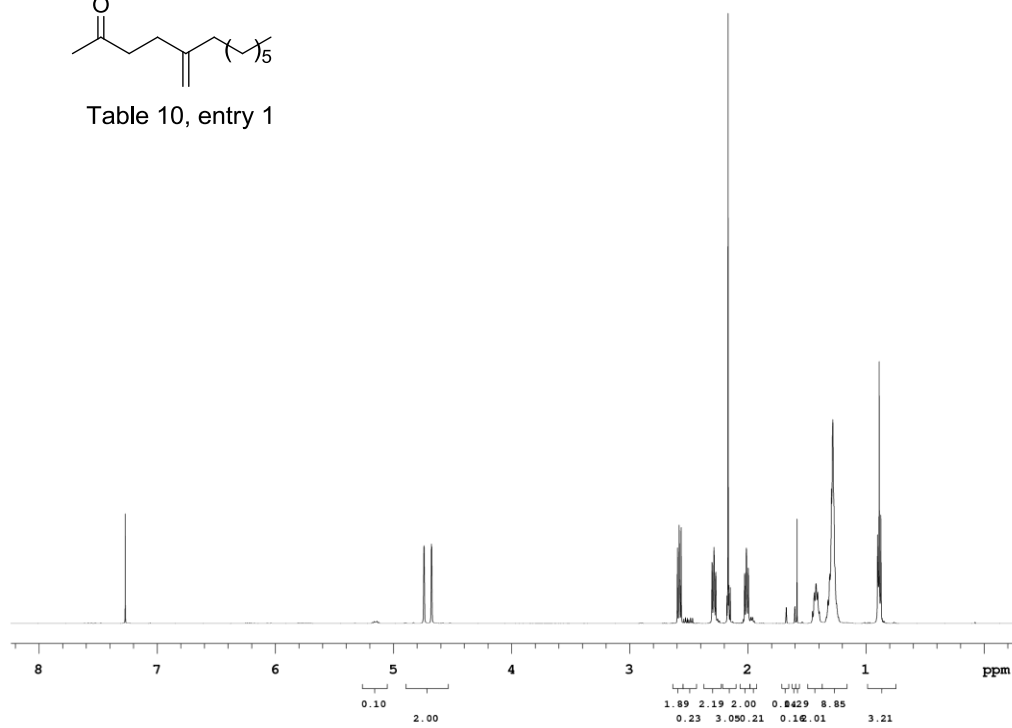


Table 10, entry 1



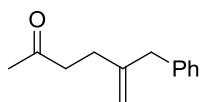
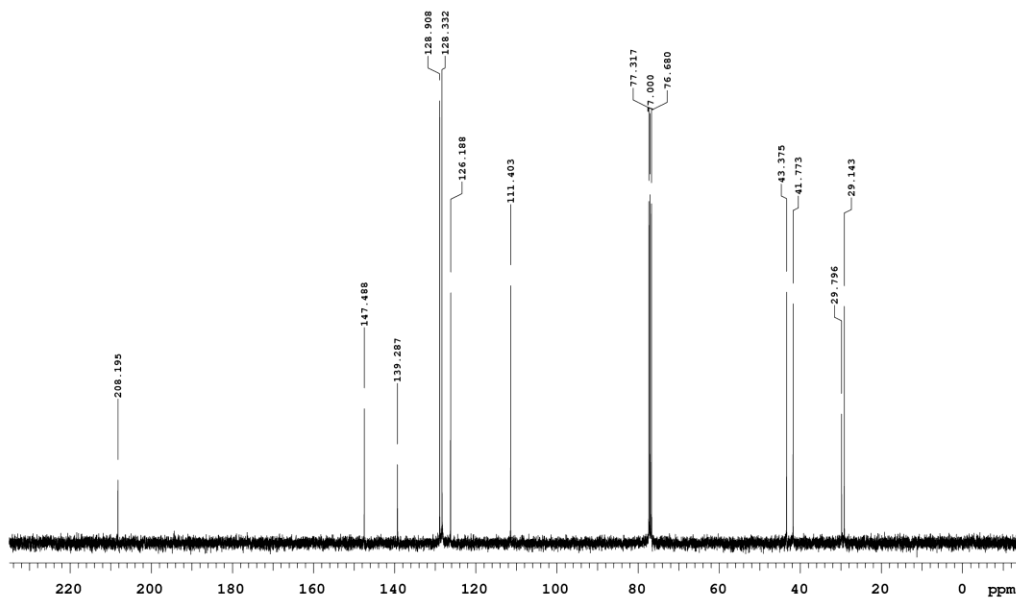
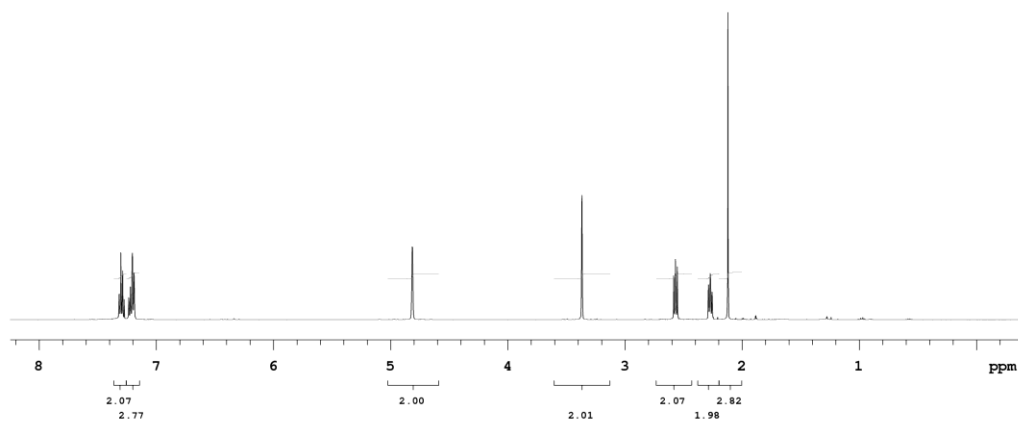


Table 10, entry 2



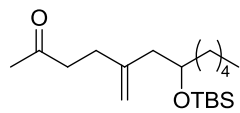
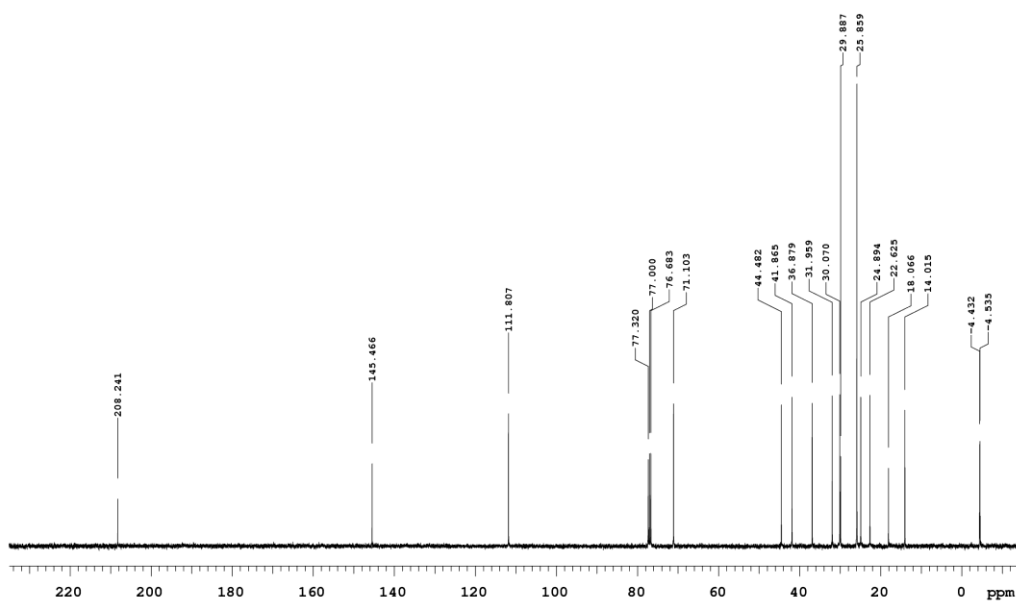
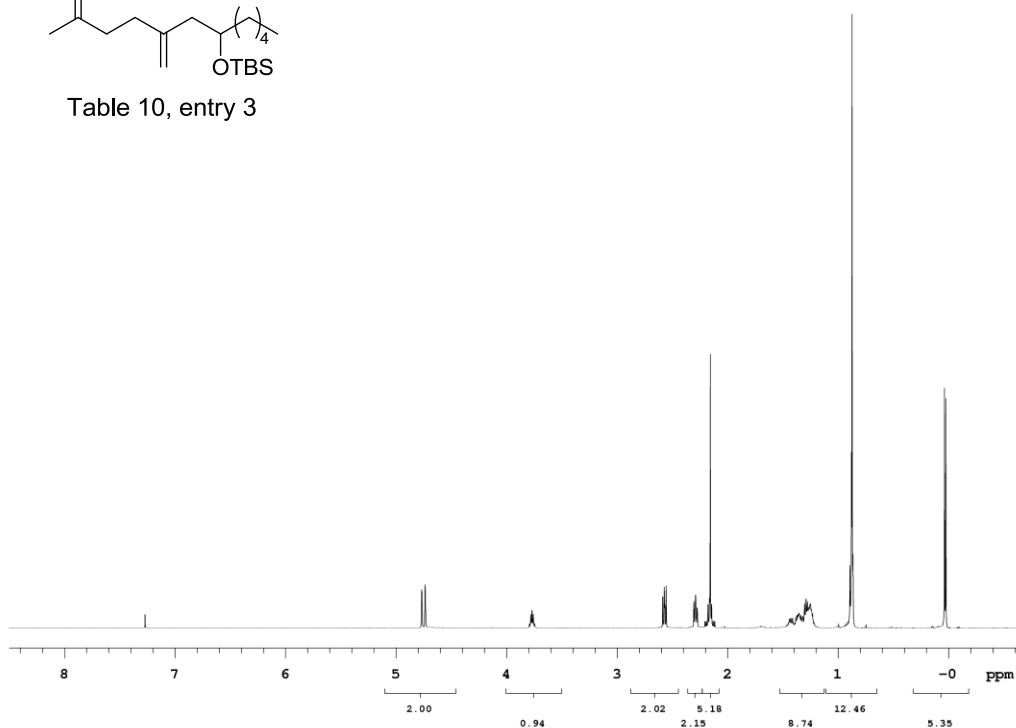


Table 10, entry 3



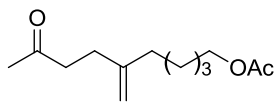
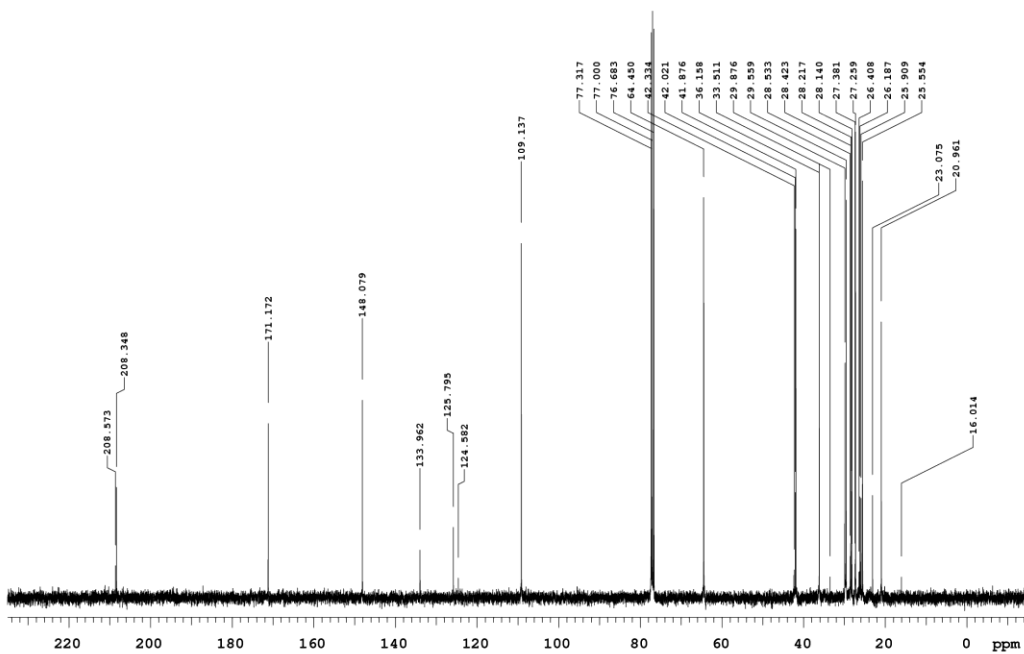
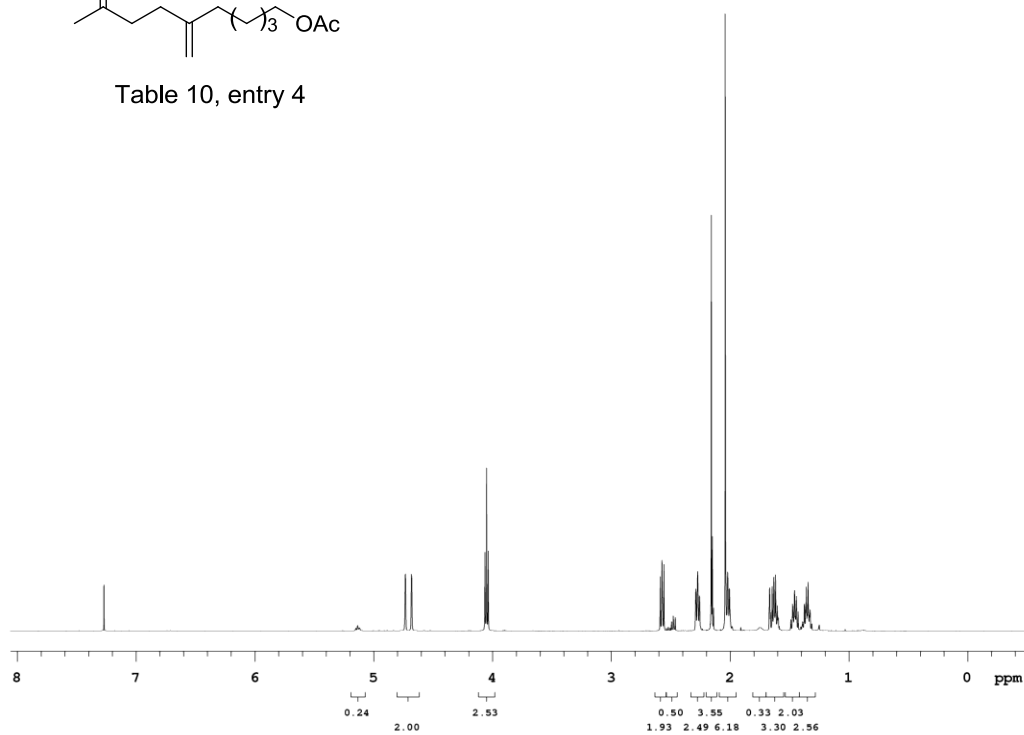


Table 10, entry 4



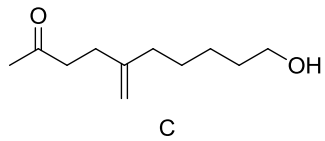
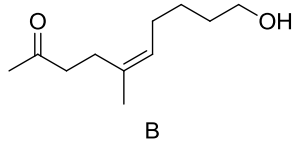
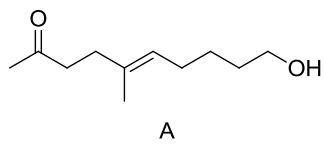
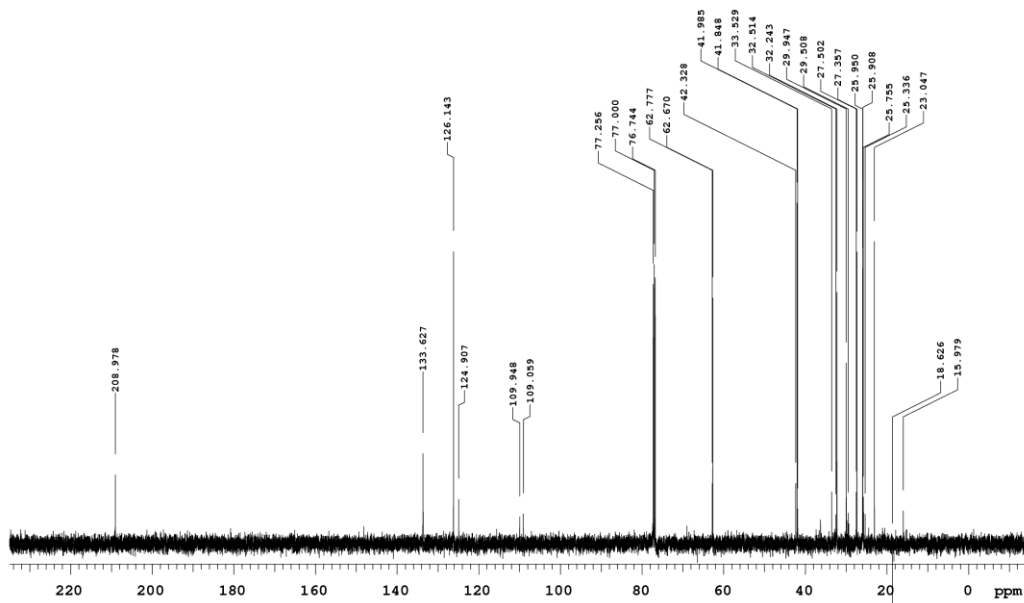
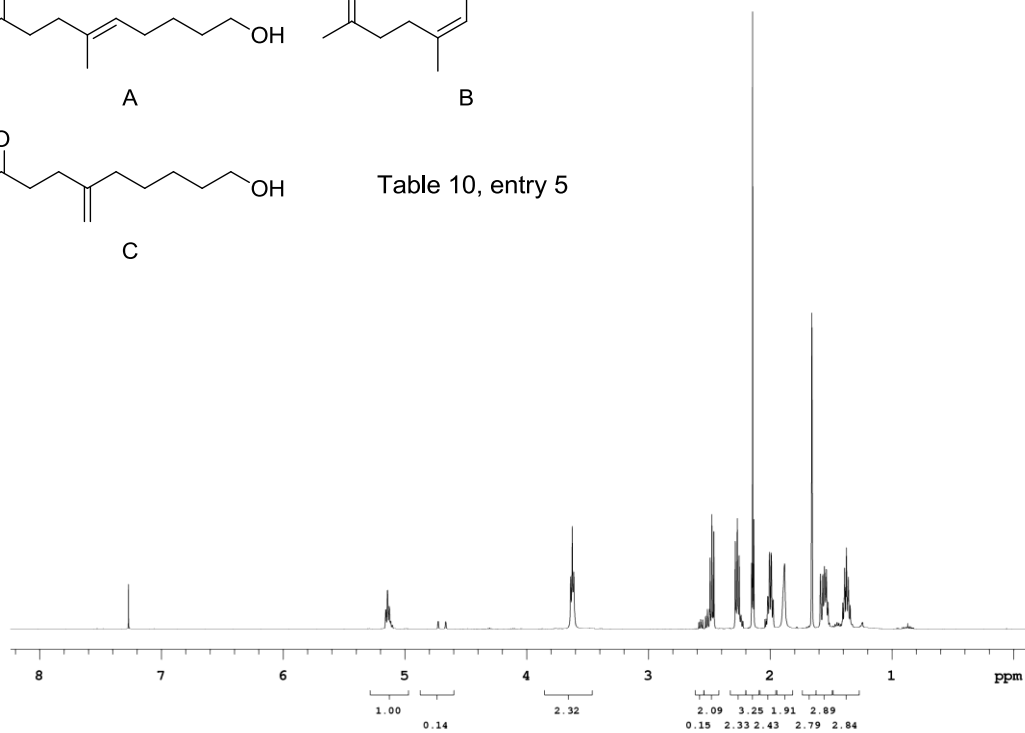


Table 10, entry 5



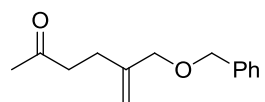
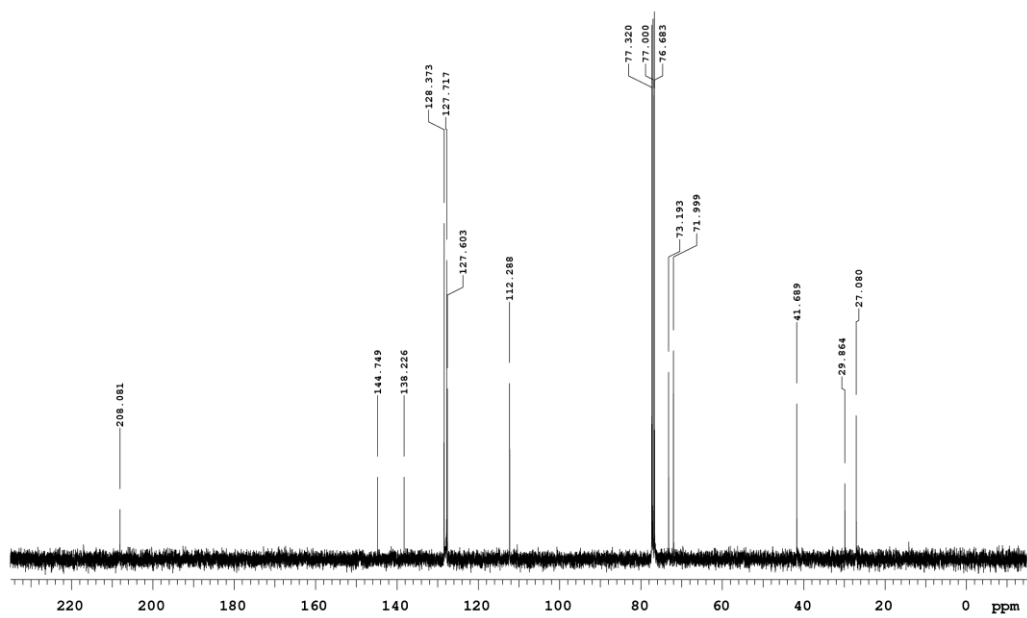
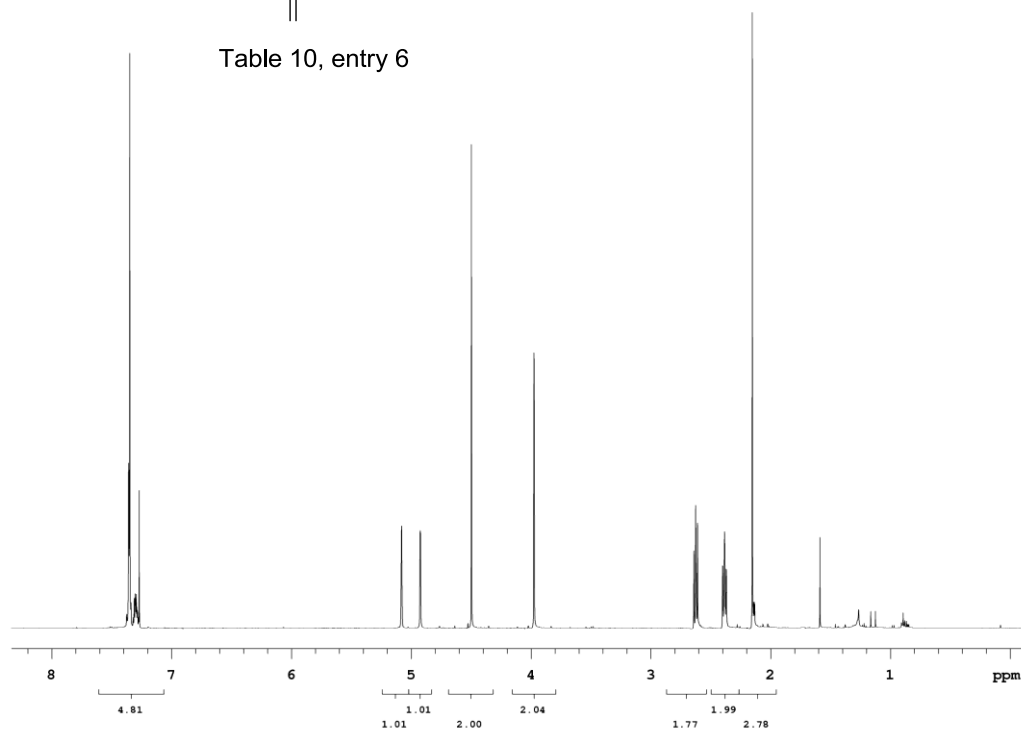


Table 10, entry 6



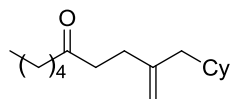
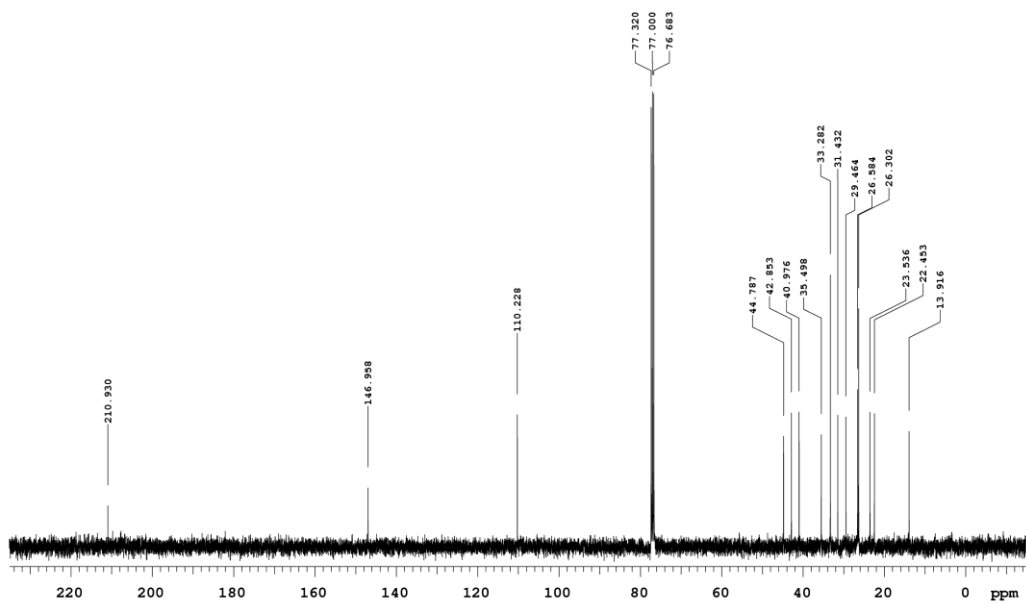
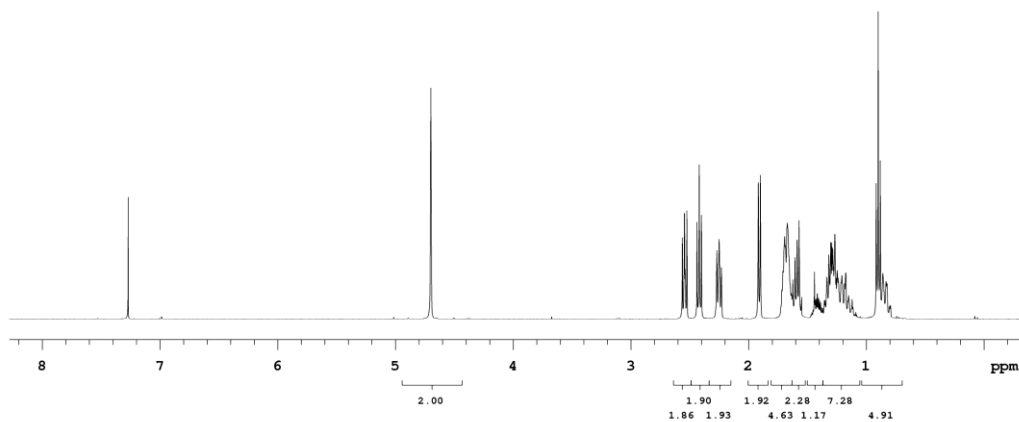


Table 10, entry 7



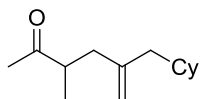
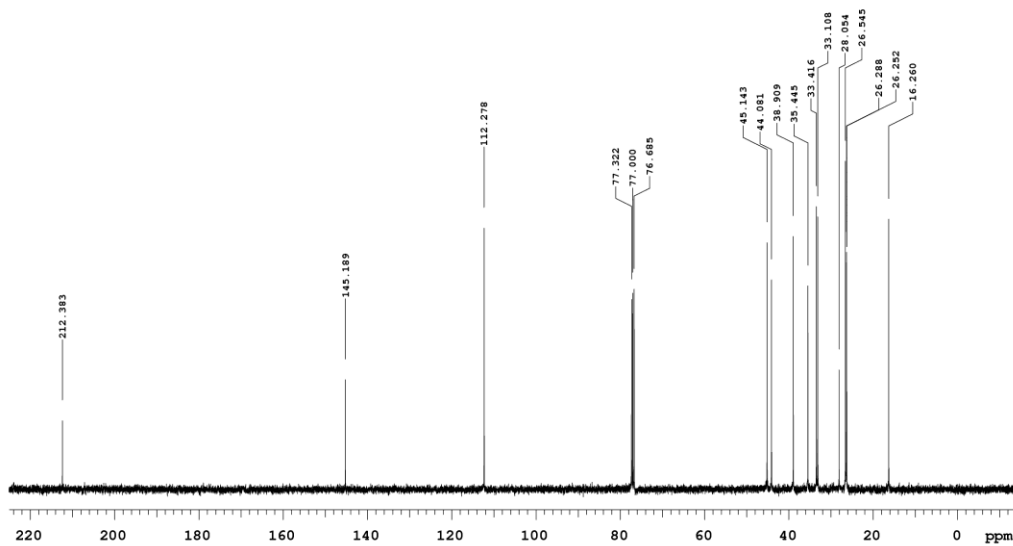
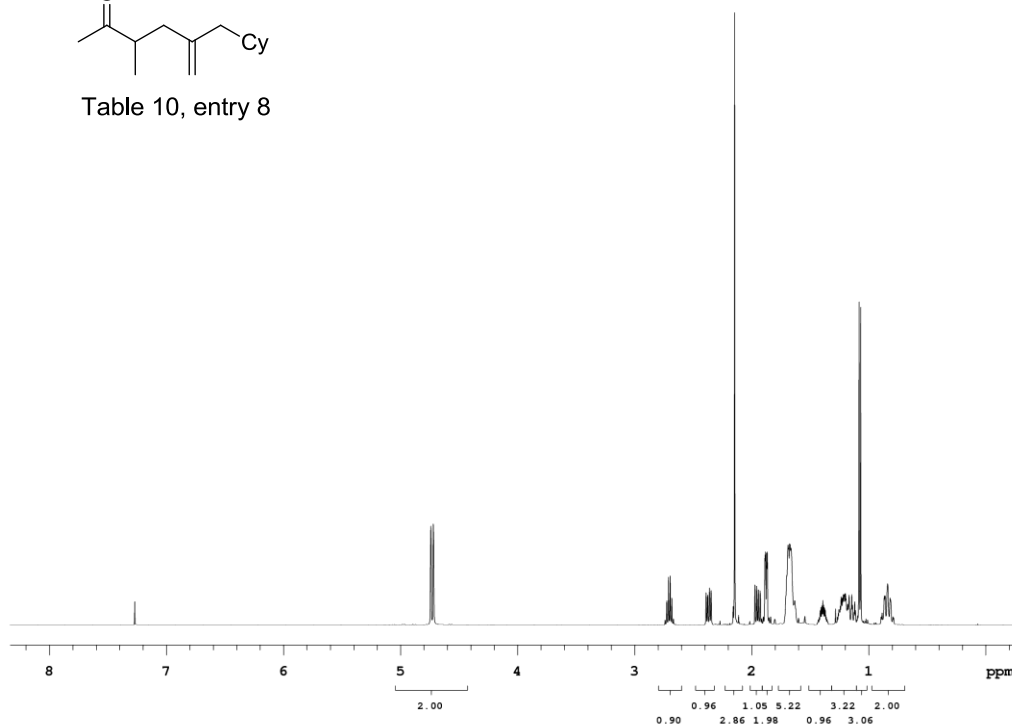


Table 10, entry 8



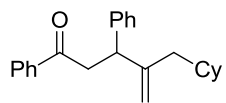
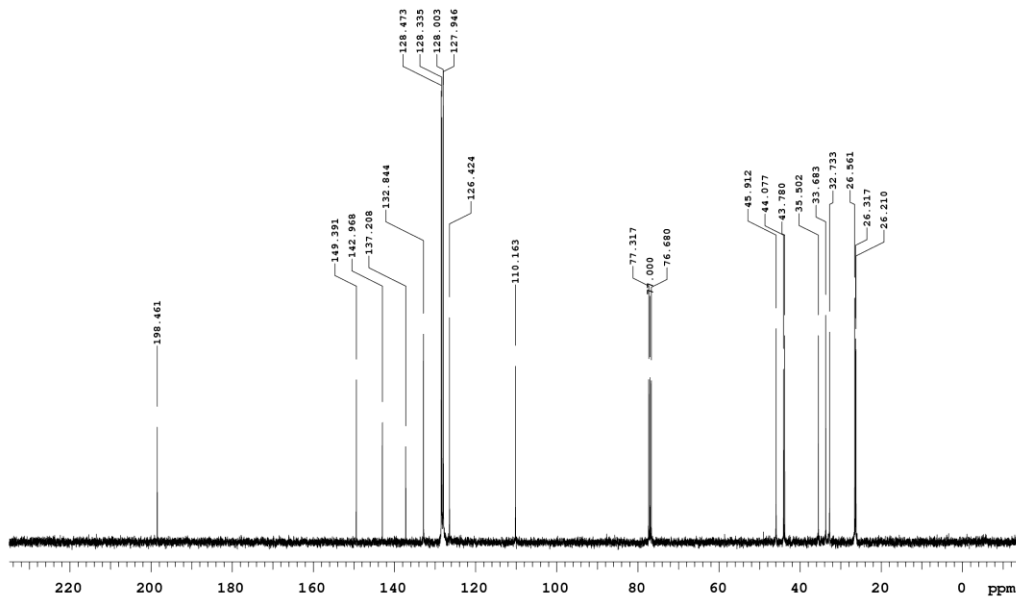
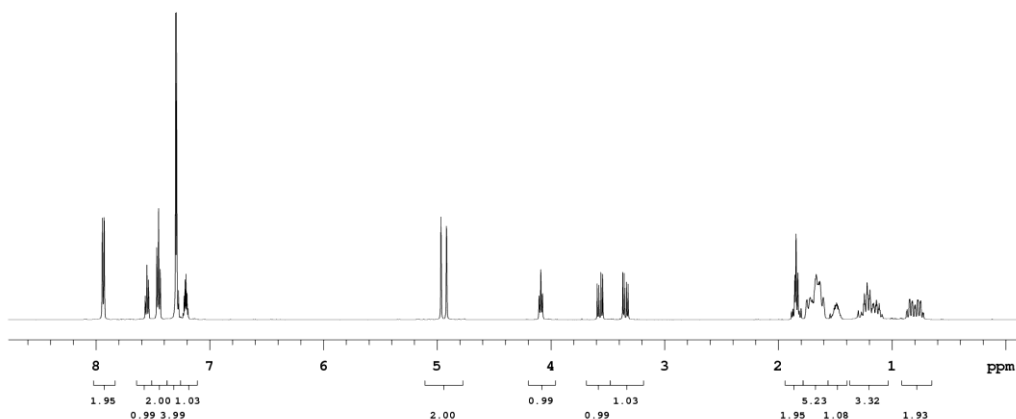


Table 10, entry 9



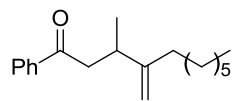
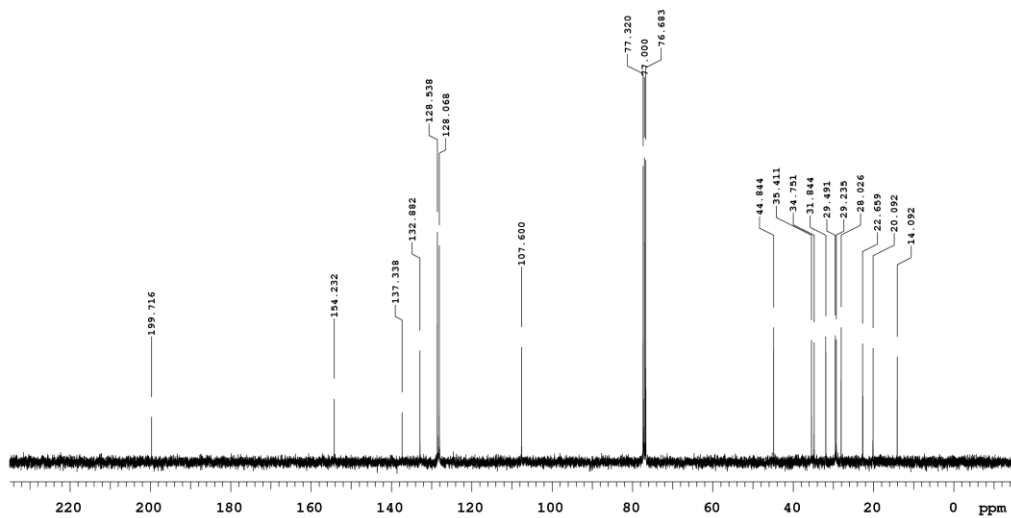
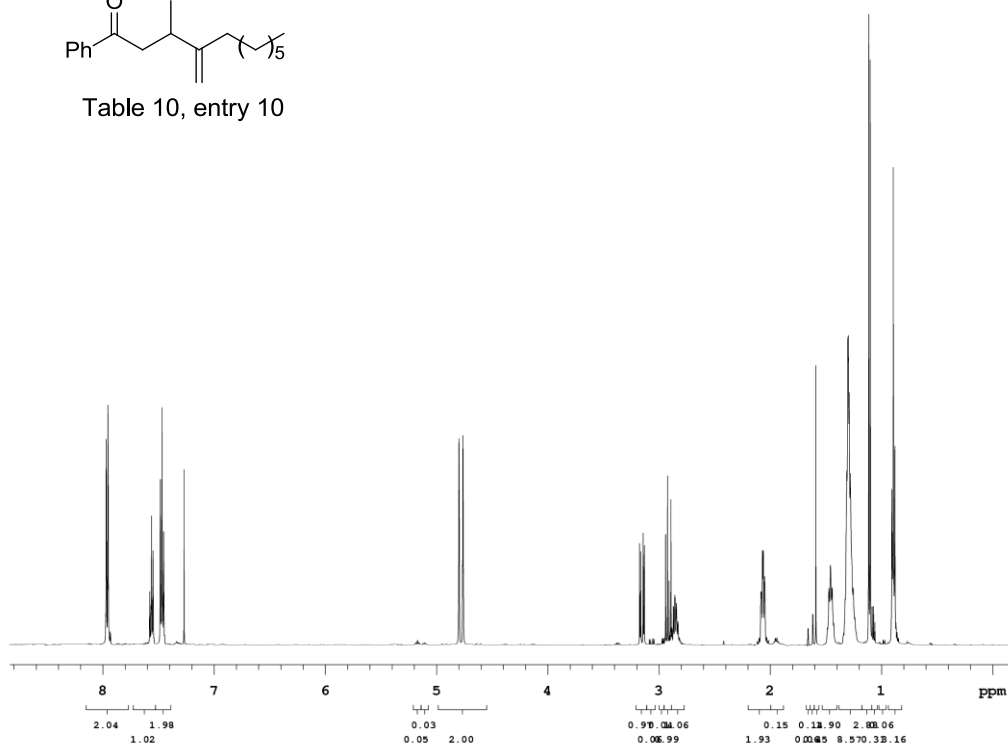


Table 10, entry 10



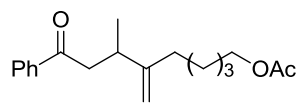
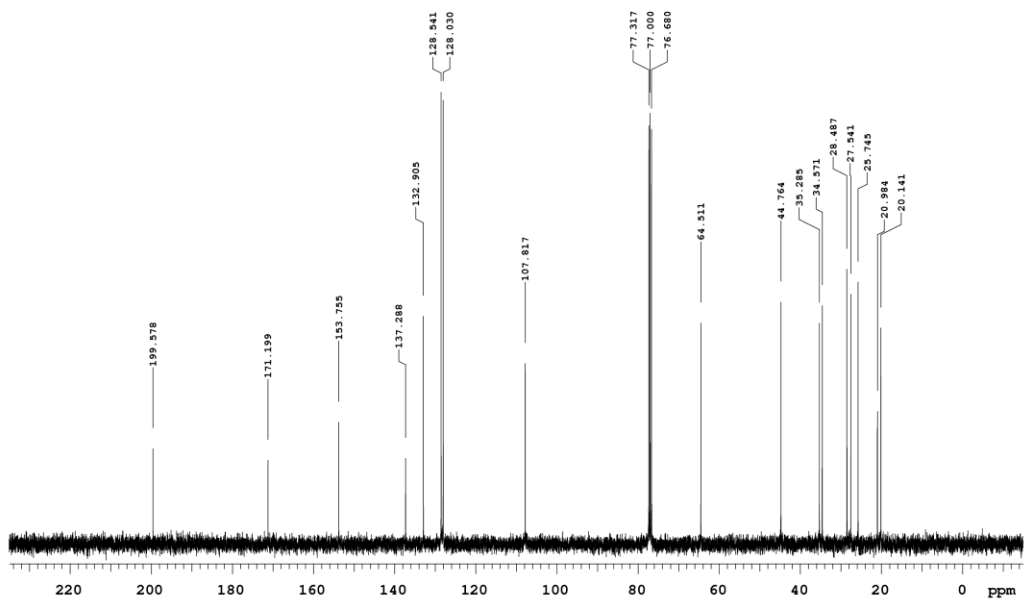
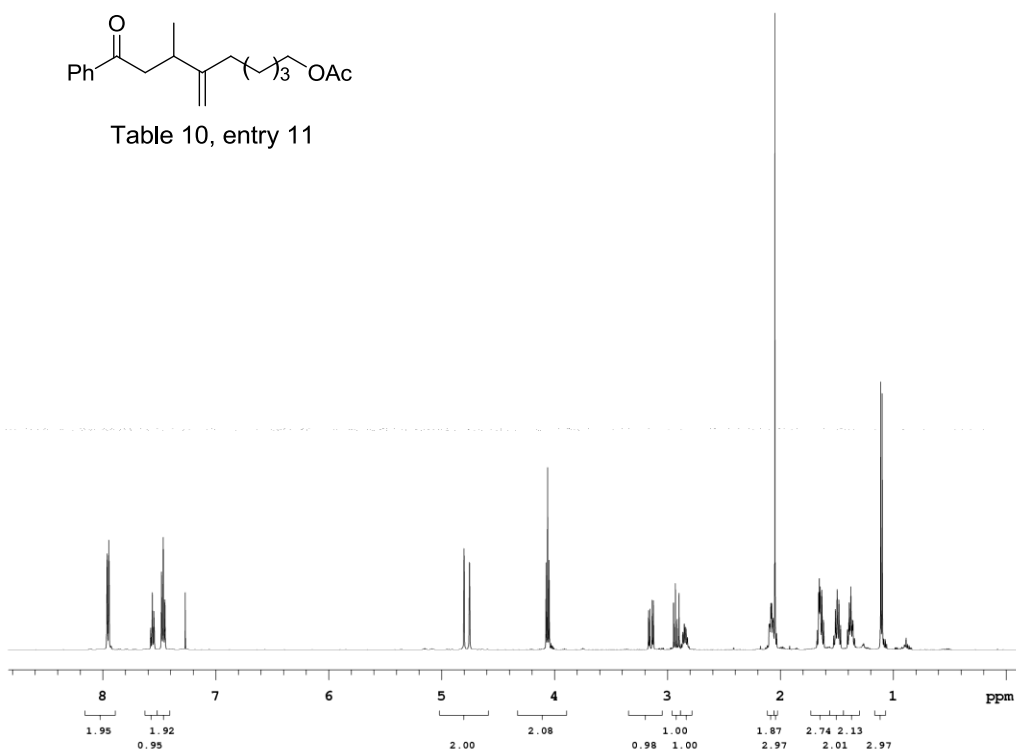


Table 10, entry 11



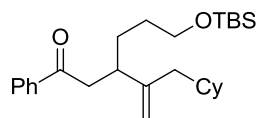
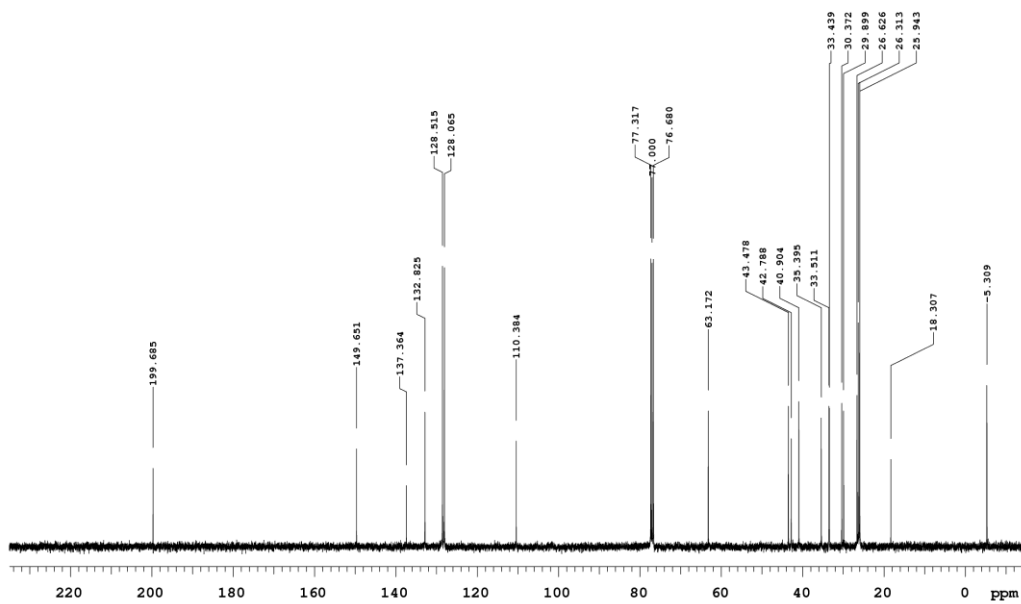
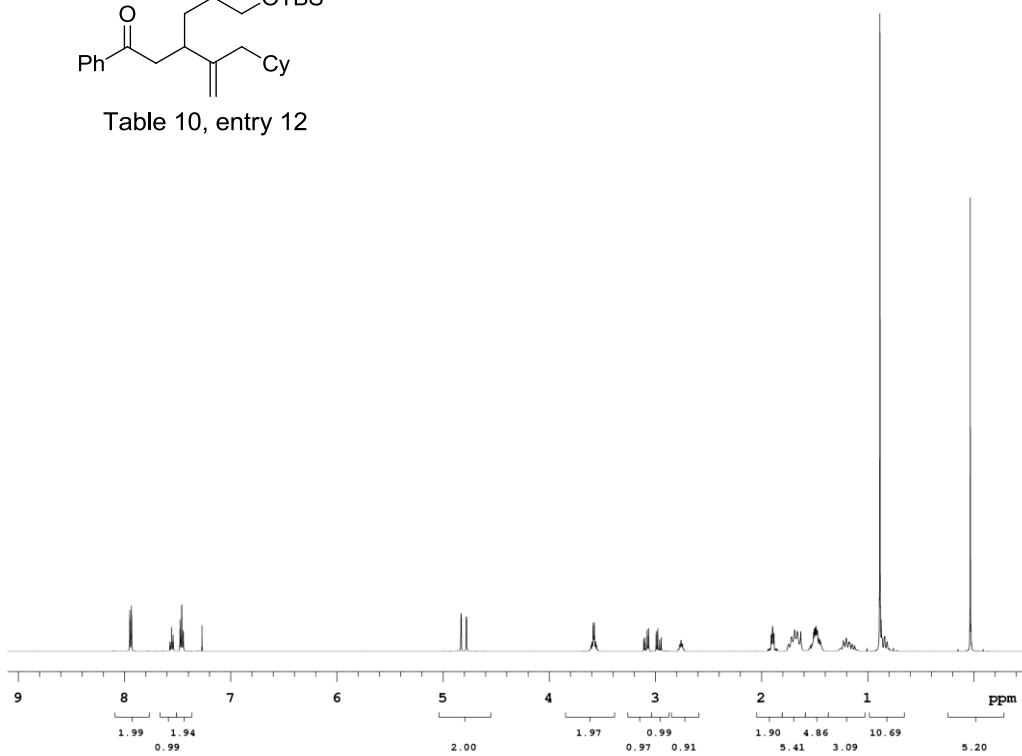


Table 10, entry 12



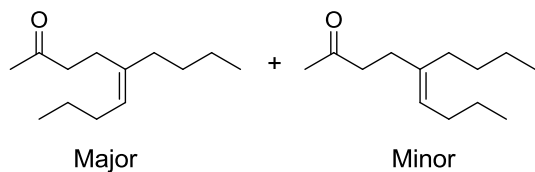
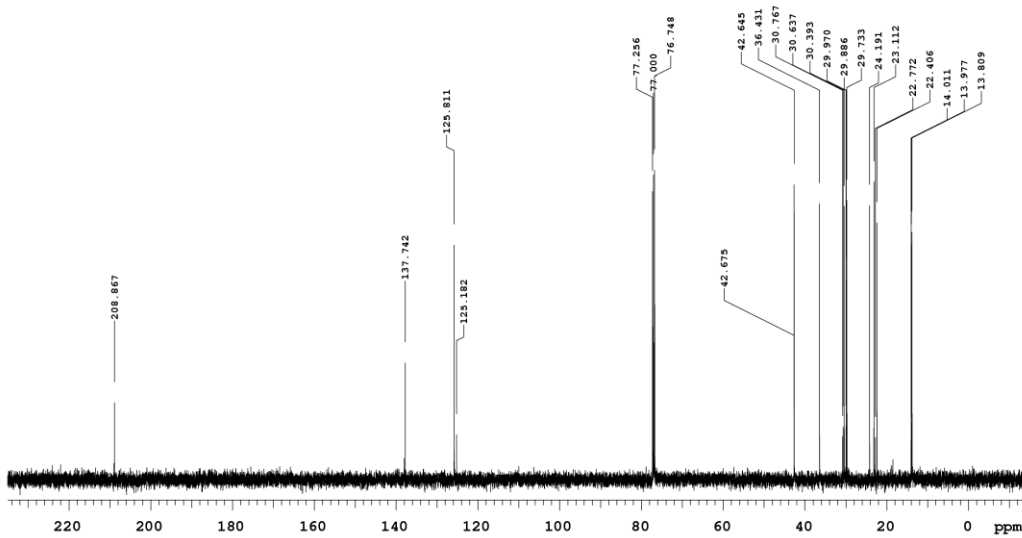
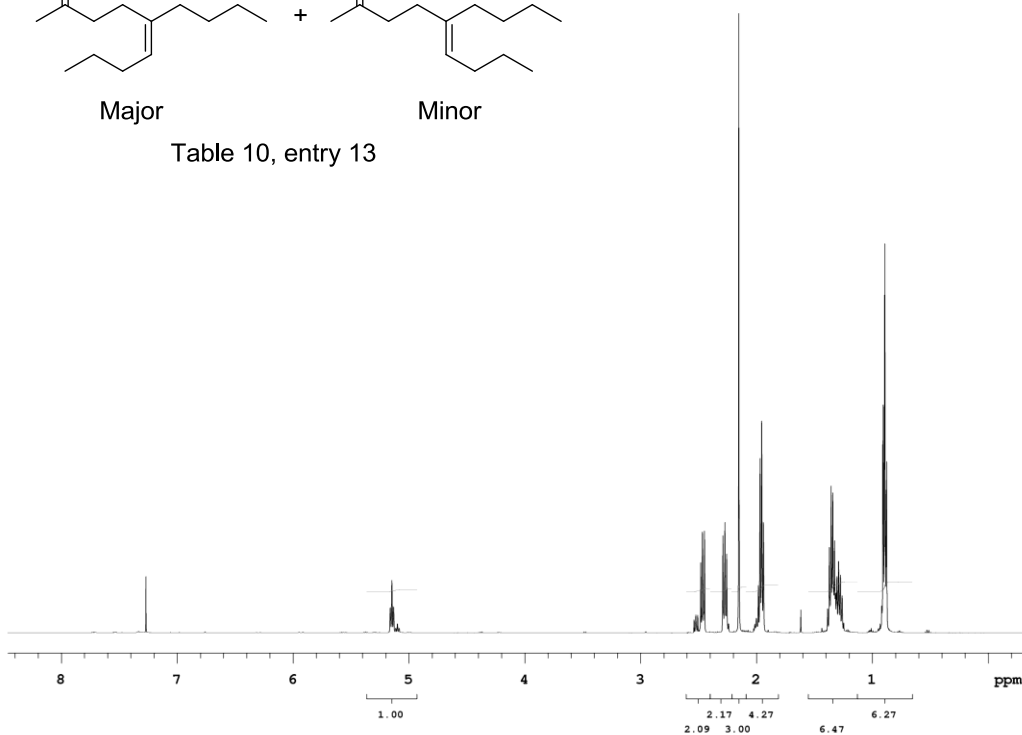
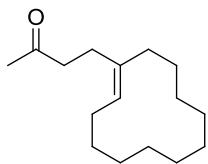
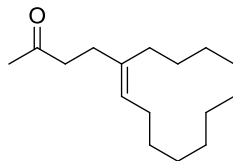


Table 10, entry 13



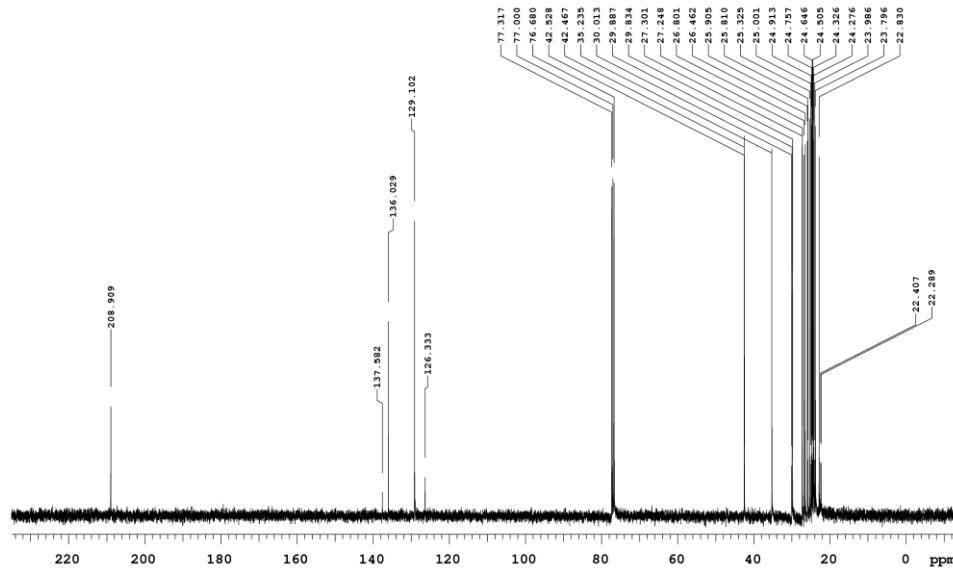
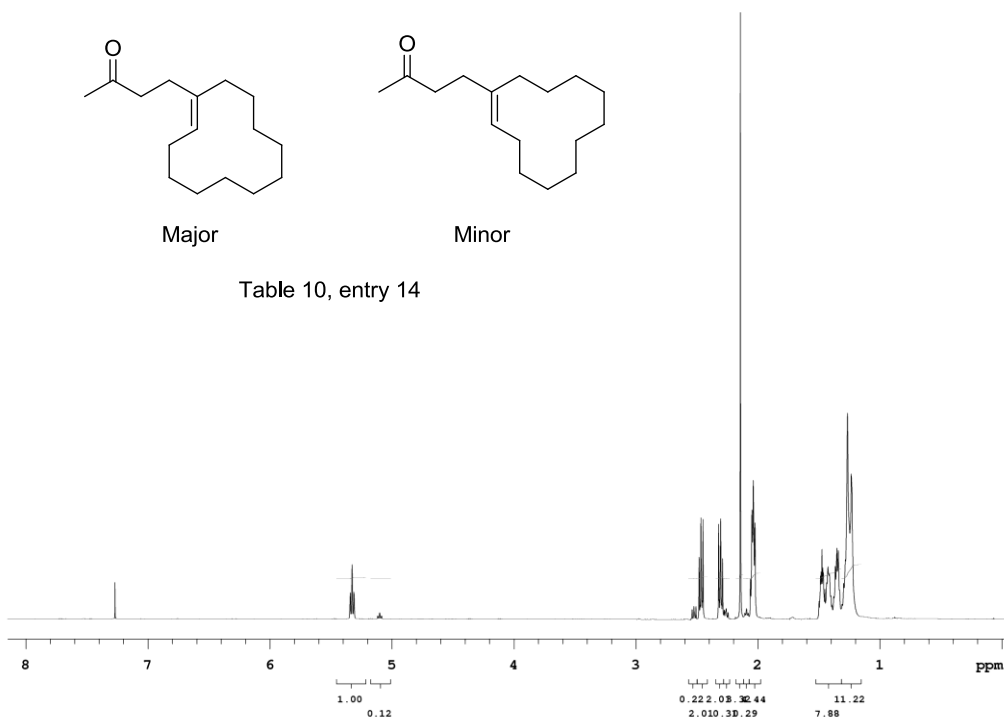


Major



Minor

Table 10, entry 14



References

- (1) Montgomery, J. *Angew. Chem. Int. Ed.* **2004**, *43*, 3890.
- (2) Takai, K.; Kimura, K.; Kuroda, T.; Hiyama, T.; Nozaki, H. *Tetrahedron.* **1983**, *47*, 5281.
- (3) Lipshutz, B. H. Sengupta, S. In *Organic Reactions*; Paquette, L. A., Ed.; Wiley: New York, 1992; Vol. 41, p 135.
- (4) Montgomery, J. *Top. Curr. Chem.* **2007**, *279*, 1.
- (5) Jin, H.; Uenshi, J.; Christ, W. J.; Kishi, Y. *J. Am. Chem. Soc.* **1986**, *108*, 5644.
- (6) Wipf, P.; Smitrovich, J. H. *J. Org. Chem.* **1991**, *56*, 6494.
- (7) Montgomery, J. *Acc. Chem. Res.* **2000**, *33*, 467.
- (8) Bower, J. F.; Kim, I. S.; Patman, R. L.; Krische, M. J. *Angew. Chem. Int. Ed.* **2009**, *48*, 34.
- (9) Hoveyda, A. H.; Evans, D. A.; Fu, G. C. *Chem. Rev.* **1993**, *93*, 1307.
- (10) Wipf, P. In *Comprehensive Organic Synthesis*; Trost, B. M., Ed.; Pergamon Press: Oxford, 1991; Vol. 4, p 585.
- (11) Oblinger, E.; Montgomery, J. *J. Am. Chem. Soc.* **1997**, *119*, 9065.
- (12) Huang, W. S.; Chan, J.; Jamison, T. F. *Org. Lett.* **2000**, *2*, 4221.
- (13) Tang, X.-Q.; Montgomery, J. *J. Am. Chem. Soc.* **1999**, *121*, 6098.
- (14) Tang, X.-Q.; Montgomery, J. *J. Am. Chem. Soc.* **2000**, *122*, 6950.
- (15) Manhandru, G.; Liu, G.; Montgomery, J. *J. Am. Chem. Soc.* **2004**, *126*, 3698.
- (16) Baxter, R. D.; Montgomery, J. *J. Am. Chem. Soc.* **2008**, *130*, 9662.
- (17) Gilman, H.; Jones, R. G.; Woods, L. A. *J. Org. Chem.* **1952**, *17*, 1630.
- (18) Wipf, P.; Jahn, H. *Tetrahedron.* **1996**, *52*, 12853.
- (19) Lipshutz, B. H.; Wood, M. R. *J. Am. Chem. Soc.* **1993**, *115*, 12625.
- (20) Loots, M. J.; Schwartz, J. *J. Am. Chem. Soc.* **1977**, *99*, 8045.
- (21) Takaya, T.; Ogasawa, M.; Hayashi, T. *Tetrahedron Lett.* **1998**, *39*, 8479.
- (22) Ikeda, S.; Sato, Y. *J. Am. Chem. Soc.* **1994**, *116*, 5975.
- (23) Ikeda, S.-I.; Yamamoto, H.; Kondo, K.; Sato, Y. *Organometallics.* **1995**, *14*, 5015.
- (24) Montgomery, J.; Savchenko, A. V. *J. Am. Chem. Soc.* **1996**, *118*, 2099.

- (25) Mahandru, G. M.; Skauge, A. L.; Chowdhury, S. K.; Amarasinghe, K. K. D.; Heeg, M. J.; Montgomery, J. *J. Am. Chem. Soc.* **2003**, *125*, 13481.
- (26) Amarasinghe, K. K. D.; Chowdhury, S. K.; Heeg, M. J.; Montgomery, J. *Organometallics*. **2001**, *20*, 370.
- (27) Hratchian, H. P.; Chowdhury, S. K.; Gutiérrez-García.; Amarasinghe, K. K. D.; Heeg, M. J.; Schlegel, B.; Montgomery, J. *Organometallics*. **2004**, *23*, 4636.
- (28) Petrier, C.; de Souza Barbosa, J. C.; Dupuy, C.; Luche, J. L. *J. Org. Chem.* **1985**, *50*, 5761.
- (29) Herath, A.; Thompson, B. B.; Montgomery, J. *J. Am. Chem. Soc.* **2007**, *129*, 8712.
- (30) Herath, A.; Montgomery, J. *J. Am. Chem. Soc.* **2006**, *128*, 14030.
- (31) Herath, A.; Montgomery, J. *J. Am. Chem. Soc.* **2008**, *130*, 8132.
- (32) Chang, H.-T.; Jayanth, T. T.; Wang, C.-C.; Cheng, C.-H. *J. Am. Chem. Soc.* **2007**, *129*, 12032.
- (33) Han, S. B.; Kim, I. S.; Han, H.; Krische, M. J. *J. Am. Chem. Soc.* **2009**, *131*, 6916.
- (34) Skucas, E.; Zbieg, J. R.; Krische, M. J. *J. Am. Chem. Soc.* **2009**, *131*, 5054.
- (35) Patman, R. L.; Chaulagain, M. R.; Williams, V. M.; Krische, M. J. *J. Am. Chem. Soc.* **2009**, *131*, 2066.
- (36) Gilgorich, K. M.; Cummings, S. A.; Sigman, M. S. *J. Am. Chem. Soc.* **2007**, *129*, 14193.
- (37) Saito, N.; Katayama, T.; Sato, Y. *Org. Lett.* **2008**, *10*, 3829.
- (38) Huddleston, R. R.; Jiang, H. Y.; Krische, M. J. *J. Am. Chem. Soc.* **2003**, *125*, 11488.
- (39) Jiang, H. Y.; Huddleston, R. R.; Krische, M. J. *J. Am. Chem. Soc.* **2004**, *126*, 4664.
- (40) Miller, K. M.; Jamison, T. F. *J. Am. Chem. Soc.* **2004**, *126*, 15342.
- (41) Bahadoor, A. B.; Flyer, A.; Micalizio, G. C. *J. Am. Chem. Soc.* **2005**, *127*, 3694.
- (42) Malik, H. A.; Sormunen, G. J.; Montgomery, J. *J. Am. Chem. Soc.* **2010**, *132*, 5966.
- (43) Ng, S. S.; Jamison, T. F. *Tetrahedron*. **2006**, *62*, 11305.
- (44) Montgomery, J.; Song, M. *Tetrahedron*. **2002**, *4*, 4009.
- (45) Bausch, C. C.; Patman, R. L.; Breit, B.; Krische, M. J. *Angew. Chem. Int. Ed.* **2011**, *123*, 5805.
- (46) Li, W.; Herath, A.; Montgomery, J. *J. Am. Chem. Soc.* **2009**, *131*, 17024.
- (47) Li, W.; Montgomery, J. *Chem. Comm.* Accepted.
- (48) Herath, A.; Li, W.; Montgomery, J. *J. Am. Chem. Soc.* **2008**, *130*, 469.
- (49) Ni, Y. K.; Amarasinghe, K. K. D.; Montgomery, J. *Org. Lett.* **2003**, *5*, 3771.

- (50) Wang, C.-C.; Lin, P. S.; Cheng, C.-H. *J. Am. Chem. Soc.* **2002**, *33*, 511.
- (51) Ho, C. Y.; Ohmiya, H.; Jamison, T. F. *Angew. Chem. Int. Ed.* **2008**, *120*, 1919.
- (52) Ho, C. Y.; Ohmiya, H.; Jamison, T. F. *Angew. Chem. Int. Ed.* **2008**, *47*, 1893.
- (53) Trost, B. M.; Pinkerton, A. B.; Seidel, M. *J. Am. Chem. Soc.* **2001**, *123*, 12466.
- (54) Chang, H.-T.; Jayanth, T. T.; Cheng, C.-H. *J. Am. Chem. Soc.* **2007**, *129*, 4166.
- (55) Chevliakov, M. V.; Montgomery, J. *J. Am. Chem. Soc.* **1999**, *121*, 11139.
- (56) Li, W.; Chen, N.; Montgomery, J. *Angew. Chem. Int. Ed.* **2010**, *49*, 8712.
- (57) Herath, A.; Thompson, B. B.; Montgomery, J. *J. Am. Chem. Soc.* **2007**, *129*, 8712.
- (58) El-Batta, A.; Hage, T. R.; Plotkin, S.; Bergdahl, M. *Org. Lett.* **2004**, *6*, 107.
- (59) See reference (30).
- (60) Ebner, D. C.; Novak, Z.; Stoltz, B. M. *Synlett.* **2006**, *20*, 3533.
- (61) Searles, S.; Li, Y.; Nassim, B.; Lopes, M.-T. R.; Tran, P. T.; Crabbé, P. *J. Chem. Soc. –Perkin Trans.* **1984**, *4*, 747.
- (62) Compound **87** was prepared by Crabbé homologation of the corresponding alkynol, followed by *tert*-butyldimethyl silyl protection with TBSCl and imidazole. Cheng, X.; Jiang, X. F.; Yu, Y. H.; Ma, S. M. *J. Org. Chem.* **2008**, *73*, 8960.
- (63) See reference (53).
- (64) Crabbé, P.; Fillion, H.; André, D.; Luche, J.-L. *J. Chem. Soc. –Chem. Comm.* **1979**, 859.
- (65) Trost, B. M.; Xie, J. *J. Am. Chem. Soc.* **2008**, *130*, 6231.
- (66) Ng, S.-S.; Jamison, T. *J. Am. Chem. Soc.* **2005**, *127*, 7320.
- (67) Brummond, K. M.; Dingess, E. A.; Kent, J. L. *J. Org. Chem.* **1996**, *61*, 6096.
- (68) Aho, J. E.; Salomäki, E.; Rissanen, K.; Pihko, P. M. *Org. Lett.* **2008**, *10*, 4179.